

University of Alberta

*The Function of Lipid Phosphate Phosphatase-2 in Fibroblasts*

by

*Katherine Elizabeth Morris*



A thesis submitted to the Faculty of Graduate Studies and Research in  
partial fulfillment of the

requirements for the degree of *Doctor of Philosophy*

Department of *Biochemistry*

Edmonton, Alberta

Fall 2006



Library and  
Archives Canada

Bibliothèque et  
Archives Canada

Published Heritage  
Branch

Direction du  
Patrimoine de l'édition

395 Wellington Street  
Ottawa ON K1A 0N4  
Canada

395, rue Wellington  
Ottawa ON K1A 0N4  
Canada

*Your file* *Votre référence*  
*ISBN: 978-0-494-23084-8*  
*Our file* *Notre référence*  
*ISBN: 978-0-494-23084-8*

#### NOTICE:

The author has granted a non-exclusive license allowing Library and Archives Canada to reproduce, publish, archive, preserve, conserve, communicate to the public by telecommunication or on the Internet, loan, distribute and sell theses worldwide, for commercial or non-commercial purposes, in microform, paper, electronic and/or any other formats.

The author retains copyright ownership and moral rights in this thesis. Neither the thesis nor substantial extracts from it may be printed or otherwise reproduced without the author's permission.

#### AVIS:

L'auteur a accordé une licence non exclusive permettant à la Bibliothèque et Archives Canada de reproduire, publier, archiver, sauvegarder, conserver, transmettre au public par télécommunication ou par l'Internet, prêter, distribuer et vendre des thèses partout dans le monde, à des fins commerciales ou autres, sur support microforme, papier, électronique et/ou autres formats.

L'auteur conserve la propriété du droit d'auteur et des droits moraux qui protègent cette thèse. Ni la thèse ni des extraits substantiels de celle-ci ne doivent être imprimés ou autrement reproduits sans son autorisation.

---

In compliance with the Canadian Privacy Act some supporting forms may have been removed from this thesis.

Conformément à la loi canadienne sur la protection de la vie privée, quelques formulaires secondaires ont été enlevés de cette thèse.

While these forms may be included in the document page count, their removal does not represent any loss of content from the thesis.

Bien que ces formulaires aient inclus dans la pagination, il n'y aura aucun contenu manquant.

  
**Canada**

## Abstract

Many phospholipids are signaling molecules that regulate cell proliferation, survival, apoptosis, adhesion, and migration. Bioactive lipid phosphate signaling is instrumental in development, angiogenesis and wound healing, and its dysregulation is implicated in inflammation, autoimmune diseases, and tumor growth and metastasis. The concentrations of bioactive lipids at their sites of activity are regulated by enzymes that catalyze the synthesis, degradation, and interconversion of glycerolipids and sphingolipids. These enzymes are therefore crucial regulators of the processes affected by lipid signaling. The lipid phosphate phosphatases regulate cell signaling and physiology by controlling the balance between the bioactive lipid phosphates lysophosphatidic acid, sphingosine-1-phosphate, phosphatidic acid, and ceramide-1-phosphate and their dephosphorylated products monoacylglycerol, sphingosine, diacylglycerol, and ceramide. *In vitro* studies and animal models have demonstrated that the lipid phosphate phosphatases have important and isoform-specific physiological roles. However, the functions of lipid phosphate phosphatase-2 in cell signaling and physiology has been largely unexplored. This thesis provides a detailed characterization of fibroblasts with increased and decreased expression of lipid phosphate phosphatase-2. Our results provide the first evidence of an endogenous and isoform-specific function of lipid phosphate phosphatase-2 activity in regulating cell cycle progression. Decreasing endogenous lipid phosphate phosphatase-2 mRNA expression results in delayed S-phase entry. The overexpression of catalytically active lipid phosphate phosphatase-2 results in

premature progression into S-phase after exit from quiescence. Cells that have prolonged overexpression of lipid phosphate phosphatase-2 activity eventually arrest in G<sub>2</sub>-phase of the cell cycle and display hallmarks of senescence. The regulation of S-phase entry by lipid phosphate phosphatase-2 is dependent on the timing of cyclin A expression, but could not be attributed to a change in the bulk cellular concentration of any known substrate or product of the enzyme's activity. In addition, lipid phosphate phosphatase-2 regulates fibroblast migration to lysophosphatidic acid and the activity of secreted matrix metalloproteinases. Although the mechanisms and physiological implications of our results require further investigation, this thesis provides the first comprehensive description of an endogenous and isoform-specific function of lipid phosphate phosphatase-2 activity in fibroblasts.

## Acknowledgements

There were many individuals who contributed to the completion of this thesis by lending both professional and personal support. I would like to acknowledge the following individuals who contributed to the results presented in this thesis. Caroline Spiers did most of the work on DNA damage and spent evenings and nights in the lab assisting with the flow cytometry experiments. Bobby Samuel produced the RT-PCR results on the regulation of endogenous LPP2 mRNA. Carlos Pilquil and Lana Stromberg did the initial cloning and characterization of LPP1 and LPP3, respectively. Cris Gaetano performed the experiments on the migration of LPP2 overexpressing cells. Meltem Sariahmetoglu contributed to the work on the MMPs, TIMP-2 and migration. Jay Dewald and Li Xie provided excellent technical support and assisted me with numerous experiments. I would especially like to thank Jay for helping me out early in the morning, at the last minute, and over the Christmas holidays on many occasions.

I would also like to acknowledge the members of other laboratories at the University of Alberta who supplied me with reagents, expertise, and advise. I would particularly like to thank Steve and others in the Ballerman lab, Dean in the Lehner lab, Darren in the Shultz lab, Steve and others in the Wang lab, Mee-Sook in the Posse De Chaves lab, Kathleen and others in the Holmes lab, Jody and others in the Michalak Lab, Gareth and others in the Berthiaume Lab, everyone in the Schang Lab, Dorothy in the flow cytometry facility, and Honey Chan in the microscopy facility. I would also like to acknowledge Drs. J-P Saulnier Blache, A. Morris, and S. Pyne for providing bacterial 1-acyl sn-glycerol-3-phosphate acyltransferase, LPP2 cDNA, and anti-LPP2 and anti-LPP3 antibodies, respectively. Thanks to Elaine Wang, Samuel Kelly and Dr. A. Merrill, Jr. for performing the mass spectrometric analysis of sphingolipids. Thanks to Yutong Zhao and Dr. V. Natarajan for providing positive control LPP2 antibody and lysate and assisting us in the generation of adenovirus. The research presented in this study was made possible by the work of all these collaborators.

I would like to acknowledge the National Sciences and Engineering Research Council, the Alberta Heritage Medical Research Foundation, and the University of Alberta for their generous salary funding.

Thanks to my committee members, Dr. Marek Michalak, Dr. Charles Holmes, and Dr. Luis Schang for your advice and time. Special thanks to Dr. Luis Schang for your mentorship and guidance that extended far beyond the typical contribution of a committee member. Without the time and expertise you generously contributed, this project would never have gone in the direction it did. I would also like to thank Dr. Luc Berthiaume and Dr. Andrew Morris for their insightful comments on my thesis. Thanks to all the members of the Signal Transduction Research Group whose advice at meetings guided my project significantly.

I would like to thank all of the current and former members of the Brindley lab including Jay, Carlos, Chif, Cris, Meltem, Nelson, Boripont, Li, Ling, Vitali, Sheri, Monika, Encarni, Anja, Atef, Indra, Anne, and Lana. I am fortunate to have found such good friends in my co-workers, and to have had such an enjoyable time at work over the years. I genuinely enjoyed my time in the lab, and I couldn't have asked for a more interesting, fun, and caring group of people to work with. You are like a second family to me, and I will miss you all very much.

Thanks to my supervisor, Dr. David Brindley, for your exceptional contribution to my career. You were always available for advice, but gave me a tremendous amount of freedom to learn for myself and develop my abilities. I appreciate the trust you showed in me and the support I knew I could always count on. Above all, I am proud to say that my supervisor is not only someone whom I respect as a scientist, but someone whom I respect as a human being. I genuinely believe that I could not have had a more educational or enjoyable experience working for anyone else.

To my parents, George and Trish Buri, who fostered my interest in academia, supported everything I did over the years, and took many, many trips to Edmonton, thank you for everything. Thanks to George, Stephanie, and Maryann, for your friendship and love. Thanks to all the friends I made in Brandon and at Brandon University who were the major reason that I developed a passion for science and who have remained in my life and encouraged me all these years. Thanks to all the family and friends I have found in Edmonton, who have made the graduate school experience a complete life experience that has exceeded all my expectations. A special thanks to Aaron for helping me discover my wand and my ability to wield it, and to all the spirits in the world that helped transform my belief in a little piece of driftwood into an instrument of true inspired sorcery when I needed it most.

Finally, to Gerald, my husband, the love of my life. Thank you for your unwavering and unending support and love. The joy and comfort you bring into my life affords me the luxury of perusing a career that consists mainly of frustration, makes the laboratory my bedroom far too many nights, and causes my friends to look at me with blank faces when I describe my latest exciting discovery. Thank you for trying to care about LPP2, and thank you for ensuring that I will always have something far more important than LPP2 to care about.

*We carry within us the wonders we seek without us*

-Thomas Browne 1642

## Table of Contents

<b>CHAPTER 1 – INTRODUCTION.....</b>	<b>1</b>
<b>1.1. Bioactive lipid signaling.....</b>	<b>3</b>
1.1.1. Metabolism of the bioactive glycerolipids and sphingolipids.....	3
1.1.2. Signaling by LPA and S1P.....	6
1.1.3. Signaling by PA and C1P.....	9
1.1.4. Signaling by DAG and ceramide.....	10
1.1.5. General trends in bioactive lipid signaling.....	11
<b>1.2. Lipid phosphate phosphatases.....</b>	<b>12</b>
1.2.1. Introduction.....	12
1.2.2. LPP family members and related proteins.....	12
1.2.3. Characteristics of the LPPs.....	15
1.2.4. Regulation of the LPPs.....	18
1.2.5. Activities and functions of the LPPs.....	19
1.2.6. Non-catalytic functions of the LPPs.....	21
1.2.7. Isoform specificity of the LPPs.....	24
1.2.8. Characteristics of the LPP2 isoform.....	28
<b>1.3. Cell cycle regulation.....</b>	<b>30</b>
1.3.1. Overview of the cell cycle .....	30
1.3.2. The traditional model of mammalian cell cycle regulation.....	31

1.3.2.1. Cyclins and cyclin-dependent kinases.....	31
1.3.2.2. G <sub>1</sub> to S-phase progression.....	35
1.3.2.3. G <sub>2</sub> to M phase progression.....	37
1.3.3. The implications of recent <i>in vivo</i> studies and new theories about cell cycle regulation.....	39
1.3.4. DNA damage pathways and checkpoint regulation.....	43
<b>1.4. Cellular senescence.....</b>	<b>47</b>
1.4.1. Characteristics of cellular senescence.....	47
1.4.2. Replicative senescence in human and rodent cells.....	48
1.4.3. Stress-induced senescence in human and rodent cells.....	48
1.4.4. Oncogene-induced senescence and tumor suppression.....	49
1.4.5. Senescence in aging and antagonistic pleiotropy.....	50
1.4.6. The p53 pathway in the senescent response.....	51
1.4.7. The p16 <sup>INK4a</sup> /Rb pathway in the senescent response.....	52
1.4.8. The role of sphingolipids in cellular senescence.....	53
<b>1.5. Matrix metalloproteinases.....</b>	<b>54</b>
1.5.1. Characteristics of the matrix metalloproteinases.....	54
1.5.2. Regulation of MMP activities.....	55
1.5.3. The gelatinases MMP2 and MMP9.....	55
1.5.4. The mechanism of activation of MMP2.....	56
<b>1.6. Thesis objectives.....</b>	<b>58</b>



<b>CHAPTER 2 – MATERIALS AND METHODS.....</b>	<b>60</b>
<b>2.1. Overexpression and knock-down of the LPPs and cell maintenance.....</b>	<b>61</b>
2.1.1. Site-directed mutagenesis and addition of GFP tag.....	61
2.1.2. Sub-cloning.....	61
2.1.3. Creation of stable cell lines and adenovirus.....	62
2.1.4. Growth and maintenance of cell lines.....	62
2.1.5. siRNA transfection.....	63
2.1.6. Induction of DNA damage.....	64
<b>2.2. Measurements of proliferation, DNA concentrations, and mRNA concentrations.....</b>	<b>65</b>
2.2.1. Cell proliferation assay.....	65
2.2.2. Measurement of DNA content.....	65
2.2.3. MTT assay for cell viability.....	66
2.2.4. Extraction of RNA and real-time RT-PCR.....	66
<b>2.3. Protein methods.....</b>	<b>68</b>
2.3.1. Extraction of proteins.....	68
2.3.2. Immunoprecipitation.....	68
2.3.3. Preparation of samples for SDS-PAGE.....	69
2.3.4. SDS-PAGE and transfer.....	70
2.3.5. Antibodies and blotting.....	70
2.3.6. Scanning and quantitation of blots.....	72

<b>2.4. Assays of LPP activity.....</b>	<b>72</b>
2.4.1. Total activity in Triton X-100 micelles.....	72
2.4.2. Ecto activity of intact cells.....	73
2.4.3. LPA depletion in media.....	74
<b>2.5. Enzyme activity assays.....</b>	<b>74</b>
2.5.1. CDK1 and CDK2 activity.....	74
2.5.2. TIMP-2 activity .....	75
2.5.3. Matrix metalloproteinase gelatin zymography.....	76
<b>2.6. Lipid analyses.....</b>	<b>76</b>
2.6.1. Extraction of lipids.....	76
2.6.2. Measurement of total phospholipid phosphate.....	77
2.6.3. Measurement of bulk PA.....	78
2.6.4. Measurement of PA, DAG, Cer, C1P, S1P, and LPA by radioactive labeling.....	79
2.6.5. Measurement of DAG and Cer by DAG kinase assay.....	80
2.6.6. Measurement of LPA by LPAAT assay.....	81
2.6.7. Measurement of sphingolipids by mass spectrometry.....	83
2.6.8. Fractionization of nuclei for nuclear lipid measurement.....	83
<b>2.7. Microscopy.....</b>	<b>83</b>
2.7.1. Preparation of coverslips.....	83
2.7.2. Visualization and co-localization analysis.....	84

2.7.3. Measurement of apoptosis .....	85
<b>2.8. Flow cytometry.....</b>	<b>85</b>
2.8.1. Synchronization of cells.....	85
2.8.2. Cell cycle analysis with propidium iodide.....	86
2.8.3. Measurement of apoptosis.....	87
<b>2.9. Migration and statistical analyses.....</b>	<b>87</b>
2.9.1. Boyden chamber assay for migration.....	87
2.9.2. Statistical analyses.....	88

**CHAPTER 3 - ESTABLISHMENT AND CHARACTERIZATION  
OF FIBROBLASTS WITH MODIFIED LEVELS OF THE LPPs.....89**

<b>3.1. Introduction.....</b>	<b>90</b>
<b>3.2. Stable overexpression of the LPPs in rat2 fibroblasts.....</b>	<b>92</b>
3.2.1. mRNA concentrations in stably transduced fibroblasts.....	92
3.2.1.1. Measurement of mRNA concentrations in cells that overexpressed the LPPs .....	92
3.2.1.2. Overexpression of each LPP does not alter the expression of the other isoforms.....	93

3.2.1.3. LPP2 overexpression can be knocked down with siRNA.....	93
3.2.1.4. LPP2 mRNA expression in cells infected with adenovirus.....	94
3.2.2. Expression of the LPP proteins.....	96
3.2.2.1. Detection of the LPP1 and LPP3 proteins by Western blot.....	96
3.2.2.2. High molecular mass aggregates appear on Western blots of lysates from cells stably transduced with LPP2.....	97
3.2.2.3. Detection of the LPP2-GFP protein after adenoviral overexpression.....	100
3.2.3. The subcellular localization of LPP2-GFP.....	103
3.2.3.1. The localization of wild-type and mutant LPP2-GFP are highly similar.....	103
3.2.3.2. LPP2 co-localizes with markers for the plasma membrane, early endosomes, and endoplasmic reticulum, and is excluded from the nucleus.....	103
3.2.4. LPP activities in cells stably overexpressing the LPPs.....	106
3.2.4.1. The activities of lysates from cells overexpressing the LPPs toward PA.....	106
3.2.4.2. The activities of lysates from cells overexpressing the LPPs toward LPA and S1P.....	106
3.2.4.3. The LPP activities of cells infected with adenovirus for LPP2-GFP .....	108
3.2.4.4. The activity of immunoprecipitated LPP2.....	109
3.2.4.5. LPP2 does not co-immunoprecipitate LPP1.....	112
3.2.4.6. Ecto activity in cells overexpressing the LPPs.....	113
3.2.5. The effects of LPP overexpression on bulk cellular lipid concentrations and ERK activation.....	116

3.2.5.1. LPP2 overexpression does not change bulk cellular PA, DAG, or LPA concentrations.....	116
3.2.5.2. LPP2 overexpression does not attenuate the activity of ERK.....	116
<b>3.3. Knock-down of the LPPs in rat2 fibroblasts.....</b>	<b>118</b>
3.3.1. Changes in mRNA expression produced by knocking down the LPPs .....	118
3.3.1.1. Each LPP was knocked down by approximately 60% with siRNAs.....	118
3.3.1.2. Knock-down of LPP2 is maintained at a maximal level between 24 and 72 hours.....	118
3.3.1.3. The knock-down of each LPP isoform does not affect the mRNA expression of the other isoforms.....	119
3.3.2. LPP activities in cells with the LPPs knocked down.....	119
3.3.2.1. Knock-down of LPP1, but not LPP2 or LPP3, decreases total LPP activity in fibroblasts.....	119
<b>3.4. Discussion.....</b>	<b>121</b>
<b>CHAPTER 4 - LPP2 REGULATES ENTRY INTO S-PHASE OF THE CELL CYCLE.....</b>	<b>130</b>
<b>4.1. Introduction .....</b>	<b>131</b>
<b>4.2. LPP2 activity changes the timing of S-phase entry in fibroblasts.....</b>	<b>131</b>

4.2.1. Cells overexpressing LPP2 enter S-phase prematurely.....	131
4.2.2. Premature S-phase entry of LPP2 overexpressing cells is not a result of incomplete synchronization in G <sub>1</sub> -phase .....	132
4.2.3. Knock-down of endogenous LPP2 results in delayed S-phase entry.....	134
<b>4.3. LPP2 activity changes the timing of cyclin A expression in fibroblasts.....</b>	<b>135</b>
4.3.1. LPP2 overexpression causes premature cyclin A expression.....	135
4.3.2. Knock-down of endogenous LPP2 delays cyclin A expression...	136
4.3.3. The activity and expression of CDK2 occur prematurely in LPP2 overexpressing cells.....	137
<b>4.4. The timing of expression of other proteins that regulate G<sub>1</sub> to S-phase progression is not regulated by LPP2 activity.....</b>	<b>138</b>
4.4.1. LPP2 overexpression does not change the expression of cyclin E.....	138
4.4.2. LPP2 overexpression does not change the expression of the D-type cyclins or CDK4, or change the activation of GSK3 $\beta$ .....	139
4.4.3. LPP2 overexpression does not change the phosphorylation of Akt, LIMK, or p38 MAPK.....	140
<b>4.5. The concentrations of bulk and nuclear lipids are not changed by LPP2 overexpression during cell cycle progression.....</b>	<b>142</b>
4.5.1. LPP2 overexpression does not change the bulk concentrations of PA, C1P, LPA, S1P, DAG, or Cer during cell cycle progression.....	142
4.5.2. LPP2 overexpression does not change the nuclear concentrations of DAG or Cer.....	142

<b>4.6. LPP2 overexpression may lead to unchecked progression into S-phase in cells with DNA damage.....</b>	<b>145</b>
4.6.1. LPP2 overexpressing cells show a decreased delay in S-phase entry following UV irradiation.....	145
4.6.2. Phosphorylated p53 (Ser15) levels are elevated following DNA damage in LPP2 overexpressing cells but p21 <sup>Cip1</sup> and p27 <sup>Kip1</sup> are not increased.....	146
4.6.3. Basal levels of activated p53 are increased in cells that stably overexpress LPP2.....	147
<b>4.7. Endogenous LPP2 mRNA expression is not regulated during cell cycle progression or by a variety of agonists.....</b>	<b>149</b>
4.7.1. Endogenous LPP2 mRNA expression does not vary throughout the cell cycle.....	149
4.7.2. LPP2 mRNA expression is not regulated by a variety of factors involved in wound healing.....	150
<b>4.8. Discussion.....</b>	<b>152</b>
<b>CHAPTER 5 – PROLONGED LPP2 OVEREXPRESSION CAUSES DECREASED PROLIFERATION, THE ACCUMULATION OF FIBROBLASTS IN G<sub>2</sub>-PHASE, AND A SENESCENT PHENOTYPE.....</b>	<b>155</b>
<b>5.1. Introduction.....</b>	<b>156</b>
<b>5.2. High passage LPP2 overexpressing cells slow in proliferation.....</b>	<b>159</b>

5.2.1. Fibroblasts overexpressing LPP2 have decreased proliferation at high passage.....	159
5.2.2. The addition of LPA, S1P, or serum does not reverse the decreased proliferation of LPP2 overexpressing cells.....	161
5.2.3. High passage LPP2 overexpressing cells do not exhibit increased apoptosis.....	162
<b>5.3. High passage LPP2 overexpressing cells accumulate in G<sub>2</sub>-phase following the activation of the G<sub>2</sub>/M checkpoint.....</b>	<b>163</b>
5.3.1. High passage LPP2 transduced cells accumulate in G <sub>2</sub> -phase.....	163
5.3.2. LPP2 overexpressing cells with decreased proliferation have increased amounts of DNA and protein per cell.....	163
5.3.3. LPP2 overexpressing cells that are arrested in G <sub>2</sub> -phase have activated the G <sub>2</sub> /M checkpoint by maintaining high levels of phosphorylation of CDK1 on Tyr15.....	165
5.3.4. LPP2 overexpressing cells that have arrested in G <sub>2</sub> -phase do not increase cyclin B expression in response to serum stimulation.....	166
<b>5.4. LPP2 overexpression is suppressed at high passage in cells arrested in G<sub>2</sub>-phase.....</b>	<b>168</b>
5.4.1. LPP2 mRNA expression is decreased in cells arrested in G <sub>2</sub> -phase.....	168
5.4.2. LPP activity in lysates from cells arrested in G <sub>2</sub> -phase is reduced to control levels.....	169
5.4.3. The concentrations of LPP1 mRNA and LPP3 mRNA in cells with suppressed LPP2 overexpression.....	169
5.4.4. The overexpression of LPP1, LPP3, and LPP2 [R214K] are not suppressed at high passage.....	170
<b>5.5. LPP2 transduced cells that are arrested in G<sub>2</sub>-phase show changes in protein expression and lipid concentrations that are characteristic of senescence.....</b>	<b>172</b>



5.5.1. The expression of proteins involved in cell cycle progression and senescence are increased in cells arrested in G <sub>2</sub> -phase.....	172
5.5.2. LPP2 transduced cells arrested in G <sub>2</sub> -phase have increased ceramide and decreased LPA concentrations .....	173
<b>5.6. Discussion.....</b>	<b>175</b>
<b>CHAPTER 6 - LPP2 REGULATES THE MIGRATION OF FIBROBLASTS TO LPA AND SECRETED MATRIX METALLOPROTEINASE ACTIVITIES.....</b>	<b>182</b>
<b>6.1. Introduction.....</b>	<b>183</b>
<b>6.2. Changes in LPP2 expression change the migration of fibroblasts to LPA.....</b>	<b>184</b>
6.2.1. Fibroblasts that overexpress LPP2 migrate less to a variety of mitogens.....	184
6.2.2. Knock-down of endogenous LPP2 decreases the migration of fibroblasts to LPA .....	184
6.2.3. Media from LPP2 overexpressing cells promotes the migration of parental fibroblasts to LPA.....	185
6.2.4. Media from cells with LPP2 knocked down inhibits the migration of fibroblasts to LPA.....	185
<b>6.3. LPP activities change the secreted activity and expression of MMP2...186</b>	

6.3.1. Secreted MMP2 activity is changed by the overexpression and knock-down of the LPPs.....	186
6.3.2. MMP mRNA expression is changed by the overexpression and knock-down of the LPPs.....	187
6.3.3. The changes in MMP2 activity produced by the stable overexpression of LPP activities can be changed by transient adenoviral overexpression of different LPP activities.....	190
6.3.4. LPA does not increase MMP2 expression in rat2 fibroblasts.....	190
<b>6.4. LPP activities change the secreted activity and expression of MMP9...191</b>	
6.4.1. Secreted MMP9 activity is changed by the overexpression and knock-down of the LPPs.....	191
6.4.2. MMP9 mRNA expression is changed by the overexpression and knock-down of the LPPs.....	192
<b>6.5. The activity and expression of TIMP-2 are decreased in cells with LPP2 knocked down.....195</b>	
6.5.1. Conditioned media from cells with LPP2 knocked down has decreased TIMP-2 activity.....	195
6.5.2. Knock-down of LPP2 decreases TIMP-2 mRNA expression.....	195
6.5.3. Knock-down of LPP2 decreases the amount of secreted TIMP-2 protein.....	196
<b>6.6. The activities and expression of MMP2 and MMP9 are changed in high passage LPP2 transduced cells that are arrested in G<sub>2</sub>-phase.....197</b>	
6.6.1. LPP2 transduced cells that are arrested in G <sub>2</sub> -phase have decreased MMP2 activity and expression.....	197
6.6.2. LPP2 transduced cells that are arrested in G <sub>2</sub> -phase have increased MMP9 activity and expression.....	197

**6.7. The premature S-phase entry of LPP2 overexpressing cells is not reversed with an MMP inhibitor.....199**

**6.8. Discussion.....200**

**CHAPTER 7 - GENERAL DISCUSSION AND**

**FUTURE DIRECTIONS.....205**

**BIBLIOGRAPHY.....217**

## List of Tables

<b>Table 1.1.</b> Mammalian proteins related to the LPPs.....	<b>15</b>
<b>Table 1.2.</b> The expression of the LPPs in adult human organs and tumors.....	<b>27</b>
<b>Table 1.3.</b> The mammalian cyclin-dependent kinases.....	<b>33</b>
<b>Table 1.4.</b> Mouse knockouts of CDKs and cyclins.....	<b>42</b>
<b>Table 2.1.</b> Determination of the dose of UV radiation to reversibly delay fibroblasts in G <sub>1</sub> -phase.....	<b>65</b>
<b>Table 5.1.</b> Lipid composition of G <sub>2</sub> arrested cells.....	<b>174</b>
<b>Table 7.1.</b> A comparison of the LPP isoforms.....	<b>211</b>

## List of Figures

<b>Figure 1.1.</b> Glycerolipid metabolism.....	4
<b>Figure 1.2.</b> Sphingolipid metabolism.....	6
<b>Figure 1.3.</b> The major signaling pathways activated by LPA and S1P receptors.....	7
<b>Figure 1.4.</b> The sequence and predicted structure and catalytic mechanism of LPP2.....	17
<b>Figure 1.5.</b> The sequences of the rat LPPs and their domains and predicted phosphorylation sites .....	23
<b>Figure 1.6.</b> Basic regulatory mechanisms of cell-cycle CDKs.....	34
<b>Figure 1.7.</b> A simplified model of G <sub>1</sub> to S-phase progression.....	37
<b>Figure 1.8.</b> A simplified model of G <sub>2</sub> to M-phase progression.....	39
<b>Figure 1.9.</b> A simplified model of the mechanisms by which DNA damage induces cell cycle arrest at the G <sub>1</sub> /S and G <sub>2</sub> /M checkpoints.....	46
<b>Figure 1.10.</b> Pathways involved in the induction of cellular senescence.....	53
<b>Figure 1.11.</b> The protein structure and activation of MMP2.....	58
<b>Figure 2.1.</b> Transfection efficiency for siRNA is approximately 95%.....	64
<b>Figure 2.2.</b> Determination the linear range of assays for bulk PA and LPA concentrations.....	79
<b>Figure 2.3.</b> Fibroblasts that have been synchronized in G <sub>2</sub> -phase by treatment with nocodazole or in G <sub>1</sub> -phase with a double thymidine block do not re-enter the cell cycle within 48 h.....	86
<b>Figure 3.1.</b> mRNA expression in cells overexpressing the LPPs.....	95
<b>Figure 3.2.</b> Expression of the LPP1 and LPP3 proteins.....	97
<b>Figure 3.3.</b> The LPP2 protein can not be detected in lysates from rat2 fibroblasts that overexpress LPP2 on Western blots with an anti-LPP2 antibody .....	98

<b>Figure 3.4.</b> Expression of the LPP2-GFP protein.....	<b>102</b>
<b>Figure 3.5.</b> Localization of LPP2 and LPP2[R214K] in rat2 fibroblasts.....	<b>105</b>
<b>Figure 3.6.</b> Total LPP activity in Triton X-100 micelles of lysates from cells overexpressing the LPPs.....	<b>107</b>
<b>Figure 3.7.</b> Total activity of lysates and immunoprecipitates from cells infected with adenovirus for LPP2-GFP.....	<b>109</b>
<b>Figure 3.8.</b> Total activity of immunoprecipitates from cells overexpressing the LPPs. LPP2 does not co-immunoprecipitate LPP1.....	<b>111</b>
<b>Figure 3.9.</b> Ecto activity of cells overexpressing the LPPs.....	<b>115</b>
<b>Figure 3.10.</b> LPP2 overexpression does not change the bulk concentrations of PA, DAG, or LPA, or attenuate ERK activation in fibroblasts.....	<b>117</b>
<b>Figure 3.11.</b> The LPP mRNA expression and LPP activity of cells treated with siRNAs for the LPPs.....	<b>120</b>
<b>Figure 4.1.</b> LPP2 overexpression causes premature S-phase entry.....	<b>133</b>
<b>Figure 4.2.</b> Knock-down of LPP2 delays S-phase entry.....	<b>134</b>
<b>Figure 4.3.</b> LPP2 activity regulates the timing of cyclin A expression.....	<b>136</b>
<b>Figure 4.4.</b> LPP2 overexpression causes premature CDK2 activity and increased CDK2 expression but does not change the expression of cyclin E.....	<b>138</b>
<b>Figure 4.5.</b> LPP2 overexpression does not change the timing or magnitude of the expression of cyclin D1, cyclin D3, CDK4, or phosphorylated GSK3 $\beta$ .....	<b>140</b>
<b>Figure 4.6.</b> LPP2 overexpression does not change the phosphorylation of LIM kinase, p38 MAP kinase, or Akt.....	<b>141</b>
<b>Figure 4.7.</b> LPP2 overexpression does not change the bulk concentrations of PA, C1P, LPA, S1P, DAG, or Cer, or the nuclear concentrations of DAG or Cer.....	<b>144</b>
<b>Figure 4.8.</b> In response to UV irradiation, fibroblasts that overexpress LPP2 do not arrest in G <sub>1</sub> -phase, do activate p53, and do not increase p21 <sup>Cip1</sup> or p27 <sup>Kip1</sup> expression.....	<b>149</b>

<b>Figure 4.9.</b> The expression of endogenous LPP2 mRNA is not regulated during starvation or cell cycle progression or by agonists involved in the regulation of wound healing.....	<b>151</b>
<b>Figure 5.1.</b> Fibroblasts that overexpress LPP2 activity have decreased proliferation at high passage .....	<b>159</b>
<b>Figure 5.2.</b> The overexpression of LPP2 but not LPP2 [R214K], LPP1, or LPP3 causes proliferation to decline at high passage.....	<b>160</b>
<b>Figure 5.3.</b> The addition of LPA, S1P, or serum to the media does not reverse the decreased proliferation of high passage LPP2 overexpressing cells.....	<b>161</b>
<b>Figure 5.4.</b> High passage LPP2 overexpressing cells do not have increased apoptosis.....	<b>162</b>
<b>Figure 5.5.</b> Cells overexpressing LPP2 at high passage have an increased percentage of cells in G <sub>2</sub> -phase and increased amounts of DNA and protein per cell.....	<b>164</b>
<b>Figure 5.6.</b> The expression of phosphorylated CDK1 (Tyr15) and cyclin B are dysregulated in cells stably overexpressing LPP2 at high passage.....	<b>168</b>
<b>Figure 5.7.</b> The overexpression of LPP2 is suppressed at high passage.....	<b>171</b>
<b>Figure 5.8.</b> Cells stably transduced with LPP2 that are arrested in G <sub>2</sub> -phase show changes in the expression of proteins that are characteristic of senescence.....	<b>173</b>
<b>Figure 6.1.</b> Changes in expression of the LPPs affect the migration of fibroblasts.....	<b>186</b>
<b>Figure 6.2.</b> Changes in LPP expression affect the activity and expression of MMP2 .....	<b>189</b>
<b>Figure 6.3.</b> Adenoviral overexpression of the LPPs alters MMP2 activity and LPA treatment does not change MMP2 expression in fibroblasts.....	<b>191</b>
<b>Figure 6.4.</b> Changes in LPP expression affect the activity and expression of MMP9.....	<b>194</b>

<b>Figure 6.5.</b> Knock-down of LPP2 decreases the expression and activity of TIMP-2.....	<b>196</b>
<b>Figure 6.6.</b> The activity and expression of MMP2 and MMP9 are changed in cells arrested in G <sub>2</sub> -phase.....	<b>198</b>
<b>Figure 6.7.</b> The MMP inhibitor Batimastat does not change the effect of LPP2 overexpression on S-phase entry.....	<b>200</b>



## Abbreviations

AC	adenylyl cyclase
AGPAT	1-acyl-sn-glycerol-3-phosphate acyltransferase (LPAAT)
Akt	serine-threonine protein kinase B
APC	anaphase-promoting complex
ARF	alternative reading frame
Arg	arginine
ATM	ataxia telangiectasia mutant
ATP	adenosine triphosphate
ATR	ATM-Rad3-related
ATX	autotaxin
BCA	bicinchoninic acid
bFGF	fibroblast growth factor-beta
B-myb	v-myb myeloblastosis viral oncogene homolog (avian)-like 2
BRAF	v-raf murine sarcoma viral oncogene homolog B1
BSA	bovine serum albumin
C1P	ceramide-1-phosphate
Cables	Cdk5 and c-Abl linker protein
CAK	CDK-activating kinase
cAMP	cyclic adenosine monophosphate
CKI	casein kinase I
CKII	casein kinase II
Cdc	characteristic of cell division cycle
CDC25	cerevisiae cell division cycle
Cdc42	cell division cycle 42/GTP-binding protein
CDK	cyclin-dependent kinase
Cer	ceramide
CHK	cell cycle checkpoint kinase
CMV	cytomegalovirus
CoA	coenzyme A
Cox2	cyclooxygenase 2
cPLA <sub>2</sub>	cytosolic phospholipase A2
c-RAF	proto-oncogene serine/threonine-protein kinase Raf
c-src	proto-oncogene tyrosine-protein kinase Src
CSS2	type 2 candidate sphingomyelin synthase
Cys	cysteine
DAG	diacylglycerol
DGPP	diacylglycerol Pyrophosphate
DMEM	Dulbecco's modified eagle medium
dNTP	deoxyribonucleotide triphosphate
DTT	dithiothreitol
ECM	extracellular matrix
EEA1	early endosome antigen-1
EGF	epidermal growth factor

ER	endoplasmic reticulum
ERK	extracellular signal-regulated kinase
EST	expressed sequence tag
Ex	exon
FAK	focal adhesion kinase
FBS	fetal bovine serum
FBS-C	charcoal-stripped fetal bovine serum
FGF-R1	fibroblast growth factor receptor 1
G <sub>1</sub> -phase	gap1 phase
G <sub>2</sub> -phase	gap2 phase
GEF	guanine nucleotide exchange factor
GFP	green fluorescent protein
GPCR	G-protein coupled receptor
GSK3β	glycogen synthase kinase 3β
HBS	Hepes buffered saline
HEK293	human embryonic kidney
I.B.	immunoblot
I.P.	immunoprecipitate
IGF	insulin-Like Growth Factor
IgG	immunoglobulin G
IL1-β	interleukin 1-beta
iPLA <sub>2</sub>	calcium-insensitive phospholipase A2
IPTG	isopropyl-β-d-thiogalactopyranoside
IR	infrared
JNK	c-jun amino-terminal kinase
K-ras	Kirsten rat sarcoma 2 viral oncogene homolog
LB	Luria Bertani
LIMK	LIM kinase
LPA	lysophosphatidic acid
LPA <sub>1-4</sub>	lysophosphatidic acid receptor
LPAAT	lysophosphatidic acid acyltransferase (AGPAT)
LPC	lysophosphatidyl choline
LPP	lipid phosphate phosphatase (phosphatidate phosphohydrolase 2)
LRP/PRG	lipid phosphatase-related proteins/plasticity-related genes
Lys	lysine
M.B.P.	myelin basic protein
MAG	monoacylglycerol
MAPK	mitogen-activated protein kinase
MARCKS	myristoylated alanine-rich C-kinase substrate
MCM	mini-chromosome maintenance
MEF	mouse embryonic fibroblasts
MEK	mitogen-activated protein kinase kinase
MLC II	myosin light chain II
MMP	matrix metalloproteinase
MOI	multiplicity of infection
M-phase	mitosis

mRNA	messenger ribonucleic acid
mSds	1,2-alpha-D-mannosidase
MT-MMP	membrane-type matrix metalloproteinase
mTOR	mammalian target of rapamycin
MTT	3-(4,5-Dimethylthiazol-2-yl)-2,5-diphenyltetrazolium bromide
Munc	mammalian homologue of the unc-18 gene
Myc	v-myc myelocytomatosis viral oncogene homolog
NF-κB	nuclear factor κB
NMDA	N-methyl-d-aspartate
ON	optic nerve
PA	phosphatidic acid
PAP1	phosphatidate phosphohydrolase 1
pBP	pBabepuro
PBS	phosphate buffered saline
PC	phosphatidylcholine
PCR	polymerase chain reaction
PDGF	platelet-derived growth factor
PE	phosphatidylethanolamine
pfu	plaque-forming units
PI	phosphatidylinositol
Pi	inorganic phosphate
PI3K	phosphatidylinositol 3-kinase
PKA	cAMP-dependent protein kinase
PKC	protein kinase C
PL	phospholipid
PLD	phospholipase D
Plk	polo-like kinase
PMSF	phenylmethylsulfonyl fluoride
PP-1	protein phosphatase 1 catalytic subunit
PP-2A	protein phosphatase 2A catalytic subunit
PPARγ	peroxisome proliferator-activated receptor-gamma
PS	phosphatidylserine
PTEN	phosphatase and tensin homolog deleted on chromosome ten
R2	rat2 fibroblasts
Rac1	ras-related C3 botulinum toxin substrate 1
RARγ	retinoic acid receptor gamma
Rb	retinoblastoma
RNA pol II	RNA polymerase II
ROCK	Rho-associated kinase
RSK	p90 ribosomal S6 kinase
RTK	receptor tyrosine kinase
RT	reverse transcription
S1P <sub>1-5</sub>	sphingosine-1-phosphate receptor
SD	standard deviation
SDS	sodium dodecyl sulfate
SDS-PAGE	sodium dodecyl sulfate polyacrylamide gel electrophoresis

Ser	serine
SIP	sphingosine-1-phosphate
siRNA	small interfering RNA
SK	sphingosine kinase
SMS	sphingomyelin synthase
SPC	sphingosylphosphorylcholine
SPH	sphingosine
S-phase	synthesis phase
sPLA <sub>2</sub>	secretory phospholipase A2
SPM	sphingomyelin
SPP	sphingosine-1-phosphate phosphatase
Stat	signal transducers and activators of transcription
Suv39h1	suppressor of variegation 3-9 homolog 1
SV40	Simian vacuolating virus 40
TGF- $\beta$	transforming growth factor-beta
Thr	threonine
TIMP	tissue inhibitor of metalloproteinases
TLC	thin layer chromatography
TNF $\alpha$	tumor necrosis factor alpha
Tyr	tyrosine
UV	ultraviolet
VEGF	vascular endothelial growth factor

## **CHAPTER 1**

### **INTRODUCTION**

In addition to being major components of cell membranes, many lipids are signaling molecules that regulate processes including cell proliferation, survival, apoptosis, adhesion, and migration. Bioactive lipid signaling can regulate processes such as development, angiogenesis and wound healing, and has been implicated in inflammation, autoimmune diseases, and tumor growth and metastasis. The concentrations of bioactive lipids at their sites of activity are regulated by a variety of enzymes that catalyze the synthesis, degradation, and interconversion of glycerolipids and sphingolipids. These enzymes are therefore crucial regulators of the processes affected by lipid signaling. The lipid phosphate phosphatases (LPPs) are a family of three enzymes that dephosphorylate lysophosphatidic acid (LPA), sphingosine-1-phosphate (S1P), phosphatidic acid (PA), and ceramide-1-phosphate (C1P). By regulating the relative concentrations these lipid mediators and their dephosphorylated products, the LPPs can regulate cellular signaling and a variety of important biological processes.

This thesis examines the function of LPP2 activity in fibroblasts. This Chapter will discuss the metabolism and signaling functions of the glycerolipids and sphingolipids that are potential substrates or products of LPP2 activity. Subsequently, the LPPs and their known functions in cell signaling will be reviewed, with an emphasis on the possible functions of LPP2 activity. In our studies, we determined that LPP2 activity regulates cell cycle progression, the induction of senescence, and secreted matrix metalloproteinase activities in

fibroblasts. Therefore, a brief overview of the relevant aspects of these processes will also be presented.

## 1.1. Bioactive lipid signaling

### 1.1.1. *Metabolism of the bioactive glycerolipids and sphingolipids –*

Phosphatidylcholine (PC) is present in abundance in cellular membranes. PC can be converted to phosphatidic acid (PA) by the phospholipase D (PLD) enzymes (Fig. 1.1). PA can then be hydrolyzed by the lipid phosphate phosphatases (LPPs) to produce diacylglycerol (DAG). DAG can be converted back to PA by diacylglycerol kinases (Fig. 1.1). PA can also be converted to lysophosphatidic acid (LPA) if either its *sn*-1 or *sn*-2 acyl chain is cleaved by a phospholipase A<sub>1</sub> or A<sub>2</sub> (PLA<sub>1/2</sub>), respectively. Secretory phospholipase A<sub>2</sub> (sPLA<sub>2</sub>) is often responsible for extracellular LPA synthesis, and is most active when hydrolyzing lipids in damaged membranes or microvesicles [1]. Calcium-independent iPLA<sub>2</sub> and calcium-dependent cPLA<sub>2</sub> synthesize LPA inside cells. LPA can be converted back into PA by the action of specific acyltransferases of the LPAAT family (Fig. 1.1). Membrane PC can also be converted into lysophosphatidylcholine (LPC) by the action of PLA<sub>1/2</sub> enzymes (Fig. 1.1). LPC can then be converted to LPA by the lysoPLD activities. Autotaxin (ATX), a protein originally known as a motility stimulating factor involved in tumor progression, is responsible for circulating lysoPLD activity [2], and the knocking out ATX in mice resulted in decreased circulating LPA levels [3]. LPA can be hydrolyzed to monoacylglycerol (MAG) by the LPPs, and MAG can be converted

back to LPA by monoacylglycerol kinases (Fig.1.1). Finally, LPA can be destroyed by cleavage of its acyl chain by specific phospholipases. Glycerolipid metabolism is depicted in Figure 1.1., and reviewed in [1, 4, 5].

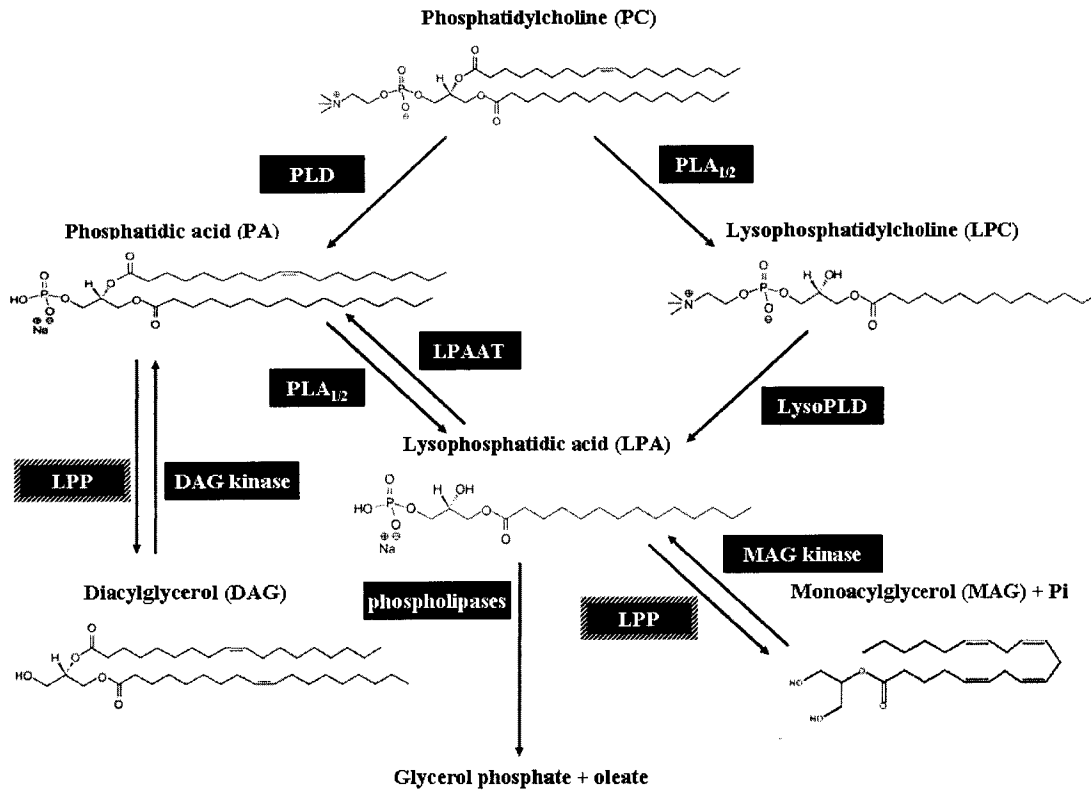


**Figure 1.1. Glycerolipid metabolism.** The major pathways for the synthesis and degradation of the bioactive glycerolipids are shown. The enzymes that catalyze the reactions are named in boxes and the structures of common, biologically active forms of the glycerolipids are provided. In the case of monoacylglycerol, the acyl chain is not conserved with the other structures to show the biologically active 2-arachadonal form. See the text for more details.

Sphingomyelin (SPM) is present in membranes and can be converted to ceramide (Cer) by sphingomyelinases (Fig. 1.2). Ceramide can also be created from palmitoyl CoA and serine in a *de novo* synthesis pathway. Ceramide can be converted back to SPM by sphingomyelin synthase activities (Fig. 1.2). Ceramide is phosphorylated by ceramide kinase to ceramide-1-phosphate (C1P), which can be hydrolyzed back to Cer by the LPPs (Fig. 1.2). Ceramide is also hydrolyzed to



sphingosine (SPH) by ceramidases, and the reverse reaction is catalyzed by ceramide synthases (Fig. 1.2). Sphingosine can be phosphorylated by sphingosine kinases (SKs) to produce sphingosine-1-phosphate (S1P). The conversion of S1P back to SPH is catalyzed by the LPPs and by specific sphingosine phosphate phosphatases (SPPs) (Fig. 1.2). Membrane sphingomyelin can also be converted to sphingosylphosphorylcholine (SPC, or lysosphingomyelin) by sphingomyelin deacylase (Fig. 1.2). SPC can then be converted to S1P by the lysoPLD activity of ATX. There is currently no evidence to suggest that this alternative pathway of S1P synthesis is physiologically relevant. The knockout of both sphingosine kinase isoforms in mice resulted in a severe deficiency in S1P, suggesting that the sphingomyelin deacylase/ATX pathway cannot substitute for the sphingosine kinase pathway in generating S1P *in vivo* [6]. Furthermore, heterozygous ATX knockout mice had decreased levels of circulating LPA, but unchanged levels of circulating S1P [3]. Sphingolipid metabolism is depicted in Figure 1.2., and reviewed in [4, 7].

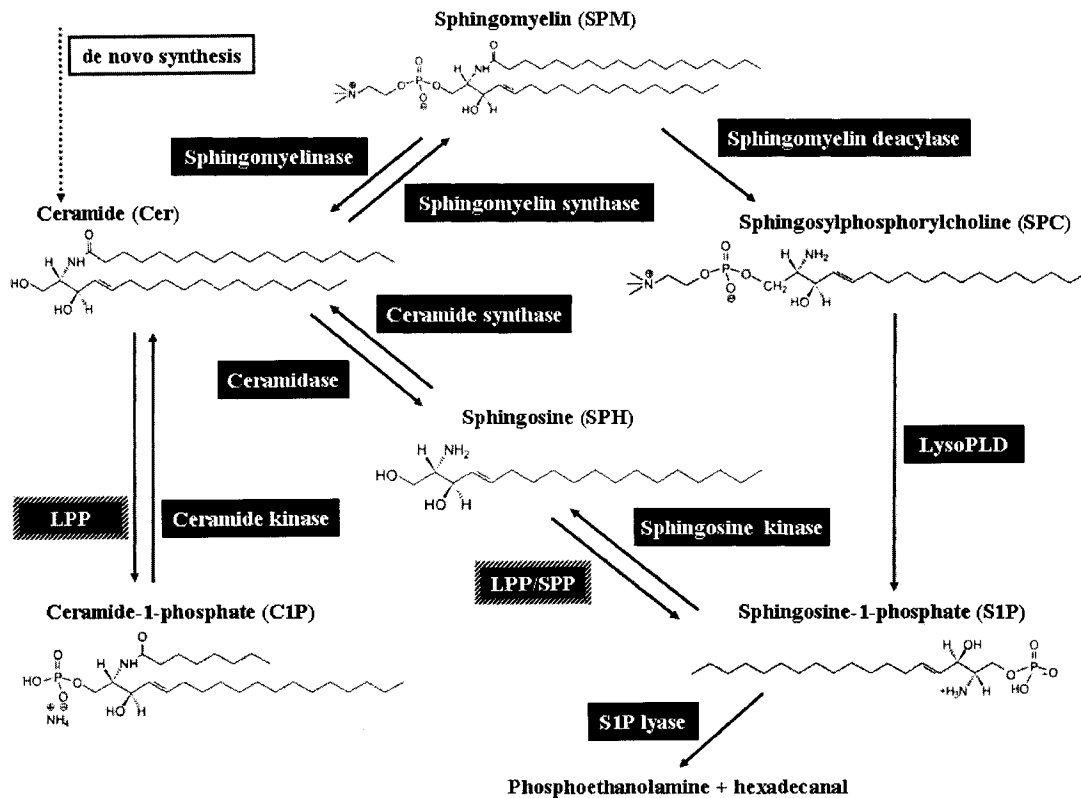


**Figure 1.2. Sphingolipid metabolism.** The major pathways for the synthesis and degradation of the bioactive sphingolipids are shown. The enzymes that catalyze the reactions are named in boxes and the structures of the sphingolipids are provided. See the text for more details.

1.1.2. *Signaling by LPA and S1P* – LPA and S1P are potent extracellular signaling molecules that activate families of G-protein coupled receptors (GPCRs). Additionally, both LPA and S1P can modify cell signaling intracellularly. Circulating LPA and S1P are produced and secreted by activated platelets, mast cells, cancer cells, and many other cell types [1, 4, 8]. LPA and S1P can also be produced extracellularly by secreted enzymes including ATX and SK1. LPA binds and activates the GPCRs LPA<sub>1-4</sub> [8-10]. Similarly, S1P binds and activates S1P<sub>1-5</sub> [11, 12]. The LPA and S1P receptors are differentially expressed, and they can preferentially activate different heterotrimeric G-proteins to transduce a variety of signals [5, 8, 12]. For example, the activation of G<sub>i</sub>

decreases cAMP concentrations and induces Ras-dependent signaling that leads to the activation of ERK and PI3K and promotes proliferation and survival (Fig. 1.3). The activation of  $G_q$  causes phospholipase C (PLC) activation which produces DAG and  $IP_3$ , which activate the PKCs and promote calcium mobilization (Fig. 1.3). The activation of  $G_{12/13}$  activates Rho and Cdc42 to regulate cell morphology and interactions with the extracellular matrix (Fig. 1.3). LPA signaling also activates PLD, promoting intracellular PA synthesis [9]. Some of the major signaling pathways that are activated by LPA and S1P receptors and the physiological consequences of these signals are depicted in Figure 1.3 [8].

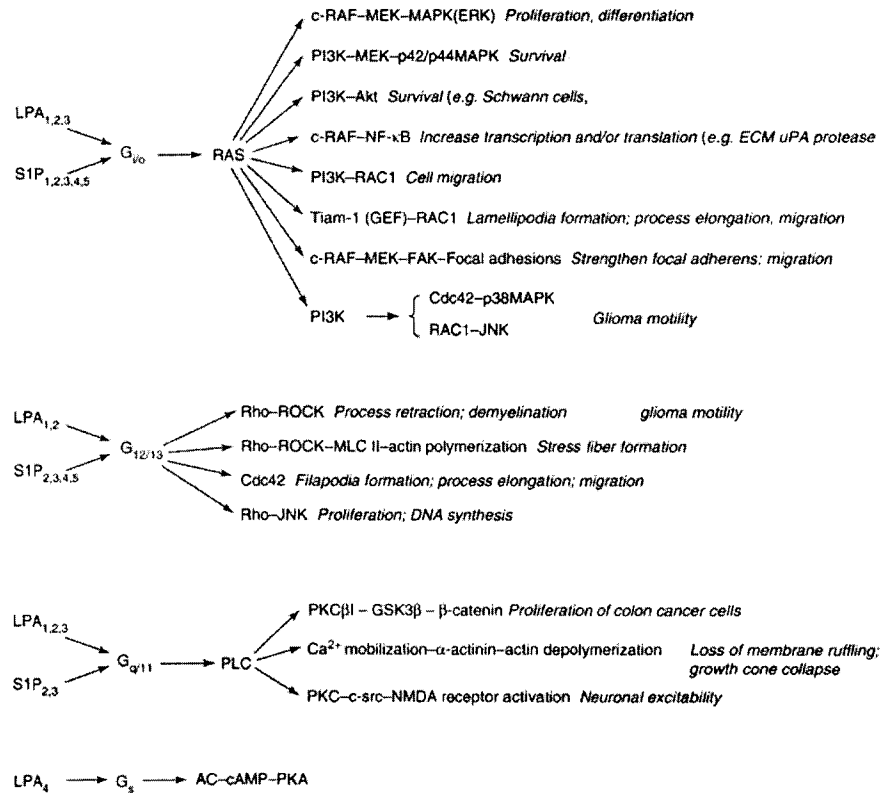


**Figure 1.3. The major signaling pathways activated by LPA and S1P receptors.** Lipid phosphate receptors (LPA1–LPA4 and S1P1–S1P5) activate diverse second messenger pathways. Examples of intracellular pathways reported for LPA and S1P receptor activation and the subsequent effect on cell function are shown (italics). From Gardell et al., 2006.

There is tremendous diversity in the signals that can be transduced by the LPA and S1P receptors, and the signaling can be regulated at several levels. The concentration and species of lipid available to the receptors affects receptor activation since different species of lipids have different affinities for each receptor. Additionally, the relative expression and location of the receptors themselves can be varied to modify signaling. Finally, the downstream pathways activated by the receptors can be modified by other signals. In addition to the signals transduced by the GPCRs themselves, LPA and S1P receptors can transactivate receptor tyrosine kinases (RTKs) including PDGF and EGF [13]. The physiological significance of the extracellular signaling of LPA and S1P through GPCRs has been well documented. Extracellular LPA promotes tissue repair and inflammation, and LPA levels are elevated in the ascites of ovarian cancer patients where LPA signaling promotes tumor growth and protects against chemotherapy [4, 10, 14, 15]. Extracellular S1P signaling is essential for promoting angiogenesis and has also been implicated in immunosuppression [6-8, 16, 17]. Due to the importance of extracellular LPA and S1P signaling in disease and biology, agonists and antagonists for the LPA and S1P receptors with possible therapeutic potential are being developed [8].

In addition to the biologically important extracellular signaling properties of lysophospholipids, emerging evidence suggests that both LPA and S1P have important intracellular signaling functions. S1P that is produced intracellularly can be secreted to activate receptors on the cell in which it was produced or on neighboring cells in an autocrine/paracrine manner [17]. Additionally, S1P acts

intracellularly, since some of its effects are independent of S1P receptors [17]. Intracellular S1P activates ERK promoting mitogenesis, causes  $\text{Ca}^{2+}$  release from intracellular stores to increase actin stress fiber formation, and activates Cox2 expression downstream of ERK, Akt, and NF- $\kappa$ B [18-20]. S1P generally promotes proliferation and survival, whereas its derivatives sphingosine and ceramide generally promote apoptosis and senescence. Therefore, it has been proposed that a “sphingolipid rheostat” exists inside cells, where the relative amounts of S1P and ceramide determine the cell’s fate. In this model, the balance between LPP activities and SK activities would regulate the relative concentrations of these lipids. It has also been proposed that the location of the generation of S1P in the cell affects the signaling by S1P and the resulting cellular outcome [21].

Recently, it has been discovered that in addition to its extracellular signaling role, LPA can signal intracellularly by activating nuclear receptors. The  $\text{LPA}_1$  receptor can be localized to the nucleus [22]. LPA signaling through  $\text{LPA}_1$  at the nuclear membrane regulates the transcription of genes that promote inflammation [23]. LPA is also an agonist for the  $\text{PPAR}\gamma$  receptor on the nuclear membrane and its activation of  $\text{PPAR}\gamma$  transcription may be important in vascular remodeling [24, 25]. This area of research is controversial, since a recent study suggests that LPA is not a  $\text{PPAR}\gamma$  agonist in adipocytes but instead it inhibits  $\text{PPAR}\gamma$  expression and adipogenesis via  $\text{LPA}_1$  receptor activation [26].

1.1.3. *Signaling by PA and CIP* – PA is a bioactive lipid that regulates cell signaling intracellularly, often by directly binding to its targets. PA activates

PI4P 5-kinase, leading to actin polymerization, and recruits Raf1 kinase to the plasma membrane [27]. PA also binds and activates the mammalian target of rapamycin (mTOR), promoting cell survival and proliferation. PA can bind to protein phosphatase-1 $\gamma$  and inhibit its activity [27]. In addition to its role in signaling, PA concentrations regulate membrane curvature, and PA has a role in regulating vesicle formation and fusion in receptor endocytosis and secretion [27, 28]. The sphingolipid analogue of PA, C1P has recently been shown to have a role in signal transduction. C1P can activate cPLA<sub>2</sub>, thereby enhancing the generation of arachidonic acid and increasing eicosanoid production in inflammation [29]. C1P also stimulates proliferation and survival by activating PI3K, and is required for degranulation in mast cells [16]. In addition to its roles in signaling, C1P may play an analogous role to PA in regulating membrane curvature and vesicle movement [4].

1.1.4. *Signaling by DAG and ceramide* – DAG, the product of hydrolysis of PA by the LPPs, is an intracellular signaling molecule. DAG activates the conventional and novel protein kinase C (PKC) isoforms, promoting PKC signaling pathways [30]. Additionally, DAG activates Ras guanyl nucleotide-releasing proteins, and recruits the chimaerins, the Munc13 proteins, and protein kinase D to membrane compartments [30]. Like PA, DAG mediates its signaling effects by directly binding to its targets. There are separate pools of DAG in the cell which are regulated independently, including pools in the nuclear and cytoskeletal compartments [30]. Additionally, DAG derived from PC and PA by PLD and the LPPs may be regulated independently from DAG derived from

phosphoinositides [30]. PKC activation is generally mitogenic, but depending on the pool of DAG that is regulated, and on cell-specific conditions, DAG can promote proliferation or proliferative arrest [30]. Ceramide regulates intracellular signal transduction by activating proteins including PP-1, PP-2A, and the protease cathepsin D [31]. By activating these and other targets, ceramide indirectly promotes apoptosis and cellular senescence in most cells. Ceramide is also involved in the formation of lipid rafts in the plasma membrane, which may serve as signaling scaffolds to recruit and integrate signaling complexes [32].

1.1.5. *General trends in bioactive lipid signaling* – The substrates and products of LPP activities are bioactive lipids with a variety of roles in cell signaling and physiology. Generally, the phosphorylated lipids (LPA, S1P, and C1P) initiate pro-proliferative, pro-survival, and pro-migratory responses, whereas their dephosphorylated products (MAG, SPH, and Cer) tend to promote cell cycle arrest, apoptosis, and senescence. However, the precise effect that any bioactive lipid has on cell signaling depends on a number of factors, such as the location of that lipid pool and the complement of receptors or other downstream targets of the pathway. It is evident that different pools of each bioactive lipid exist inside or outside a cell, and it is possible that more than one independently regulated pool of a lipid may exist in a single organelle. Therefore, the precise timing and localization of the activities that regulate lipid concentrations is an important factor in the outcome of the regulation. Additionally, it is possible that different molecular species of a lipid are regulated differently, or preferentially activate different signaling pathways. The precise regulation of pools of bioactive

lipids is an area of great interest since the regulation of lipids such as LPA, S1P, PA, DAG, Cer, and C1P is important in a number of cell signaling events and physiological processes. By catalyzing the extracellular hydrolysis of LPA and S1P and the intracellular hydrolysis of LPA, S1P, PA, and C1P, the LPPs play a crucial role in regulating bioactive lipid signaling. The LPPs can regulate the relative concentrations of many bioactive phospholipids in both extracellular and intracellular pools. It is clear that bioactive lipids that are regulated by the LPPs are crucial regulators of a variety of cell signaling pathways, and that their regulation has important physiological consequences.

## **1.2. Lipid phosphate phosphatases**

1.2.1. *Introduction* – The lipid phosphate phosphatases are integral membrane proteins that catalyze the dephosphorylation of LPA, S1P, PA, C1P, and diacylglycerol pyrophosphate (DGPP) to MAG, SPH, DAG, Cer, and PA. Their activities are the primary means of degrading these lipid phosphates in many biological systems. The LPPs regulate many aspects of cell signaling by regulating the balance between their phosphorylated substrates and dephosphorylated products.

1.2.2. *LPP family members and related proteins* – The LPPs (formerly PAP2a-c) were originally identified as members of a class of phosphatidate phosphohydrolases (PAPs). There are two types of phosphatidate phosphohydrolase activity that can be distinguished by their subcellular localization, substrate selectivities, divalent cation dependence, and sensitivity to



alkylating agents. PAP1 activity degrades PA selectively and is cytosolic and associated with the cytosolic surface of membranes [33]. This activity is activated by  $Mg^{2+}$  and inhibited by N-ethylmaleimide [34]. Until recently, the gene product responsible for this activity was not identified. New evidence suggests that *PAH1* is responsible for PAP1 activity in *Saccharomyces cerevisiae*. The PAH1 shows homology to the mammalian protein lipin, a protein known for regulating obesity [35]. Heterologous expression of human lipin-1 in *E. Coli* demonstrated that this lipin is a PA phosphatase [36]. Recent work from our laboratory has also shown that lipin-2 and lipin-3 have PA phosphatase activity (K. Reue, J. Dewald, D. Brindley, unpublished). This discovery is likely to be of great significance and provides a basis to study the role of PAP1 activities in lipid metabolism and signaling.

PAP2 (LPP) activities are not specific for PA, but also have activity toward LPA, S1P, PA, C1P, DGPP, and possibly other substrates [34]. To reflect this broader substrate specificity, the enzymes were renamed the lipid phosphate phosphatases (LPPs) [34]. LPP activities are  $Mg^{2+}$ -independent and N-ethylmaleimide-insensitive and are exclusively membrane-associated [34]. There are three mammalian LPP isoforms, named LPP1-3, all of which can hydrolyze all of the above substrates *in vitro*. The LPPs are part of a larger family of phosphatases and phosphotransferases which share a common catalytic motif and have similar transmembrane topology. These include the sphingosine-1-phosphate phosphatases (SPPs) that are specific for S1P, the sphingomyelin synthases (SMS) that catalyze the interconversion of PC and Cer

with DAG and SPM, the type 2 candidate sphingomyelin synthases (CSS2s) whose function is unknown, and the lipid-phosphatase related proteins/ plasticity related genes (LRP/PRGs), that have extended C-termini and lack critical residues in their catalytic domains [37]. A list of the mammalian enzymes in these families and their known substrates is provided in Table 1.1. The LPPs are part of a larger superfamily [38] that also includes nonspecific bacterial acid phosphatases, diacylglycerol pyrophosphate phosphatase, dihydrosphingosine/ phytosphingosine phosphate phosphatases, fungal haloperoxidase, and mammalian glucose-6-phosphatase. This family is characterized by the presence of three conserved domains that include residues which constitute the active site of the enzyme.

**Table 1.1. Mammalian proteins related to the LPPs**

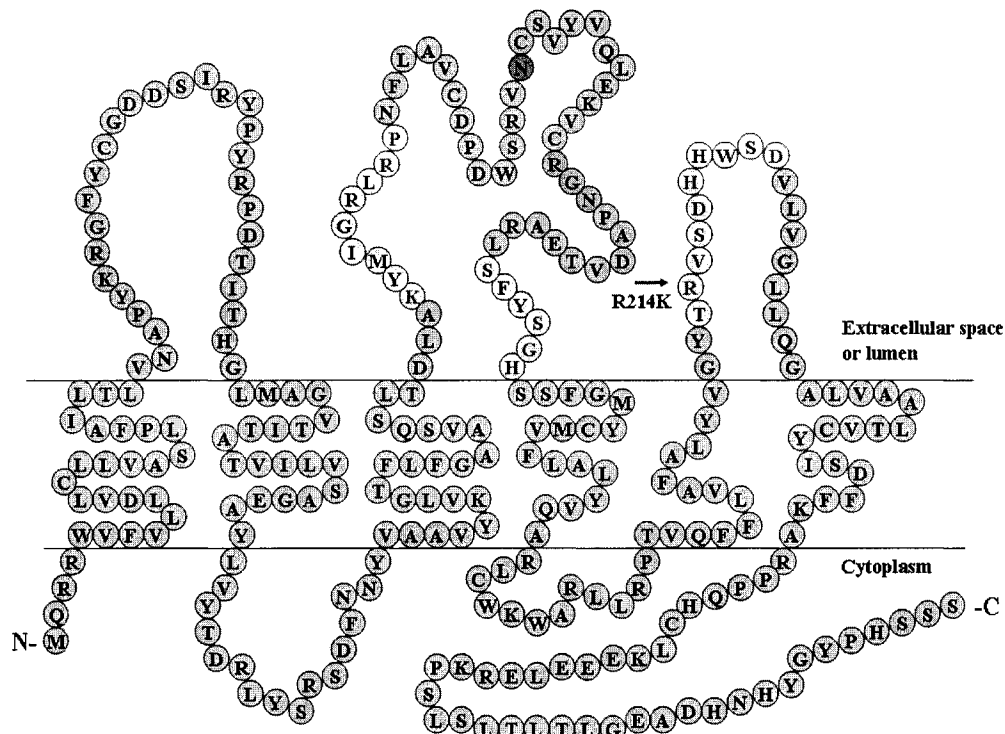
The mammalian proteins related to the LPPs are listed along with their known substrates. The proteins listed all have transmembrane domains and share three conserved motifs that constitute catalytic domains in the active enzymes. The accession numbers for the sequences of the human proteins are listed. For more detailed information see the text. Adapted from Sigal et al, 2005.

Name	Family	Substrates	GenBank accession #
LPP1 (PAP2a)	Lipid phosphate phosphatase	LPA, SIP, PA, C1P, DGPP	NP_795714
LPP2 (PAP2c)	Lipid phosphate phosphatase	LPA, SIP, PA, C1P, DGPP	NP_808211
LPP3 (PAP2b)	Lipid phosphate phosphatase	LPA, SIP, PA, C1P, DGPP	NP_003704
SPP1	Sphingosine phosphate phosphatase	S1P	NP_110418
SPP2	Sphingosine phosphate phosphatase	S1P	NP_689599
LRP1/PRG3	Lipid phosphatase related proteins/ plasticity related genes	? (no intact active site)	AAH22465
LRP2/PRG4	Lipid phosphatase related proteins/ plasticity related genes	? (no intact active site)	AAH09378
LRP3/PRG1	Lipid phosphatase related proteins/ plasticity related genes	? (no intact active site)	NP_997182
LRP4/PRG2	Lipid phosphatase related proteins/ plasticity related genes	? (no intact active site)	NP_982278
SMS1	Sphingomyelin synthases	PC + ceramide	NP_671512
SMS2	Sphingomyelin synthases	PC + ceramide	Q8NHU3
CSS $\alpha$	Type 2 candidate sphingomyelin synthases	?	NP_116117
CSS $\beta$	Type 2 candidate sphingomyelin synthases	? (no intact active site)	BAB55210

1.2.3. *Characteristics of the LPPs* - The LPPs are predicted to have 6 membrane-spanning helices, and are oriented such that the loops that contain their catalytic domain residues face the extracellular side of the plasma membrane, or the lumen of intracellular membranes [37, 39] (Fig. 1.4A). The N- and C-termini are oriented on the cytoplasmic side of the membrane, and a conserved N-

glycosylation site is present on one of the extracellular loops. The reaction mechanism used by the LPPs can be inferred from studies on the related fungal vanadate-dependent chloroperoxidase [40-43]. The proposed reaction mechanism is illustrated in Figure 1.4B [37]. According to this model, the two conserved histidine residues in domains 2 and 3 and the conserved aspartic acid in domain 3 are required for catalysis, and the 2 conserved arginine and conserved lysine and serine residues are required to form hydrogen bonds with the phosphate group (Fig 1.4B). Mutational analysis of LPP1 confirmed that the mutation of either of the two critical histidine residues, or mutations of each of the arginine, lysine, or serine residues that were predicted to be essential for catalysis abolished the activity of the enzyme by more than 95% [44]. The mutation of a conserved active site proline residue also abolished enzyme activity, while the mutation of a glycine residue that was predicted to be involved in hydrogen bonding only partially reduced the activity of LPP1 [44]. Mutations of other non-essential residues in the conserved domains or the mutation of the glycosylation site did not significantly change the activity of LPP1 [44]. The LPPs are located in the plasma membrane, and in intracellular membranes including the ER and in some cases the Golgi apparatus, endosomes, or unidentified cytoplasmic vesicles [39, 45-48].

A)



B)

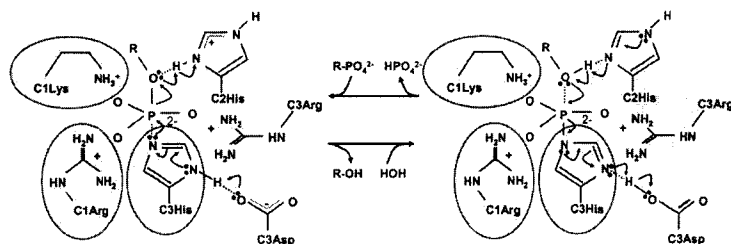


**Figure 1.4. The sequence and predicted structure and catalytic mechanism of LPP2.** Panel A depicts the protein sequence of human LPP2 in the proposed structure of the enzyme. The 6 transmembrane loops are bridged by three extracellular and two intracellular loops. The residues in the three conserved domains (C1-C3) in the phosphatase superfamily are indicated with yellow circles. The residues that are equivalent to those required for catalytic activity in LPP1 are indicated with red letters. The N-glycosylation site is indicated with a green circle, and the residues corresponding to the functional RGD sequence in human LPP3 are indicated in blue circles. The residue that was mutated in this study is indicated with an arrow. The representation is based on a drawing for LPP1 in Zhang et al, 2000. Panel B depicts the predicted catalytic mechanism used by the LPPs. The C3 histidine and aspartic acid residues (in red) promote the formation of a phosphohistidine intermediate in step one as the phosphate group is removed from the lipid substrate. In step two, the C2 histidine (in red) facilitates the hydrolysis of the phosphohistidine intermediate, freeing the active site of the LPP. The C1 lysine and arginine and C3 arginine residues (in blue) form hydrogen bonds with the oxygen molecules of the phosphate moiety that stabilize the transition state of the reaction. The C3 arginine residue depicted is the mutated R214 residue indicated in Panel A. From Sigal et al, 2005.

1.2.4. *Regulation of the LPPs* – The LPPs may be subject to many forms of regulation, including transcriptional regulation, post-translational modifications, oligomerization, and translocation. There is evidence to suggest that the LPPs translocate in response to various stimuli. It has been reported that LPP3 in a complex with SK1 translocates from the cytoplasm to perinuclear compartments following PLD stimulation in HEK293 cells [46]. Additionally, LPP3 activity translocates to caveolin-rich domains following phorbol ester stimulation [49]. A recent study reported that LPP3 translocated from unidentified cytoplasmic compartments to the plasma membrane in response to gonadotropin-releasing hormone [50]. In polarized Madin-Darby canine kidney cells, LPP1 had an exclusively apical localization, whereas LPP3 was primarily localized to the basolateral subdomain [47]. Therefore, the regulated trafficking of the LPPs induced by binding or post-translational modifications may represent a mechanism of LPP regulation. The three LPP isoforms contain many phosphorylation consensus sequences, some of which differ between isoforms (Fig. 1.5). However, there is no direct evidence to demonstrate that the LPPs are actually phosphorylated *in vivo*. The LPPs are glycosylated, but the physiological relevance of this modification is unknown, since the glycosylation of LPP1 did not affect its activity [44]. Therefore, it is unclear whether the LPPs are regulated post-translationally in a physiologically relevant manner.

The LPPs are regulated by transcription in some physiological situations. The mRNA expression of the LPPs is changed in tumor cells [1], and the downregulation of LPP1 expression in ovarian cancer cells permits increased LPA

signaling and has physiological consequences [51]. The transcription of LPP1 is also increased by androgen in prostate cancer cells [52]. LPP3 transcription is increased in HeLa cells by EGF treatment [53], in rat cells during epithelial cell differentiation [54], and by bFGF and VEGF in endothelial cells [55].

It has recently been demonstrated that the LPPs can homodimerize [56]. The *Drosophila* LPP3 ortholog, wunen-1, formed homodimers, but not heterodimers with the closely related wunen-2 or LPP3 proteins [56]. Dimer formation was dependent on the aspartic acid residue in the third conserved domain of wunen-1, and on the last 35 C-terminal amino acids of the protein [56]. In the case of wunen-1, the dimerization of the enzyme did not seem to change its biological function [56]. LPP1 and LPP3 also homodimerized, but did not heterodimerize [56]. The oligomerization of the LPPs was expected since LPP activity had been purified and detected on Western blots at molecular weights higher than the 30-35 kDa predicted from the sequences [57-59]. Therefore, it is likely that oligomerization of the LPPs occurs *in vivo*, although the physiological relevance of this phenomenon is unclear.

1.2.5. *Activities and functions of the LPPs* – By virtue of their plasma membrane localization and orientation, it has been suggested that a major function of the LPPs is to degrade exogenous LPA and S1P and attenuate signaling by their receptors. It has been demonstrated that the ecto activity of LPP1 and LPP3 on the plasma membrane can alter LPA signaling [39, 60-63]. This activity appears to be largely responsible for the some physiological effects of the LPPs, for example in attenuating the migration of ovarian cancer cells [63]. In addition

to attenuating signaling by LPA or S1P receptors, the ecto activity of the LPPs could be involved in promoting the uptake of bioactive lipids. Polar lipids including LPA, S1P, and PA cannot readily enter cells, but their dephosphorylated products can be taken up into cells more rapidly, and then the equivalent phospholipids can be resynthesized intracellularly [62, 64]. Thus, the LPPs could regulate the availability of substrates for lipid kinases and other lipid metabolizing enzymes inside the cell. Indeed, LPPs can control lipid uptake as a result of their ecto activity [62]. In addition to acting at the plasma membrane, LPPs catalyze the hydrolysis of phospholipids intracellularly. The LPPs are found in the same caveolin-rich domains as PLD [48], and can terminate PLD signaling by hydrolysing PA to DAG. This both decreases signaling by PA and activates DAG-responsive PKCs. LPPs can attenuate signaling downstream of GPCRs, possibly by altering the intracellular PA: DAG ratio [45, 65]. Recently, it was discovered that an ER-localized *Drosophila* LPP, *lazarro*, can regulate the PA: DAG ratio downstream of PIP2 signaling in the retina [66]. The regulation of PA levels by *lazarro* regulated the resynthesis of PI from DAG, and the deletion of *lazarro* enhanced light-dependent retinal degeneration [66]. This study demonstrates that by regulating the relative levels of lipid intermediates, the LPPs can regulate signaling by regulating the generation of other lipids species including phosphoinositides. Additionally, recent evidence suggests that LPP2 and LPP3 form complexes with SK1. LPP2, but not LPP3, degraded PA that was produced by PLD in HEK293 cells [46]. It was suggested in the same study that LPP3 has a role in regulating intracellular S1P concentrations [46]. It is also



possible that the LPPs may regulate the intracellular ratios of Cer: C1P and LPA: MAG and affect their intracellular signaling functions. LPA has been recently implicated in nuclear signaling since the LPA<sub>1</sub> receptor translocates to the nucleus [22] and since LPA may be an agonist for the nuclear PPAR $\gamma$  receptor [24]. Although there are no reports of the LPPs localizing to the nucleus, they may regulate the availability of lipids to nuclear pools. The LPPs are localized in the ER which forms a continuous network with the nuclear envelope. The combination of studies to date suggest that both the extracellular and intracellular activities of the LPPs are important in regulating different cellular signaling processes.

1.2.6. *Non-catalytic functions of the LPPs* – In addition to their enzymatic activities, there is some evidence that the LPPs may have non-catalytic functions. The deletion of LPP3 in mice resulted in early embryonic lethality, in part due to unexpected defects in the Wnt signaling pathway [67]. Surprisingly, the ability of LPP3 to negatively regulate the Wnt signaling pathway in cells from LPP3 knockout mice was apparently not dependent on the catalytic activity of the enzyme, since the overexpression of inactive mutant LPP3 mimicked the effects of the overexpression of active LPP3 [67]. An unrelated study demonstrated that human LPP3 modified cell-cell interactions by binding integrins through a RGD motif in one of its extracellular loops [68]. The RGD motif in human LPP3 is not conserved in mouse LPP3 which has an RGE motif. RGE motifs are commonly used as negative controls for integrin binding, and would not be expected to be active. Surprisingly, the RGE motif in mouse LPP3 was recently shown to be

functional for integrin binding, [69]. Rat LPP3 also has an RGE motif, while human LPP1 and LPP2 have RGN sequences in the corresponding locations (Fig. 1.4 and Fig. 1.5). The rat LPP1 and LPP2 sequences have QGN and RGS sequences, respectively (Fig. 1.5). The functional significance of these divergent sequences is not known, but the lack of conservation casts doubt on the importance of these sequences. It is unclear whether the regulation of integrin binding is a conserved function of the LPPs. Nonetheless, the fact that LPP3 appears to have non-catalytic functions raises the possibility that the other LPPs may have non-catalytic functions that could contribute to their overall function *in vivo*.

```

rLPP1 -----MFDKTRLPYVVLVDVICVLLAGLP
rLPP2 -----MERRWVFLLDVLCVLVASLP
rLPP3 MQSYKYDKAIVPESKNGGSPALNNNPRKGGSKRVLLICLDLFCFLFMAALP
      . * : **::*::**.*

rLPP1 FIIILTS-RHTPFQRGVFCTDESIKYPYRE-DTIPYALLGGIVIPFCIIVM
rLPP2 FIIILTL-VNAPYKRGFYCGDDSI RYPYRP-DTITHGLMAGVIITATVVLV
rLPP3 FLIIETSTIKPYRRGFYCNDESIKYPLKVSETINDAVLCAVGIVIAILAI
*:*: *::**:* *:*:** ** : ** .:: .: * :::

rLPP1 ITGETLSVYFNVLHSNSFVSNHYIATIYKAVGAFVLFASASQSLTDIAKY
rLPP2 SSGEAYLVYTDRLYSRSDFN-NYVAAIYKVLGTFVFGAAVSQSLTDLAKY
rLPP3 ITGEFYRIYYLKEKSRSTIQNPYVAALYKQVGCFLFGCAISQSFTDIAKV
: ** : * * . * .. *:::** : * ***. : **::**:*

rLPP1 SIGRLRPHFLAVCNPDWSKINCSDGYIENFVCQGNEQKVREGRLSFYSGH
rLPP2 MIGRLRPSFLAVCDPDWSRVNCSG-YVQVEVCRGSPANVTEARLSFYSGH
rLPP3 SIGRLRPHFLSVCDFDSQINCSEGYIQNYRCRGEDSKVQEARKSFFSGH
***** **:*:**:*::** *:: *:* . : * * . * **::**

rLPP1 SSFSMYCMLFVALYLQARMKGDWARLLRPMLQFGLVALSIYVGLSRVSDY
rLPP2 SSFGMYCMLFLALYVQARLCWKWARLLRPTVQFFLVAFAIYVGYTRVSDN
rLPP3 ASFSMFTMLYLVLVYLQARFTWRGARLLRPLLQFTLLMMAFYTGLSRVSDY
:*:*: **::**:*:**: ***** ** * : : : * . * :****

rLPP1 KHHWSDVLIQGLIQGAVVAILVVLYVTDFFKTTESNKERKEDSHTTLHETT
rLPP2 KHHWSDVLVGLLQGALVACLTVCYVSDFFKSRPPO$CQENEESEKPKPLS
rLPP3 KHHPSDVLAGEAQQALVACCIVFFVSDLFKTKTTL$LPAPAIRREILSPV
*** ** * : **:* ** * : **::**: . . .

rLPP1 NRQSYARNHEP-
rLPP2 LTLTLGDRP---
rLPP3 DIMDRSNHHNMV

```

**Figure 1.5. The sequences of the rat LPPs and their domains and predicted phosphorylation sites.** The protein sequences of the rat LPPs (gi\_47940642, gi\_21245102, and gi\_38197674 for LPP1, LPP2, and LPP3, respectively) were aligned using ClustalW software (<http://www.ebi.ac.uk/clustalw/>). \* indicate sequence identities, : indicate that conserved substitutions are observed, and . indicate that semi-conserved substitutions are observed. Predicted transmembrane domains were determined using a Kyte & Doolittle plot and are indicated with green shading. The regions corresponding to the three conserved catalytic domains are indicated with orange shading. The sequence that corresponds to the RGD sequence in human LPP3 is indicated with yellow shading. The N-glycosylation site is indicated with blue shading. Red circles indicate residues on cytoplasmic loops that are predicted to be phosphorylated as determined by NetPhos1.0/2.0 (<http://www.cbs.dtu.dk/services/NetPhosK/>). See text for details.

1.2.7. *Isoform specificity of the LPPs* – It is clear from many *in vitro* and *in vivo* studies that the three LPP isoforms have specific, non-redundant roles in regulating cell signaling and physiology. Transgenic mice that overexpress LPP1 have decreased birth weight, sparse curly hair, and defective spermatogenesis causing male infertility [70]. The unexpected effects of LPP1 overexpression in mice imply that LPP1 has a role in spermatogenesis, hair development, liver function, and prenatal development in mice [70]. Unfortunately, these effects could not be directly correlated with the activity of LPP1. A knockout model of LPP1 has not yet been produced. The deletion of LPP3 in mice resulted in early embryonic lethality [67]. LPP3 knockout mouse embryos were unable to form a functional chorio-allantoic placenta and yolk sac vasculature. Additionally, LPP3 knockout mice showed defects in axis formation, characteristic of defects in the Wnt signaling pathway [67]. Once again, the precise role of LPP3 activity or non-catalytic functions in producing these defects was unclear. LPP2 knockout mice are viable and overtly normal [71]. Therefore the LPPs have distinct and possibly tissue-specific biological roles in mice. In *Drosophila*, the LPP orthologs *wunen-1* and *wunen-2* act as repellent factors by modifying the concentration of an undetermined lipid factor, and *wunen-1/2* activity is essential for embryonic germ cell migration [72]. LPP3 can substitute for *wunen-1* and *wunen-2* to direct the correct migration of germ cells in *Drosophila*, but LPP1 cannot [73]. This clearly demonstrates that LPP1 and LPP3 function differently *in vivo*. The basis of this difference is unknown. In addition to having different functions in the regulation of physiology and cell signaling, several studies

indicate that the different LPPs have different substrate preferences [45, 60, 74, 75]. Since the crucial active site residues in the three isoforms are conserved, the reasons for these differences are unclear. Furthermore, there is little evidence of what the actual *in vivo* substrate preferences of the isoforms are. The three LPP isoforms have high sequence homology in their transmembrane and catalytic domains (Fig. 1.5). The greatest source of variation between the isoforms is in their N- and C-terminal tails. The different isoforms have different combinations of phosphorylation consensus sequences on their cytoplasmic loops, which provides a possible mechanism for how they could be specifically regulated (Fig. 1.5). Rat LPP1 has possible consensus sequences for phosphorylation by PKC, PKA, CKI, and CKII. Rat LPP2 has possible consensus sequences for phosphorylation by PKA, RSK, and CKII. Rat LPP3 has possible consensus sequences for phosphorylation by PKC, PKA, p38 MAPK, GSK3, and CDK5. Rat LPP1 and LPP2 also have consensus sequences for tyrosine phosphorylation. However, as mentioned previously, there is no evidence that any of the LPPs are phosphorylated *in vivo*. The differences in substrate preferences could be a result of the subcellular distribution of the LPPs, or their differential binding to other proteins or membrane domains. Alternatively, it could be a result of uncharacterized differences in the sequences of the enzymes that confer specificity, since even in micelles, the enzymes do not show the same preference for all substrates (see Chapter 3). While LPP1 and LPP3 are present in cells from nearly all organs and tissues, LPP2 has a much more limited expression profile (Table 1.2) [37, 48, 53, 71, 76]. Even in tissues in which all three isoforms are

expressed, LPP2 is often the least abundant transcript. LPP2 is absent from some tissues where LPP activities are presumed to be important, such as in the vascular system (Table 1.2). The tissue distribution pattern of the LPPs suggests that LPP2 is likely to have a very different function from LPP1 and LPP3. This is further supported by mRNA expression data from cancer cells (Table 1.2) [1]. In tumor types where LPP1 and LPP3 expression are decreased (breast, colon, gastric), LPP2 expression is increased (Table 1.2). Conversely, in prostate and kidney tumors, where LPP1 and LPP3 expression are increased, LPP2 expression is decreased or unchanged (Table 1.2). This suggests that LPP2 could possibly have an different function to LPP1 and LPP3 in tumor progression. Additionally, while it has been conclusively demonstrated that ecto activities of LPP1 and LPP3 alter cell signaling, biological consequences of LPP2 ecto activity have not been described. In fact, there is no conclusive evidence to suggest that LPP2 is a functional ecto enzyme, and results presented in this thesis indicate that it is not. Therefore, LPP2 is likely to have a specific role in the regulation of signaling and physiology.

**Table 1.2. The expression of the LPPs in adult human organs and tumors**

The abundance of EST transcripts corresponding to each gene in human adult organs is given as transcripts per million. The data is compiled from information available online at <http://www.ncbi.nlm.nih.gov/UniGene/>. Adapted from Sigal et al, 2005. The gene expression profiles for each gene in human tumors are expressed relative to the average expression in normal epithelial cells and are from microarray hybridization experiments. The sample sizes varied between 6 and 28 for tumor cells. A sample size of 36 was used for control epithelial tissues. The information is available online at <http://gnf.org/cancer/epican>. Adapted from Umezu-Goto et al, 2004.

	LPP1	LPP2	LPP3
<b>Expression of transcripts in adult human organs and tissues</b>			
Bladder	191	0	47
Bone marrow	27	0	136
Brain	107	30	166
Cervix	72	48	24
Colon	64	347	58
Eye	80	43	222
Heart	161	0	287
Kidney	172	44	202
Liver	22	7	197
Lung	67	56	106
Lymph node	39	0	724
Mammary gland	132	24	490
Ovary	63	116	21
Muscle	119	0	82
Pancreas	74	211	161
Nervous system (peripheral)	318	0	238
Placenta	108	4	535
Prostate	483	38	576
Skin	30	12	6
Testes	60	7	68
Uterus	196	156	214
Vascular system	154	0	656
<b>mRNA expression in human tumors</b>			
Ovarian	0.2 ± 0.1 ↓	1.1 ± 1.2 ≈	1.0 ± 1.1 ≈
Breast	0.4 ± 0.1 ↓	2.8 ± 1.5 ↑	0.6 ± 0.5 ↓
Colon	0.3 ± 0.1 ↓	3.1 ± 1.0 ↑	0.5 ± 0.4 ↓
Prostate	6.0 ± 2.2 ↑	1.0 ± 1.0 ≈	2.9 ± 1.2 ↑
Kidney	2.6 ± 1.3 ↑	0.4 ± 0.8 ↓	4.7 ± 2.6 ↑
Pancreas	0.7 ± 0.2 ↓	3.7 ± 1.3 ↑	0.9 ± 0.4 ≈
Gastric	0.4 ± 0.4 ↓	2.1 ± 1.8 ↑	0.2 ± 0.4 ↓
Lung	0.5 ± 0.3 ↓	2.2 ± 1.0 ↑	1.1 ± 0.4 ≈
<b>Overall trend</b>	↓	↑	≈

1.2.8. *Characteristics of the LPP2 isoform* – LPP2 is the least uniformly expressed LPP in human tissues, showing high expression in the colon, ovary, pancreas, and uterus and lower expression in the brain, cervix, eye, kidney, lung, mammary gland, prostate, skin, and testes (Table 1.2). The human LPP2 sequence has 54% identity with human LPP1 and 43% identity with human LPP3 [60]. Human LPP2 is 93% and 91% identical to mouse and rat LPP2, respectively (public domain, NCBI). There are two other alternative splice variants of LPP2, one with a longer N-terminus and one with a shorter N-terminus, but it is unknown whether either is actually expressed (public domain, NCBI). This study will discuss only the first splice variant, a 288 amino acid protein in the human form, with a predicted molecular mass of 32.6 kDa and the sequence represented in Figure 2.4 [60]. LPP2 is the least studied of the LPP isoforms, and its role in cell signaling and physiology was, prior to this study, relatively unknown. Since LPP2 knockout mice are viable and fertile with no obvious abnormalities, it can be concluded that LPP2 is not essential for embryonic or post-natal development in mice. There is a report suggesting that LPP2 knockout mice may have deficiencies in retina development or degeneration, and that LPP2 interacted with the metabotropic glutamate receptor-6 to mediate the migration of ON bipolar cells [77]. This is particularly interesting in light of the recent studies in *Drosophila* showing that the deletion of an LPP can cause retinal degeneration. However these results have not been pursued any further. Therefore, although the LPP2 knockout mice have no obvious phenotypic abnormalities, there may be tissue-specific or subtle phenotypes associated with the animals. Comprehensive



studies with these animals or cells derived from them have not been performed. *In vitro*, LPP2 has been shown to attenuate signaling by GPCR agonists including LPA and thrombin by altering the intracellular PA: DAG ratio in HEK293 cells [45]. Furthermore, the intracellular activity of LPP2 on PA was implicated in sequestering SK1 in the cytosol and rendering cells hypersensitive to apoptosis [46]. These studies were performed in HEK293 cells that had low endogenous expression of the LPPs and employed very high levels of overexpression [45]. In these cells, endogenous LPP2 protein was undetectable so the levels of protein overexpression were not determined, but LPP2 overexpression resulted in enormous 21-, 74-, and 271-fold increases in activity toward PA, LPA, and S1P, respectively [45]. With the exception of these studies, very little information was available about the possible functions of LPP2 in cell signaling prior to the results presented in this thesis. Additionally, our results provide the first information about the function of endogenous LPP2, since previous studies employed only overexpression techniques. Based on the restricted tissue expression of LPP2 and its unique expression profile in tumor cells, it is likely that LPP2 has an isoform-specific function in the regulation of cell signaling that has been unexplored. This thesis focuses on exploring the functions of LPP2 in fibroblasts, employing both overexpression and knock-down techniques in an attempt to examine the endogenous roles of LPP2 activity.

### 1.3. Cell cycle regulation

1.3.1. *Overview of the cell cycle* – Organisms rely on mitotic cell divisions to produce cells for growth and differentiation. The series of stages that a cell passes through from one cell division to the next is called the cell cycle.

Following cell division, continuously dividing cells enter GAP1 ( $G_1$ ) phase in which the cells prepare themselves for DNA replication in response to mitogens. The DNA is then replicated in synthesis (S) phase, which is followed by GAP2 ( $G_2$ ) phase in which the cells prepare for mitosis. In mitosis (M-phase) the cells divide into two daughter cells. Mitosis is composed of a series of stages in which paired chromosomes line up and separate, and the DNA and cytoplasmic content of the cell is divided into two cells in an orderly fashion. When mitosis is complete, the two new cells either continue dividing and progress into  $G_1$ -phase, or exit the cell cycle and enter quiescence (reversible cell cycle arrest), also known as  $G_0$ -phase.

The progression of cells through the cell cycle is regulated by many proteins, including a subset of the cyclin-dependent kinases (CDKs) whose activities drive cell cycle progression, and their activating binding partners, the cyclins. Inhibitory mechanisms ensure that cells in unfavorable growth conditions or harboring damage do not continue cycling. Cell cycling is stopped in response to unfavorable stimuli at two main checkpoints. These occur at the transition between  $G_1$  and S-phases and at the transition between  $G_2$  and M-phases. Dysregulation of either of the cell cycle checkpoints can lead to aberrant

cell proliferation or the proliferation of damaged cells which can result in the development of many pathologies including cancer.

1.3.2. *The traditional model of mammalian cell cycle regulation* – For many years *in vitro* studies have contributed to the development of a model of the regulation of cell cycle progression. This model involves the sequential action of CDK-cyclin complexes acting on specific substrates to promote cell cycle progression. Recently, several *in vitro* observations and the phenotypes resulting from the genetic deletion of cell cycle regulatory genes in mice have cast doubt on the validity of this model. Despite recent developments, the mechanisms traditionally associated with cell cycle regulation are likely to be important processes that affect cell cycle progression in certain situations, even if they are not all explicitly necessary for normal proliferation *in vivo*. The following discussion outlines the traditional model of cell cycle regulation, and then introduces the new studies that question aspects of this model.

1.3.2.1. *Cyclins and cyclin-dependent kinases* – Cyclins were originally discovered and named on the basis that their expression cycled synchronously with the cell cycle. All proteins that share sequence homology with the originally identified A- and B-type cyclins are now termed cyclins. These proteins share a region of homology known as the cyclin box that forms an  $\alpha$ -helical fold composed of five helices that is important for binding to the cyclin-dependent kinases [78]. The cyclins whose expression fluctuates with the cell cycle contribute to cell cycle progression by binding to and activating a family of serine/threonine protein kinases known as the cyclin-dependent kinases (CDKs).

Different cyclins have different binding partners and are expressed at different intervals during the cell cycle (reviewed in [79]). The cyclins that have been traditionally considered important for cell cycle progression are as follows: the D-type cyclins are synthesized in early G<sub>1</sub>-phase and destroyed before S-phase and activate CDK4 and CDK6; the E-type cyclins are synthesized in mid G<sub>1</sub>-phase and destroyed at the beginning of S-phase and activate CDK2; the A-type cyclins are synthesized in late G<sub>1</sub>-phase and destroyed in metaphase in mitosis and activate CDK2 and CDK1; the B-type cyclins are synthesized in S-phase and destroyed at the metaphase/anaphase transition in mitosis and activate CDK1 (Table 1.3). Cyclins are primarily regulated by transcription and degradation. Some cyclins are synthesized in response to mitogens (for example, the D-type cyclins), and others are synthesized subsequent to the activity of other cyclin-dependent kinases (for example, cyclins E and A). Many cyclins are ubiquitinated by various signal-activated E3 ubiquitin ligases and are subsequently rapidly degraded by the proteasome [79, 80]. Cyclins can also be regulated by sequestration from their binding partners and by translocation in and out of the nucleus [81].

The cyclin-dependent kinases are a family of 11 serine/threonine protein kinases that are activated by cyclin partners [82] (Table 1.3). There are also 9 proteins that are related to the CDKs but have no known cyclin activators [82]. The activities of some CDKs are thought to be important in promoting cell cycle progression as follows: CDK4 and CDK6 activities promote progression through G<sub>1</sub>-phase; CDK2 activity promotes progression from G<sub>1</sub> to S-phase and through

S-phase; CDK1 activity promotes progression from G<sub>2</sub> to M-phase and through mitosis. A list of the known cyclin-dependent kinases and their binding partners and selected substrates is provided in Table 1.3.

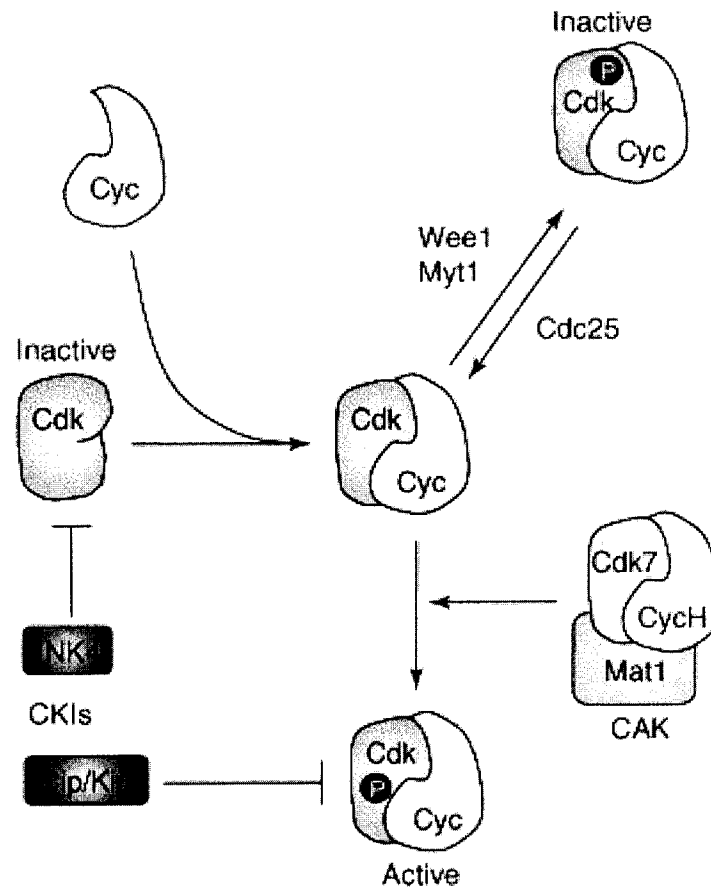
**Table 1.3. The mammalian cyclin-dependent kinases**

The cyclin-dependent kinases, their known cyclin binding partners, a selected list of their substrates, and their known cell cycle functions are listed. Adopted from Malumbres and Barbacid, 2005.

Symbol	Cyclin Partner	Substrates	Cell cycle function
CDK1	A1, A2, B1, B2 (E, B3)	APC, CDC25A, Histone H1, Rb, MCM2, p53, Separase, many others	G <sub>2</sub> -M progression
CDK2	A1, A2, E1, E2 (D1, D2, B1, B3)	Rb, p107, p27 <sup>Kip1</sup> , p21 <sup>Cip1</sup> , cdc6, ctd1, cdc7, CDK7, MCM2, MCM4, p53, BRCA1, B-myb, Marcks, others	G <sub>1</sub> -S progression
CDK3	E1, E2, A1, A2, C	Cables1	G <sub>0</sub> -G <sub>1</sub> -S progression
CDK4	D1, D2, D3	Rb, p130, p107, Marcks, Cdt1, Smad3	G <sub>1</sub> -S progression
CDK5	p35, p39 (D-, E-, and G-type)	Cables, Munc18, p53, Pctaire1, Stat3, mSds3, PP1-I1, others	None (senescence, neuronal functions)
CDK6	D1, D2, D3	Rb, p130, p107	G <sub>1</sub> -S progression
CDK7	H	CDK1-6, p53, RAR $\gamma$ , RNA pol II	CAK (transcription)
CDK8	C (K)	RNA pol II	None (transcription)
CDK9	T1, T2, K	Rb, RNA pol II	None (transcription)
CDK10	unknown	unknown	G <sub>2</sub> -M progression
CDK11	L1, L2, D	Cyclin L, 9G8	M-phase progression

The activity of cyclin-dependent kinases is regulated on several levels (Fig. 1.5). In order to be active, CDKs must bind to their cyclin partner and must be phosphorylated on the T-loop by CDK activating kinase (CAK) which is a complex composed of CDK7, cyclin H, and Mat1 [83]. CDK-cyclin complexes are inhibited by the phosphorylation of adjacent residues by the kinases Wee1 and Myt1, and activated by the dephosphorylation of these residues by the CDC25 phosphatases [84] (Fig. 1.5). Additionally, there are two families of proteins that are inhibitors of CDK activity. The Cip/Kip family includes the proteins p21<sup>Cip1</sup> and p27<sup>Kip1</sup> [85]. These proteins bind to CDK-cyclin complexes to inhibit their

kinase activity (Fig. 1.5). The INK4 family of proteins that includes p16<sup>INK4a</sup> bind specifically to monomeric CDK4 and CDK6 and prevent their association with the D-type cyclins [85] (Fig. 1.5).



T/BS

**Figure 1.6. Basic regulatory mechanisms of cell-cycle CDKs.** These CDKs must bind to their cyclin partners to activate their kinase activity. Some CDKs (CDK4 and CDK6) are inhibited by direct binding of the INK4 family of CKIs. By contrast, Cip and Kip inhibitors block kinase activity by forming inactive trimeric complexes (CDK2–Cyclin E, CDK2–Cyclin A, CDK1–Cyclin A, CDK1–Cyclin B, and possibly CDK4–Cyclin D and CDK6–Cyclin D). CDK–cyclin complexes can be activated by phosphorylation in their conserved T-loop of the CDK subunit by CAK. By contrast, CDK–cyclin complexes can be negatively regulated by phosphorylation in adjacent threonine or tyrosine residues by the dual-specificity kinases Wee1 and Myt1. These inhibitory phosphorylations can be reversed by the dual-specificity CDC25 phosphatases that act as positive regulators of CDK–cyclin activity. From Malumbres and Barbacid, 2005.

1.3.2.2. *G<sub>1</sub> to S-phase progression* – The induction of cell cycle progression requires the transcription of genes that are regulated by the E2F family of transcription factors [86]. Proteins in the E2F family form heterodimers with DP proteins, and these complexes bind regions of DNA [87-89]. E2F1-3 are considered activators and can transactivate target genes to promote their expression [90]. E2F4-5 are considered transcriptional repressors [90]. The pocket proteins retinoblastoma (Rb), p130, and p107 can bind to the E2F proteins and inhibit their transactivating activity [90]. E2F1-3 preferentially bind to Rb while E2F4 predominantly binds p107 and p130 and E2F5 mainly binds to p130 [91]. In normal proliferating cells, mitogens stimulate cell cycle progression by increasing the functional pool of the D-type cyclins. Mitogens stimulate the transcription of cyclins D1-3, in addition to promoting their stability and increasing their import into the nucleus [79] (Fig. 1.6). The D-type cyclins bind to CDK4 and CDK6, and the activated CDK4/6-cyclin D complexes in the nucleus phosphorylate Rb [79] (Fig. 1.6). The phosphorylation of Rb releases Rb from the activating E2Fs and allows the E2Fs to transactivate target gene expression. Among the genes activated by E2F are cyclin E and cyclin A (Fig. 1.6). CDK4/6-cyclin D complexes also bind to and sequester the cell cycle inhibitor p27<sup>Kip1</sup>, thereby out competing CDK2-cyclin E/A complexes for the inhibitor and permitting subsequent CDK2 activities [92].

The newly synthesized E-type cyclins bind to CDK2 and the active CDK2-cyclin E complexes phosphorylate Rb on distinct residues from those phosphorylated by CDK4/6 [79] (Fig. 1.6). CDK2-cyclin E also phosphorylates

unbound p27<sup>Kip1</sup> on Thr187 which provides a recognition motif for an E3 ubiquitin ligase and results in the rapid degradation of p27<sup>Kip1</sup> by the proteasome [79] (Fig. 1.6). The inhibition of Rb and p27<sup>Kip1</sup> by CDK2-cyclin E alleviates the cells' reliance on continued mitogenic signaling. Once cells have passed this "restriction point" they will continue on to DNA replication even in the absence of mitogens [79]. CDK2-cyclin E complexes also phosphorylate substrates involved in DNA replication and cell duplication. For example, the phosphorylation of the Cdc6 and Ctd1 proteins by CDK2-cyclin E facilitates the loading of the MCM chromosome maintenance proteins onto origins of replication in cells that re-enter the cell cycle following quiescence [82] (Fig. 1.6) This is an essential step in promoting DNA replication, since it "licences" the origins for replication.

Cyclin E is rapidly degraded in early S-phase [91]. CDK2 and GSK3 $\beta$  phosphorylate cyclin E, targeting it for ubiquitination and subsequent proteasomal destruction [93]. As cyclin E levels decline, CDK2 binds predominantly to cyclin A2 (Fig. 1.6). CDK2-cyclin A2 complexes phosphorylate substrates that start DNA replication from the pre-assembled replication initiation complexes [94-96] (Fig. 1.6). CDK2-cyclin A complexes also inhibit the assembly of new replication complexes to prevent the re-replication of DNA [96]. It has been suggested that cyclin A associated kinase activity can be rate-limiting for progression from G<sub>1</sub> to S-phase [97]. A model of the sequence of events resulting in G<sub>1</sub> to S-phase progression is given in Figure 1.6.



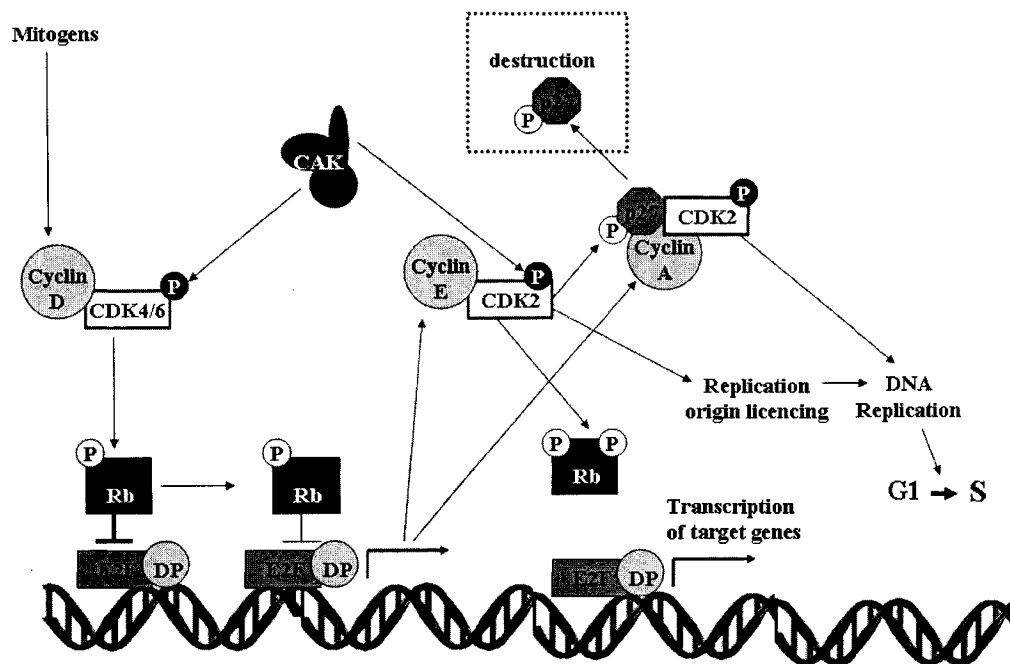


**Figure 1.7. A simplified model of G<sub>1</sub> to S-phase progression.** Mitogens increase the transcription of cyclin D. The binding of CDK4/6 to the D-type cyclins and phosphorylation on the T-loop by CAK activate CDK4/6. The active CDK4/6-cyclin D complex phosphorylates Rb, relieving its inhibition of E2F transactivation. E2F target genes are synthesized including cyclin E and cyclin A. CDK2 binds to cyclin E and is phosphorylated by CAK. The active complex further phosphorylates Rb, causing its dissociation from E2F and activating further transcription. CDK2-cyclin E also phosphorylates the inhibitor p27<sup>Kip1</sup>, promoting its degradation by the proteasome. CDK2-cyclin E facilitates the loading of MCM proteins onto replication origins, licensing the origins for replication. Cyclin E levels decline and CDK2-cyclin A complexes become abundant. CDK2-cyclin A complexes inhibit origin licensing to prevent re-replication, and then initiate DNA replication from pre-assembled licensed origins. Cells progress into S-phase and replicate their DNA.

1.3.2.3. *G<sub>2</sub> to M-phase progression* – Once the DNA has been replicated, cells promote CDK1 activity to progress into mitosis and divide into two daughter cells. The progression from G<sub>2</sub> to M-phase and through mitosis is dependent on the activity of the CDK1-cyclin B1 complexes that phosphorylate more than 70 substrates and regulate processes such as centrosome separation, chromosomal condensation, fragmentation of the Golgi, and breakdown of the nuclear lamina [82]. Exit from mitosis requires the inactivation of CDK1-cyclin

B, which is mediated by the ubiquitination and proteosomal degradation of the B-type cyclins by the anaphase promoting complex [82]. The activity of CDK1-cyclin B complexes is regulated in several ways. First, the expression of cyclin B is highly upregulated prior to the G<sub>2</sub>/M transition [80] (Fig. 1.7). CDK1-cyclin B complexes must also translocate to the nucleus in order to promote mitotic progression. The 14-3-3 protein sequesters cyclin B, CDK1-cyclin B complexes, and CDC25C in the cytoplasm. Polo-like kinase-1 (Plk-1) phosphorylates cyclin B and CDC25C, increasing their nuclear import just prior to mitosis [80, 81] (Fig. 1.7). CDK1 is inhibited prior to the G<sub>2</sub>/M transition by phosphorylation on Thr14 and Tyr15 that is mediated by the dual-specificity kinases Wee1 and Myt1 [81] (Fig. 1.7). CDC25C dephosphorylates these residues to activate CDK1-cyclin B and promote G<sub>2</sub> to M-phase progression [80] (Fig. 1.7). The CDC25C phosphatase is activated by CDK1 in a positive feedback loop to create the high transient levels of CDK1-cyclin B activity that are required to promote progression into mitosis (Fig. 1.7). It has recently been suggested that CDK2-cyclin A complexes activate CDC25 proteins, thus promoting mitosis [98]. The exact role of CDK1-cyclin A complexes in mitotic progression is obscure, though some studies suggest that this activity is important (reviewed in [80]). A model of the mechanisms involved in promoting G<sub>2</sub> to M-phase progression is provided in Figure 1.7.

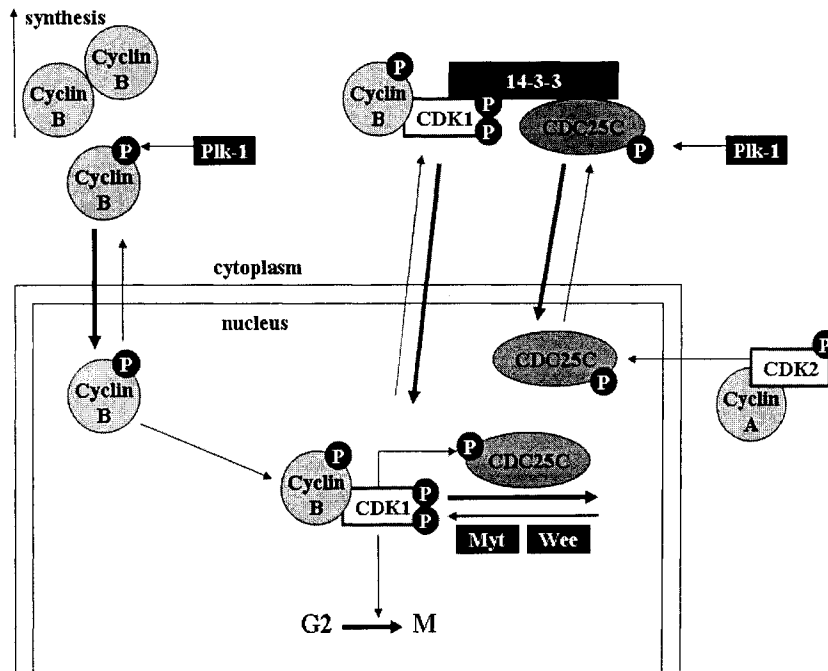


**Figure 1.8. A simplified model of G<sub>2</sub> to M-phase progression.** Cyclin B is synthesized leading to an increase in its concentration. Cyclin B binds to CDK1. CDK1 is phosphorylated by Wee and Myt on Thr14/Tyr15, inactivating it. The complex is sequestered in the cytoplasm by binding to 14-3-3. Plk-1 phosphorylates cyclin B, leading to an increase in its nuclear import relative to its nuclear export, and the complex translocates to the nucleus. CDC25C is sequestered to the cytoplasm by binding to 14-3-3. Plk-1 phosphorylates CDC25C, increasing its nuclear import. CDK2-cyclin A complexes activate CDC25C. In the nucleus, CDC25C dephosphorylates CDK1 on Thr14/Tyr15, activating the enzyme. Active CDK1 phosphorylates CDC25C, increasing its activity in a positive feedback loop. CDK1-cyclin B complexes phosphorylate >70 substrates involved in progression into and through mitosis. High levels of CDK1-cyclin B activity promote progression from G<sub>2</sub> to M-phase.

1.3.3. *The implications of recent in vivo studies and new theories about cell cycle regulation* – Recently, many members of the CDK and cyclin families have been deleted in mice without severely impacting fetal development. This had raised many doubts about the mechanisms thought to be essential for cell cycle progression, since cell cycle progression occurs *in vivo* in the absence of genes that were previously considered essential (Table 1.4). The knockout of any single member of the D-type or E-type cyclins produced viable animals whose cells exhibited relatively normal cell cycle progression [99-104] (Table 1.4). A

knockout of all three D-type cyclins resulted in very late embryonic lethality (E16.5 to just after birth) and the mice died of anemia as a result of poor proliferation of hematopoietic cells [105] (Table 1.4). However, loss of all three of the D-type cyclins did not result in severe proliferative defects in all cells, and embryonic fibroblasts (MEFs) from the cyclin D1/2/3 knockout mice exited quiescence in response to mitogens *in vitro* [105]. Similarly, mice in which both CDK4 and CDK6 were knocked out died at E14.5 and onward as a result of hematopoietic proliferative defects, but were still able to develop normally until this stage [106] (Table 1.4). MEFs from these animals also entered S-phase after starvation in response to mitogens. These results demonstrated that the D-type cyclins and CDK4/6 kinases are not essential for cell cycle progression or exit from quiescence in response to mitogens *in vivo*. The compensatory activity of CDK2-cyclin E may have been an important factor in allowing cells from these animals to cycle and enter S-phase [79].

Knocking out both E-type cyclins in mice resulted in embryonic lethality at E11.5 due to defective endoduplication in megakaryocytes [103, 107] (Table 1.4). However, mice lacking E-type cyclins still developed to mid-gestation and did not have major cell cycle defects. MEFs from these embryos were defective in their ability to enter S-phase after quiescence due to an inability to load MCM proteins onto replication origins (Table 1.4). However, if not forced into quiescence, these cells were able to cycle and grow with only a minor decrease in their proliferation rate. Most surprisingly, mice in which CDK2 was knocked out were viable and relatively normal and lived for 2 years [108, 109] (Table 1.4).

CDK2 knockout mice were sterile, indicating that CDK2 has an essential role in meiosis, but not mitosis (Table 1.4). Although they senesced prematurely, fibroblasts from CDK2 knockout mice had no cell cycle defects. Surprisingly, the deletion of CDK2 did not impair the loading of MCM proteins onto origins of replication, indicating that this essential process can be mediated by cyclin E independently of CDK2 activity. Recent evidence suggests that cyclin E can bind and activate CDK1, and that CDK1-cyclin E activity can compensate for CDK2-cyclin E activity and initiate S-phase entry in the absence of CDK2 [110]. The fact that CDK2 appears to be dispensable for normal cell cycle progression *in vivo*, brings many aspects of our understanding of cell cycle progression into question. A summary of the consequences of knocking down various CDKs and cyclins in mice is given in Table 1.4.

**Table 1.4. Mouse knockouts of CDKs and cyclins**

The major phenotypes that result from the deletion of cell cycle regulating genes in mice are summarized. The cell cycle phenotypes of embryonic fibroblasts derived from the knockout animals are also summarized. See the text for more detailed discussion. Adopted from Malumbres and Barbacid, 2005, and Sherr and Roberts, 2006.

<b>Disrupted gene(s)</b>	<b>Survival</b>	<b><i>In vivo</i> pathology</b>	<b><i>In vitro</i> phenotype in MEFs</b>
CDK1	Lethal		
CDK2	Viable	Male and female sterility	Early senescence, no cell cycle defects in mitosis, defective meiosis
CDK4	Viable	Small size, sterility, abnormal $\beta$ -islet development	Decreased ability to exit G <sub>0</sub> , high p21 <sup>Cip1</sup>
CDK6	Viable	Defective erythroid lineage	T-lymphocytes have slow S-phase entry
CDK4/6	Lethal E14.5	Hematopoiesis defects	Delayed cell cycle
CDK11	Lethal E3.5	Mitotic defects in blastocyst	Proliferative defects
Cyclin D1	Viable	Small size, neuropathy, retinopathy	
Cyclin D2	Viable	Female sterility, abnormal cerebellar development	B-lymphocytes proliferate poorly
Cyclin D3	Viable	Hypoplastic thymus, T-cell maturation defects	
Cyclin D1-3	Lethal E16.5	Severe hematopoietic deficits	Reduced susceptibility to transformation
Cyclin E1	Viable	Normal	
Cyclin E2	Viable	Male infertility	
Cyclin E1-2	Lethal E11.5	Endoreduplication defects in megakaryocytes, cardiac abnormalities	Cannot exit G <sub>0</sub> due to failure to load MCM proteins on replication origins, slow growth and senescence
Cyclin A1	Viable	Male sterility	
Cyclin A2	Lethal		
Cyclin B1	Lethal		
Cyclin B2	Viable	No significant defects	

Recent studies also suggest that the phosphorylation of Rb and transactivation by E2F activators may not be essential for cell cycle progression. Endogenous Rb is rarely found on E2F target promoters during normal cell cycle progression (reviewed in [91]). The predominant complex found in G<sub>1</sub>-phase of the cell cycle is E2F4 bound to p107 or p130. Furthermore, while some evidence suggests that the E2Fs serve an important role in repressing transcription in early

G<sub>1</sub>-phase, and that the repression must be alleviated for cell cycle progression, the transactivation of target genes by E2F proteins may be dispensable for their role in regulating cell cycle progression [91].

The abundance of new and surprising information about cell cycle regulation *in vivo* has cast doubt on whether the traditional mechanisms thought to be essential for cell cycle regulation are essential. It is evident that significant redundancy exists in the processes that regulate cell cycle progression, and that the loss of one or more regulators can often be compensated for by related factors. The new studies have also raised questions about the importance of proteins such as CDK11, whose deletion results in early embryonic lethality due to cell cycle defects. There is speculation that mammals could, like yeast, have only one essential cyclin-dependent kinase activity, that of CDK1. Even if many of the regulatory pathways that have been described are not essential for cell cycle progression, it is likely that they are important in providing a complex regulatory system that allows cell cycle progression to be altered and fine tuned in response to a variety of diverse stimuli. As further studies revisit the role of various pathways involved in promoting cell cycle progression, we will understand more about why certain non-essential mechanisms exist, and how cells are able to proliferate without them.

1.3.4. *DNA damage pathways and checkpoint regulation* – When cells encounter stresses that could compromise the correct replication of their DNA or their correct division, they activate a stress response pathway to halt cell cycle progression. The DNA damage response is activated by various types of DNA

damage, and by events that occur as a result of aberrant cycling, including low levels of ribonucleoside triphosphate pools that often occur as a result of a shortened G<sub>1</sub>-phase. Cellular stresses cause the activation of phosphatases or acetylases that post-translationally modify the p53 protein. This leads to an increase in its half-life and enhances its ability to bind to specific DNA sequences to promote the transcription of p53-responsive genes [111]. Two of the best characterized activators of p53 are the serine/threonine kinases ataxia telangiectasia mutated (ATM) and ATM-Rad3-related (ATR) which respond best to DNA damage induced by IR and UV light, respectively. Both ATM and ATR also respond to other cellular stresses including oxidative stress, nutrient withdrawal, and aberrant cell cycle progression. ATM and ATR phosphorylate p53 on Ser15, enhancing its stability [112, 113], and phosphorylate the kinases CHK2 and CHK1, respectively (Fig. 1.8). CHK1/2 phosphorylate p53 on Ser20, further stabilizing the protein [81, 114] (Fig. 1.8). The phosphorylation of p53 on Ser15/20 prevents binding by the ubiquitin ligase MDM2 that serves as the major negative regulator of p53 activity by targeting p53 for proteosomal destruction [111]. ATM also directly phosphorylates MDM2, hindering its ability to bind to p53 [115] (Fig. 1.8).

p53 activation results in the transcription of genes that arrest cells, promote DNA repair, or cause the induction of apoptosis or senescence. p53 activity initiates both positive and negative feedback loops, and depending upon other signaling in the cell, cells will either arrest temporarily and repair their



DNA, or progress irreversibly toward apoptotic death or permanent proliferative arrest [111].

The temporary cell cycle arrest induced by the DNA damage response pathway can occur at the G<sub>1</sub>/S checkpoint (prior to DNA replication) or at the G<sub>2</sub>/M checkpoint (prior to cell division). The arrest at G<sub>1</sub>/S is mediated largely by the transcriptional activation of p21<sup>Cip1</sup> by p53 (Fig. 1.8). p21<sup>Cip1</sup> inhibits the activity of CDK-cyclin complexes, preventing the induction of DNA replication. Activated p53 can also assist in arresting cells at the G<sub>2</sub>/M boundary by upregulating the expression of 14-3-3 [116] (Fig. 1.8). The 14-3-3 proteins are localized in the cytoplasm, and bind CDC25C, thus sequestering it in the cytoplasm (Fig. 1.8). CDC25C is therefore unable to enter the nucleus where its activity is required to alleviate the inhibitory phosphorylation of CDK1 on Thr14/Tyr15. DNA damage also arrests cells at the G<sub>2</sub>/M checkpoint independent of p53 activation. The ATM/ATR substrates CHK1 and CHK2 can phosphorylate CDC25C at Ser216, causing its inactivation, and therefore locking CDK1 in an inactive state [117] (Fig. 1.8). ATM and ATR also inhibit Plk-1 which promotes the nuclear translocation of both CDC25C and cyclin B complexes [118] (Fig. 1.8).

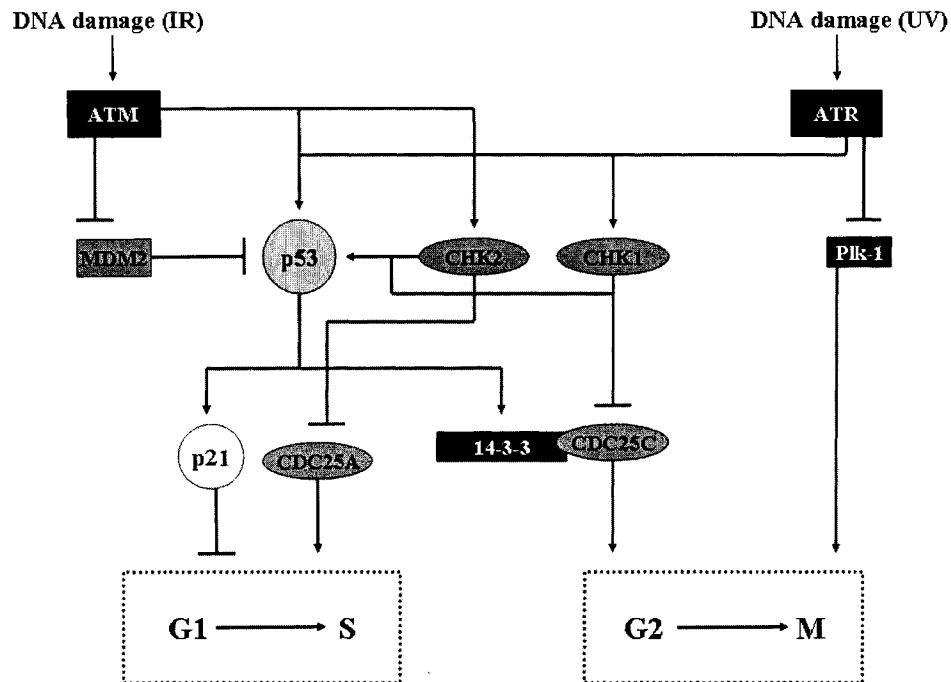


**Figure 1.9. A simplified model of the mechanisms by which DNA damage induces cell cycle arrest at the G<sub>1</sub>/S and G<sub>2</sub>/M checkpoints.** DNA damage or other cell stresses induce the activation of the kinases ATM and ATR. ATM and ATR phosphorylate p53 on Ser15, stabilizing the protein. ATM and ATR also activate CHK2 and CHK1, respectively, which phosphorylate p53 on Ser20, further stabilizing p53. ATM phosphorylates the ubiquitin ligase MDM2, preventing its binding to p53. Activated p53 promotes transcription of p21<sup>Cip1</sup> and 14-3-3. p21<sup>Cip1</sup> binds to and inhibits CDK-cyclin complexes, preventing the transition from G<sub>1</sub> to S-phase. CHK1/2 also inactivate CDC25A that normally promotes entry into S phase. Therefore, cells arrest at the G<sub>1</sub>/S transition. The 14-3-3 protein sequesters CDC25C in the cytoplasm, so it cannot enter the nucleus to activate CDK1-cyclin B. Independent of p53 action, CHK1 phosphorylates and inhibits CDC25C so that it cannot activate CDK1-cyclin B. Additionally, ATR inhibits the activity of Plk-1, a kinase that increases the nuclear import of cyclin B and CDC25C. The result of the combined mechanisms of inhibition of CDC25C is that CDK1-cyclin B cannot be activated, and cells arrest at the G<sub>2</sub>/M checkpoint.

The regulation of cell cycle progression is orchestrated by a number of pathways that respond to signals from the cellular environment and promote cell division in an orderly fashion only when conditions are favorable. There is considerable redundancy in the regulation of the cell cycle, and many non-essential pathways allow the fine-tuning of the process to ensure that cells are not

duplicated incorrectly and that damaged cells are excluded from continued mitotic progression. The correct regulation of cell cycle progression and its checkpoints is crucial for the successful growth and development of an organism.

#### **1.4. Cellular senescence**

1.4.1. *Characteristics of cellular senescence* – Cellular senescence is a state of irreversible proliferative arrest. The finite replicative lifespan of human fibroblasts in culture was first described by Hayflick and colleagues in 1961 [119]. After 50-100 passages, human fibroblasts reached the end of their replicative life span, irreversibly stopped growing, and adopted a large, flat cell morphology. This “intrinsic” type of senescence is termed replicative senescence, and is predominantly a result of telomere shortening in the absence of telomerase activity [120]. It is now well established that in addition to replicative senescence, “extrinsic” senescence can be induced in the absence of telomere shortening by many cellular stresses including DNA damage, oxidative stress, and the overexpression of tumor suppressors or oncogenes (reviewed in [121]). While senescence is typically characterized simply by irreversible proliferative arrest and cell cycle exit, other hallmarks of senescence include enlarged cell size, flattened cell morphology, senescence-associated neutral  $\beta$ -galactosidase activity, resistance to apoptosis, and a variety of changes in protein expression [122]. Senescence is generally thought to be maintained by two pathways, the p53 DNA damage pathway, and the p16<sup>INK4a</sup>/Rb pathway.

1.4.2. *Replicative senescence in human and rodent cells* – Telomeres are DNA-protein structures composed of repetitive DNA sequences (TTAGGG in vertebrates) and specialized proteins that cap the ends of linear chromosomes and prevent chromosome end fusions and genomic instability [123, 124]. Human telomeres are 5-15 kilo base pairs long, and rodent telomeres are 40-60 kilo base pairs long. Since the DNA replication machinery cannot fully replicate 3'-termini, telomeres shorten an average of 50-200 base pairs each cell division. Telomeres can be resynthesized in cells that express the enzyme telomerase. Human germ cells express telomerase, but most human somatic cells do not. In contrast, many rodent somatic cells express telomerase. Once a telomere reaches a critically short length, a senescence program is initiated. This likely occurs by the activation of a DNA damage response involving the p53 DNA damage response pathway (reviewed in [121]) (Fig. 1.9). Replicative senescence caused by telomere shortening regulates the replicative lifespan of human somatic cells. Although mouse cells can undergo senescence induced by telomere shortening [125, 126], mouse cells in culture usually reach a finite life span and undergo senescence without telomere shortening, predominantly as a result of oxidative culture stress [120, 127].

1.4.3. *Stress-induced senescence in human and rodent cells* – A senescence phenotype can be induced prematurely in cells with functional telomeres in response to DNA damage or oxidative stress. For example, some mouse cells that have long telomeres and express telomerase arrest in culture after 10-20 doublings due to their sensitivity to oxidative stress incurred from being

cultured in atmospheric oxygen (reviewed in [121]). In the case of this “extrinsic” senescence, the activation of the DNA damage response pathway involving p53 and p21<sup>Cip1</sup> is crucial for maintaining proliferative arrest. The induction of senescence following DNA damage or stress can be regarded as a protective mechanism to prevent cells with irreparable damage or those in unfavorable growth conditions from proliferating. This can be viewed as an alternate outcome to apoptosis for damaged cells, and can serve as a backup mechanism for cells whose apoptotic signaling is disrupted. It is not clear exactly what combination of signals results in a cell undergoing senescence rather than apoptosis *in vivo*. Since permanent proliferative arrest can act as a failsafe against the propagation of damaged cells, it is not surprising that the upregulation of many tumor suppressors including p16<sup>INK4a</sup> and p14(ARF) also cause the induction of senescence [128].

1.4.4. *Oncogene-induced senescence and tumor suppression* – Activated oncogenes can also induce premature cellular senescence both in culture and *in vivo*. It has been well described that the overexpression of oncogenes in culture often results in cellular senescence. For example, the overexpression of c-Ras causes senescence in some cells in culture, even though expression of oncogenic K-ras often results in increased proliferation and transformation. The ability of cells to senesce in response to oncogenic stimulation represents a mechanism whereby malignancy can be avoided. Several recent studies demonstrate that oncogene-induced senescence is a physiologically relevant process that contributes to tumor suppression *in vivo*. In one study, oncogenic K-ras<sup>V12</sup> was

conditionally activated in mice to promote the formation of both pre-malignant and malignant tumors in the lung and pancreas. The pre-malignant tumors showed hallmarks of senescence including the upregulation of p16<sup>INK4a</sup>, the expression of senescence-associated  $\beta$ -galactosidase, and the presence of heterochromatin foci [129]. In contrast, the malignant tumors did not show hallmarks of senescence. Therefore, oncogenic K-Ras induced cellular senescence *in vivo*, and the senescence may have prevented malignancy, whereas cells that failed to senesce became malignant. Another study demonstrated that early stage prostate tumors exhibited hallmarks of senescence [130]. When the tumor suppressor PTEN was inactivated, p53-dependent cellular senescence pathways were initiated both *in vitro* and *in vivo* in prostate cells. Furthermore, secondary inactivation of p53 reversed the senescent phenotype, and the combined inactivation of PTEN and p53 resulted in invasive prostate cancer in mice [130]. Another study demonstrated that sustained expression of an oncogenic mutant of BRAF, a downstream effector of Ras, promoted a cellular senescence response *in vivo* in melanocytes [131]. After initially promoting proliferation, oncogene-induced senescence resulted from BRAF<sup>V600E</sup>-induced cell cycle arrest. This oncogenic mutation of BRAF is commonly found in benign human naevi that typically remain growth arrested [131]. These studies collectively demonstrate that oncogene-induced senescence is a physiologically relevant process *in vivo* that prevents malignancy.

1.4.5. *Senescence in aging and antagonistic pleiotropy* – Since replicative senescence occurs when cells reach their finite life span, senescence has always

been associated with aging. Cells with hallmarks of senescence accumulate with age in human and rodent tissues, and are abundant in various age-related pathologies (reviewed in [122]). Antagonistic pleiotropy refers to the hypothesis that organisms develop processes that are favorable in the short-term at the expense of unfavorable long-term effects. There is evidence that senescence prevents malignancy in the short-term by arresting the proliferation of damaged cells, but contributes to long-term malignancy (reviewed [132]). There are various factors including matrix metalloproteinases, epithelial growth factors, and inflammatory cytokines, that are increased in senescent cells and promote chronic tissue remodeling, inflammation, and the proliferation of other cells, (reviewed in [122]). Senescent fibroblasts can promote the growth and morphological differentiation of epithelial cells due to the secretion of MMP3 [133]. Therefore, the accumulation of senescent cells in the long-term may contribute to the development of late-life cancer.

1.4.6. *The p53 pathway in the senescent response* – Cellular senescence induced by telomere shortening, DNA damage, oxidative stress, and oncogene overexpression requires the activation of p53 [132] (Fig. 1.9). p53 is activated by a DNA damage response in the case of stress-induced senescence or telomere shortening, and by p14(ARF) in the case of oncogene-induced senescence. In some senescent cells, inactivation of p53 reverses the proliferative arrest [134, 135], whereas in other cells it does not. However, p53 upregulation is a common feature of senescence. p53 likely contributes to senescence primarily by

upregulating p21<sup>Cip1</sup> which inhibits CDK activities and prevents cell cycle progression and proliferation (Fig. 1.9).

1.4.7. *The p16<sup>INK4a</sup>/Rb pathway in the senescent response* – The second pathway responsible for the maintenance of cellular senescence is mediated by increased expression of p16<sup>INK4a</sup>, a CDK4/6 inhibitor that is induced in senescence and prevents the phosphorylation of Rb [136]. Dephosphorylated retinoblastoma inhibits E2F, thereby preventing the transcription of genes required for cell cycle progression and proliferation. In human fibroblasts, after Rb-mediated senescence has been induced, the inactivation of p16<sup>INK4a</sup>, p53, or Rb does not necessarily reverse the proliferative arrest [135]. This indicates that activating the p16<sup>INK4a</sup> pathway may make cellular senescence irreversible. This irreversibility is likely caused by the formation of dense foci of heterochromatin [137, 138] (Fig. 1.9). The changes in chromatin organization that make senescence irreversible are dependent on Rb repression of E2F target genes and the methylation of Histone H3 on lysine 9 by the histone methyltransferase Suv39h1 [137, 139]. Recently, it was shown that oncogenic Ras promotes Suv39h1-dependent senescence in mice [139].



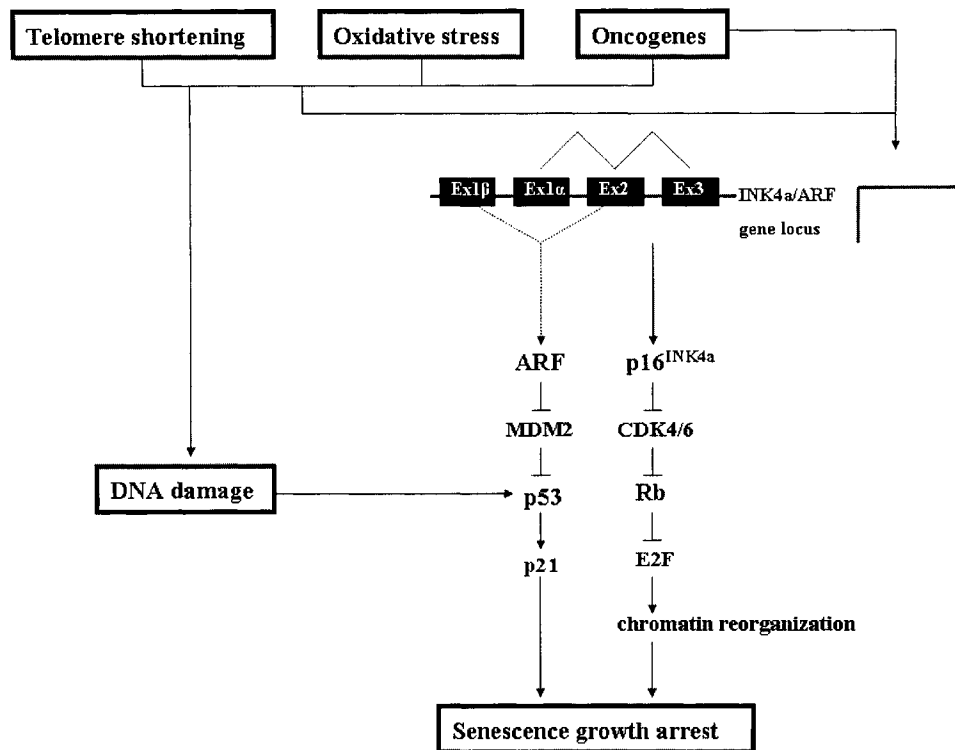


**Figure 1.10. Pathways involved in the induction of cellular senescence.** Many types of cellular stress result in DNA damage which activates p53 by post-translational modifications. Oncogenes and other cellular stresses also activate the transcription of the genes p16<sup>INK4a</sup> and p14(ARF). ARF inhibits the p53 inhibitor, MDM2, causing the activation of p53. p53 increases the transcription of p21<sup>Cip1</sup> that inhibits CDK-cyclin complexes. The p16<sup>INK4a</sup> protein inhibits monomeric CDK4 and CDK6, preventing the phosphorylation and inactivation of Rb. Hypophosphorylated Rb inhibits the transactivating E2F transcription factors, preventing the transcription of proteins required for cell cycle progression. The sustained inhibition of E2F in proliferative arrest results in the activation of the histone methyltransferase Suv39h1 which promotes chromatin reorganization that renders the proliferative arrest of cells irreversible.

#### 1.4.8. *The role of sphingolipids in cellular senescence* – Endogenous

levels of ceramide increase in cellular senescence in human fibroblasts, implying that sphingolipid signaling may be involved in maintaining a senescent phenotype [140]. When high passage senescent human fibroblasts were compared to low passage cycling cells, the senescent cells had increased ceramide levels by 4-fold as a result of 8-10 fold increases in neutral sphingomyelinase activity [140]. The

addition of 15  $\mu\text{M}$  D-erythro- $\text{C}_6$ -ceramide to young fibroblasts inhibited DNA synthesis and promoted a senescence-like morphology [140]. Exogenous ceramide also promoted the dephosphorylation of Rb [140]. These results suggest that activation of neutral sphingomyelinase activity and the maintenance of high ceramide concentrations may be involved in activating the Rb pathway in cellular senescence.

## **1.5. Matrix metalloproteinases**

1.5.1. *Characteristics of the matrix metalloproteinases* – The matrix metalloproteinases (MMPs), also known as the matrixins, are a family of more than 20 members of endopeptidases. As indicated by their name, the MMPs degrade components of the extracellular matrix (ECM), thereby promoting extracellular matrix remodeling. In addition to destroying ECM components, the cleavage of ECM proteins can expose new recognition sites for receptors or release ECM-sequestered cytokines [141]. It has recently been discovered that MMPs have additional non-ECM substrates, and regulate signaling by cleaving a variety of proteins including growth factors, growth factor receptors, cytokines, and other enzymes (reviewed in [141, 142]). MMPs are important regulators of processes such as development, wound healing, inflammation, and tumorigenesis [141, 143]. MMPs are normally expressed at low levels in most tissues, but are dramatically upregulated by cytokines, oncogenes, and other factors in situations where extracellular matrix degradation or remodeling are required. MMPs can be regulated transcriptionally, and are regulated by their secretion and cleavage

[141]. MMPs are also regulated by specific inhibitors [141]. The MMPs are divided into families based on their substrates and characteristics, although recent studies have demonstrated that there is significant overlap in substrates between families.

1.5.2. *Regulation of MMP activities* – The minimal domains in MMPs are a secretory signal sequence, a propeptide domain, and a catalytic domain containing a zinc binding consensus motif. The MMPs are all produced as pro-enzymes that require cleavage to be activated. Most MMPs are secreted as inactive zymogens and cleaved extracellularly, although the membrane-type MMPs (MT-MMPs) are bound to the plasma membrane by a C-terminal transmembrane domain or tether. The propeptide domains of the MMPs have a consensus motif with a critical cysteine residue. The sulfhydryl group on the cysteine residue co-ordinates with the zinc in the active site to inhibit the activity of the enzyme. For the MMPs to be fully activated, the Cys-zinc binding must be disrupted by cleavage of the propeptide domain. The MMPs are inhibited by a variety of natural inhibitors. Some inhibitors including  $\alpha$ 2-macroglobulin form a complex with MMPs that is cleared by scavenger receptors [144, 145]. A class of proteins called the tissue inhibitor of metalloproteinases (TIMPs) bind to MMPs in a 1:1 ratio and inhibit the MMP activities. There are 4 TIMP proteins, each of which inhibits a select group of MMPs.

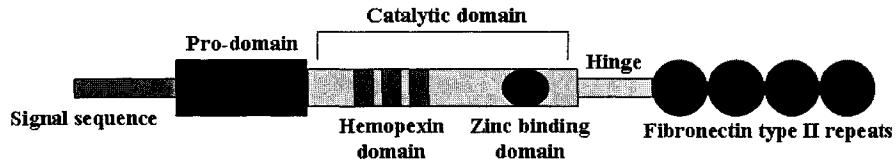
1.5.3. *The gelatinases MMP2 and MMP9* – In addition to the minimal MMP protein domains, MMP2 and MMP9 contain a hemopexin domain, which confers binding specificity, and three fibronectin type II repeats in their catalytic

domain, which facilitate the binding of gelatin. The gelatinases are secreted enzymes, although there is some evidence to suggest that they must be associated with the plasma membrane for their correct function [141]. MMP2 and MMP9 preferentially degrade denatured collagen (gelatin). Their ECM substrates include collagen I,/IV,/V,/VII,/X,/XI, elastin, fibronectin, laminin, aggrecan, and vitronectin. In addition, MMP2 and MMP9 can cleave other proteins to regulate signal transduction. MMP2 is important in regulating the transactivation of the EGF receptor downstream of LPA-induced GPCR receptor activation [146-148] This process is important for mediating many of the effects of extracellular LPA in some cells. Additionally, MMP2 and MMP9 can cleave pro-TGF- $\beta$ 2, pro-IL1- $\beta$ , and pro-TNF $\alpha$ , producing the active forms of the cytokines. MMP2 can also cleave decorin, increasing the pool of available TGF- $\beta$ , can cleave FGF-R1, rendering the receptor unable to signal, and can cleave pro-MMP 1/2/13. MMP9 can cleave plasminogen to form the angiogenesis inhibitor, angiostatin (reviewed in [142]). Both MMP2 and MMP9 are often pro-migratory and enhance tissue remodeling and signaling that promote blood vessel formation and inflammation.

1.5.4. *The mechanism of activation of MMP2* – MMP2 exists in two forms, a 72 kDa pro-enzyme, and a fully cleaved 60 kDa enzyme. Although the 72 kDa pro-MMP2 is considered inactive, it does have activity. It is simply less active than the 62 kDa MMP2. The basis for this is unknown. MMP2 is the only MMP for which the physiological mechanism of activation has been elucidated. Although TIMP-2 inhibits the active MMP enzyme, it is also required for the activation of MMP2. The membrane bound MT-MMP1 (also called MMP14) is

also required for MMP2 activation. A complex forms between one membrane anchored MT-MMP1 protein and one TIMP-2 protein (Fig. 1.10). The N-terminus of TIMP-2 binds to the catalytic domain of MT-MMP1, inhibiting it. The secreted 72 kDa pro-MMP2 is recruited to the TIMP-2/ MT-MMP1 complex and binds to the C-terminus of TIMP-2 through its hemopexin domain (Fig. 1.10). A second MT-MMP1 protein that is not inhibited by TIMP-2 subsequently cleaves the propeptide domain of pro-MMP2, which partially activates the enzyme (Fig. 1.10). Another active MMP2 enzyme must complete the propeptide cleavage to produce the fully active 62 kDa MMP2 [149-151] (Fig. 1.10). Based on this mechanism, it is evident that the ratio of MMP2, MT-MMP1, and TIMP-2 is in large part responsible for determining the activity of secreted MMP2. A certain amount of TIMP-2 is required to activate MMP2, but excesses of TIMP-2 relative to MT-MMP1 or MMP2 will inhibit all the MT-MMP1, preventing the activation of MMP2, and inhibit the active 60 kDa MMP2. Therefore, changes in the MMP2: MT-MMP1: TIMP-2 ratios can regulate MMP2 activity and the signaling pathways effected by MMP2 activity.

### A) The protein structure of MMP2 and MMP9



### B) The activation of MMP2

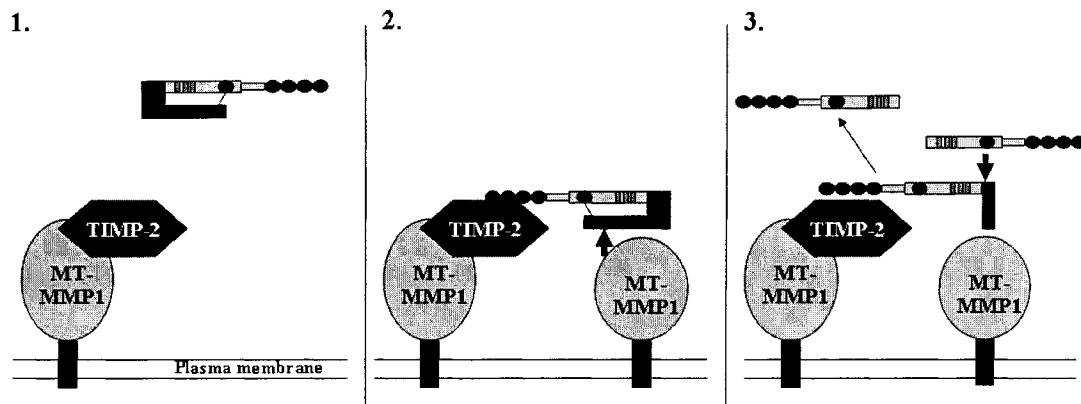


**Figure 1.11. The protein structure and activation of MMP2.** Panel A depicts the protein structure of the gelatinases MMP2 and MMP9. Panel B depicts the mechanism by which MT-MMP1, TIMP-2, and MMP2 co-operate to activate secreted MMP2. See the text for details.

## 1.6. Thesis objectives

The lipid phosphate phosphatases are important regulators of cell signaling due to their ability to degrade bioactive lipid phosphates extracellularly and intracellularly. The three LPP isoforms have non-redundant, isoform-specific roles in regulating signal transduction and physiology. LPP2 is the least studied of the LPP enzymes. The restricted tissue expression and unique expression profile of LPP2 in tumors suggests that LPP2 has a unique role in regulating cell signaling and physiology. However, prior to this study, little was known about the role of endogenous LPP2 in cell signaling.

The aim of this study is to evaluate the hypothesis that LPP2 has isoform-specific functions in regulating signaling in fibroblasts. We intent to evaluate the role of LPP2 expression and activity in regulating fibroblast functions.

Fibroblasts that had high endogenous overall LPP activities and endogenously expressed LPP2 were used to evaluate the functions of LPP2. We overexpressed wild-type and catalytically inactive mutant LPP2 and knocked down endogenous LPP2 expression. Our first aim was to determine what effects the overexpression and knock-down of LPP2 would have on fibroblast function and signaling. We wanted to evaluate whether effects were dependent on the catalytic activity of LPP2 by comparing the effects of an inactive mutant. Additionally, we wanted to evaluate whether LPP2 activity had an isoform-specific role by comparing the overexpression and knock-down of LPP2 with the overexpression and knock-down of LPP1 and LPP3. The elucidation of the role of endogenous LPP2 activity in cells that normally express LPP2 would provide insight into the specific role of LPP2 in signaling and physiology.

## **CHAPTER 2**

### **MATERIALS AND METHODS**



## 2.1 Overexpression and knock-down of the LPPs and cell maintenance

2.1.1. *Site-directed mutagenesis and addition of the GFP tag* – cDNA for human LPP2 was from Dr. A. Morris (Department of Medicine, Veterans Affairs Medical Center, Lexington KY). The polymerase chain reaction (PCR) was used to generate a point mutation in LPP2 in which an arginine residue required for catalytic activity was mutated to a lysine residue (R214K). PCR was also used to add a C-terminal green fluorescent protein (GFP) tag to both the wild-type and mutant LPP2 and to add Bam HI and Sal I sites to the N- and C-termini, respectively.

2.1.2. *Sub-cloning* - The resulting PCR products were ligated into pCR2.1-TOPO (Invitrogen Life Technologies, Carlsbad, CA ) according to the manufacturer's directions and amplified in *E. coli*. LPP2, LPP2-GFP, and LPP2[R214K]-GFP sequences and the pBabepuro (pBP) ([152], Addgene plasmid 1764) and pShuttle-CMV (Stratagene, La Jolla, CA) expression vectors were cut with the restriction enzymes Bam HI and Sal I (Invitrogen) according to the manufacturer's directions. The products were purified and ligated with T4 DNA ligase (Invitrogen) according to the manufacturer's directions. The plasmids were sequenced to confirm that no random mutations had occurred during cloning. Constructs for GFP, mLPP1, and mLPP1-GFP were engineered by Q.X. Zhang . The myc-mLPP1 construct was engineered by C. Pilquill, and the myc-rLPP3 and rLPP3-GFP constructs were engineered by L. Stromberg in the laboratory. These were subcloned into the pBP and pShuttle-CMV vectors.

2.1.3. *Creation of stable cell lines and adenovirus* – For the creation of stably overexpressing cells, the previously described constructs in pBP or the empty pBP vector were transfected into Bosc31 packaging cells [153] using a standard calcium phosphate transfection protocol [154] or lipofectamine 2000 (Invitrogen) according to the manufacturer's directions. Virion-containing media were collected after 48 and 72 h, filtered, and pooled. Virion-containing media were used to infect rat2 fibroblasts that had been treated with 6 µg/ml polybrene for 48 h. Fibroblasts were selected in media containing 25 µg/ml puromycin (Sigma-Aldrich, Oakville, ON). Clones were not selected. To create adenovirus, GFP-tagged hLPP2 and myc-tagged mLPP1, driven by a cytomegalovirus promoter, were transferred into an adenovirus-packing cell line using the AdEasy™ vector system (Stratagene) following the manufacturer's directions. The recombinant plasmids were linearized and propagated in HEK 293 cells, and high-titre purified preparations ( $1 \times 10^{10}$  plaque-forming units/ml) were generated by the University of Iowa Gene Transfer Vector Core. For adenoviral transfections, various multiplicity of infection (pfu/cell) were added to cells in antibiotic-free media for 24 h.

2.1.4. *Growth and maintenance of cell lines* - Rat2 fibroblasts [155] and Bosc31 cells were maintained in DMEM (Invitrogen) supplemented with 10% fetal bovine serum (FBS) (Medicorp Inc., Montreal, PQ, Canada) and an antibiotic/antimycotic cocktail (penicillin/ streptomycin/amphoterecin B) (Invitrogen) at 5% CO<sub>2</sub>, 95% humidity, and 37°C. Transduced cells were maintained in medium containing 25 µg/ml puromycin to maintain selective

pressure. Experiments were performed in the absence of puromycin and the antibiotic/antimycotic cocktail. Stably transduced cells were generally split 1:20 at confluence and used between passages 5 and 25 post-transduction, with the exception of the studies on high passage cells.

2.1.5. *siRNA transfection*- Double stranded *SMARTpool*® small interfering RNAs (siRNAs) targeting rat LPP1, rat LPP2, human LPP2, rat LPP3, rat cyclophilin B, non-targeting controls, and Cy3-conjugated non-targeting controls (siGLO) were purchased from Dharmacon (Lafayette, CO). Lipofectamine 2000 (Invitrogen) in opti-MEM (Invitrogen) media was used at 0.625 µg/ml according to the manufacturer's directions. The final concentration of siRNA in each transfection was 200 nM. Controls for the knock-downs were performed with cyclophilin B, non-targeting control siRNAs, and lipofectamine alone. The transfection efficiency for the introduction of the siRNAs was about 95%, as evaluated by the number of fluorescent cells transfected with siGLO, divided by the number of nuclei stained with Hoescht 33258 (not shown) or phase contrast microscopy (Fig. 2.1). For cell cycle analysis, transfections were performed in antibiotic-free media that contained serum, and media were changed 6 h after transfection. After a further 18 h, cells were treated with serum-free media for 20 h before the re-addition of serum to promote cell cycle progression. Lysates were collected for real time RT-PCR 12 h after the addition of serum in each experiment to determine the extent of knock-down achieved at approximately the point of S-phase entry.

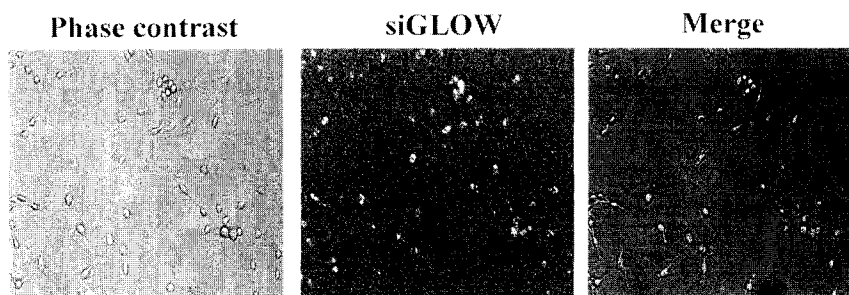


**Figure 2.1. Transfection efficiency for siRNA is approximately 95%.** Rat2 fibroblasts were transfected with siGLO® fluorescent siRNAs. The total number of cells in each field was detected with phase contrast microscopy (left). The incorporation of siRNA into cells was detected by viewing the fluorescence at 570 nm (centre). The two images were merged (right) and the percentage of cells transfected was calculated by dividing the number of fluorescent cells by the number of total cells. Panels depict typical cells from 1 of 12 fields. Results are from one experiment.

2.1.6. *Induction of DNA damage* – To induce reversible DNA damage, cells were exposed to ultraviolet (UV) radiation (254 nm) using a *Stratalinker*<sup>TM</sup> crosslinker (Stratagene). A dose curve was performed in rat2 fibroblasts. Cells were seeded at 300,000 cells/dish for 4 h. Media were removed, and cells were washed and incubated in 0.5 ml HEPES buffered saline, pH 7.4 (HBS). The lids were removed from dishes, and each dish was placed in the center of the crosslinker and treated with the indicated dose of UV radiation. The HBS was removed, and the cells were washed and media were replaced for 16 h. Cells were collected and analyzed for cell cycle phase by flow cytometry. Parallel dishes were trypsinized, re-seeded, and allowed to grow for another 12 h. Floating and attached cells were counted. The dose that most effectively reversibly delayed cells in G<sub>1</sub>-phase was 50 J/m<sup>2</sup> (Table 2.1). In subsequent experiments, cells were trypsinized and seeded for 4 h, treated with 50 J/m<sup>2</sup> UV, and analyzed by flow cytometry 4-24 h later.

**Table 2.1. Determination of the dose of UV radiation to reversibly delay fibroblasts in G<sub>1</sub>-phase.**

Rat2 fibroblasts were treated with the indicated amounts of UV and grown for 16 h. Flow cytometry was performed to evaluate the cell cycle distribution. The percentage of viable cells after trypsinization and re-seeding was determined by counting on a hemocytometer.

	Energy (J/m <sup>2</sup> )						
	0	15	30	40	50	60	100
% G1	39.43	36.82	31.84	27.94	74.17	72.2	70.73
% S	38.61	40.28	58.86	72.06	15.85	10.47	11.99
% G2	21.96	21.91	9.3	0	9.98	17.34	17.27
% viable	100	100	100	100	50	20	0

## 2.2. Measurements of proliferation, DNA concentrations, and mRNA concentrations

2.2.1. *Cell proliferation assay* - Cells were seeded at 30,000 cells/dish and grown for 8 days, with media replaced each day. Under these conditions, fibroblasts proliferated exponentially for 2-3 days before encountering contact inhibition, irrespective of passage number. Cells were washed with HBS, trypsinized, resuspended in serum-containing media, and counted on a hemocytometer. Parallel determinations of total protein in cells scraped from dishes were performed in some cases using the bicinchoninic acid (BCA) assay (Bio-Rad) according to the manufacturer's directions.

2.2.2. *Measurement of DNA content* - The amount of DNA in cell populations was measured by Hoescht staining in a 96-well plate. [156]. Cells were grown for 8 days as described above, trypsinized, and counted. One thousand cells/well were seeded into black 96-well plates and incubated for 4 h. Wells were emptied and 100 µl of distilled water was added to each well. Plates

were frozen at -80 °C and thawed to room temperature to lyse cells. To each well, 100 µl of 1 µg/ml Hoescht 33258 (Molecular Probes Inc., Eugene, OR) solution was added, and fluorescence was measured on a Fluoroskan Ascent FL plate reader (ThermoLabsystems, Waltham, MA) using an excitation of 350 nm and an emission of 460 nm. Standard curves were performed in each plate using calf thymus DNA (Invitrogen) as a control. Wells without cells were used to provide blank values which were subtracted.

*2.2.3. MTT assay for cell viability* – Cells were seeded at 1-10,000 cells/well in 96-well plates and grown for 8 days, with media replaced each day. Media were replaced with 100 µl of fresh media/well, and 10 µl of 12 mM 3-(4,5-dimethylthiazol-2-yl)-2,5-diphenyltetrazolium bromide (MTT) (Sigma) solution was added to each well. Plates were incubated at 37 °C for 4 h. To each well, 100 µl of 1% SDS in 0.01 M HCl was added, and plates were incubated for 12 h. Absorbance was measured at 540 nm on an EAR 340AT plate reader (SLT Labinstruments, Austria).

*2.2.4. Extraction of RNA and real-time RT-PCR* - Total RNA was collected using the RNAaqueous kit (Ambion Inc., Austin TX.) according to the manufacturer's directions. Contaminating DNA was removed using the DNA-free kit (Ambion) according to the manufacturer's directions. RNA was quantitated spectrophotometrically at 260 nm on a Shimodzu UV-160 spectrophotometer (Mandel Scientific, Guelph, ON). Reverse transcriptions were performed using Superscript II (Invitrogen), random primers (Invitrogen), RNAout (Invitrogen), and dNTPs (Invitrogen) according to the manufacturer's

directions. Negative controls lacking RNA or Superscript II were performed with each reverse transcription reaction. PCR was performed on an Icycler (Bio-Rad, Hercules, CA) or a 7500 System (Applied Biosystems, Foster City, CA). Each reaction contained 0.2  $\mu$ M of each primer, approximately 100 ng of cDNA from the reverse transcription reaction, and SYBR green® PCR master mix (Applied Biosystems). Standard curves were generated for each primer pair and the slope and efficiency that were calculated from the curves were used to calculate target RNA levels relative to the levels of the housekeeping gene cyclophilin A.

Melting curves were performed with each analysis to confirm product specificity, and amplified products were run out in 2% agarose to confirm the presence of a single band of the expected size. An annealing temperature of 57 °C was used for cyclophilin A, LPP1, LPP2, LPP3, MMP2, and TIMP-2 reactions. An annealing temperature of 62 °C was used for MMP9 and cyclophilin B reactions. Primers for the LPPs were designed to recognize human, mouse, and rat sequences.

Primers for PCR were as follows: LPP2 forward TGGCCAAGTACATGATTGG and reverse AGCAGCCGTGCCCACTTCC; LPP1 forward GGTCAAAAATCAACTGCAG and reverse TGGCTTGAAGATAAAGTGC; LPP3 forward CCCGGCGCTCAACAACAACC and reverse TCTCGATGATGAGGAAGGG; mouse cyclophilin A forward CACCGTGTTCGACATCAC and reverse CCAGTGCTCAGAGCTCGAAAG; rat cyclophilin B forward GCCAACGATAAGAAGAAGGGACC and reverse TGATGACACGATGGAAGTTGCTG; rat TIMP-2 forward

CAAGCAGATAAAGATGTTCAAAGGG and reverse  
TGATGTGCATCTTGCCGTCC; rat MMP2 forward  
CTATTCTGTCAGCACTTTGG and reverse CAGACTTTGGTTCTCCAACCT;  
rat MMP9 forward AAATGTGGGTGTACACAGGC and reverse  
TTCACCCGGTTGTGGAAACT.

### 2.3. Protein methods

2.3.1. *Extraction of proteins* – Cells were washed twice with ice-cold HBS and harvested by scraping in lysis buffer. For most Western blots, cells were collected in standard lysis buffer (1% Nonidet P-40, 10% glycerol, 50 mM HEPES, 137 mM NaCl, 1 mM MgCl<sub>2</sub>, 1 mM CaCl<sub>2</sub>, 10 mM Na<sub>4</sub>P<sub>2</sub>O<sub>7</sub>, 5 µg/ml aprotinin, 1 mM phenylmethylsulfonyl fluoride (PMSF), and 1 µg/ml leupeptin). For LPP2 Western blots and LPP activity assays, cells were collected in LPP solubilization lysis buffer (50 mM HEPES, 137 mM NaCl, 1mM MgCl<sub>2</sub>, 1mM CaCl<sub>2</sub>, 10% glycerol, 0.1% SDS, 1% Triton X-100, 0.5% sodium deoxycholate, 2.5 mM EDTA, 0.1 mM PMSF, 10 µg/ml aprotinin, 10 µg/ml leupeptin). Lysates were sonicated at 35% output for 30 sec. and insoluble debris was removed by centrifugation. Samples were assayed for protein concentration with a BCA assay (Bio-Rad) according to the Manufacturer's directions.

2.3.2. *Immunoprecipitation* – Equal amounts of lysate in terms of total protein were diluted to 500 µl with lysis buffer and pre-cleared with 10 µl of protein A sepharose beads (GE Healthcare Bio-Sciences AB, Uppsala, Sweden) at 4 °C for 1 h. Lysates were incubated with antibodies for 12 h at 4 °C with



shaking, and 20  $\mu$ l of protein A sepharose beads were added for an additional 4 h. Beads were collected by centrifugation and washed three times with IP washing buffer (50mM Tris base, pH 7.5, 1% Triton X-100, 100 mM NaCl, 5 mM EDTA, 1  $\mu$ g/ml aprotinin, 20 mM leupeptin, 1 mM PMSF) for LPP Western blots, or with RIPA buffer (50 mM Tris-HCl, 150 mM NaCl, 50 mM NaF, 2 mM DTT, 0.1% Triton X-100, 0.1 mM sodium orthovanadate, 10  $\mu$ M leupeptin, 100  $\mu$ g/ml aprotinin, 40 mM  $\beta$ -glycerophosphate, and 20 mM *p*-nitrophenyl phosphate) for CDK kinase assays. Antibodies were monoclonal anti-GFP (B-2, Santa Cruz, Biotechnology Inc., Santa Cruz, CA) at 1:100, goat and rabbit polyclonal anti-GFP (Dr. L. Bertiaume, University of Alberta, Edmonton AB) at 1:500, mouse anti-myc 9E10 (Dr. T. Hobman, University of Alberta, Edmonton AB) at 1:200, anti-CDK1 (Cell Signaling) at 1:100, and anti-CDK2 (sc-163, Santa Cruz) at 1:100.

*2.3.3. Preparation of Samples for SDS-PAGE* – A standard method of sample preparation was used for analysis of all proteins except LPP2. Lysates were dissolved in sample loading buffer (0.25 M Tris base, pH 6.8, 13% glycerol, 2.5% SDS, 0.1 mg/ml bromophenol blue).  $\beta$ -mercaptoethanol was added to 5%, and samples were boiled for 10 min and then cooled to 4  $^{\circ}$ C before loading. The LPP2 protein could not be visualized on Western blots using the standard method described above. Therefore, additional methods of sample preparation were used to resolve LPP2. Method A: Lysates were diluted in 20 mM Tris, pH 6.8, 10% glycerol, 10% SDS, and 0.1 mg/ml bromophenol blue.  $\beta$ -mercaptoethanol was added to 10%, and samples were loaded without boiling. Method B: Lysates were

diluted in sample buffer with final concentrations of 10 mM Tris, pH 8.3, 2% SDS, 10% glycerol, and 8 M urea.  $\beta$ -mercaptoethanol was added to 5%, and samples were boiled for 10 min and then cooled to 4 °C before loading. Method C: Lysates were dissolved in 20 mM Tris, pH 8.3, 20 mM DTT, and 4% SDS, and boiled for 5 min. 100 mM iodoacetamide was added, and samples were incubated at room temperature for 1 h. Loading buffer containing 20 mM Tris, pH 6.5, 10% glycerol, and 0.1 mg/ml bromophenol blue was added, and samples were loaded at room temperature.

2.3.4. *SDS-PAGE and transfer* – Samples were loaded onto stacking gels composed of 0.375 M Tris-HCl, pH 8.8, 0.1% SDS, 3.9 % acrylamide, and 0.1% bisacrylamide. Separating gels were composed of 0.125 M Tris-HCl, pH 6.8, 0.1% SDS, and 7.5% acrylamide/ 0.2% bisacrylamide to resolve proteins larger than 60 kDa, or 10% acrylamide/ 0.27% bisacrylamide to resolve proteins between 30 and 60 kDa, or 12% acrylamide/ 0.32% bisacrylamide to resolve proteins less than 30 kDa. Gels were run in Laemmli electrophoresis buffer at 100 volts at 4 °C. Prestained molecular mass markers were loaded on each gel (Bio-Rad). Proteins were transferred onto 0.45  $\mu$ M Transblot® nitrocellulose membranes (Bio-Rad) in Tris-glycine containing 20% ethanol at 500 mA for 12 h. Membranes were stained with 2% ponceau red in 5% acetic acid to confirm that there was an even transfer of proteins from the gels onto the membranes.

2.3.5. *Antibodies and blotting* – Membranes were blocked in Odyssey™ blocking buffer (Li-Cor Biosciences, Lincoln, NE) for 1 h. Membranes were incubated with primary antibodies that were diluted in blocking buffer containing

0.1% Tween 20 for 4 h, and then with fluorescence-conjugated secondary antibodies that were diluted in blocking buffer containing 0.1% Tween 20 for 1 h. Membranes were washed for 1 h with PBS and stored at 4 °C in the dark until scanning. Antibodies and dilutions were: anti-cyclin A (rabbit, 1:200 sc-751, Santa Cruz); anti-cyclin D2 (mouse, 1:200, sc-181, Santa Cruz); anti-cyclin E (rabbit, 1:500, sc-481, Santa Cruz); anti-CDK1 (rabbit, Cell Signaling, 1:500); anti-CDK2 (rabbit, 1:200, sc-163, Santa Cruz); anti-CDK4 (rabbit, 1:200, sc-601, Santa Cruz) anti-LIMK (mouse, Cell Signaling, 1:500); anti-phospho (Thr508/Thr505) LIMK (rabbit, Cell Signaling, 1:500); anti-Akt (mouse, Cell Signaling, 1:1000) anti-ERK1 (rabbit, 1:500, sc-93, Santa Cruz); anti-phospho p42/44 MAPK (rabbit, Cell Signaling, 1:1000); anti-p38 MAPK (mouse, Cell Signaling, 1:1000), anti-phospho p38 MAPK (rabbit, Cell Signaling, 1:500); anti-p27 (mouse, 1:500, sc-528, Santa Cruz); anti-phospho-cdc2, Tyr15 (rabbit, 1:1000, Cell Signaling,); anti-phospho-p53, Ser15 (rabbit, 1:1000, Cell Signaling); anti-cyclin D1 (rabbit, 1:200, Cell Signaling); anti-cyclin D3 (rabbit, 1:200, sc-6283, Santa Cruz); anti-p21 (mouse, 1:500, sc-6246, Santa Cruz); anti-cyclin B1 (mouse, 1:200, sc-245, Santa Cruz), anti-GFP (mouse, 1:200, B-2, Santa Cruz), anti-p16 (mouse, 1:200, sc-1661, Santa Cruz). Anti-LPP2 antibodies were from a gift from Dr. S. Pyne (University of Strathclyde, Glasgow, U.K.), and purchased from Exalpa Biologicals, Inc. (Watertown, MA). Rabbit anti-mLPP1 antibody was produced as described previously [39]. Secondary antibodies were: Alexa Fluor<sup>®</sup> 680 goat anti-mouse IgG, A-21057 (Invitrogen), 1:10,000; and

IRDye 800 goat anti-rabbit IgG (Rockland Immunochemicals, Philadelphia, PA), 1:10,000.

*2.3.6. Scanning and quantitation of blots* - Blots were scanned on the Odyssey™ Imager (Li-Cor) at 700 nm for anti-mouse and 800 nm for anti-rabbit IgG simultaneously, and quantitated using Odyssey™ software. Values were always expressed relative to a control lane after background subtraction. The amount of protein that was loaded resulted in the fluorescence of the bands being within the linear range for quantitation and below saturation. Results are comparable within but not between membranes.

## **2.4. Assays of LPP activity**

*2.4.1. Total activity in Triton X-100 micelles* – For each sample, 5, 10, and 20 µg of lysate or the beads from 50, 100, and 200 µg of lysate that had been immunoprecipitated were assayed. Lysates or immunoprecipitates were diluted into 100 mM Tris-maleate, 0.5% Triton X-100, and 1 mM N-ethylmaleimide. At 15 sec intervals, 0.6 mM [<sup>3</sup>H] PA (0.27 µCi/ µl) was added, and samples were incubated with shaking at 37 °C for 30 min. The reaction was stopped with the addition of chloroform and alumina. Phosphatidic acid bound to the basic alumina, and the extent of formation of <sup>3</sup>H-labeled DAG was determined by counting an aliquot of the dried chloroform phase in a scintillation counter. Results were expressed as specific activities determined from the slope calculated for each sample. Samples that contained lysis buffer but no cells were incubated under the same conditions for each experiment and their values were subtracted as

a reagent blank. The hydrolysis of PA was proportional to the amount of lysate added in the range of protein used. In some experiments, the hydrolysis of 1.5 mM [ $^{32}\text{P}$ ]-LPA or [ $^{32}\text{P}$ ]-S1P (1 Ci/ mol) were measured. In this case the reaction was stopped and [ $^{32}\text{P}$ ]-Pi was extracted as described for the measurement of ecto activity described below.

2.4.2. *Ecto activity of intact cells* – Fibroblasts were seeded at 300,000 cells/ 35 mm dish and cultured for 24 h. Cells were starved in DMEM containing 0.6% fatty acid free BSA (Sigma) for 4 h. Media were replaced with DMEM containing 0.6% fatty acid free BSA and [ $^{32}\text{P}$ ]-labeled 0.01-50  $\mu\text{M}$  LPA or S1P (approximately 1 Ci/mol) for 10, 20, or 30 min. Since LPA could be converted to glycerol 3-phosphate by phospholipase A-type activities and subsequently to Pi by an ecto alkaline phosphatase, *rac*-glycerol-3-phosphate was included in the media when LPA hydrolysis was measured. The reaction was stopped by removing the medium and mixing it with an equal volume of 1 M perchloric acid to precipitate the protein and most of the labeled lipid. After centrifugation, the supernatant was extracted twice with 1-butanol to remove any remaining lipid. The aqueous phase was mixed with a tenth the volume of 125 mM ammonium molybdate to allow the formation of phosphomolybdate complexes which were extracted with benzene: isobutanol (1:1). A sample of the organic phase was measured by scintillation counting. Dishes containing no cells were processed in parallel and used as a blank in each experiment. Dishes were washed twice with ice-cold PBS, and cells were collected in lysis buffer. Lysates were weighed to calculate the exact volume of buffer and protein was measured using a BCA assay

(Bio-Rad) according to the Manufacturer's directions. The production of [ $^{32}\text{P}$ ]-Pi that was determined by scintillation counting was normalized to the total amount of protein on each dish. In each experiment at least three concentrations of LPA or SIP or three incubation times were used, and slopes of the responses were used to calculate the specific activity.

2.4.3. *LPA depletion in media* – In some experiments, the concentration of [ $^{32}\text{P}$ ]-labeled LPA in the media was measured as a complementary measure to the amount of [ $^{32}\text{P}$ ]-Pi produced. In this case, the reaction was stopped by combining the media with an equal volume of 0.2 M acetic acid. After centrifugation, an equal volume of butanol was added. Butanol extracts containing labeled and unlabeled LPA were pooled. The aqueous layer was removed for subsequent addition of molybdate and extraction as described above. Butanol extracts were processed as described below for the radioenzymatic quantitation of LPA. Dual-label scintillation counting was set up to allow for the quantitation of both  $^{32}\text{P}$ -labeled and subsequently  $^{14}\text{C}$ -labeled LPA. Dishes without cells were used as positive controls to calculate the total LPA added to the plates. Results were normalized to the amount of total protein on each dish.

## 2.5. Enzyme activity assays

2.5.1. *CDK1 and CDK2 activity* - Prior to the kinase assay, beads from immunoprecipitations were washed with RIPA buffer (50 mM Tris-HCl, 150 mM NaCl, 50 mM NaF, 2 mM DTT, 0.1% Triton X-100, 0.1 mM sodium orthovanadate, 10  $\mu\text{M}$  leupeptin, 100  $\mu\text{g}/\text{ml}$  aprotinin, 40 mM  $\beta$ -

glycerophosphate, and 20 mM *p*-nitrophenyl phosphate) and then with kinase buffer (40 mM Tris, pH 7.6, 2 mM DTT, 10 mM MgCl<sub>2</sub>). Immunoprecipitates were incubated in 10 µl kinase buffer containing 1 µg Histone H1, 50 pmol ATP and 1 µCi [ $\gamma$ -<sup>32</sup>P]ATP for 10 min. Reactions were stopped by adding gel loading buffer and products were separated on SDS-PAGE. Phosphorylated substrate was visualized and quantitated on a phosphorimager (Bio-Rad) and the bands were cut and quantitated in a scintillation counter. Results were expressed relative to the activity in control cells at the time of re-entry into the cell cycle (0 h) after background values were subtracted.

2.5.2. *TIMP-2 activity* – Cells were incubated for 12 h in DMEM, and media were collected and concentrated. Medium (40 µl) was added to 90 µl of reaction buffer (150 mM NaCl, 10 mM HEPES, pH 7.5, 0.25 mM DTT, 5 mM CaCl<sub>2</sub>, 0.1% Triton X-100, and 5 µg/ml sodium azide) and 10 µl 100 ng/ml recombinant MMP2 (Calbiochem, San Diego, CA) in a 96-well plate. Fluorescein-conjugated DQ<sup>TM</sup> gelatin (Molecular Probes) was dissolved in water to a final concentration of 1 mg/ml and 10 µl was added to each sample. Plates were incubated at 37 °C and fluorescence was measured (excitation of 485 nm and emission of 527 nm) every 10 min for 4 h. MMP2 activity on gelatin was measured as the slope of activity over time in duplicate and blanks containing unconditioned media alone (with no TIMP-2) were used as positive controls. TIMP-2 inhibition was measured as the decrease in the slope of MMP2 activity compared to controls. The amount of recombinant MMP2 was large compared to

amounts in conditioned media and saturated any changes in MMP activities in the samples.

2.5.3. *Matrix metalloproteinase gelatin zymography* – Cells were incubated in DMEM for 12 h. Media were collected, cells were removed by centrifugation, and media were concentrated 4-fold with Amicon™ ultra 4-10,000 MWCO filters (Millipore, Billerica, MA). Separation gels were made of (0.3 M Tris-HCl, pH 8.8, 8% acrylamide, 0.1% SDS, 2 mg/ml gelatin) and stacking gels were made of (0.1 M Tris-HCl, pH 6.8, 4% acrylamide, 0.1% SDS). Conditioned media from adenocarcinoma cells that had been treated with phorbol ester was used as a standard for 72kDa and 62 kDa MMP2 and 92 kDa MMP9 and run on each gel. Samples were loaded and gels were run in Laemmli electrophoresis buffer at 100 volts at 4 °C. Gels were washed for 2 h in 2.5% Triton X-100 in water. Gels were then incubated at 37 °C in incubation buffer (50 mM Tris-HCl, 0.15 M NaCl, 5 mM CaCl<sub>2</sub>) for 8-24 h until bands were visible. Gels were stained with 0.25% Coomassie R250 in 40% methanol and 10% acetic acid, and destained with 40% methanol and 10% acetic acid. Gels were scanned at 700 nm on the Odyssey™ imager and quantitated using Odyssey™ software. The values from each band were normalized to the amount of protein or number of cells on dishes from which media were collected.

## 2.6. Lipid analyses

2.6.1. *Extraction of lipids* – For analysis of PA, DAG, Cer, C1P, LPA, and SIP by bulk lipid mass, radioactive labelling, or DAG kinase assays, cells were



washed twice with HBS and scraped twice in 0.5 ml of methanol. Methanol extracts were pooled and mixed with 0.9 ml 0.5 M NaCl in water and 1 ml chloroform. 800  $\mu$ l of the lower chloroform layer was removed, and evaporated under a stream of nitrogen. Extracts were resuspended in a small volume of chloroform for subsequent analyses, and an aliquot was taken for the measurement of total phospholipid phosphate. For measurement of LPA using the LPAAT assay, cells were washed twice with HBS and scraped with 1 ml water. 1.1  $\mu$ l concentrated acetic acid and 1 ml water-saturated 1-butanol were added. The butanol layer was collected. An additional 1 ml of water-saturated 1-butanol was added, and butanol extracts were pooled. One tenth of the extract was removed for the measurement of total phospholipid phosphate, and the remaining butanol was evaporated under a stream of nitrogen.

*2.6.2. Measurement of total phospholipid phosphate* – A standard curve of 1-100 nmol glycerol-3-phosphate was measured with every experiment. Glycerol-3-phosphate standards in water and samples in chloroform or butanol were heated at 180 °C until the solvents were evaporated. 50  $\mu$ l of concentrated perchloric acid was added to each sample, and samples were heated at 180 °C for 30 min with beads covering the tubes to prevent evaporation. 278  $\mu$ l water, 55  $\mu$ l 2.5% ammonium molybdate, and 55  $\mu$ l 10% ascorbic acid were added. Samples were boiled for 15 min. Samples were pipetted in duplicate into a 96-well plate and the absorbance was measured on a plate reader at 700 nm. For each experiment, blanks containing each solvent used without sample were run in

parallel and subtracted, and concentrations for the samples were determined using the standard curve.

2.6.3. *Measurement of bulk PA* – Chloroform extracts and 1-10 µg PA standards in chloroform were loaded 10 cm above the origin of a plastic backed Silica gel 60 thin layer chromatography (TLC) plate. The plate was developed twice in chloroform: methanol: ammonium hydroxide (65:35:7.5). The plate was cut 12 cm above the origin and inverted, and developed in the opposite direction in chloroform: methanol: acetic acid: acetone: water (10:2:3:4:1). The plate was dried and was either sprayed with 0.05% primulin in 80% acetone, or stained for 1 h in 0.03% Coomassie R250 in 20% methanol and 100 mM NaCl and then destained for 15 min in 20% methanol. Plates were dried. In the case of primulin staining, plates were quantitated by scanning on a phosphorimager (Bio-Rad) at 525 nm. In the case of Coomassie staining, plates were scanned at 700 nm on an Odyssey™ imager. In both cases, bands were quantitated using each scanner's software, blanks of samples containing only solvent were subtracted, and concentrations were determined based on the slope of the standard curve and were expressed relative to the amount of total phospholipid phosphate in the sample. Samples were run within the linear range of the assay, as determined experimentally for the Coomassie technique (Fig. 2.2A)

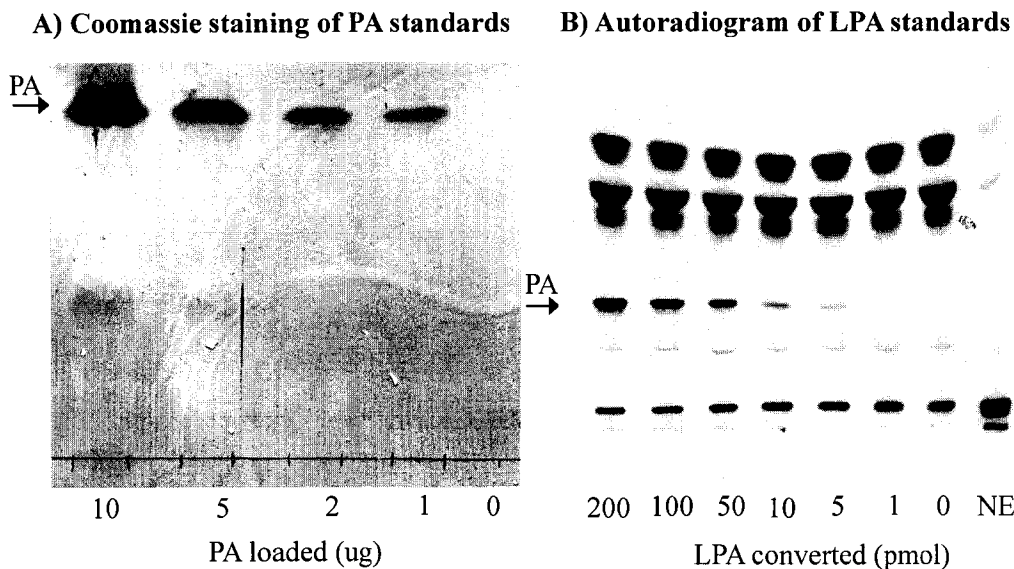


**Figure 2.2. Determination of the linear range of assays for bulk PA and LPA concentrations.** Panel A shows a thin layer chromatography plate stained with Coomassie R250 and scanned on the Odyssey™ imager at 700 nm. PA standards containing the amount of lipid indicated in chloroform were loaded. Panel B shows an autoradiogram of a thin layer chromatography plate developed with an enhancer screen for 12 h. Standards containing the indicated amounts of LPA were converted to PA in a radioenzymatic assay and products were resolved by TLC. NE denotes a standard processed in the absence of enzyme. The band resulting from the acylation of LPA that co-migrated with a cold PA standard is indicated. The band at the origin corresponds to oleoyl-CoA and the band beneath to oleate. The three upper bands correspond to neutral lipids including DAG and TAG. The band beneath the PA band is of unknown origin. The bands we observed corresponded to the bands observed and characterized in Saulnier-Blache et al, 2000. Results are from one representative of at least three experiments.

#### 2.6.4. Measurement of PA, DAG, Cer, CIP, SIP, and LPA by radioactive

*labeling* – Cells were incubated in starvation medium (DMEM with 0.1% BSA) for 2 h. Media were replaced with DMEM containing 0.1% BSA and 8  $\mu\text{Ci/ml}$  [ $^3\text{H}$ ]palmitate and 2  $\mu\text{Ci/ml}$  [ $^{14}\text{C}$ ]oleate for 20 h. Media were removed and cells were washed twice with HBS. Chloroform extracts were collected as described previously and washed twice with synthetic top phase containing 1 M KCl and 1 M HCl. Samples were resuspended in 50  $\mu\text{l}$  of chloroform. Half the samples were loaded 1.5 cm from the origin of a Silica gel 60 TLC plate and run 70% of the plate length in chloroform: methanol: acetic acid: acetone: water

(50:10:10:20:5). The plate was dried and run in the same direction to its full length in hexane: diethyl ether: acetic acid (60:40:1). Unlabeled standards were added to each plate, and labeled bands were cut and quantitated by scintillation counting. The retention factors ( $R_f$ ) for standards in this solvent system were as follows: palmitate, 0.94; DAG, 0.91 and 0.89; PA, 0.77; PE, 0.47; PC, 0.31; PS, 0.3; PI, 0.24. The other half of the sample was loaded 10 cm from the origin of a Silica gel 60 TLC plate and run twice in chloroform: methanol:  $\text{NH}_4\text{OH}$  (55:45:7.5). The plate was cut 12 cm above the origin, inverted, and run in the opposite direction in chloroform: methanol: acetic acid: acetone: water (50:10:10:20:5). LPA, S1P, and C1P standards were loaded on the plate, and labeled bands from the samples were cut and quantitated by scintillation counting.

2.6.5. *Measurement of DAG and Cer by DAG kinase assay* – Standards of 0.1-4 nmol each of diolein *sn*-1,2-DAG and mixed long-chain ceramides were prepared in heptane, and the solvents from the samples and standards were evaporated under a stream of nitrogen. To each standard and sample, 1 mM DETAPEC, 12.5 mM  $\text{MgCl}_2$ , 50 mM NaCl, 1 mM EGTA, 50 mM Imidazole/HCl, 1 mM cardiolipin, 1.5% N-octyl- $\beta$ -D-glucopyranoside, 10 mM DTT, 1 mM ATP, and 0.01 units of DAG kinase, pH 6.6 were added, and tubes were pre-incubated at 37 °C for 20 min to phosphorylate contaminants without radioactivity. 1  $\mu\text{Ci}$  [ $\gamma$ - $^{32}\text{P}$ ] ATP was added to each sample, and the samples were incubated at 37 °C for 45 min with periodic sonication. Reactions were stopped with the addition of 1 ml methanol. 1 ml chloroform and 0.8 ml 2 M KCl/ 0.2 M  $\text{H}_2\text{PO}_4$  were added. The upper aqueous layer was discarded, and the lower organic layer was washed

twice with synthetic top phase (prepared by separating the top phase from a mix of 300 ml chloroform, 300 ml methanol, and 240 ml 2 M KCl/ 0.2 M H<sub>2</sub>PO<sub>4</sub> in water). 800 µl of the lower organic phase was extracted and the chloroform was evaporated under a stream of nitrogen. Samples were resuspended in 25 µl chloroform and loaded 1.5 cm from the origin of a Silica gel 60 TLC plate. Plates were developed in chloroform: methanol: ammonium hydroxide (65:35:7.5), dried, and developed in the same direction in chloroform: methanol: acetic acid: acetone: water (50:10:10:20:5). Plates were dried and stained with iodine vapor to visualize an unlabelled PA standard loaded on each plate. Plates were exposed to film with the use of an enhancer screen (Kodak) for 12 h. Films were used to match bands to each plate on a light box, and bands were cut and soaked in 0.5 ml water, before 4 ml of scintillation fluid was added and the samples were counted in a scintillation counter. Blanks containing solvent but no cells were run with every experiment and subtracted. DAG and Cer concentrations in each sample were determined using the slopes of the standard curves for each lipid. Concentrations were normalized to the total phospholipid phosphate in each sample.

*2.6.6. Measurement of LPA by LPAAT assay* – To prepare the bacterial acyl transferase, *E. Coli* were transformed with the pTrcHis-AGPAT plasmid (Dr. J-P Saulnier Blache, Toulouse, France). Bacteria were grown in Luria-Bertani (LB) medium (1 % Tryptone, 0.5% yeast extract, 1% NaCl, pH 7.0) until they reached the log phase of growth, and were cultured for 3 h in the presence of 1 mM isopropyl-β-D-thiogalactopyranoside (IPTG) to induce expression of AGPAT

(LPAAT). Bacteria were pelleted, and the pellet was sonicated in 0.2 M Tris-HCl, pH 7.4, and centrifuged at 10,000 g for 20 min. Supernatants were centrifuged at 100,000 g for 90 min to precipitate microsomes containing the active LPAAT enzyme. The amount of total protein in the pellet was measured and the pellet was suspended in 0.2 M Tris-HCl, pH 7.4 at 1 µg/µl and aliquots were frozen. For each experiment, 0.1-10 µM LPA standards were assayed in parallel with the samples. The acylation reaction was performed with 20 mM Tris, pH 7.5, 1 mg/ml Tween 20, 20 µM Na<sub>3</sub>VO<sub>4</sub>, 1 µl [<sup>14</sup>C]oleoyl-CoA (55 mCi/mmol), and 10 µl of the microsomal pellet containing AGPAT/LPAAT for 2 h at room temperature with periodic mixing. Reactions were stopped with the addition of chloroform: methanol: 12 M HCl (40:40:0.26). The upper phase was removed and the lower organic phase was washed twice with synthetic top phase and extracted. The chloroform was evaporated under a stream of nitrogen, and samples were resuspended in 20 µl chloroform: methanol (1:1) and loaded 1.5 cm from the origin of a Silica gel 60 TLC plate. Plates were developed with chloroform: methanol: NH<sub>4</sub>OH: water (65:25:0.9:3). Plates were dried and radioactive PA was exposed to film with an enhancer screen. Unlabeled PA standards were run on each plate and stained with iodine vapor to confirm the location of the correct band. Bands were cut or scraped into water, and 4 ml of scintillation fluid was added before samples were counted in a scintillation counter. For each experiment, blanks containing only solvent were run in parallel with samples and subtracted. The amount of sample used was within the linear range of the assay, which was determined experimentally (Fig. 2.2B). The

concentration of LPA in each sample was calculated by comparing samples to the standard curve. The concentration of LPA was normalized to the amount of total phospholipid phosphate in the sample.

*2.6.7. Measurement of sphingolipids by mass spectrometry* - For mass spectrometric analysis, methanol extracts were combined with internal standards of 0.5 nmol of each of C<sub>12</sub>-sphingomyelin, C<sub>12</sub>-ceramide, C<sub>12</sub>-galactosylceramide, C<sub>12</sub>-lactosylceramide, C<sub>20</sub>-sphingosine, C<sub>20</sub>-sphinganine, C<sub>17</sub>-sphingosine-1-phosphate, and C<sub>17</sub>-sphinganine-1-phosphate. Samples were analyzed using liquid chromatography and tandem mass spectrometry by Elaine Wang, Samuel Kelly and Dr. A. Merrill, Jr., Georgia Institute of Technology, Atlanta, GA [157].

*2.6.8. Fractionization of nuclei for nuclear lipid measurement* - For the determination of nuclear DAG and Cer, nuclei were purified by centrifugation through a 16% sucrose cushion. Nuclei were washed twice with buffer containing 10% sucrose and lipids were extracted as above. The presence of intact nuclei was confirmed by Hoechst staining using a fluorescence microscope [158].

## **2.7. Microscopy**

*2.7.1. Preparation of coverslips* – Coverslips (12 mm<sup>2</sup>) were coated with fibronectin (Sigma) for 2 h, and washed. Cells were seeded at 30,000 cells/well onto coated coverslips and allowed to attach and spread for 12 h. Coverslips were washed twice with HBS and fixed with buffered 4% formaldehyde for 20 min at room temperature. Cells were permeabilized with 0.1% Triton X-100, washed with HBS, and blocked with 4% nonfat milk and 0.6% BSA for 1 h. Coverslips

were incubated with primary and secondary antibodies for 1 h each, and washed. Coverslips were mounted on slides in Prolong<sup>®</sup> antifade mounting media (Invitrogen). For staining of DNA, coverslips were incubated with 1 µg/ml Hoescht 33258 for 1 h. Primary antibodies were as follows: for LPP2-GFP and R214K-GFP, goat polyclonal anti-GFP, from Dr. L. Berthiaume (University of Alberta, Edmonton, AB, Canada), 1:200; for early endosomes, mouse anti-early endosome antigen-1 (BD Biosciences Canada, Mississauga, ON, E41120), 1:200; for caveolae, rabbit anti-caveolin-1 (Upstate Biotechnology, Charlottesville, VA, 06-591), 1:100; for endoplasmic reticulum, rabbit anti-calreticulin (from Dr. T. Hobman, University of Alberta, Edmonton, AB, Canada), 1:50; for Golgi apparatus, rabbit anti-giantin, (from X.-Z. Wang, University of Alberta, Edmonton AB, Canada), 1:100; for nuclear envelope, rabbit anti-lamin A/C (Santa Cruz), 1:50; and for mitochondria, mouse anti-cytochrome C, (Dr. M. Barry, University of Alberta, Edmonton, AB, Canada), 1:100. Secondary antibodies were chicken anti-rabbit Alexa Fluor<sup>®</sup> 594 (A-21442), chicken anti-mouse Alexa Fluor<sup>®</sup> 594 (A-21201), and chicken anti-goat Alexa Fluor<sup>®</sup> 488 (A-21467) from Invitrogen and were diluted 1:500.

*2.7.2. Visualization and co-localization analysis* – To determine the localization of LPP2-GFP, fluorescence was viewed on a Zeiss 510 confocal microscope using a pinhole of 1 airy unit (AU) and the extent of co-localization of LPP2-GFP with organelle markers was determined using LSM5 Software (Carl Zeiss Inc., Germany).



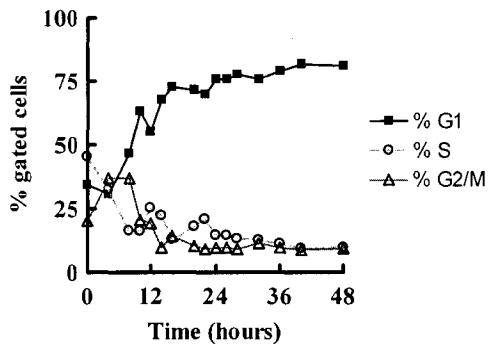
2.7.3. *Measurement of apoptosis* – Cells were seeded on coverslips and grown for 2, 4, 8, 12, or 24 h with or without treatment with 50 J/m<sup>2</sup> of UV radiation to induce apoptosis. Coverslips were fixed with 4% buffered formaldehyde and stained with 1 µg/ml Hoescht 33258 for 1 h. Nuclei were visualized using a fluorescence microscope (Leica Microsystems GmbH, Wetzlar, Germany) and normal and apoptotic nuclei were counted on the basis of nuclear condensation and fragmentation. For each treatment, 8 independent fields were averaged.

## 2.8. Flow cytometry

2.8.1. *Synchronization of cells* - Cells were synchronized by starvation in DMEM containing 0.1% fatty-acid free BSA (Sigma Chemical Co. St. Louis, MO) and released after 24 h by adding DMEM containing 10% FBS. In the case of knock-down experiments, cells were seeded in media containing serum without antibiotic and grown for 12 h, and then transfected with siRNAs for 6 h before the medium was changed. The transfected cells were then grown in media containing serum for an additional 18 h before the addition of starvation media for 24 h, and release with the re-addition of FBS. Cells were also synchronized by trypsinization after being grown to confluence. Nocodazole treatment and double-thymidine block techniques were not used because of their inability to produce adequate cell cycle re-entry after synchronization in the rat2 cell line. Treatment with 40-50 ng/ml nocodazole produced arrest in G<sub>2</sub>-phase only after 24 h, but this arrest was not reversible, and cells did not enter S-phase in the next 48

h (Fig. 2.3A). Treatment with 2 mM thymidine for 24 and 16 h at 6 h intervals produced G<sub>1</sub>-phase arrest that could not be overcome, and cells failed to cycle for the next 48 h (Fig. 2.3B). To determine the effectiveness of the various methods of synchronization, flow cytometry was used to measure the DNA content of cells every two hours from the point at which starvation or synchronization treatment began until 48 h after the re-addition of FBS for each method.

### A) Nocodazole treatment



### B) Double Thymidine treatment

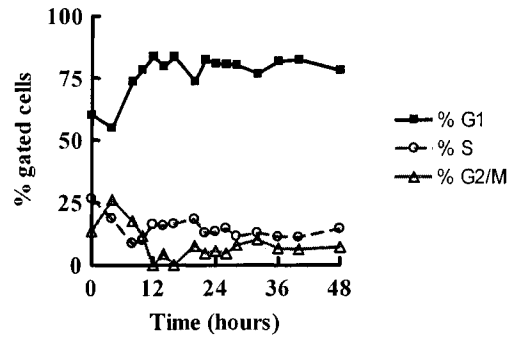


**Figure 2.3. Fibroblasts that have been synchronized in G<sub>2</sub>-phase by treatment with nocodazole or in G<sub>1</sub>-phase with a double thymidine block do not re-enter the cell cycle within 48 h.** Panels A and B show the percent of gated cells in each cell cycle phase at various times after the removal of synchronization reagent. Results are from one of at least two representative experiments.

2.8.2. *Cell cycle analysis with propidium iodide* - At specific times after serum stimulation, cells were harvested and nuclei were suspended at  $1 \times 10^6$  cells/ml in Vindelov's reagent (0.01 M Tris base, 10 mM NaCl, 700 U RNase I, 50  $\mu$ g/ml propidium iodide (PI) (Sigma), 0.1% NP-40). Samples were analyzed between 1-6 h after collection and were stored at 4 °C in the dark until analysis. Analysis was performed on a FACScan flow cytometer (BD Biosciences) using Cellquest software. A minimum of 20,000 cells were gated based on forward scatter (FSC) versus side scatter (SSC) and area versus width to exclude doublets,

polyploids, and cell fragments. Modfit Lt. Software (Verity Software House, Inc.) was used to quantitate G<sub>1</sub>, S, and G<sub>2</sub>/M peaks.

2.8.3. *Measurement of apoptosis* - To determine the percentage of apoptotic cells, cells were collected by centrifugation and fixed in 70% ethanol for 18 h and then stained with 100 µg/ml PI in PBS. The subdiploid peak was quantitated using Cellquest software (BD Biosciences). Positive control samples were treated with UV radiation to ensure the presence of a large subdiploid peak for correct gating. The percentage of apoptotic cells that is estimated by this method is an overestimation, since each fragmented nuclei that would normally correspond to a single event would produce more than one event in the subdiploid peak.

## **2.9. Migration and statistical analyses**

2.9.1. *Boyden chamber assay for migration* – 350,000 cells were seeded in a 10 cm dish 48 h before the migration assay and starved in DMEM containing 0.1% fatty-acid free BSA for the last 12 h. Transwells (polycarbonate, 6.5 mm, 80 µM pore size, Corning, Corning, NY) were coated with 40 µl of 0.15 mg/ml fibronectin for 12 h prior to seeding cells. Cells were washed twice with HBS, trypsinized, and resuspended in DMEM containing 0.1% BSA. 100,000 cells were seeded into each fibronectin-coated filter and incubated for 2 h to allow for attachment and spreading. Filters were then transferred into bottom chambers that had DMEM containing 0.1% BSA or conditioned media from cells supplemented with 0.4% charcoal-stripped FBS (FBS-C) and agonist. In most cases, the

migration to 0.5  $\mu$ M LPA was measured, and media without LPA was used as a negative control. Cells were incubated at 37 °C for 6 h to allow the migration of cells through the pores in the membrane toward the stimulus in the bottom chamber. After 6 h, filters were removed and the media was removed from the top chamber. The top side of the filters were cleaned with a moist cotton swap to remove cells that had not migrated. Filters were then fixed in 5% buffered formaldehyde for 30 min at room temperature. Filters were washed, and stained with 1  $\mu$ g/ml Hoescht 33258 for 2 h. Filters were washed again, and migrated cells that were attached to the bottom side of the filter were visualized under a fluorescent microscope. At least 5 random fields were photographed for each filter, and the number of cells in each field were counted blindly. Results were averaged and counts were expressed relative to a control filter for each experiment.

2.9.2. *Statistical analyses* – Results were presented as representative experiments without error bars, or as means  $\pm$  SD from at least 3 independent experiments. When means were compared for statistically significant differences, a 1-way ANOVA was used, followed by a Sheffe post-hoc test when all means were compared against each other to determine multiple differences, or a Tukey post-hoc test when all means were compared to a single control mean. A 95% confidence interval was used, and statistical significance was based on  $p < 0.05$ . Statistical analyses and graphing were performed using GraphPad 4 software (Prism).

## **CHAPTER 3**

### **ESTABLISHMENT AND CHARACTERIZATION OF FIBROBLASTS WITH MODIFIED LEVELS OF THE LPPs**

*A version of this chapter has been published. Morris KE, Schang LM, Brindley  
DN. 2006. J Biol Chem. 281:9297-306.*

### 3.1. Introduction

Fibroblasts are an ideal model system for studying wound healing, one of the major physiological processes regulated by bioactive lipids. Using this model, the migratory and proliferatory responses of fibroblasts to bioactive lipid mediators and the effect of the lipid phosphate phosphatases on these processes can be studied in great detail in a culture system. Rat2 fibroblasts express all three LPP isoforms and have high endogenous levels of LPP activities compared to many other cell types, including smooth muscle and endothelial cells. This suggests that fibroblasts are a physiologically relevant cell type in which to determine the endogenous functions of LPP2. Rat2 fibroblasts have been well characterized in the laboratory, and their complement of LPA receptors and signaling responses to lipid mediators such as LPA, PA, and Cer have been studied extensively.

To study the role of LPP2 in fibroblasts, LPP2 was stably overexpressed in rat2 fibroblasts using a retroviral expression system. The retroviral system allowed an overexpression large enough to produce increased LPP activity in cell lysates, but modest enough to avoid producing toxic effects or extreme changes in bulk lipid concentrations in the cell. To avoid the risk of studying compensatory mutations and artifacts, clones were not selected, but a mixed population of transduced cells was maintained and studied. Stable cell lines were produced independently on several occasions and exhibited the same characteristics. Additionally, to confirm that the effects of LPP2 overexpression were not due to a compensatory mutation in the cell population, drift, or cell damage, the

overexpression of LPP2 was reversed temporarily with the use of siRNAs. LPP2 was overexpressed with a GFP tag to allow it to be visualized by confocal microscopy and immunoprecipitated, since there were no adequate specific antibodies for LPP2 available. LPP2 was also overexpressed without a tag, to ensure that the tag did not affect the expression or function of the protein. A point mutant of LPP2 in which an arginine residue in the active site required for catalytic activity was mutated to lysine was also overexpressed. The overexpression of the catalytically inactive mutant allowed us to distinguish between catalytic and possible non-catalytic functions of LPP2.

To complement the stable overexpression, adenovirus for LPP2-GFP was produced. The induction of LPP2 overexpression by adenoviral transfection allowed us to study the effects of a transient overexpression of LPP2, thus avoiding any effects produced by long-term LPP2 expression, such as compensatory mutations or population drift. The adenovirus also allowed us to vary the levels of overexpression obtained to look at dose-dependent effects, and to achieve much higher levels of overexpression than could be obtained with stable overexpression. Unfortunately, expression of the adenoviral empty vectors produced some artifactual effects on the cells such as altering the rate of cell cycle progression. Therefore, adenoviral overexpression was used sparingly to validate results from the stable overexpression only where appropriate. siRNA was used to knock down endogenous LPP2 expression to complement the overexpression studies and to directly evaluate the endogenous function of LPP2 in fibroblasts.

To evaluate the potential isoform-specific role of LPP2 in fibroblasts, LPP1 and LPP3 were overexpressed and knocked down in parallel with LPP2, using the same methods. This allowed us to discover effects produced by LPP2 that were not mimicked by LPP1 or LPP3, and to understand the independent roles of the three isoforms in fibroblasts.

### **3.2. Stable overexpression of the LPPs in rat2 fibroblasts**

#### *3.2.1. mRNA concentrations in stably transduced fibroblasts*

*3.2.1.1. Measurement of mRNA concentrations in cells that overexpressed the LPPs* – RNA was collected from cells that were stably transduced with the empty vector (pBP), mLPP1, hLPP2, hLPP2-GFP, myc-rLPP3, or catalytically inactive hLPP2 [R214K]-GFP, and real-time RT-PCR was performed to determine the level of LPP mRNA overexpression resulting from each. Cells transduced with untagged LPP2, LPP2-GFP, and LPP2 [R214K]-GFP had 33-fold, 42-fold, and 29-fold increases in LPP2 mRNA expression, respectively (Fig. 3.1A). Cells transduced with LPP1 had a 9.5-fold increase in LPP1 mRNA expression compared to parental fibroblasts (Fig. 3.1E). Cells transduced with LPP3 had a 49-fold increase in LPP3 mRNA expression compared to control cells (Fig. 3.1F). These results are averages from at least three independent populations of cells. The level of mRNA overexpression was between 7- and 15-fold every time cells transduced with LPP1 were selected, between 20- and 50-fold every time cells transduced with LPP2 were selected, and between 30- and 100-fold every time cells transduced with LPP3 were



selected. The RT-PCR primers were designed to recognize the rat, mouse, and human isoforms of all three LPPs, so that the mRNA expression detected was the sum of endogenous and induced expression. These results demonstrate that each of the LPPs was overexpressed in the stably transduced cell lines at an mRNA level. RT-PCR also demonstrated that LPP1, LPP2, and LPP3 were all endogenously expressed in rat2 fibroblasts (Fig. 3.1A, E-F). When RT-PCR reactions were performed on parental rat2 cells using the same reagents and RNA concentrations, in a typical experiment the three isoforms had primer efficiencies of 1.88, 1.62, and 1.64, and required 18, 25, and 20 cycles to reach the threshold for endogenous LPP1, LPP2, and LPP3, respectively. The higher number of threshold cycles required for LPP2 indicated that LPP2 is likely to be the least abundant isoform in rat2 fibroblasts. LPP1 is likely the most abundant isoform in rat2 fibroblasts.

*3.2.1.2. Overexpression of each LPP does not alter the expression of the other isoforms* – It was possible that overexpression of one LPP isoform could affect the expression of the other isoforms. Therefore, mRNA expression levels of all three LPP isoforms were measured in cells overexpressing each of the LPPs. Overexpression of each of the three LPPs did not significantly change the mRNA expression of the other isoforms (Fig. 3.1B, E and F).

*3.2.1.3. LPP2 overexpression can be knocked down with siRNA* – To test whether the effects produced by the stable overexpression of LPP2 were a result of LPP2 activity, and were reversible, transfections with siRNAs for human LPP2 were performed to knock down the overexpression. The siRNAs for human

LPP2 had partial homology with the rat LPP2 sequence, so both the human LPP2 and endogenous rat LPP2 could have been knocked down. When cells that stably overexpressed LPP2 were treated with non-targeting control siRNAs, there was no change in LPP2 mRNA expression (Fig. 3.1C). However, when cells stably overexpressing hLPP2 were transfected with siRNAs for hLPP2, there was a 60% decrease in LPP2 mRNA overexpression (Fig. 3.1C). The 60% decrease still resulted in a 13-fold remaining overexpression of LPP2 mRNA.

#### 3.2.1.4. *LPP2 mRNA expression in cells infected with adenovirus –*

Rat2 fibroblasts were infected with 0-100 MOI (pfu/cell) of adenovirus expressing LPP2-GFP. Compared to uninfected cells, cells infected with 10, 25, 50, and 100 pfu/cell of adenovirus had 34-, 53-, 84-, and 135-fold increases in LPP2 mRNA expression, respectively (Fig. 3.1D). Infection with 10 pfu/cell of adenovirus expressing LPP1 did not alter the expression of LPP2 mRNA (Fig. 3.1D). These results demonstrate that adenoviral infection resulted in a dose-dependent overexpression of LPP2 mRNA, and was able to produce much higher levels of overexpression than were obtained by creating stably overexpressing cells.

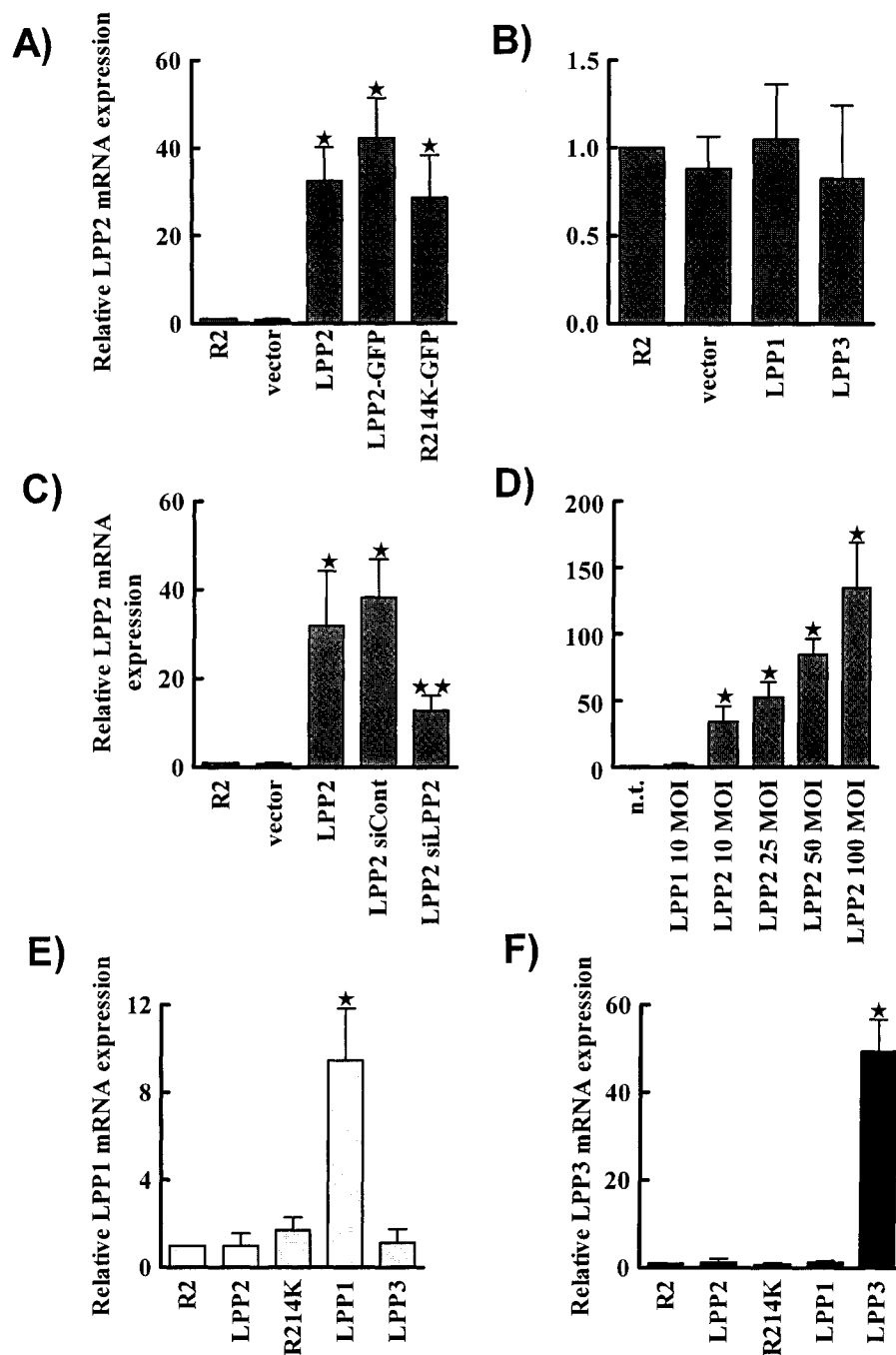


**Figure 3.1. mRNA expression in cells overexpressing the LPPs.** Panels A-C and E-F show mRNA concentrations for stable cell lines transduced with empty vector, LPP2, LPP2-GFP, LPP2[R214K]-GFP, LPP1, or LPP3. In Panel C some cells that stably overexpressed LPP2 were transfected with siRNAs for non-targeting control (siCont) or human LPP2 (siLPP2). Panel D shows rat2 cells (n.t.) or rat2 cells infected with various MOI (pfu/cell) of LPP2-GFP adenovirus. mRNA concentrations are normalized to that of the housekeeping gene, cyclophilin A. Results are expressed as fold change compared to rat2 fibroblasts which is given as 1. Results are means  $\pm$  SD from at least 4 independent experiments, except Panel D which are mean  $\pm$  SD for triplicates in one experiment. Statistically significant differences ( $p < 0.05$ ) from control are indicated by \*.

### 3.2.2. Expression of the LPP proteins

#### 3.2.2.1. Detection of the LPP1 and LPP3 proteins by Western blot

– To confirm that the LPP proteins were overexpressed in the stably transduced cells, Western blots were performed. Lysates from stably transduced cells were run on SDS-PAGE and membranes were blotted with antibodies that recognized the GFP and myc tags and the LPP proteins. Lysates from cells that were transduced with mLPP1 showed a doublet at approximately 35 and 33 kDa when probed with an anti-LPP1 antibody (Fig. 3.2A). Since the anti-LPP1 antibody only recognized the mouse isoform [39], there was no corresponding band in the control lane representing endogenous rat LPP1 (Fig. 3.2A). Lysates from cells transduced with myc-rLPP3 showed an increase in a band at approximately 33 kDa when blotted with an anti-LPP3 antibody (Fig. 3.2B). Since the LPP3 antibody recognized the rat isoform, the endogenous rat LPP3 was visualized with anti-LPP3 and the level of protein overexpression could be estimated. A comparison of the intensity of the 33 kDa band in the rat2 fibroblasts and in the stably transduced cells indicated that the amount of overexpression of the LPP3 protein was approximately 10-fold (Fig. 3.2B). Lysates from cells transduced with rLPP3-GFP showed a band that was not present in control cells with anti-LPP3 antibody at 72 kDa, slightly higher than the predicted molecular mass of 60 kDa (Fig. 3.2B). Bands at 78 kDa and 98 kDa were also observed, in addition to the endogenous protein at 33 kDa (Fig. 3.2B). The molecular weight discrepancies are most likely the result of the inherent imprecision of the prestained molecular

weight markers. The 98 kDa band could possibly be the product of homodimers between endogenous LPP3 and LPP3-GFP ( $\sim 70 + \sim 30 \approx 100$ ).

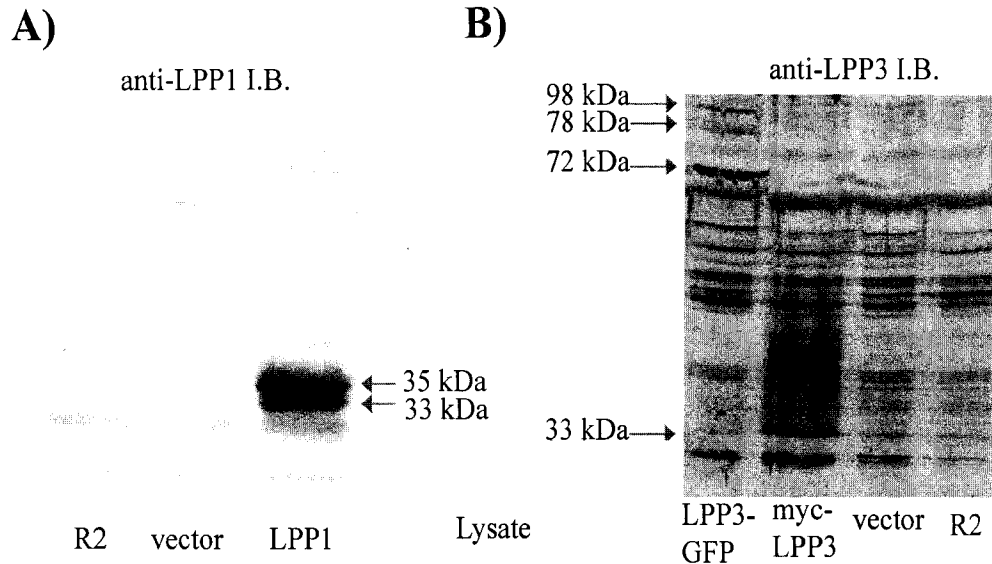


**Figure 3.2. Expression of the LPP1 and LPP3 proteins.** Panels A and B show Western blots as scanned by the Odyssey™ imager at 800 nm. Lysates were collected from rat2 cells (R2) and cells stably transduced with empty vector, mLPP1, myc-rLPP3, or rLPP3-GFP. Blots were incubated with rabbit polyclonal anti-mLPP1 at 1:1000 in Panel A and rabbit polyclonal anti-LPP3 at 1:500 in Panel B. Bands representing possible species of LPP1 and LPP3 proteins are indicated by arrows along with their molecular masses. Results are one representative of at least three independent experiments. The blot in Panel A was performed by C. Pilquil.

#### 3.2.2.2. High molecular mass aggregates appear on Western blots

*of lysates from cells stably transduced with LPP2-* In lysates from cells that were stably transduced with untagged LPP2, LPP2-GFP, or LPP2 [R214K]-GFP, no obvious bands were observed at the expected molecular masses of 33 kDa for the untagged protein, or 60 kDa for the GFP-tagged protein, using two different anti-LPP2 antibodies (Fig. 3.3A-B). Endogenous LPP2 protein could also not be visualized with anti-LPP2 antibodies (Fig. 3.3A-B), although this was not unexpected since both antibodies were designed against human LPP2, and since mRNA studies indicated that LPP2 is the least abundant isoform in fibroblasts.

Various sample preparation techniques were employed, including the addition of urea and iodoacetamide, as described in Chapter 2, but all failed to resolve LPP2 (Fig. 3.3B). Lysates from human bronchial epithelial cells showed a doublet at ~32 kDa representing the LPP2 protein (Fig. 3.3A). This demonstrates that our blotting techniques and anti-LPP2 antibodies were effective.

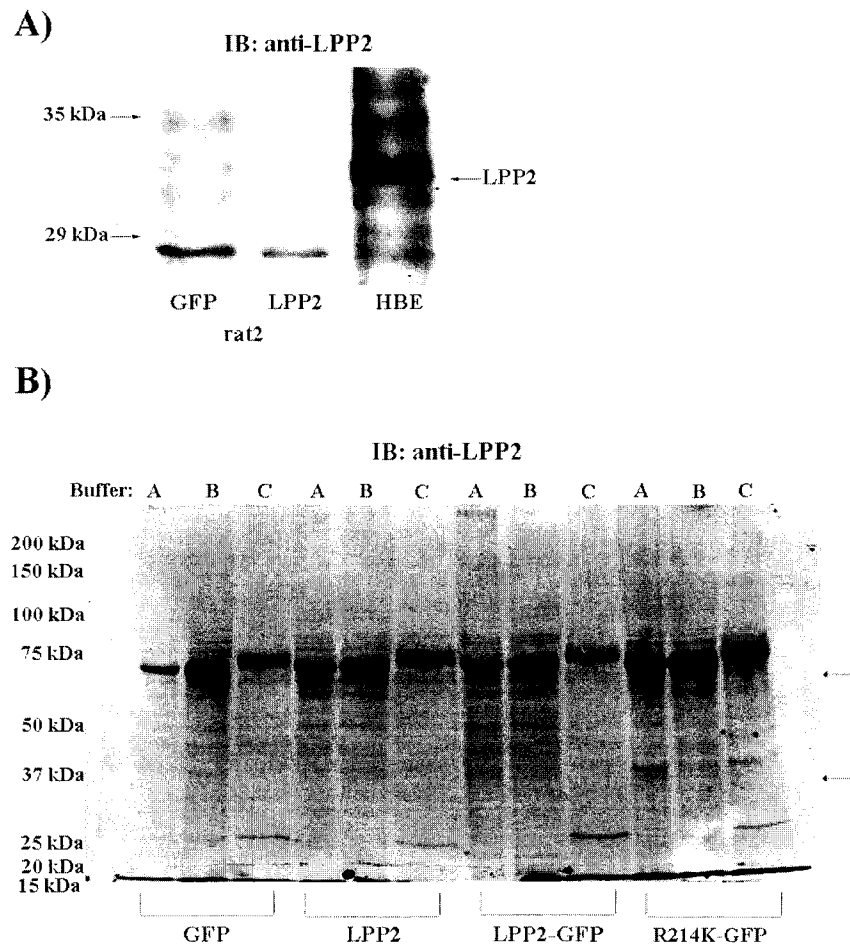


**Figure 3.3. The LPP2 protein can not be detected in lysates from rat2 fibroblasts that overexpress LPP2 on Western blots with an anti-LPP2 antibody.** Panel A shows lysates from rat2 cells that were stably transduced with GFP or LPP2 and human bronchial epithelial cells (HBE) in RIPA buffer. Panel B shows lysates from cells that were stably transduced with GFP, LPP2, LPP2-GFP, or LPP2[R214K]-GFP and were prepared using the three methods (A-C) described in Chapter 2. Western blots were probed with polyclonal anti-LPP2 antibody (1:100) and scanned at 800 nm to detect the secondary antibody. The molecular masses of the markers are given. In Panel A the arrow indicates the band representing LPP2, and in Panel B the arrows indicate the expected locations of the untagged and tagged LPP2 proteins at 33 kDa and 60 kDa. The results are from two representatives of at least four independent experiments.

When lysates from cells that were transduced with LPP2-GFP were blotted with anti-GFP using method A from Chapter 2, a very faint band was present at ~60 kDa, but a stronger band was observed at ~90 kDa (Fig. 3.4A). The 90 kDa band could be a result of LPP2-GFP monomers running at an unexpected molecular weight, or it more likely could represent LPP2-GFP/endogenous LPP2 dimers ( $\sim 60 + \sim 33 \approx 93$ ). Anti-GFP immunoprecipitates from cells transduced with GFP, LPP2-GFP, or LPP2 [R214K]-GFP were treated according to methods B or C from Chapter 2, run on SDS-PAGE, and blotted with anti-GFP or anti-LPP2. Immunoprecipitates from cells transduced with LPP2-GFP and LPP2 [R214K]-GFP, but not GFP, showed a high molecular mass doublet when probed with both anti-GFP and anti-LPP2 (Fig. 3.4C-E). This doublet could not be resolved further by any of the techniques described in Chapter 2. The same immunoprecipitates showed only a faint diffuse band at 60 kDa, the expected molecular weight for LPP2-GFP (Fig. 3.4C-E). mLPP1 and hLPP3 homodimerize, but do not heterodimerize [56]. It is therefore possible that LPP2 also forms homodimers. The two high molecular mass bands occurred at approximately 125 kDa and 175 kDa. The band at 125 kDa could be a result of the formation of LPP2-GFP/ LPP2-GFP dimers ( $\sim 60 + \sim 60 \approx 120$ ). The 175 kDa band could be a result of LPP2-GFP trimers ( $\sim 60 \times 3 \approx 180$ ) or of tetramers with two LPP2/ LPP2-GFP dimers. Other investigators have had difficulties resolving LPP2 on SDS-PAGE as a result of the formation of enzymatically active high molecular mass aggregates [159]. These authors overexpressed LPP2 in HEK293 cells and observed a prominent high molecular mass doublet at ( $>185$  kDa) and

(115 kDa to 185 kDa) and a prominent band at ~80 kDa, but only a small band at ~33 kDa [159]. These observations are very similar to our observations in rat2 fibroblasts. Pyne and colleagues determined that the gel filtration fractions that corresponded to the >80 kDa bands had LPP activity *in vitro* and attributed the bands to multimers [159]. Therefore, it is probable that the LPP2 protein was not detected at its expected molecular mass on Western blots due to its being present predominantly in the high molecular mass multimers that were not separated by the methods we used. It is also possible that the high molecular mass bands contained proteins other than the LPPs that were present with the LPPs in detergent-insoluble microdomains. We did not determine the composition of these bands. Nevertheless, our Western blots suggest that the GFP-tagged LPP2 proteins were expressed in the stable cell lines.

#### 3.2.2.3. *Detection of the LPP2-GFP protein after adenoviral*

*overexpression* – To enhance the possibility of detecting the LPP2 protein in its monomeric form, fibroblasts were transfected with adenovirus expressing GFP or LPP2-GFP and lysates were collected. In anti-GFP immunoprecipitates from cells infected with 100 pfu/cell of LPP2-GFP adenovirus, a strong band was seen at approximately 60 kDa with anti-LPP2 antibodies (Fig. 3.4B). In the same immunoprecipitates, a band was observed at approximately 120 kDa, approximately the same molecular weight observed in immunoprecipitates from stably transduced cells (Fig. 3.4B,E). These results demonstrate that adenoviral infection resulted in the overexpression of the LPP2-GFP protein, and that monomeric LPP2-GFP can only be detected at 60 kDa with anti-LPP2 antibodies



at very high levels of overexpression (greater than 100-fold overexpression of mRNA, Fig. 3.1D). Since neither LPP2 antibody was able to detect endogenous LPP2 in the rat2 cells, the level of overexpression of the LPP2 protein that was achieved by stable transduction or adenoviral infection could not be estimated.

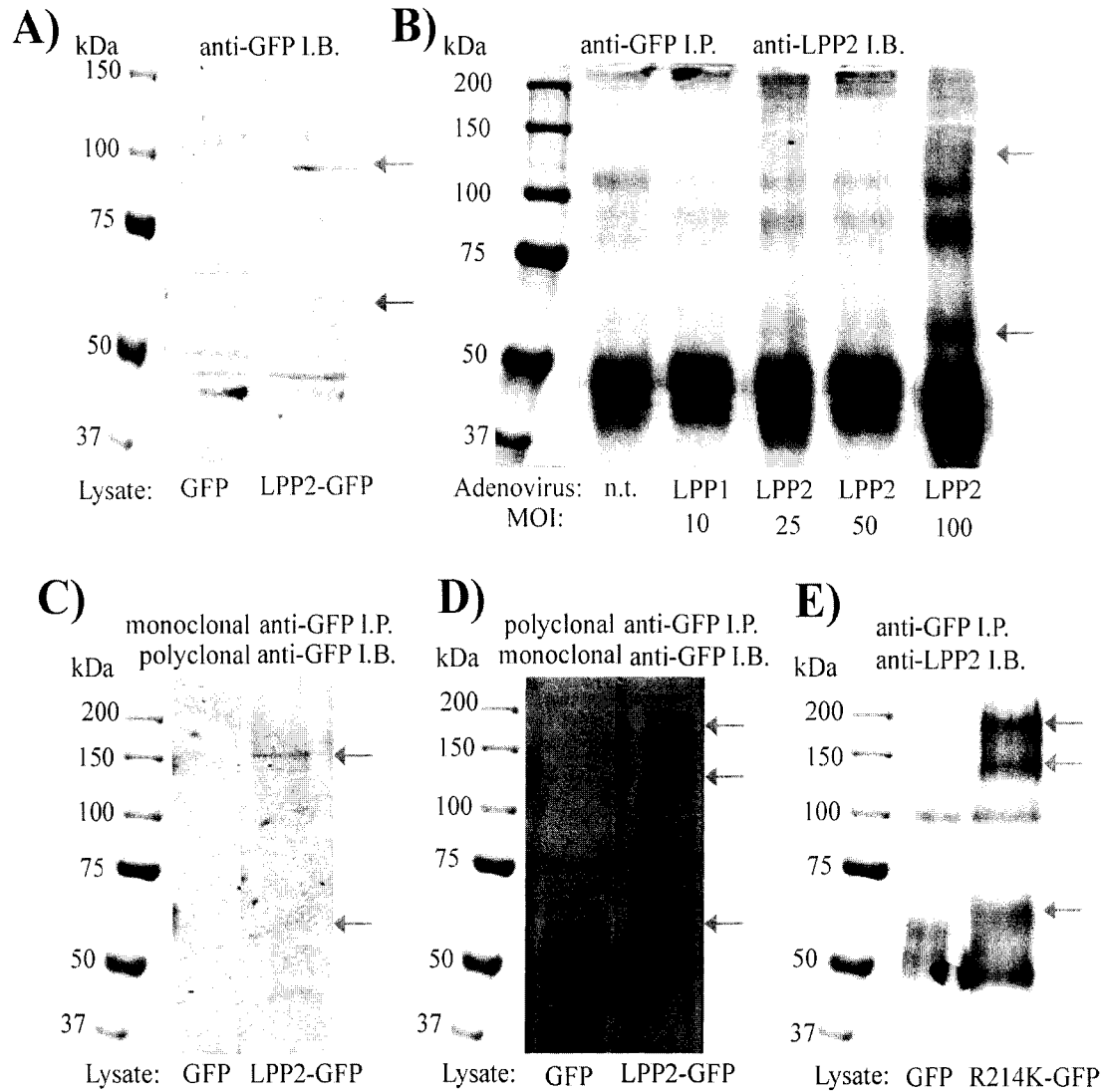


**Figure 3.4. Expression of the LPP2-GFP protein.** Panels A-E show Western blots scanned on the Odyssey™ imager at 700 nm for anti-mouse or 800 nm for anti-rabbit secondary antibodies. Panel A shows lysates from cells stably transduced with GFP or LPP2-GFP. Panel B shows anti-GFP immunoprecipitates from uninfected rat2 fibroblasts (n.t.) or those infected with the indicated concentrations of myc-mLPP1 or LPP2-GFP adenovirus. Panel C shows lysates from cells stably transduced with GFP or LPP2-GFP and immunoprecipitated with mouse monoclonal anti-GFP. Panels D and E show lysates from cells stably transduced with GFP, LPP2-GFP, or LPP2[R214K]-GFP and immunoprecipitated with rabbit polyclonal anti-GFP. Membranes were incubated with rabbit polyclonal anti-GFP at 1:1000 in panels A and C, with mouse monoclonal anti-GFP at 1:500 in panel D, and with rabbit polyclonal anti-LPP2 at 1:100 in panels B and E. The 50 kDa bands in panels B and E are rabbit IgG. Molecular mass markers are shown in the left-most lane on each blot. Arrows indicate bands that may represent the LPP2 protein. Results are each one independent experiment

### 3.2.3. *The subcellular localization of LPP2-GFP*

3.2.3.1. *The localization of wild-type and mutant LPP2-GFP are highly similar* – Cells transduced with GFP, LPP2-GFP, or LPP2 [R214K]-GFP were fixed and stained with an affinity-purified anti-GFP antibody to visualize the recombinant proteins with a confocal microscope. Cells transduced with GFP expressed the GFP protein, and its localization was primarily cytoplasmic and distributed evenly throughout the entire cell (Fig. 3.5A). In contrast, the LPP2-GFP protein was expressed in the plasma membrane, and in intracellular membranes in a punctate pattern with the most pronounced staining in the paranuclear region (Fig. 3.5A). Mutant LPP2 [R214K]-GFP had an indistinguishable localization pattern from the wild-type enzyme (Fig. 3.5A). Additionally, based on the intensity of fluorescence, the wild-type and mutant proteins seemed to be expressed to a similar level. These results confirmed that the GFP-tagged proteins were expressed and that they associated with membranes at expected. Additionally, these results justified the use of the mutant to distinguish the catalytic from non-catalytic functions of LPP2, since the mutation did not appear to affect the expression level or localization of the protein.

3.2.3.2. *LPP2 co-localizes with markers for the plasma membrane, early endosomes, and endoplasmic reticulum, and is excluded from the nucleus* – To determine which membranes LPP2 was localized in, cells overexpressing LPP2-GFP and LPP2 [R214K]-GFP were fixed and stained with anti-GFP and antibodies to various organelle markers. Confocal microscopy was used to look at slices through the cells to evaluate co-localization. LPP2-GFP and LPP2

[R214K]-GFP co-localized with early endosome antigen-1 in endosomes (Fig. 3.5B) and with caveolin-1 on the plasma membrane and in intracellular membranes (Fig. 3.5C). LPP2 also co-localized partially with the endoplasmic reticulum marker, calreticulin (Fig. 3.5D). LPP2 did not co-localize significantly with giantin in the Golgi apparatus or cytochrome C in the mitochondria (not shown). LPP2 also did not co-localize with lamin A in the nuclear membrane (Fig. 3.5E), or with the DNA stain Hoescht 33258 in the nucleus (not shown). It did appear superficially that there was some immunofluorescence from LPP2-GFP in the nucleus (Fig. 3.5). However, when the pinhole size was reduced from 1 AU to 0.6 AU and the focus was adjusted to optimize viewing of the center of the cell and the nuclear membrane, the apparent nuclear localization of LPP2-GFP was eliminated. Additionally, when slices through the images were evaluated as histograms using LSM5 software, the peaks of fluorescence for Lamin A did not coincide with the peaks of fluorescence for LPP2-GFP. Therefore, although there may be a very small amount of nuclear localization of LPP2-GFP, we concluded that there was not a substantial co-localization of LPP2 with the nuclear envelope or nucleus. The apparent nuclear localization of LPP2-GFP is most likely an artifact derived from coincidental staining due to the focus used to optimize organelle marker and plasma membrane fluorescence. These results indicate that the most likely sites of action for the LPP2 protein are the plasma membrane, the endosomes, and the ER. Additionally, it is likely that LPP2 is present in caveolin-rich regions of the plasma membrane as has been described previously for LPP1 and LPP3 [49].

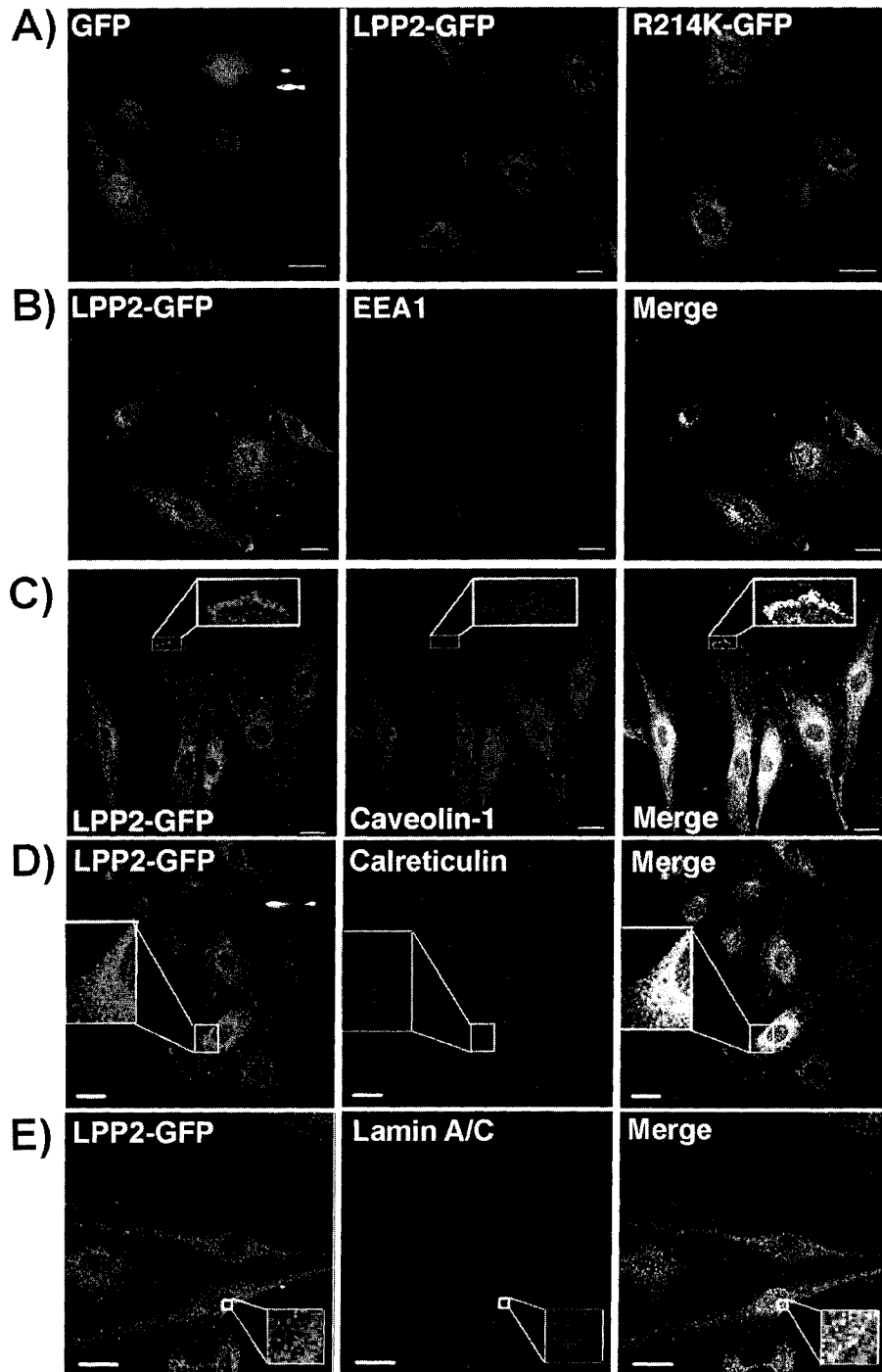


**Figure 3.5. Localization of LPP2 and LPP2[R214K] in rat2 fibroblasts.** Fibroblasts that were stably transduced with GFP, LPP2-GFP, and LPP2[R214K]-GFP were grown on coverslips and fixed. GFP was detected using polyclonal goat anti-GFP and Alexa 488 anti-Goat. Early endosome antigen-1, caveolin-1, calreticulin, and lamin A were detected with rabbit anti-EEA1, rabbit anti-caveolin-1, rabbit anti-calreticulin, and rabbit anti-lamin A/C respectively, and with Alexa 594 anti-Rabbit. Panels depict typical cells from 4 independent experiments. The bars represent 20  $\mu$ M and the insets were magnified 4 times more in Panels C-D and 5 times more in Panel E.

### 3.2.4. *LPP activities in cells stably overexpressing the LPPs*

#### 3.2.4.1. *The activities of lysates from cells overexpressing the*

*LPPs toward PA* – Lysates from rat2 fibroblasts stably overexpressing the LPPs were assayed for LPP activity toward PA in Triton X-100 micelles. The activity measured was the sum of LPP activities in the lysate. Cells stably overexpressing LPP1 and LPP3 had 3.9- and 2.2-fold increases in total LPP activity, respectively, compared to parental fibroblasts or those transduced with the empty vector (Fig. 3.6A). Cells overexpressing LPP2 and LPP2-GFP had 2.9- and 2.2-fold increases in LPP activity, respectively (Fig. 3.6A). Cells transduced with LPP2 [R214K]-GFP showed a consistent decrease in LPP activity, compared to parental cells or those transduced with the empty vector, suggesting a possible dominant-negative effect, but this decrease was not statistically significant (Fig. 3.6A). In cells stably overexpressing LPP2, the addition of control non-targeting siRNAs did not alter the LPP activity of the cells, but the addition of siRNAs for human LPP2 that knocked down mRNA overexpression by 60% reduced the total LPP activity to a level not statistically different from controls (Fig. 3.6A).

#### 3.2.4.2. *The LPP activities of lysates from cells overexpressing the*

*LPPs toward LPA and SIP* – The LPP activities of cell lysates in Triton X-100 micelles were also measured using LPA and SIP as substrates. Cells overexpressing LPP1 had a 4-fold increase in LPP activity toward LPA, and a 50% decrease in activity toward SIP (Fig. 3.6B). Cells overexpressing LPP2 had no change in activity toward LPA and a 5-fold increase in activity toward SIP (Fig. 3.6B). Cells overexpressing LPP3 had a 3-fold increase in activity toward

LPA and a 13-fold increase in activity toward S1P (Fig. 3.6B). These results indicate that LPP1 overexpression increases the hydrolysis of LPA and PA, but not S1P, LPP2 overexpression increases the hydrolysis of PA and S1P, but not LPA, and LPP3 overexpression increases the hydrolysis of PA, LPA, and S1P.

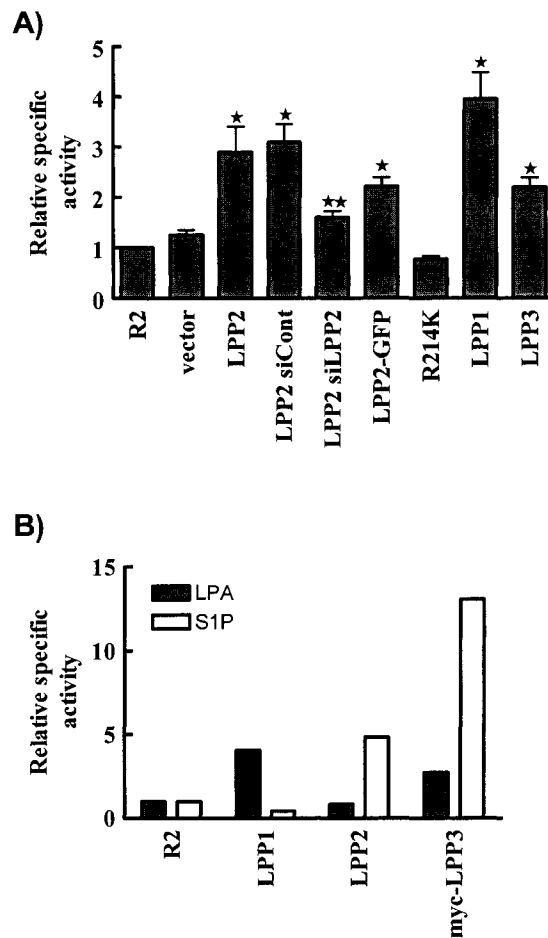


**Figure 3.6. Total LPP activity in Triton X-100 micelles of lysates from cells overexpressing the LPPs.** Panel A shows the activity toward PA of lysates from rat2 fibroblasts (R2) or those stably transduced with the empty vector, LPP2, LPP2-GFP, LPP2[R214K]-GFP, LPP1, or LPP3. In some cases cells that stably overexpressed LPP2 were transfected with siRNAs for non-targeting control (siCont) or hLPP2 (siLPP2). Results are means  $\pm$  SD from at least 4 independent experiments. Statistically significant differences ( $p < 0.05$ ) from control and from LPP2 siCont are indicated by \* and \*\*, respectively. Panel B shows the activity of lysates from rat2 cells (R2) or those stably transduced with mLPP1, hLPP2, or myc-rLPP3 toward LPA or S1P, indicated in black or white bars, respectively. Results are from one representative of two experiments.

#### 3.2.4.3. *The LPP activities of cells infected with adenovirus for*

*LPP2-GFP* – The total LPP activity of lysates toward PA was measured in cells that were infected with various MOI of adenovirus vectors expressing LPP2-GFP. Compared to uninfected cells, cells infected with 50-500 pfu/cell of adenovirus expressing LPP2-GFP had between 1.4- and 2-fold increases in total LPP activity (Fig. 3.7A). The peak of total activity occurred at MOIs of 150-200 pfu/cell (Fig. 3.7A). Therefore, even though the level of mRNA overexpression for LPP2 produced by adenoviral infection was much higher than levels produced by stable transduction (Fig. 3.1), the resulting changes to the total LPP activity in lysates were similar. When anti-GFP immunoprecipitates from cells infected with LPP2-GFP adenovirus were assayed for activity, the LPP activity of the immunoprecipitates increased with increasing multiplicity of infection (pfu/cell) (Fig. 3.7B). These results indicate that increasing the MOI of LPP2-GFP adenovirus results in the expression of increasing amounts of immunoreactive enzymatically active LPP2-GFP protein. We previously observed that increasing MOIs resulted in increasing LPP2 mRNA expression (Fig. 3.1D). Interestingly, although the amount of immunoprecipitated LPP2-GFP activity increased with increasing MOI, this did not translate into increases in overall LPP activity in the lysates (Fig. 3.7A). Furthermore, although mRNA expression levels of LPP2 after adenoviral transfection were in excess of 100-fold above controls in cells infected with 100 pfu/cell or more (Fig. 3.1D), the activity of immunoprecipitates from these cells was comparable to those from stably transfected cells with less than 40-fold increases in LPP2 mRNA (Fig. 3.7B and Fig 3.8B). Therefore, it



appears that fibroblasts are able to regulate the amount of total LPP activity in cells. Thus, higher levels of mRNA expression for LPP2 does not translate directly into higher expression of functional and active LPP2 protein, and does not necessarily result in increases in overall cellular LPP activity. This suggests that the activity of the LPPs may be regulated post-translationally or post-transcriptionally.

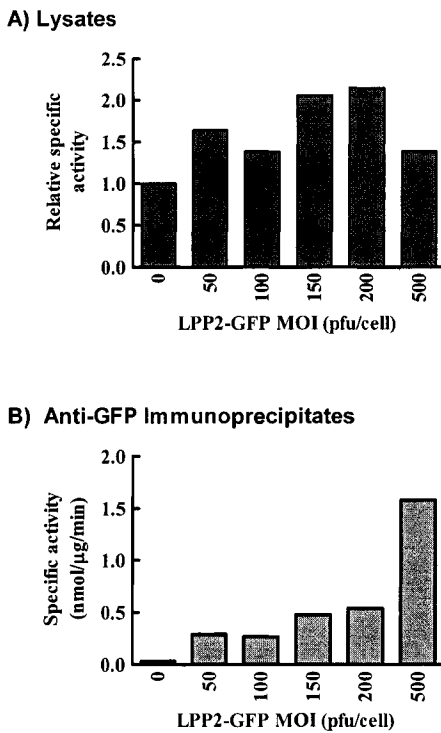


**Figure 3.7. Total activity of lysates and immunoprecipitates from cells infected with adenovirus for LPP2-GFP.** Panel A shows LPP activity toward PA in rat2 cells infected with the indicated amounts of adenovirus for LPP2-GFP. Results are from one representative of two independent experiments. Panel B shows the activity of anti-GFP immunoprecipitates from cells infected with the indicated amounts of adenovirus for LPP2-GFP. Results are from one experiment.

#### 3.2.4.4. *The activity of immunoprecipitated LPP2-* The GFP-tagged

constructs were immunoprecipitated and assayed for LPP activity to confirm that functional and enzymatically active LPP2-GFP was expressed in fibroblasts.

Anti-GFP immunoprecipitates from cells transduced with GFP, LPP2-GFP, and

LPP2 [R214K]-GFP were assayed for activity toward PA. The anti-GFP immunoprecipitate from cells transduced with LPP2-GFP was active, and its LPP activity increased with the amount of lysate immunoprecipitated (Fig. 3.8A). In contrast, immunoprecipitates from cells stably transduced with GFP alone did not show increased activity with increasing amount of lysate immunoprecipitated (Fig. 3.8A). This demonstrates that an active LPP2-GFP fusion protein was expressed in the stably transduced cells. Surprisingly, anti-GFP immunoprecipitates from cells transduced with LPP2 [R214K]-GFP also showed LPP activity (Fig. 3.8B). One explanation for this is that the mutant protein was active, but had a reduced level of activity. It is unlikely that the mutant protein itself could catalyze the hydrolysis of PA, since the residue that was mutated is predicted to have a critical role in forming hydrogen bonds with the phosphate group of the substrate to stabilize the complex during catalysis (Chapter 1). Furthermore, when the equivalent arginine was mutated to lysine in LPP1, the mutation decreased the activity of the enzyme by 98% [44]. Therefore, the most likely explanation for this result is that LPP2 [R214K]-GFP co-immunoprecipitated an active lipid phosphatase. It has been reported that the LPPs homodimerize but do not heterodimerize [56]. Western blots of immunoprecipitates from cells transduced with LPP2 [R214K]-GFP showed high molecular mass bands when probed with anti-LPP2 antibodies (Fig. 3.4E). These could be multimers composed of mutant LPP2-GFP and endogenous LPPs. Additionally, these could be complexes from detergent-resistant microdomains that contain both LPP2 [R214K]-GFP and endogenous LPP activities. Therefore

the activity in the immunoprecipitate could be attributed to co-immunoprecipitated endogenous LPP2, or endogenous LPP1 or LPP3.

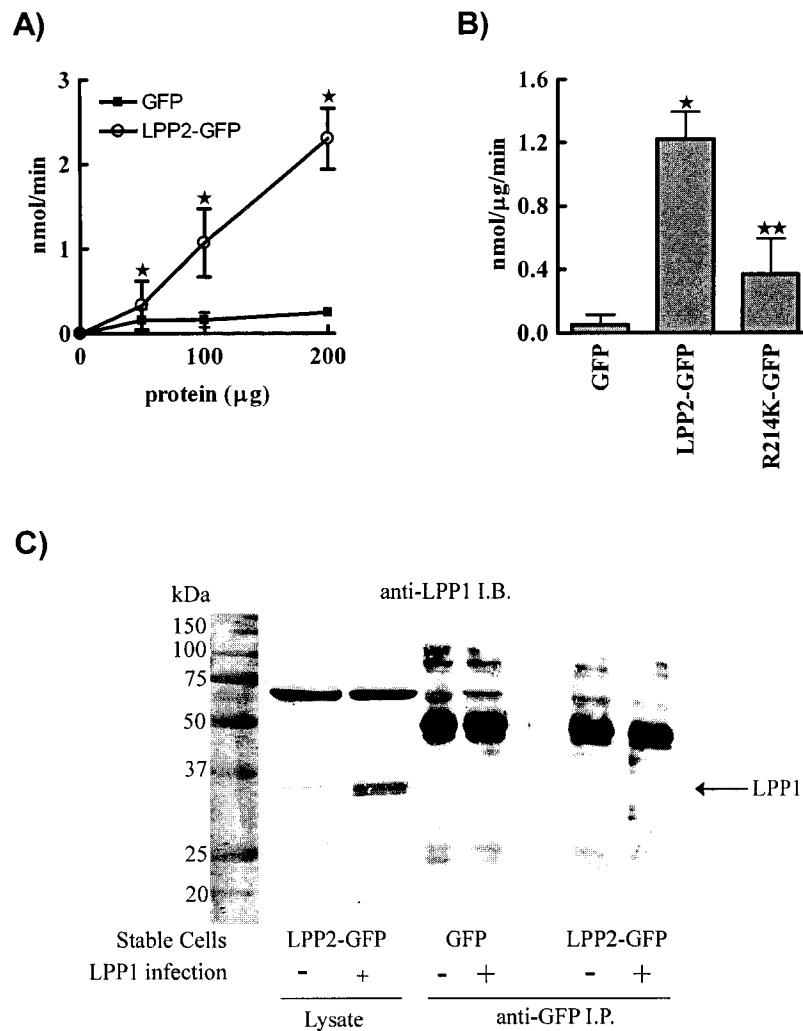


**Figure 3.8. Total activity of immunoprecipitates from cells overexpressing the LPPs. LPP2 does not co-immunoprecipitate LPP1.** Panel A shows the activity toward PA of anti-GFP immunoprecipitates that were obtained by treating the indicated amount of lysate protein from cells stably transduced with GFP or LPP2-GFP. Results are means  $\pm$  SD from 3 independent experiments. Statistically significant differences ( $p < 0.05$ ) from control are indicated by \*. Panel B shows the activity of anti-GFP immunoprecipitates from cells stably transduced with GFP, LPP2-GFP, or LPP2[R214K]-GFP. Results are means  $\pm$  SD from at least 3 independent experiments. Statistically significant differences ( $p < 0.05$ ) from control and from both control and LPP2-GFP are indicated by \* and \*\*, respectively. Panel C shows a Western blot of lysates and anti-GFP immunoprecipitates from cells stably transduced with GFP or LPP2-GFP that were uninfected or infected with 12 pfu/cell myc-LPP1 adenovirus. The membrane was blotted with anti-mLPP1 and scanned on the Odyssey™ imager at 800 nm to detect the secondary antibody. The result is from one experiment. The 35 kDa band representing myc-LPP1 is indicated by the arrow. The band at 50 kDa represent rabbit IgG. The band at ~70 kDa is an unknown non-specific band that interacts with the anti-LPP1 antibody.

3.2.4.5. *LPP2 does not co-immunoprecipitate LPP1* – The isoform responsible for the majority of the LPP activity and the most highly expressed LPP in rat2 fibroblasts is LPP1 (Figure 3.1 and results shown later in this Chapter). Therefore, endogenous LPP1 would be the most likely protein to have been co-immunoprecipitated with LPP2 [R214K]-GFP. We investigated the possibility that LPP2 co-immunoprecipitated LPP1. We optimized the possibility of heterodimer formation and of detecting a possible interaction by transfecting cells that stably overexpressed LPP2-GFP with myc-LPP1 adenovirus. Anti-GFP immunoprecipitates were collected from cells that were stably transduced with GFP or LPP2-GFP with and without myc-LPP1 adenoviral infection, and the presence of LPP activity in the LPP2-GFP immunoprecipitates was confirmed. Immunoprecipitates were analyzed by SDS-PAGE and blotted with anti-myc and anti-LPP1 to detect any co-immunoprecipitated LPP1 protein. In lysates from cells that were stably overexpressing LPP2 and infected with myc-LPP1 adenovirus, but not lysates from uninfected cells, a 35 kDa doublet was detected with an anti-LPP1 antibody, confirming that LPP1 was overexpressed (Fig. 3.8C). Anti-GFP immunoprecipitates from cells stably transduced with GFP or LPP2-GFP and infected with adenovirus for myc-LPP1 did not have an immunoreactive band at 35 kDa, indicating that neither GFP alone, nor LPP2-GFP co-immunoprecipitated the LPP1 protein (Fig. 3.8C). There were also no high molecular mass bands in the lanes from LPP2-GFP immunoprecipitates that were absent from the anti-GFP immunoprecipitates (Fig. 3.8C). Therefore, there is no evidence that high molecular mass aggregates from LPP1/ LPP2 heterodimers or

from complexes containing LPP1 were immunoprecipitated. Therefore, it is more likely that the activity in immunoprecipitates from LPP2 [R214K]-GFP transduced cells was due to co-immunoprecipitated endogenous LPP2.

3.2.4.6. *Ecto activity in cells overexpressing the LPPs* – The extracellular hydrolysis of LPA and S1P was measured in fibroblasts that stably overexpressed the LPPs. Cells overexpressing LPP1 had a 1.9-fold increase in ecto activity toward LPA compared to parental fibroblasts (Fig. 3.9A). Cells overexpressing LPP3 showed no significant change in LPA hydrolysis, while cells overexpressing catalytically active or inactive LPP2 had decreased extracellular LPA hydrolysis by ~50% (Fig. 3.9A,C). Cells overexpressing LPP3 had increased ecto activity toward S1P by 2-fold compared to control fibroblasts (Fig. 3.9B). Cells overexpressing LPP1 may have slightly increased S1P hydrolysis, but the change was not statistically significant (Fig. 3.9B). Cells overexpressing LPP2 or LPP2 [R214K] had decreased extracellular hydrolysis of S1P by ~50% (Fig. 3.9B). These results suggest that LPP1 is mainly responsible for the extracellular hydrolysis of LPA in fibroblasts, whereas LPP3 is mainly responsible for the extracellular hydrolysis of S1P. The hydrolysis of both LPA and S1P appears to be antagonized by LPP2 overexpression, and this appears to be a non-catalytic function of LPP2. To evaluate whether LPP2 could inhibit ecto activity in a dose-dependent manner, the effect of the adenoviral overexpression of LPP2-GFP on ecto activity was evaluated. The inhibition of LPA hydrolysis increased with increasing MOI of adenovirus for LPP2-GFP (Fig. 3.9D). Increasing the MOI of adenovirus for the empty vector did not affect ecto activity,

while ecto activity toward LPA increased with increasing MOI of adenovirus for myc-LPP1 (Fig. 3.9D). These results indicate that the increases and decreases in the extracellular hydrolysis of LPA produced by LPP1 and LPP2 overexpression, respectively, are dependent on the expression levels of the two enzymes and can be regulated by changing the relative levels of the LPPs in fibroblasts.

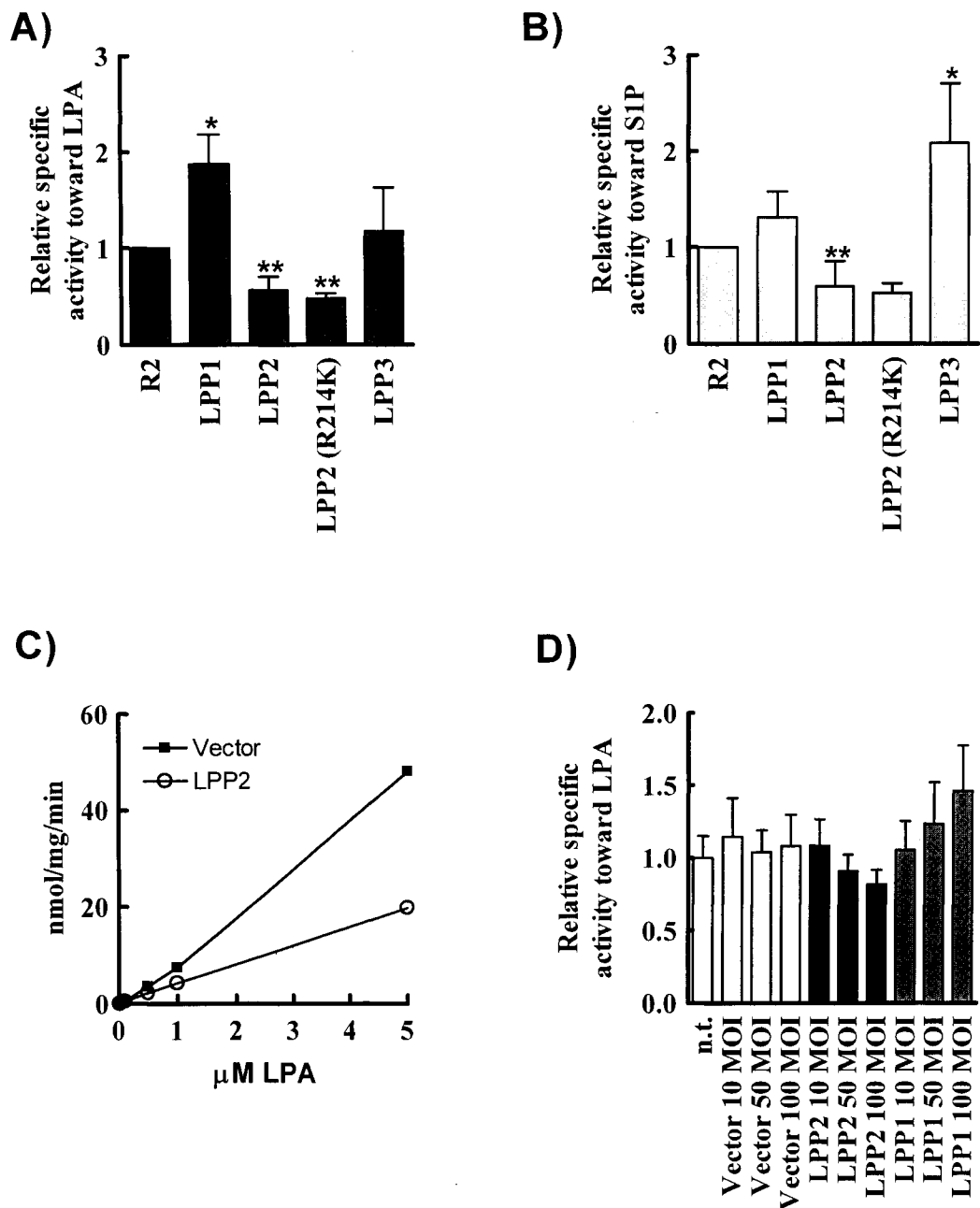


**Figure 3.9. Ecto activity of cells overexpressing the LPPs.** Panels A and B show the extracellular hydrolysis of LPA and S1P, respectively, in rat2 cells (R2) or those stably transduced with mLPP1, hLPP2, hLPP2[R214K], or rLPP3. Activity is expressed relative to the activity in rat2 cells which is given as 1. Results are means  $\pm$  SD from at least 3 independent experiments. Statistically significant increases and decreases from rat2 are indicated by \* and \*\*, respectively. Panel C shows the ecto activity of fibroblasts stably transduced with empty vector or LPP2 toward the indicated concentrations of LPA. Results are from one representative of 3 independent experiments. Panel D shows the ecto activity toward LPA of uninfected rat2 cells (n.t.) and those infected with the indicated MOI (pfu/cell) of vector control, LPP2-GFP, or myc-LPP1 adenovirus. Results are from one experiment.

*3.2.5. The effects of LPP overexpression on bulk cellular lipid concentrations and ERK activation*

*3.2.5.1. LPP2 overexpression does not change bulk cellular PA, DAG, or LPA concentrations* – It has been previously shown that the overexpression of the LPPs can change the bulk concentrations of PA and alter the PA: DAG ratio in some cells [45, 46]. Other investigators in the laboratory have demonstrated that bulk cellular PA is decreased in rat2 fibroblasts that stably overexpress LPP1 (C. Pilquill, unpublished). To determine whether the stable overexpression of LPP2 in our fibroblasts changed the bulk concentrations of PA, DAG, or LPA, cell extracts from overexpressing cells were collected and bulk lipid concentrations were measured. The stable overexpression of LPP2 did not produce significant changes in the concentrations of bulk PA, DAG, or LPA in rat2 fibroblasts (Fig. 3.10A).

*3.2.5.2. LPP2 overexpression does not attenuate the activity of ERK* – It has been previously shown that overexpression of the LPPs can attenuate the activation of ERK by LPA and other G-protein coupled receptor agonists [39, 45]. Other investigators in our laboratory have demonstrated that LPP1 overexpression can significantly decrease the phosphorylation of ERK downstream of LPA signaling in rat2 fibroblasts (C. Pilquill, unpublished). To investigate whether the overexpression of LPP2 attenuated signaling to ERK in fibroblasts, Western blots were performed to measure the phosphorylation of ERK after stimulation of cells with LPA. SIP was not used as an agonist since it



does not promote ERK phosphorylation in rat2 fibroblasts. In three separate experiments, the overall amount of phosphorylated p42/44 MAPK following LPA stimulation was not significantly different in LPP2 overexpressing cells compared to control cells (Fig. 3.10B). It did appear that LPP2 overexpression may have delayed the activation of ERK by approximately 10 min. However, there were no significant changes that were consistent between experiments in the total amount of phosphorylated ERK in LPP2 overexpressing cells compared to control cells at any given time. Therefore, the level of overexpression of LPP2 achieved in our fibroblasts did not alter the intracellular PA: DAG ratio, and did not decrease the amount of LPA-dependent ERK activation.

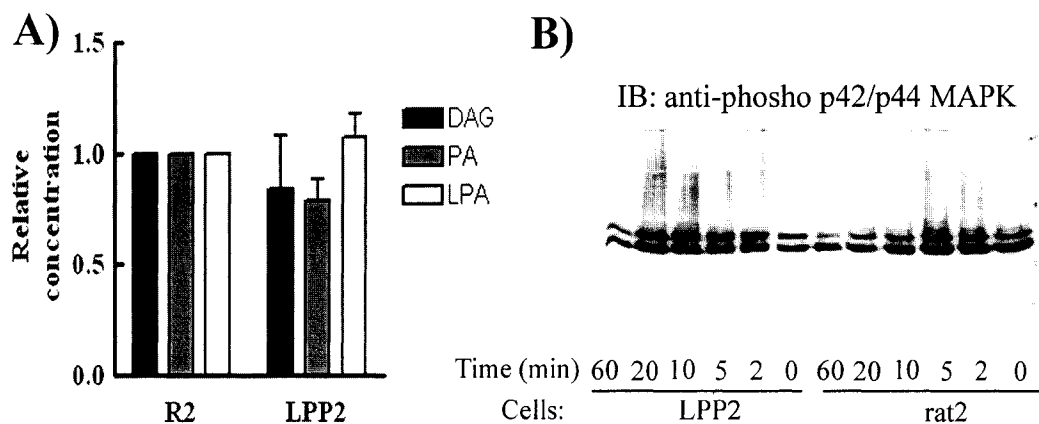


**Figure 3.10. LPP2 overexpression does not change the bulk concentrations of PA, DAG, or LPA, or attenuate ERK activation in fibroblasts.** Panel A shows the bulk concentrations of DAG, PA, and LPA, in rat2 cells (R2) or those stably transduced with hLPP2. Concentrations are expressed relative to those in rat2 cells which are given as 1. Results are means  $\pm$  SD from at least 3 independent experiments. Panel B shows a Western blot with lysates from rat2 cells or those stably transduced with LPP2 that have been treated for the indicated amount of time with 10  $\mu$ M LPA. The membrane was blotted with anti-phospho p42/44 MAPK and scanned on the Odyssey<sup>TM</sup> imager. Results are one representative of 3 independent experiments.

### 3.3. Knock-down of the LPPs in rat2 fibroblasts

#### 3.3.1. *Changes in mRNA expression produced by knocking down the LPPs*

3.3.1.1. *Each LPP was knocked down by approximately 60% with siRNAs* – To complement the overexpression studies, and to directly evaluate the functions of LPP2 in fibroblasts, siRNA technology was used to specifically knock-down the expression of each of the LPP isoforms. A mixture of four small interfering RNA duplexes designed for the rat sequence of each of the LPPs were transfected into fibroblasts to specifically knock down the expression of each LPP. Cells transfected with siRNAs for rat LPP2 showed a 61% decrease in the expression of LPP2 mRNA on average (Fig. 3.11A). Fibroblasts that were transfected with siRNAs for rat LPP1 and rat LPP3 showed 52% and 57% decreases in LPP1 mRNA and LPP3 mRNA expression, respectively, on average (Fig. 3.11C). Therefore, the endogenous expression of each of the LPPs could be decreased by 50-60%, using siRNA in rat2 fibroblasts.

3.3.1.2. *Knock-down of LPP2 is maintained at a maximal level between 24 and 72 hours* – To determine how long the LPP2 knock-down maintained its efficacy, mRNA levels were measured for 120 h after transfection. A 50% knock-down of LPP2 was achieved by 24 h after transfection with siRNAs, and was maintained until 72 h after transfection, with the maximum knock-down occurring approximately 48 h after transfection (Fig. 3.11B). After 120 h of transfection, LPP2 mRNA levels had recovered to the endogenous level (Fig. 3.11B). In subsequent experiments, all measurements were performed between 24 and 72 h after siRNA transfections.

3.3.1.3. *The knock-down of each LPP isoform does not affect the mRNA expression of the other isoforms* – The mRNA expression level of each of the LPPs was measured in cells in which each LPP had been knocked down to confirm that the siRNA effects were specific for each isoform. Knocking down rat LPP2 by ~60% did not significantly change the mRNA expression of LPP1 or LPP3 (Fig. 3.11C). Similarly, knocking down LPP1 by ~50% did not significantly change the mRNA expression of LPP2 or LPP3, and knocking down LPP3 by ~50% did not significantly change the mRNA expression of LPP1 or LPP1 (Fig. 3.11A,C). Therefore, knocking down the endogenous expression of any of the LPPs did not change the mRNA expression of the other isoforms, and the knock-downs were specific for each isoform. As a result, we could use knock-downs produced by siRNA transfection to evaluate the endogenous role of each LPP isoform in fibroblasts.

### 3.3.2. *LPP activities in cells with the LPPs knocked down*

3.3.2.1. *Knock-down of LPP1, but not LPP2 or LPP3, decreases total LPP activity in fibroblasts* – The LPP activity toward PA was measured in lysates from cells with each LPP knocked down. The knock-down of LPP1 mRNA by ~50% resulted in a ~50% decrease in LPP activity in cell lysates (Fig. 3.11D). In contrast, the ~60% and ~55% knock-downs of LPP2 and LPP3 mRNA expression did not change the total LPP activity in cell lysates significantly (Fig. 3.11D). These results strongly suggest that LPP1 is responsible for most of the endogenous LPP activity toward PA in fibroblasts.

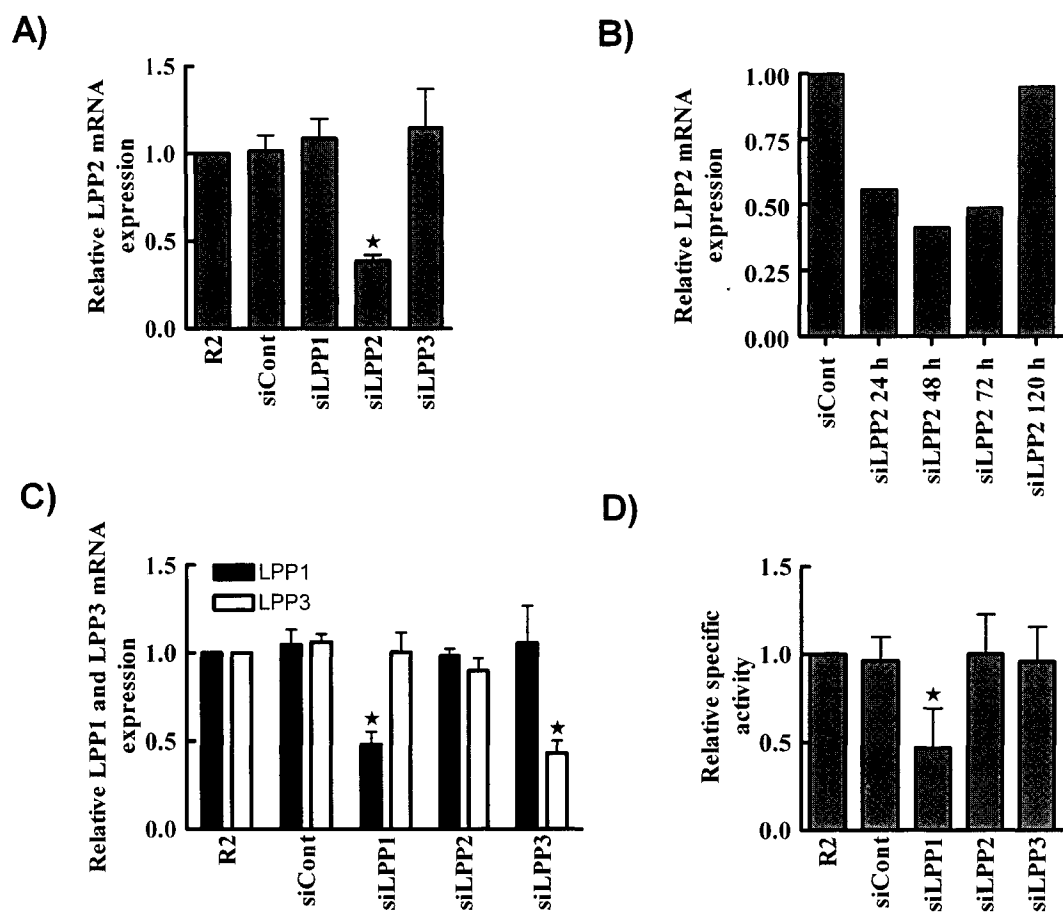


**Figure 3.11. The LPP mRNA expression and LPP activity of cells treated with siRNAs for the LPPs.** Panels A and C show mRNA concentrations of the indicated target for untreated parental fibroblasts (R2) or cells treated with siRNAs for non-targeting control, or rat LPP1, LPP2, or LPP3. mRNA concentrations are normalized to that of the housekeeping gene, cyclophilin A. Results are expressed as fold change compared to rat2 fibroblasts which is given as 1. Results are means  $\pm$  SD from at least 4 independent experiments. Statistically significant differences ( $p < 0.05$ ) from control are indicated by \*. Panel B shows LPP2 mRNA concentrations in rat2 fibroblasts treated with non-targeting control or rat LPP2 siRNAs for the indicated times. mRNA concentrations are normalized to that of the housekeeping gene, cyclophilin A. Results are from one experiment. Panel D shows LPP activities toward PA in parental rat2 fibroblasts (R2) or those transfected with siRNAs for non-targeting control (siCont) or for rat LPP1, LPP2, or LPP3. Results are expressed as fold change compared to rat2 fibroblasts (R2) which is given as 1. Results are means  $\pm$  SD from at least 3 independent experiments. Statistically significant differences ( $p < 0.05$ ) from control are indicated by \*.

### 3.4. Discussion

To evaluate the role of LPP2 in fibroblasts, cells lines were created that stably overexpressed untagged, GFP-tagged, and catalytically inactive LPP2. The C-terminal GFP tag did not significantly change the mRNA expression level or LPP activity of the LPP2 enzyme, and it enabled us to immunoprecipitate LPP2 and visualize the tagged protein using confocal microscopy. The R214K point mutant was expressed to a similar level as wild-type LPP2 in terms of mRNA, and was not mislocalized. Adenovirus was used to produce high levels of transient overexpression of LPP2, and siRNA was used to reverse LPP2 overexpression in stable cell lines and to decrease the expression of endogenous LPP2 by ~60% in parental fibroblasts. LPP1 and LPP3 were overexpressed and knocked down in parallel with LPP2 so that the effects of each of the three isoforms could be compared.

In fibroblasts that stably overexpressed the LPPs, the levels of mRNA overexpression were approximately 10-fold for LPP1 and approximately 40- and 50-fold for LPP2 and LPP3, respectively. Since we did not have antibodies that detected the endogenous rat LPP1 or LPP2 proteins, the corresponding levels of protein overexpression could not be estimated. Using antibodies for the rat LPP3 protein, it was estimated that there was approximately a 10-fold overexpression of protein that corresponded to the 50-fold increase in mRNA expression. LPP1 appears to be the most abundant endogenous isoform in rat2 fibroblasts. This assumption can be made based on the primer efficiencies from RT-PCR, and based on the fact that only the knock-down of endogenous LPP1 changed the

overall LPP activity in cells. In addition, the fact that LPP1 was only overexpressed 10-fold, whereas LPP2 and LPP3 were expressed 40 to 50-fold using the same protocols, implies that the endogenous expression of LPP1 may have been higher. The low abundance of LPP2 indicated by RT-PCR suggests that it is not likely to have a role in maintaining bulk cellular phospholipid concentrations in fibroblasts. Additionally, LPP2 overexpression did not change the concentrations of PA, DAG, or LPA in the fibroblasts, and the knock-down of endogenous LPP2 by ~60% did not significantly change the amount of total cellular LPP activity toward PA.

The overexpression of all three LPP isoforms increased the hydrolysis of PA in Triton X-100 micelles by 2- to 4-fold, with LPP1 overexpression having the greatest effect on PA hydrolysis, and LPP3 overexpression the smallest effect. LPP1 overexpression also increased the hydrolysis of LPA in Triton X-100 micelles and in an ecto assay, whereas it did not increase S1P hydrolysis in either assay. LPP2 overexpression increased S1P, but not LPA hydrolysis in Triton X-100 micelles, and decreased the extracellular hydrolysis of both substrates. LPP3 overexpression increased both S1P and LPA hydrolysis in Triton X-100 micelles and increased S1P hydrolysis in ecto activity assays. These results suggest that LPP1 is active on the cell surface, and has a substrate preference for PA and LPA, but is not effective at degrading S1P. LPP3 is likely active on the cell surface, degrades PA, LPA, and S1P, and appears to have a strong preference for S1P. LPP2 degrades both PA and S1P in Triton X-100 micelles, but does not hydrolyze LPA, and does not increase ecto activity on the cell surface. It is evident from

these studies that the three LPP isoforms have different substrate preferences, and different sites of activity in fibroblasts.

Surprisingly, anti-GFP immunoprecipitates from cells transduced with LPP2 [R214K]-GFP had LPP activity. This raises the possibility that the mutant version of LPP2 could be somewhat catalytically active. This is unlikely since mutating the equivalent arginine residue to lysine in LPP1 abolished the activity of the enzyme [44]. However, it is possible that the active site conformation of LPP2 could be slightly different from that of LPP1, and a lysine residue could at least partially substitute for the arginine and stabilize the interaction between the phosphate group of the substrate in LPP2, but not in LPP1. Casting doubt on this possibility are the observations that the stable transduction of LPP2 [R214K] does not increase the total LPP activity in lysates, does not produce effects on the cell cycle (discussed in Chapter 4), and appears to exhibit a dominant-negative effect in regulating MMP2 expression (discussed in Chapter 6). Another possible explanation for the LPP activity in the LPP2 [R214K]-GFP immunoprecipitates is that LPP2 [R214K] co-immunoprecipitated an active lipid phosphatase. This possibility is supported by the fact that Western blots of LPP2 [R214K]-GFP immunoprecipitates show high molecular mass aggregates that are immunoreactive to anti-LPP2 antibodies. Therefore, it is probable that the activity in the LPP2 [R214K]-GFP immunoprecipitates could be attributed to a co-immunoprecipitated lipid phosphate phosphatase.

It has been reported that LPP1 and LPP3 form homodimers, but not heterodimers [56]. It has also been suggested that LPP2 forms active multimers

[159]. Studies on the *Drosophila* LPP3 orthologue wunen-1 suggested that the C-terminus of the enzyme and the catalytic activity might be required for homodimerization [56]. The assumption that activity was required for dimerization was based on the fact that a D248T mutation in the active site that abolished activity also prevented dimer formation. The authors acknowledged that other residues would have to be mutated to determine whether it was the absence of activity or the mutation of the specific residue that resulted in a loss of dimerization. Our results suggest that the R214K mutation, a mutation in the same third conserved domain but a more conservative mutation in terms of charge, does not prevent LPP2 from being present in high molecular mass complexes on Western blots. The point mutation of LPP2 did not allow monomeric LPP2 to be resolved on SDS-PAGE, and immunoprecipitates from cells transduced with LPP2 [R214K]-GFP showed aggregates on Western blots, at the same molecular masses as immunoprecipitates from cells transduced with LPP2-GFP. Interestingly, we also used a large C-terminal GFP tag, that did not appear to prevent LPP2 from being present in high molecular mass species. Therefore, the requirements for multimerization of LPP2 may be different from the requirements for dimerization of wunen-1, or the high molecular mass aggregates containing LPP2 that we observed on Western blots may not have been dimers.

We could not detect the formation of LPP2/ LPP1 heterodimers or LPP2/ LPP1 multimeric complexes, even when we optimized conditions to detect a possible interactions between the isoforms. This agrees with previous reports that



the LPPs homodimerize but do not heterodimerize [56]. We did not test whether LPP2 and LPP3 heterodimerize since LPP3 has a much lower endogenous expression than LPP1, and since we had no adenovirus for myc-LPP3. Therefore, we cannot exclude the possibility that LPP2 binds LPP3. However, it is more likely that LPP2 homodimerizes, and that the high molecular mass bands on the Western blots from LPP2 [R214K]-GFP transduced cells resulted from R214K/R214K homodimers, while the activity in the immunoprecipitates was a result of the less abundant R214K/ endogenous LPP2 dimers. These dimers would form with much lower abundance than R214K/ R214K dimers due to the low endogenous expression of LPP2. The amount of activity in the immunoprecipitates from cells transduced with LPP2 [R214K] was ~30% of the amount in equivalent immunoprecipitates from cells transduced with wild-type LPP2. If both wild-type and mutant LPP2 always formed dimers that permitted the catalytic activity of both proteins, and if mutant LPP2 formed dimers with mutant and wild-type LPP2 with equal frequency, then for a wild-type enzyme you would have 4 active units immunoprecipitated (LPP2/ LPP2 and LPP2/ LPP2) for every one unit of activity immunoprecipitated from cells overexpressing the mutant (R214K/ LPP2 and R214K/ R214K). Thus, based on these assumptions, we would expect that the maximum amount of activity in the mutant immunoprecipitate would be 25% of the activity in the wild-type immunoprecipitate. It is doubtful that mutant LPP2 would have formed dimers with mutant and wild-type LPP2 with equal frequency, since the endogenous expression of LPP2 is very low. Therefore, we would expect to have much less

than 25% of the activity in wild-type immunoprecipitates in the mutant immunoprecipitates. It is unclear why the activity in LPP2 [R214K]-GFP immunoprecipitates was so high. It is possible that LPP2/ LPP2 [R214K] dimers are more active than LPP2/ LPP2 dimers or that a more complex multimeric complex of LPP2 proteins exists. These are possible explanations for the results we observed. More studies are needed to understand what complexes of LPP2 proteins are formed in cells and what the relative activities and physiological roles of different oligomers may be. Our experiments did not directly evaluate the dimerization of the LPPs. Rather, we observed aggregates on Western blots and LPP activity that we attributed to co-immunoprecipitation. The LPPs could co-immunoprecipitate other lipid phosphatases without forming dimers. For example, scaffolding proteins could be involved in tethering LPPs together, which would result in co-immunoprecipitation without dimerization. It is possible that higher order complexes containing proteins other than the LPPs were co-immunoprecipitated with the LPPs. This could account for the discrepancy between our results and the previous study on LPP dimerization. Our results indicate that LPP2-GFP and LPP2 [R214K]-GFP exist in higher order complexes in fibroblasts, and that complexes containing LPP2 [R214K]-GFP are catalytically active.

Fibroblasts that were stably transduced with LPP2 or LPP2 [R214K] had decreased the extracellular hydrolysis of LPA and S1P compared to parental fibroblasts. Assuming that the LPP2 [R214K] construct is inactive, this effect was a non-catalytic function of LPP2 overexpression. LPP2-GFP and LPP2

[R214K]-GFP were both expressed on the plasma membrane to similar levels. It is possible that there are a limited number of LPP proteins that can be localized to the plasma membrane of cells. The increase in the amount of LPP2 protein produced by stable overexpression could have allowed LPP2 to out-compete LPP1 and LPP3 for plasma membrane binding sites or plasma-membrane associated binding partners. Therefore, LPP2 could have displaced, or titrated out the more active isoforms of the LPPs on the plasma membrane. This could account for the decrease in LPA and S1P hydrolysis in the LPP2 overexpressing cells. In this scenario, LPP2 would have to be much less effective at hydrolyzing both LPA and S1P at the plasma membrane than LPP1 or LPP3. LPP2 did not effectively hydrolyze LPA *in vitro* but did effectively hydrolyze S1P *in vitro*. It is not likely that LPP2 decreased ecto activity by directly binding and antagonizing the other LPP isoforms, since LPP1 was responsible for almost all the ecto activity toward LPA, and LPP2 did not co-immunoprecipitate LPP1. Additionally, we determined that LPP2 overexpression did not change the mRNA concentrations of LPP1 or LPP3. It is possible that LPP2 overexpression changed the post-translational regulation or the concentration of the LPP1 and LPP3 proteins. The results with adenoviral overexpression that showed that increased LPP2-GFP activity did not correlate with increased cellular LPP activity suggest that LPP2 overexpression may cause the downregulation of endogenous LPP activities in the cell.

The overexpression of LPP2 was knocked down by approximately 60% with siRNAs for hLPP2. The knock-down resulted in a 13-fold overexpression of

LPP2 mRNA, but abolished the increase in total LPP activity in the cells. When we attempted to create cells that stably overexpressed LPP2 using a lipofectamine 2000 transfection technique followed by puromycin selection, the mRNA overexpression achieved was less than 20-fold on each occasion. This modest overexpression failed to produce an increase in total LPP activity in cell lysates. Therefore, these cells were not used for further study. Furthermore, adenoviral transfections with LPP2-GFP using a pfu/cell of 10 or less (~30-fold mRNA overexpression or less) did not produce changes in the LPP activity in cells. In experiments described later in Chapter 4, LPP2 overexpression produces a phenotype that is completely reversed by the 60% knock-down of expression with siRNA. Taken together, these results suggest that LPP2 activity may be regulated post-transcriptionally or post-translationally. In this case, a threshold level of approximately 20- or 30-fold overexpression of LPP2 mRNA may be required to overcome this negative regulation. The total activity of cell lysates toward PA did not increase until cells overexpressed LPP2 mRNA by at least 40-fold, and never increased beyond 3-fold no matter how high the levels of mRNA were. The regulation of LPP2 activity could be mediated by phosphorylation or other modifications of the protein, since there are several putative consensus sites in the LPP2 sequence. The protein could also be regulated by degradation, or by translocation and sequestration from its substrates. The possible regulation of the LPP2 protein was not investigated further in these studies.

In summary, LPP2 was stably and transiently overexpressed and transiently knocked down in rat2 fibroblasts. LPP2 was localized to the plasma

membrane, early endosomes, and endoplasmic reticulum, and appeared to exist mainly in homomultimers. LPP2 mRNA overexpression of greater than 40-fold produced increases in the total cellular hydrolysis of PA and S1P, but not LPA. The increase in LPP activity did not alter bulk concentrations of PA, DAG, or LPA, or attenuate ERK signaling. Overexpression of LPP2 decreased the extracellular hydrolysis of LPA and S1P by a non-catalytic mechanism. The knock-down of LPP2 mRNA did not decrease the total LPP activity in cells, since LPP1 is responsible for the majority of endogenous LPP activity in fibroblasts. The specific overexpression and knock-down of each of the LPP isoforms that was achieved provides a system in which to evaluate the role of LPP2 activity in fibroblasts.

## **CHAPTER 4**

### **LPP2 REGULATES ENTRY INTO S-PHASE OF THE CELL CYCLE**

*A version of this chapter has been published. Morris KE, Schang LM, Brindley*

*DN. 2006. J Biol Chem. 281:9297-306.*

## 4.1. Introduction

In our studies on cells stably overexpressing the LPPs, we noticed that the overexpression of catalytically active LPP2 produced a phenotype in which proliferation declined gradually as cells increased in passage number. This observation led us to examine whether LPP2 overexpression was affecting cell cycle progression in fibroblasts. We discovered that LPP2 overexpression resulted in premature entry into S-phase of the cell cycle following the premature expression of cyclin A. The cell populations that entered S-phase prematurely eventually arrested in G<sub>2</sub>-phase and exited the cell cycle. This resulted in the low proliferation rates observed at late passages (discussed in Chapter 5). Knock-down studies confirmed that LPP2 has an endogenous role in cell cycle regulation. Decreasing endogenous LPP2 expression caused delayed cyclin A expression and delayed entry into S-phase of the cell cycle. This Chapter describes our findings on the effect of LPP2 on G<sub>1</sub> to S-phase progression in fibroblasts.

## 4.2. LPP2 activity changes the timing of S-phase entry in fibroblasts

4.2.1. *Cells overexpressing LPP2 enter S-phase prematurely* – Cells stably overexpressing the LPPs were synchronized in G<sub>1</sub>-phase by serum deprivation and their progression through the cell cycle after the addition of FBS was measured by flow cytometry. Cells overexpressing LPP2, but not catalytically inactive LPP2, entered S-phase  $2.4 \pm 0.70$  h (mean  $\pm$  SD from 6 experiments) before parental rat2 cells (Fig. 4.1A). Cells overexpressing LPP1 or LPP3 entered

S-phase at approximately the same time as control cells (Fig. 4.1B). These results demonstrate the the regulation of the timing of S-phase entry is an isoform-specific function of LPP2 that requires its catalytic activity. In LPP2 overexpressing cells, transfection with non-targeting control siRNAs did not affect the 2 h premature S-phase entry, whereas transfection with siRNAs specific for hLPP2 (that knocked down LPP2 mRNA expression by ~60%) reversed the premature S-phase entry (Fig. 4.1C). Since transient reductions in LPP2 overexpression using siRNA reversed the effect, the regulation of S-phase entry is a function of the activity of LPP2, not the result of a compensatory change in the stably overexpressing cells.

*4.2.2. Premature S-phase entry of LPP2 overexpressing cells is not a result of incomplete synchronization in G<sub>1</sub>-phase-* To ensure that the premature entry into S-phase by LPP2 overexpressing cells was not due to their incomplete synchronization in G<sub>1</sub>-phase, flow cytometry was used to monitor the progression of cells into G<sub>1</sub>-phase during serum deprivation. Rat2 fibroblasts and those overexpressing LPP2-GFP or LPP2 [R214K]-GFP all progressed into G<sub>1</sub>/G<sub>0</sub>-phase at the same rate during serum withdrawal, and all contained approximately the same percentage of cells in each phase of the cell cycle prior to the re-addition of FBS (Fig. 4.1E). Additionally, when LPP2 overexpressing cells were synchronized by trypsinization instead of serum withdrawal, they showed the same phenotype of premature S-phase entry (Fig. 4.1D).



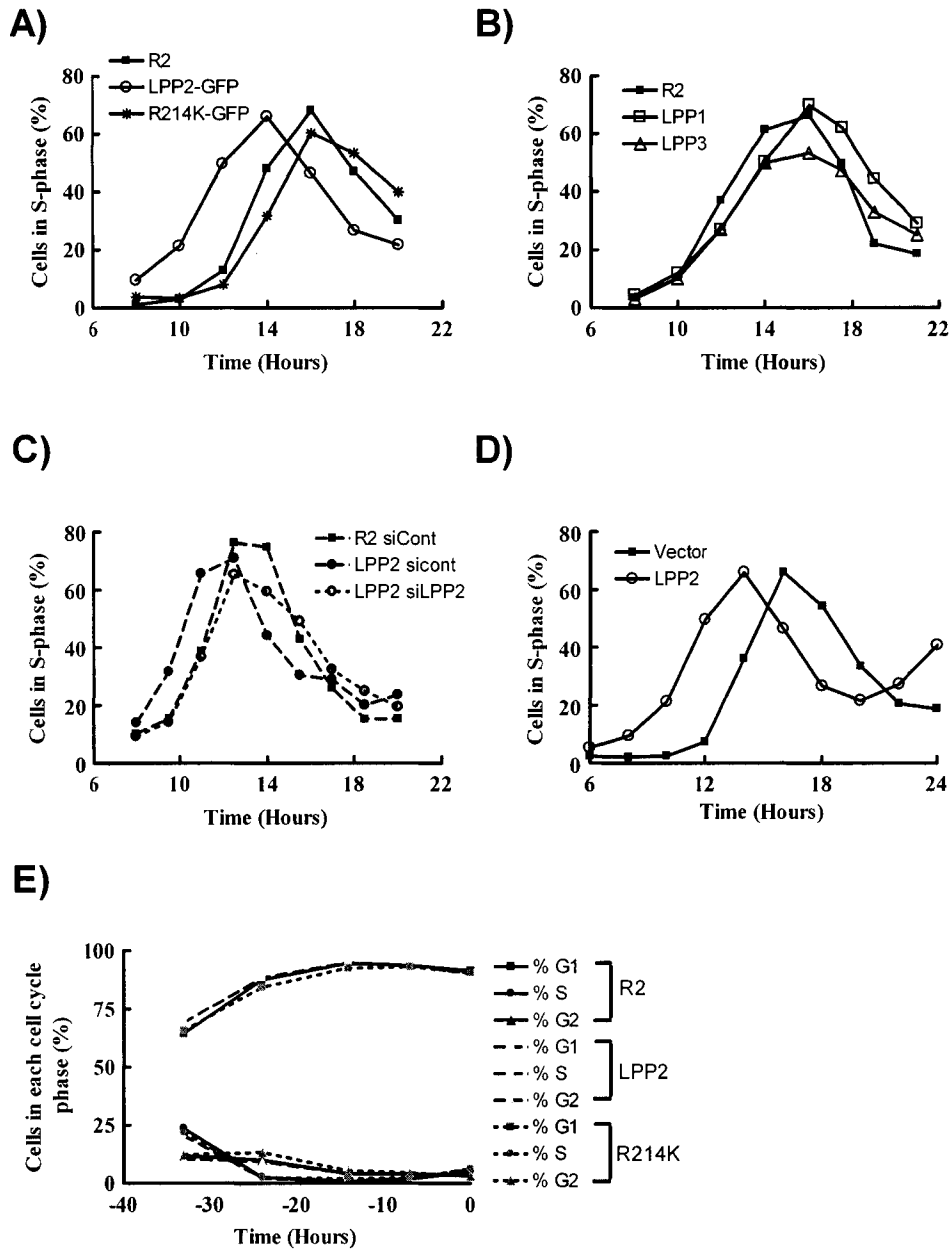


**Figure 4.1. LPP2 overexpression causes premature S-phase entry.** Panels A-D show the percent of gated cells in S-phase at various times after the addition of FBS. Panels A, B, and D show parental rat2 fibroblasts (R2) and those stably transduced with empty vector, LPP2, LPP2-GFP, LPP2[R214K]-GFP, LPP1, or LPP3. Panel C shows parental rat2 fibroblasts transfected with non-targeting control siRNAs, and cells stably overexpressing LPP2 and transfected with non-targeting control siRNAs or with siRNAs for human LPP2. Cells were synchronized by starvation in Panels A-C and by trypsinization at confluence in Panel D. Results are from one representative of at least 3 independent experiments. Panel E shows the percent of gated cells in G<sub>1</sub>, S, and G<sub>2</sub>-phases at various times after the addition of starvation media and prior to starvation (-36 h). Results are from one experiment.

#### 4.2.3. Knock-down of endogenous LPP2 results in delayed S-phase entry –

Knock-down studies were performed to determine whether the regulation of the timing of S-phase entry is an endogenous function of LPP2. The knock-down of endogenous LPP2 expression by ~60% in fibroblasts resulted in a  $1.2 \pm 0.14$  h (mean  $\pm$  SD for 3 independent experiments) delay in S-phase entry, compared to rat2 cells or those transfected with control siRNAs (Fig. 4.2A). The knock-down of LPP1 or LPP3 by 50-60% did not significantly change the rate of S-phase entry (Fig. 4.2B). Therefore, the regulation of the timing of S-phase entry is an isoform-specific endogenous function of LPP2.

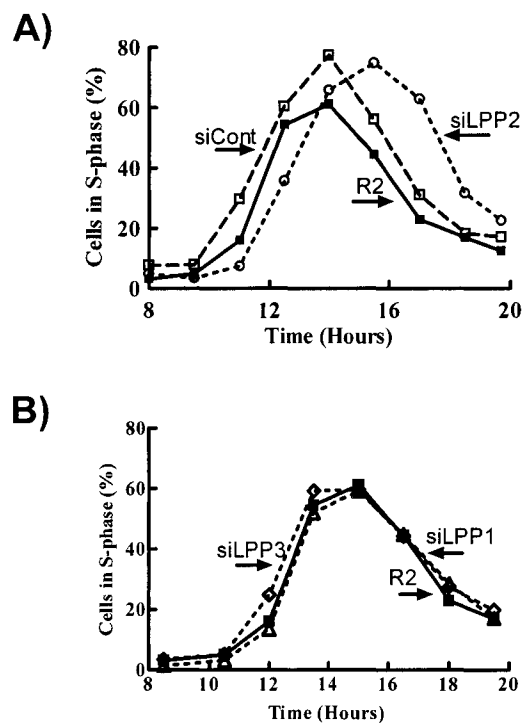


**Figure 4.2. Knock-down of LPP2 delays S-phase entry.** Panels A-B show the percent of gated cells in S-phase at various times after the addition of FBS. Panel A shows parental rat2 fibroblasts (R2, ■), or cells transfected with siRNAs for non-targeting control (siCont, □), or rat LPP2 (siLPP2, ○). Panel B shows parental rat2 fibroblasts (R2, ■), or cells transfected with siRNAs for rat LPP1 (siLPP1, ◇), or rat LPP3 (siLPP3, △). Results are from one representative of at least 3 independent experiments.

### 4.3. LPP2 activity changes the timing of cyclin A expression in fibroblasts

#### 4.3.1. *LPP2 overexpression causes premature cyclin A expression* –

Parental rat2 fibroblasts or those overexpressing LPP2 and entering S-phase prematurely were synchronized by serum deprivation, and lysates were collected at various times after the re-addition of FBS. Western blots were performed to measure the expression of cyclins and other proteins that regulate G<sub>1</sub> to S-phase progression. In cells overexpressing LPP2, cyclin A expression increased prematurely compared to the expression in rat2 control cells (Fig. 4.3A). The levels of cyclin A in the LPP2 overexpressing cells were similar to the levels of cyclin A in the control fibroblasts approximately 2 h later. These differences occurred between 12-16 h after the addition of FBS. The changes in cyclin A expression produced by LPP2 preceded and coincided with entry into S-phase, and the 2 h acceleration of cyclin A expression paralleled the 2 h acceleration of progression into S-phase. Cyclin A is a partner of cyclin-dependent kinase-2 (CDK2) which regulates G<sub>1</sub> to S-phase progression. Dysregulation of cyclin A expression and subsequent increases in cyclin A associated CDK2 activity results in unscheduled progression into S-phase [160-168]. Fibroblasts that stably overexpressed LPP1 and LPP3 did not show significant differences in the timing of cyclin A expression compared to parental control cells (Fig. 4.3B). When cells that stably overexpressed LPP2 were treated with control siRNAs or siRNAs for human LPP2, the treatment with siRNAs for LPP2 that transiently knocked down stable LPP2 overexpression by ~60% delayed cyclin A expression (Fig. 4.3C).

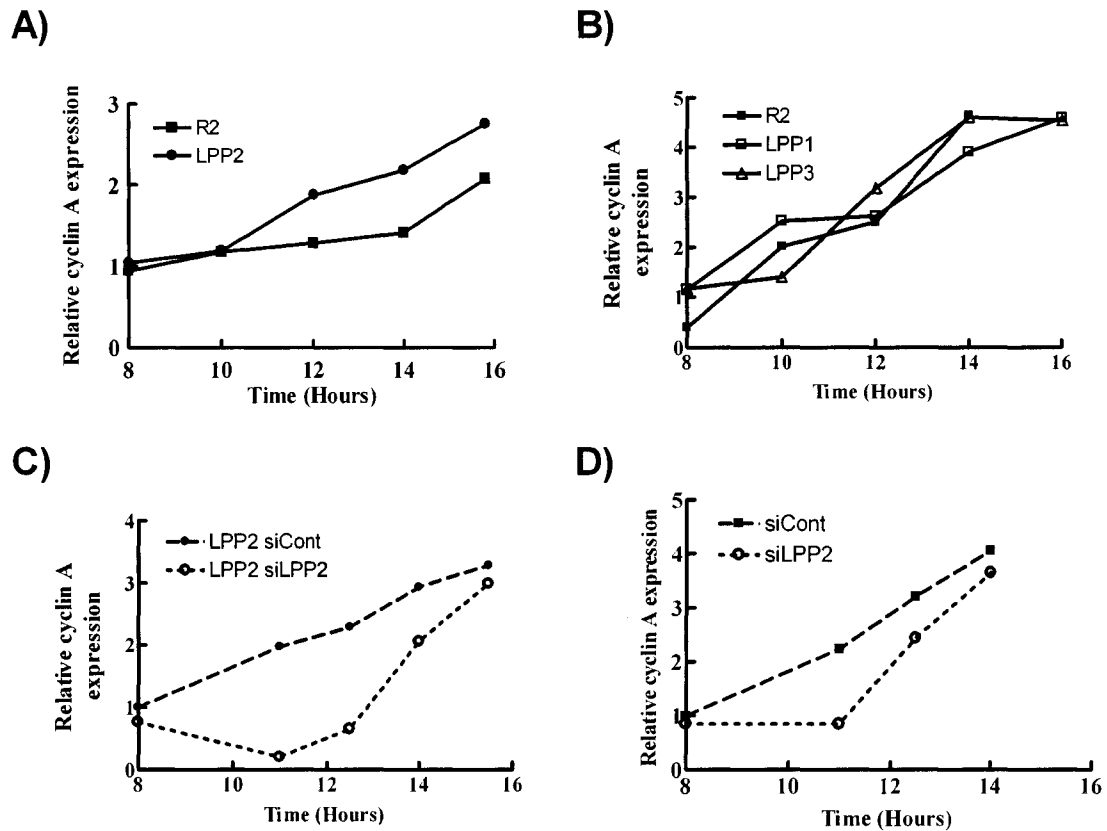


**Figure 4.3. LPP2 activity regulates the timing of cyclin A expression.** Panels A-D show the relative expression of cyclin A after synchronization and the re-addition of FBS. Cyclin A expression was determined by the quantitation of bands from Western blots and is normalized to total protein and expressed relative to R2, LPP1, LPP2 siCont, or siCont, respectively, at time 0, which is given as 1. Panels A-B show parental rat2 fibroblasts or cells stably overexpressing LPP2, LPP1, or LPP3. Panel C shows cells stably overexpressing LPP2 that have been transfected with siRNAs for non-targeting control or human LPP2. Panel D shows parental rat2 fibroblasts transfected with siRNAs for non-targeting control or rat LPP2. Results are from one representative of at least 3 independent experiments.

4.3.2. *Knock-down of endogenous LPP2 delays cyclin A expression* – The timing of cyclin A expression was evaluated in fibroblasts in which endogenous LPP2 was knocked down with siRNAs. Fibroblasts transfected with siRNAs for rLPP2 that had delayed progression into S-phase also showed delayed expression of the cyclin A protein compared to cells treated with non-targeting control siRNAs (Fig. 4.3D). The delay in cyclin A expression was approximately 1.5-2 h, similar to the delay in the timing of entry into S-phase.

4.3.3. *The activity and expression of CDK2 occur prematurely in LPP2 overexpressing cells* – CDK2 was immunoprecipitated from fibroblasts stably transduced with the empty vector or LPP2 at various times after the re-addition of FBS. The overall levels of CDK2 activity were similar in vector control cells and those overexpressing LPP2 (Fig. 4.4A). LPP2 overexpressing cells had two peaks in CDK2 activity at approximately 8 and 18 h after the addition of FBS (Fig. 4.4A). These peaks occurred at approximately 10 and 20 h in the cells transduced with empty vector (Fig. 4.4A). The 2 h acceleration in the timing of CDK2 activity caused by LPP2 paralleled the 2 h premature S-phase entry caused by LPP2. The premature expression of cyclin A could result in the premature formation of active cyclin A-CDK2 complexes, and could account for the change in the timing of CDK2 activity in the LPP2 overexpressing cells. Surprisingly, the expression of the CDK2 protein was also increased in LPP2 overexpressing cells between 6 and 12 h after the addition of FBS (Fig. 4.4B). Therefore, LPP2 activity may also enhance the expression of CDK2, either by increasing its production or by stabilizing the protein, and this may contribute to the premature S-phase entry in the LPP2 overexpressing cells.

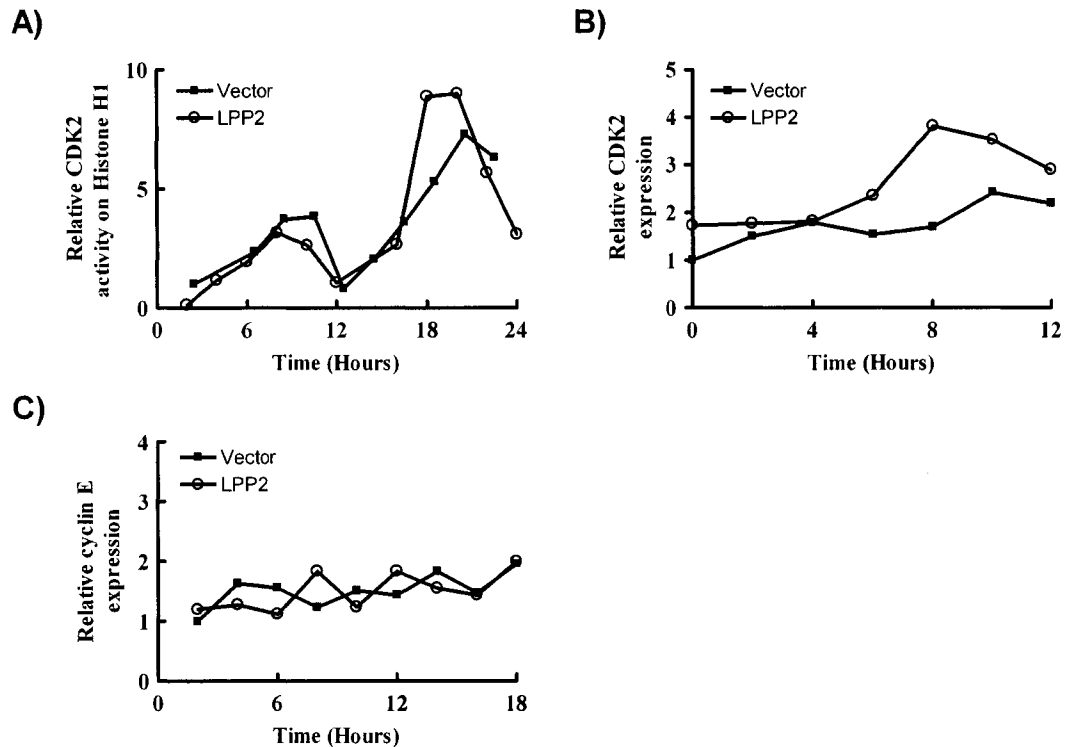


**Figure 4.4. LPP2 overexpression causes premature CDK2 activity and increased CDK2 expression but does not change the expression of cyclin E.** Panel A shows the activity of immunoprecipitated CDK2 in cells stably transduced with the empty vector or LPP2. The activity toward Histone H1 was measured at the indicated times after synchronization and the re-addition of FBS. Results are from one representative of 3 independent experiments. Panels B-C show the quantitation of Western blots for CDK2 and cyclin E, respectively, in cells stably transduced with the empty vector or LPP2. Expression is given relative to the vector control cells at 0 or 2 h, respectively, which is given as 1. Results are from one representative of at least two independent experiments.

#### 4.4. The timing of expression of other proteins that regulate G<sub>1</sub> to S-phase progression is not regulated by LPP2 activity

##### 4.4.1. LPP2 overexpression does not change the expression of cyclin E –

Cyclin E is another partner of CDK2. According to the conventional model of cell cycle progression, the earlier activity of cyclin E-CDK2 complexes allows cells to progress through G<sub>1</sub>-phase of the cell cycle past the “restriction point” (reviewed in [82]). The expression of cyclin E was not significantly changed in

LPP2 overexpressing cells compared to control fibroblasts during cell cycle progression (Fig. 4.4C).

4.4.2. *LPP2 overexpression does not change the expression of the D-type cyclins or CDK4, or change the activation of GSK3 $\beta$*  – Mitogen-dependent progression through early G<sub>1</sub>-phase is mediated by CDK4 and CDK6 complexed with cyclin D1, D2, or D3 (reviewed in [82]). GSK3 $\beta$  inhibits progression through early G<sub>1</sub>-phase by phosphorylating cyclin D, causing it to be translocated from the nucleus and targeted for proteolysis. Growth factors that promote cell cycle progression activate the Akt signaling pathway to increase cyclin D expression and promote the inhibitory phosphorylation of GSK3 $\beta$  [169]. Since the activities of CDK4/6-cyclin D complexes precede and promote cyclin A expression, we wanted to determine if LPP2 overexpression caused changes to the expression of CDK4 or the D-type cyclins, or changed the phosphorylation state of the cyclin D inhibitor GSK3 $\beta$ . Western blots demonstrated that LPP2 overexpression did not significantly change the expression of cyclin D1, cyclin D3, or CDK4, or the phosphorylation of GSK3 $\beta$  in fibroblasts that were re-entering the cell cycle after the addition of FBS (Fig. 4.5A-D). The expression of CDK6, cyclin D2, and the phosphatase CDC25A that activates CDK2, CDK4, and CDK6 were not measured because our antibodies could not effectively detect the endogenous proteins.

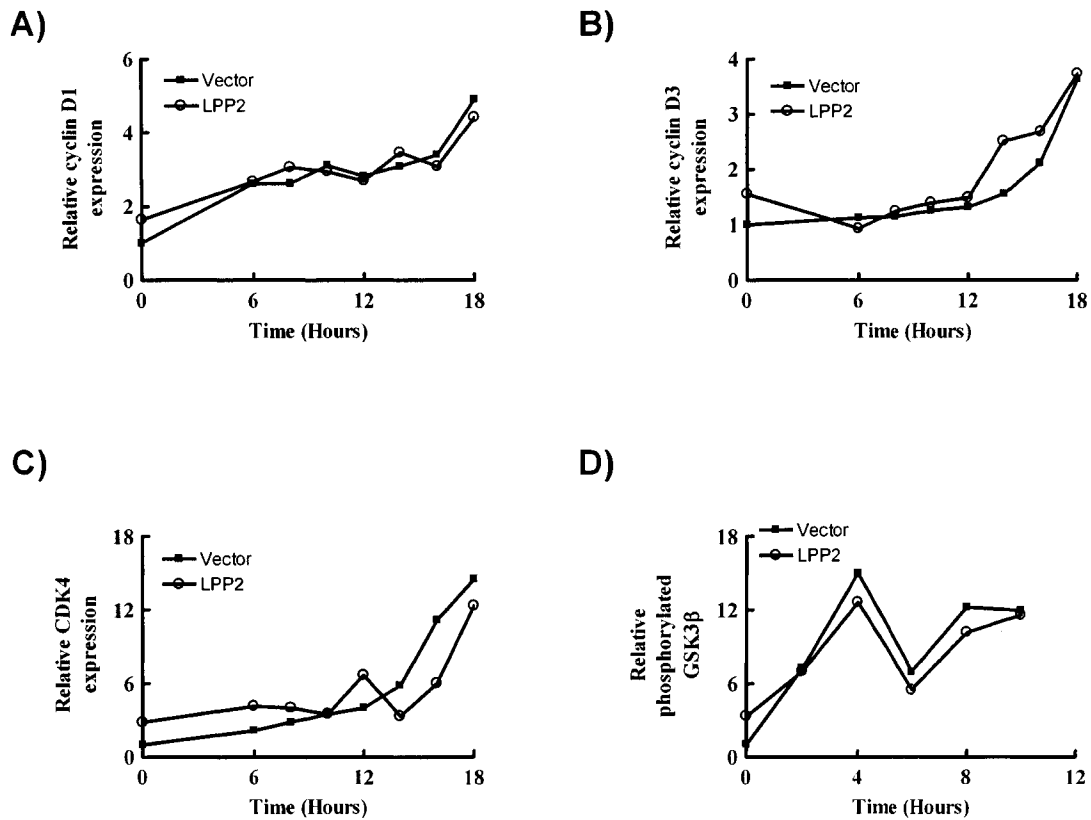


**Figure 4.5. LPP2 overexpression does not change the timing or magnitude of the expression of cyclin D1, cyclin D3, CDK4, or phosphorylated GSK3 $\beta$ .** Panels A-C show the quantitation of Western blots for cyclin D1, cyclin D3, or CDK4, respectively. Panel D shows the quantitation of Western blots for phosphorylated GSK3 $\beta$  (Ser9) divided by total GSK3 $\beta$ . The two antibodies were detected simultaneously by scanning the membrane at 800 nm and 700 nm, respectively on the Odyssey<sup>TM</sup> imager. Lysates were from cells stably transduced with the empty vector or LPP2 that were synchronized by serum deprivation and stimulated with FBS for the indicated times. Expression is relative to the vector control cells at time 0 which is given as 1. Results are from one representative of two independent experiments.

#### 4.4.3. LPP2 overexpression does not change the phosphorylation of Akt,

*LIMK*, or *p38 MAPK* – The phosphorylation of Akt downstream of PI3K

activation, the phosphorylation of LIMK downstream of Rho, and the

phosphorylation of p38 MAPK have all been shown to regulate the duration of

G<sub>1</sub>-phase and the timing of S-phase entry [170-172]. Therefore, we evaluated

whether LPP2 overexpression changed the phosphorylation of Akt, LIMK1/2, or

p38 MAPK in cells re-entering the cell cycle. The overexpression of LPP2 in



fibroblasts did not significantly change the phosphorylation of Akt, LIMK, or p38 MAPK during cell cycle progression (Fig. 4.6 A-C). We therefore conclude that LPP2 activity does not accelerate S-phase entry upstream of the regulation of these kinases.

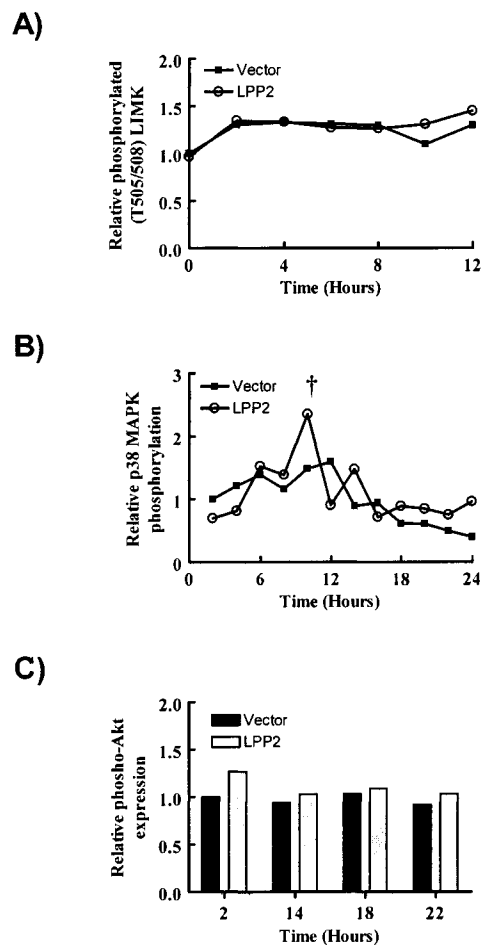


**Figure 4.6. LPP2 overexpression does not change the phosphorylation of LIM kinase, p38 MAP kinase, or Akt.** Panels A-C show the quantitation of Western blots for phosphorylated LIMK1/2 (Thr 505/508) divided by total LIMK, phosphorylated p38 MAPK (Thr180/Tyr182) divided by total p38 MAPK, or phosphorylated Akt (Ser473) divided by total Akt, respectively. In each case antibodies for phosphorylated and total protein were detected simultaneously by scanning the membrane at 800 nm and 700 nm, respectively. Lysates are from cells stably transduced with the empty vector or LPP2 that were synchronized by serum deprivation and stimulated with FBS for the indicated times. Expression is relative to the vector control cells at time 0 which is given as 1. Results are from one representative of at least two independent experiments. †In Panel B, the increase in phosphorylated p38 MAPK at 10 h in LPP2 overexpressing cells was not reproducible in two other experiments.

#### **4.5. The concentrations of bulk and nuclear lipids are not changed by LPP2 overexpression during cell cycle progression.**

4.5.1. *LPP2 overexpression does not change the bulk concentrations of PA, C1P, LPA, S1P, DAG, or Cer during cell cycle progression* – The effect of LPP2 overexpression on S-phase entry was dependent on the catalytic activity of the enzyme. To determine which lipid pool could have been affected by LPP2 to promote cell cycle progression, the concentrations of bioactive phospholipids and their dephosphorylated products were measured during cell cycle progression in control fibroblasts and those stably overexpressing during cell cycle progression. It was technically impractical to obtain enough cells to separate cell fractions and determine the subcellular concentrations of low abundance lipids at multiple time points during the cell cycle. Even if this could be achieved, it is doubtful that lipids like LPA and S1P would remain associated with the original organelle during fractionation. Therefore, the bulk concentrations of lipids from whole cell extracts were measured. In all cases, the bulk lipid mass and the incorporation of radioactive oleate or palmitate into lipids were measured in parallel, giving similar results. There were no reproducible significant changes in the bulk concentrations of PA, C1P, LPA, S1P, DAG, or ceramide in cells overexpressing LPP2 compared to cells transduced with the empty vector between 4 and 14 hours after the addition of FBS (Fig. 4.7A-F).

4.5.2. *LPP2 overexpression does not change the nuclear concentrations of DAG or Cer* – Intact nuclei are relatively easy to purify in large amounts compared to other organelles. Nuclear DAG can regulate S-phase entry [30].

Sensitive radioenzymatic assays allowed us to determine the concentrations of DAG and ceramide in nuclear preparations during cell cycle progression.

In one experiment, there were no significant differences in the concentrations of nuclear DAG or ceramide between 4 and 18 hours after the addition of FBS in cells overexpressing LPP2 compared to cells transduced with the empty vector (Fig. 4.7 G, H). Since we did not observe any significant changes in the bulk or nuclear concentrations of any lipids as a result of LPP2 activity, we cannot directly attribute the regulation of cell cycle progression to the regulation of any specific lipid pool in fibroblasts. It is probable that the activity responsible for the premature S-phase entry is localized to a specific lipid pool in a specific subcellular compartment. The technical limitations of our assays prevented us from investigating this possibility.

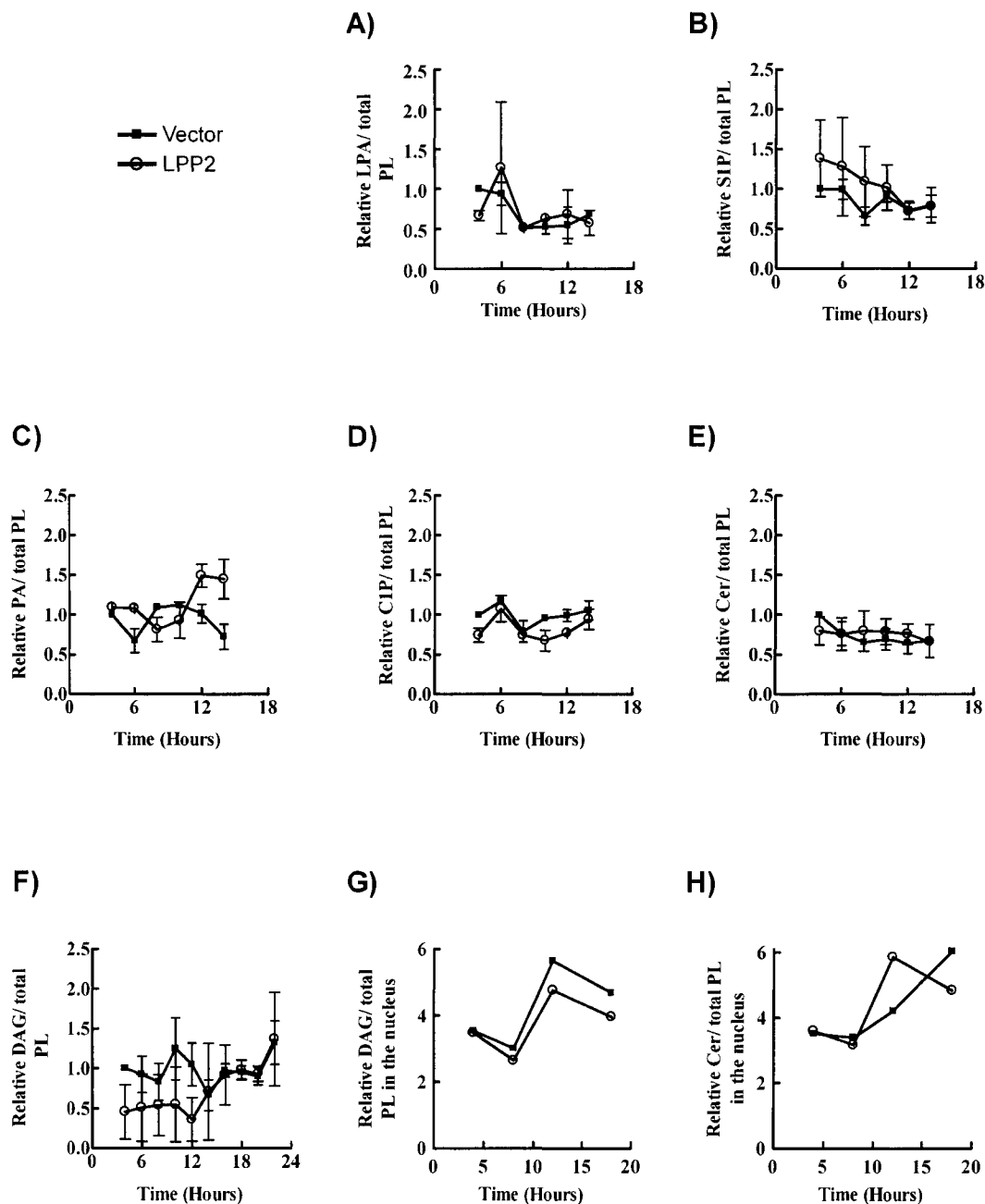


**Figure 4.7. LPP2 overexpression does not change the bulk concentrations of LPA, S1P, PA, CIP, DAG, or Cer, or the nuclear concentrations of DAG or Cer.** Panels A-H show the concentrations of bulk or nuclear lipids in cells stably transduced with the empty vector or LPP2 that were synchronized by serum deprivation and stimulated with FBS for the indicated times. Concentrations are expressed as the amount of labeled oleate incorporated into the lipid divided by the total labeled phospholipid except in panels E-H, where concentrations are expressed as total bulk lipid divided by total phospholipid phosphate. Concentrations are expressed relative to concentrations in the vector control cells at time 4 h or time zero in panels G-H which is given as 1. Results means  $\pm$  SD from at least two independent experiments for panels A-F and single experiments in panels G-H.

#### **4.6. LPP2 overexpression may lead to unchecked progression into S-phase in cells with DNA damage**

4.6.1. *LPP2 overexpressing cells show a decreased delay in S-phase entry following UV irradiation* – Since the transition from G<sub>1</sub> to S-phase occurred prematurely in cells that overexpressed LPP2, it was possible that the G<sub>1</sub>/S checkpoint was not functional in these cells. To investigate this possibility, non-lethal DNA damage was induced in cells synchronized in G<sub>1</sub>-phase using ultraviolet (UV) radiation. In response to UV irradiation, cells with a functional G<sub>1</sub>/S checkpoint should spend an increased amount of time in G<sub>1</sub>-phase and should activate the p53 pathway. Cells were synchronized in G<sub>1</sub>-phase by trypsinization, re-seeded in FBS to promote cell cycle entry, and treated with UV 4 h later. Vector control cells that were untreated had 27% of their cells in S-phase 10 h after mock treatment (14 h after release from synchronization), whereas vector control cells treated with UV had only 10% of cells in S-phase at this time (Fig. 4.8A). This indicated that, as expected, the progression into S-phase had been delayed following UV-induced DNA damage in cells transduced with the empty vector. In contrast, in LPP2 overexpressing cells there were more than 20% of cells in S-phase 10 h after mock treatment or UV treatment (Fig. 4.8A). The lack of a decrease in the number of cells in S-phase following UV irradiation suggested that the LPP2 overexpressing cells were not lengthening the time spent in G<sub>1</sub>-phase in response to UV-induced DNA damage. At 24 h after synchronization, the untreated vector control cells had completed a full cell cycle and 70% of the cells were in G<sub>1</sub>-phase, only 11% in S-phase, and 19% in G<sub>2</sub>-

phase (Fig. 4.8B). Rat2 fibroblasts completed the cell cycle in ~24 h when synchronized by serum deprivation or trypsinization. The vector control cells that had been treated with UV were still delayed in their cell cycle progression by approximately 3-4 h and had only 14% of cells in G<sub>1</sub>-phase, 58% of cells still in S-phase, and 28% of cells in G<sub>2</sub>-phase (Fig. 4.8B). The untreated LPP2 overexpressing cells completed the cell cycle ~2.5 h earlier than the vector control cells due to their premature S-phase entry. 24 h after release from synchronization, the mock-treated LPP2 overexpressing cells had already completed a cell cycle and had progressed into S-phase again. Cells undergo a shortened G<sub>1</sub>-phase when they have just completed a cycle and are continuing cycling, rather than exiting from quiescence. The distribution of cells in LPP2 overexpressing cells after 24 h was approximately equal between the three cell cycle phases (Fig. 4.8B). The LPP2 overexpressing cells that were treated with UV cycled at the same rate as untreated cells, and 24 h after synchronization, their cell cycle distribution was not statistically different from untreated LPP2 overexpressing cells (Fig. 4.8B). These results suggest that the overexpression of LPP2 prevented cells from arresting at the G<sub>1</sub>/S checkpoint in response to DNA damage.

*4.6.2. Phosphorylated p53 (Ser15) levels are elevated following DNA damage in LPP2 overexpressing cells but p21<sup>Cip1</sup> and p27<sup>Kip1</sup> are not increased –*  
In response to DNA damage caused by UV irradiation, ATR is activated and phosphorylates p53 on Ser15. Activated p53 mediates the transcriptional activation of p21<sup>Cip1</sup> that causes activation of the G<sub>1</sub>/S checkpoint and delay in G<sub>1</sub>-

phase of the cell cycle (reviewed in [173]). p27<sup>Kip1</sup> is also frequently upregulated in response to DNA damage and inhibits cyclin-dependent kinase activities, resulting in delay in G<sub>1</sub>-phase (reviewed in [174]). In rat2 fibroblasts stably transduced with the empty vector, treatment with UV resulted in 5-fold increases in phosphorylated (Ser15) p53 and only modest 1.5-fold increases in the expression of p21<sup>Cip1</sup> and p27<sup>Kip1</sup> (Fig. 4.8 C,D). In fibroblasts that stably overexpressed LPP2, there was a 3-fold increase in the amount of phosphorylated (Ser15) p53 after the induction of DNA damage, but no increase in the expression of p21<sup>Cip1</sup> or p27<sup>Kip1</sup> (Fig. 4.8C,D). These results demonstrate that LPP2 overexpressing cells do activate p53 in response to DNA damage caused by UV. However, this p53 activation does not cause a significant delay in the timing of progression into S-phase. This could be because activated p53 does not enhance the expression of p21<sup>Cip1</sup>. However, in control cells the activation of p21<sup>Cip1</sup> was also very modest in response to the dose of UV that we used. The delay in G<sub>1</sub>-phase was also relatively short in control cells (3-4 h), consistent with the lack of large increases in p21<sup>Cip1</sup> expression. It is unclear why LPP2 overexpressing cells activate p53 after DNA damage but do not arrest in G<sub>1</sub>-phase.

*4.6.3. Basal levels of activated p53 are increased in cells that stably overexpress LPP2* – Cells that stably overexpressed LPP2 and had undergone unscheduled S-phase entry for at least 15 passages contained 16-fold more phosphorylated (Ser15) p53 than cells transduced with vector control at the same passage number (Fig. 4.8C). This indicated that the LPP2 overexpressing cells that were entering S-phase prematurely may have been accumulating DNA

damage and activating p53 in response to this accumulated DNA damage. Random DNA damage that occurs in all cells would not be repaired in cells that persistently entered S-phase prematurely due to the lack of a functional G<sub>1</sub>/S checkpoint, and would accumulate over time. The levels of basal p21<sup>Cip1</sup> and p27<sup>Kip1</sup> were also elevated in the LPP2 overexpressing cells (Fig. 4.8D). This indicated that p21<sup>Cip1</sup> expression had been increased by p53 activation. Levels of p21<sup>Cip1</sup> and p27<sup>Kip1</sup> may have not increased following UV radiation because they were already elevated.



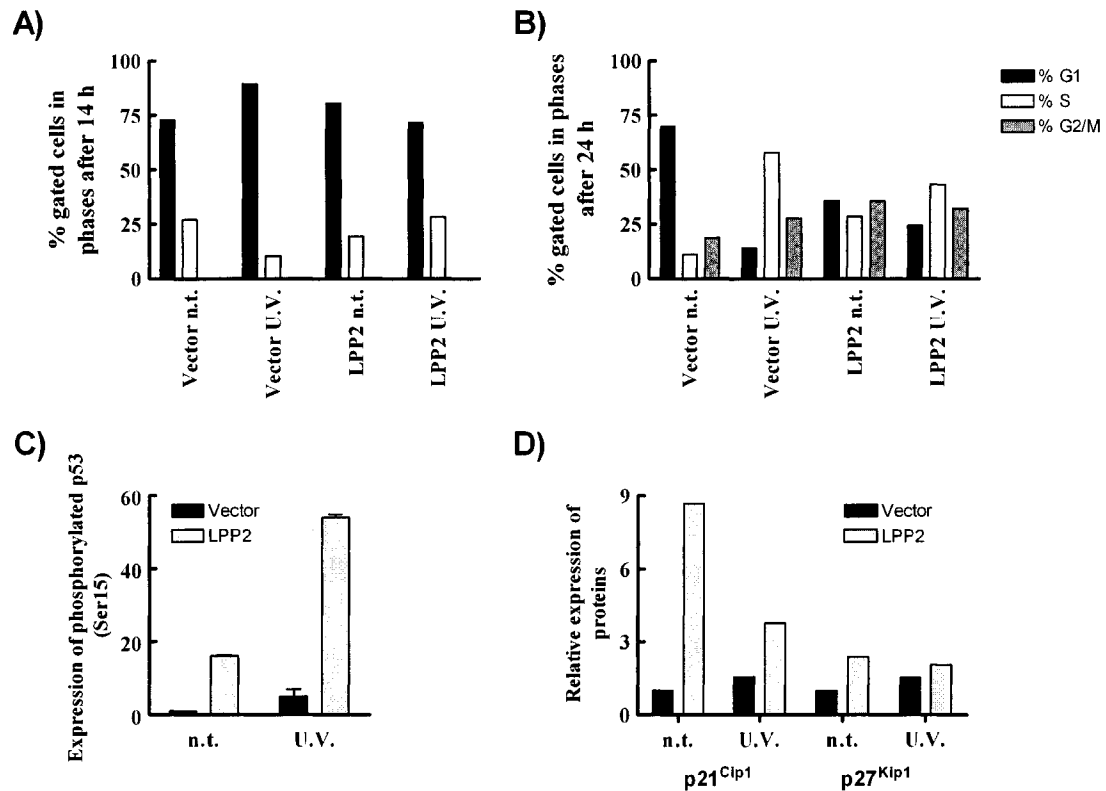


**Figure 4.8. In response to UV irradiation, fibroblasts that overexpress LPP2 do not arrest in G<sub>1</sub>-phase, do activate p53, and do not increase p21<sup>Cip1</sup> or p27<sup>Kip1</sup> expression.** Panels A-B show the percent of gated cells in each of G<sub>1</sub>-, S-, and G<sub>2</sub>-phases at the indicated times after synchronization by trypsinization and the addition of FBS. Results are from one representative of 3 independent experiments. Panels C-D show the quantitation of Western blots of phosphorylated (Ser15) p53, p21<sup>Cip1</sup>, or p27<sup>Kip1</sup>, respectively. Expression is relative to untreated vector control cells which is given as 1. Cells stably transduced with the empty vector or LPP2 were not irradiated (n.t.) or were irradiated with 50 J/m<sup>2</sup> of UV after 4 h. In Panel C, lysates were collected 2 h after irradiation or mock treatment. Results are mean ± SD from 3 independent experiments. In Panel D, lysates were collected 2-10 h after irradiation or mock treatment. Results are averages of 3 timepoints (2, 6, and 10 h after treatment) from one representative of at least two independent experiments. Results shown in Panels A-B are from experiments performed by C. Spiers.

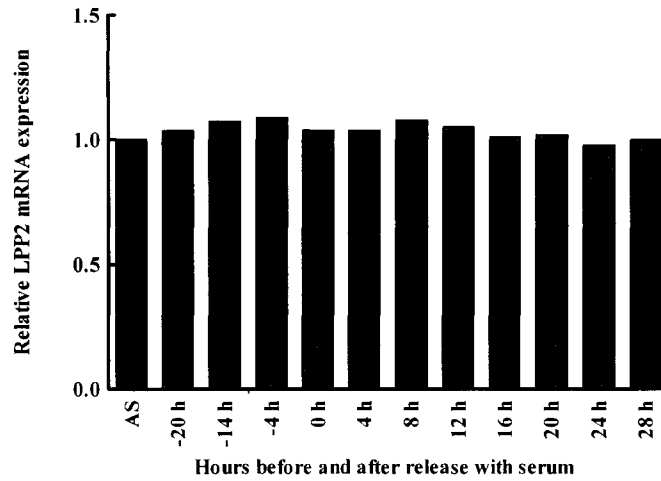
#### 4.7. Endogenous LPP2 mRNA expression is not regulated during cell cycle progression or by a variety of agonists.

4.7.1. *Endogenous LPP2 mRNA expression does not vary throughout the cell cycle* – Since endogenous LPP2 activity regulates the timing of G<sub>1</sub> to S-phase progression, we investigated whether endogenous LPP2 mRNA expression was regulated during starvation and cell cycle progression in fibroblasts. Rat2

fibroblasts were synchronized by serum deprivation and FBS was added to promote cell cycle progression. Endogenous LPP2 mRNA concentrations were measured at various times during starvation and cell cycle progression. There were no significant changes in the mRNA concentration of endogenous LPP2 during serum deprivation or cell cycle progression (Fig. 4.9A). At all times throughout the cell cycle, LPP2 mRNA levels remained similar to levels in an asynchronous population of cells.

*4.7.2. LPP2 mRNA expression is not regulated by a variety of factors involved in wound healing* – In processes such as wound healing, rapid progression into S-phase may be induced in cells that are normally quiescent. This is the type of physiological situation in which it might be expected that LPP2 activity would be upregulated. Therefore, we investigated whether the mRNA expression of endogenous LPP2 is regulated by mitogens and factors involved in regulating wound healing in fibroblasts. The expression of endogenous LPP2 mRNA was not significantly changed when fibroblasts were stimulated for 1, 2, or 8 h with 10  $\mu$ M LPA, 1  $\mu$ M S1P, 50 ng/ml EGF, 50 ng/ml PDGF, 10 ng/ml TNF $\alpha$ , 2.5 ng/ml TGF- $\beta$ , 100 ng/ml IGF, or 20 ng/ml FGF (Fig. 4.9B). These results do not exclude the possibility that LPP2 mRNA expression is regulated by other mitogenic signals. For example, the combination of two or more mitogenic signals may be required to induce LPP2 expression. These results also do not exclude the possibility that LPP2 is regulated post-transcriptionally or post-translationally in relevant physiological situations.

**A)**



**B)**

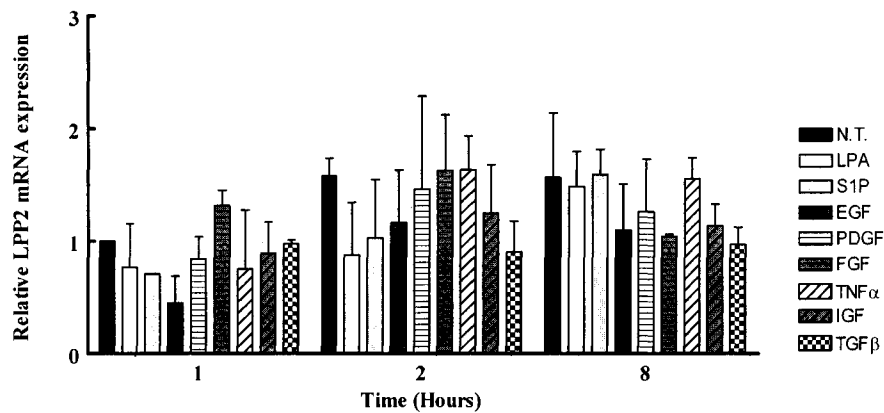


**Figure 4.9. The expression of endogenous LPP2 mRNA is not regulated during starvation or cell cycle progression or by agonists involved in the regulation of wound healing.** Panels A-B show the concentrations of LPP2 mRNA in rat2 fibroblasts during synchronization by serum deprivation and at the indicated times after the re-addition of FBS, or at the indicated times after the addition of the indicated mitogens. mRNA concentrations are normalized to that of the housekeeping gene, cyclophilin A. Results are expressed as fold change compared to asynchronous (AS) rat2 fibroblasts in Panel A or untreated fibroblasts at 1 h in Panel B which is given as 1. Results are one representative of at least two independent experiments. Results shown in Panel B are from experiments performed by B. Samuel.

#### 4.8. Discussion

The overexpression of LPP2, but not LPP2 [R214K], LPP1, or LPP3, promoted premature entry into S-phase in fibroblasts. The knock-down of endogenous LPP2, but not LPP1 or LPP3, caused a delay in S-phase entry in fibroblasts. These results demonstrate that LPP2 activity regulates the duration of G<sub>1</sub>-phase following quiescence and the timing of entry into S-phase in fibroblasts. This is an isoform-specific function of LPP2 that is dependent on the catalytic activity of the enzyme.

The regulation of the timing of S-phase entry by LPP2 appears to be mediated primarily by regulating the timing of cyclin A expression. Cyclin A expression increased approximately 2 h prematurely in LPP2 overexpressing cells and approximately 2 h late in cells in which LPP2 was knocked down. The change in the timing of cyclin A expression led to changes in the timing of CDK2 activity that resulted in the premature or delayed progression from G<sub>1</sub>-phase into S-phase of the cell cycle. LPP2 overexpression also increased the expression of CDK2, which may have contributed to the early S-phase entry. Cyclin A expression is induced by the release of inhibitory pocket proteins from cyclin A promoters [175]. This is thought to occur as a result of the activity of CDK4/6-cyclin D complexes and CDK2-cyclin E complexes. In turn, the production of D-type cyclins is increased in response to mitogens by pathways that involve PI3K/Akt, Rho/LIMK, and p38 MAPK. Our results show that LPP2 does not appear to influence cyclin A expression by regulating the phosphorylation of Akt, LIMK, or p38 MAPK, or by increasing the expression of the D-type cyclins or

inhibiting GSK3 $\beta$ . Therefore, the mechanism by which LPP2 regulates cyclin A expression is unclear.

The bulk concentrations of lipids that are substrates or products of LPP2 activity including LPA, S1P, C1P, PA, DAG, and Cer were not changed significantly by LPP2 overexpression at various stages of the cell cycle. The nuclear concentrations of DAG and ceramide were also not significantly different in LPP2 overexpressing cells compared to control cells during cell cycle progression. Since the catalytically inactive mutant LPP2 did not change the timing of S-phase entry, the regulation of the timing of S-phase entry did require the catalytic activity of LPP2. Therefore, it is likely that the regulation of a specific lipid pool by LPP2 activity contributed to the regulation of the cell cycle. Since LPP2 was localized to the ER and the endosomes in fibroblasts, pools at these organelles are the most likely to have been affected. Changes in intracellular pools of DAG, LPA, S1P, or Cer could all possibly change cell cycle progression. Unfortunately, the mechanism by which LPP2 activity increases cyclin A expression and promotes cell cycle progression remains unknown.

Sustained LPP2 overexpression caused cells to accumulate high levels of activated, phosphorylated p53 and high levels of p21<sup>Cip1</sup> and p27<sup>Kip1</sup>. The p53 DNA damage response pathway is often activated in cells with premature S-phase entry resulting from cyclin overexpression [81, 176, 177]. This could be a result of insufficient ribonucleoside triphosphate levels due to the shortened G<sub>1</sub>-phase or it could be the result of the accumulation of DNA damage. Cells with a non-functional G<sub>1</sub>/S checkpoint that repeatedly entered S-phase prematurely could

accumulate DNA damage since randomly occurring DNA damage would not be repaired due to the lack of arrest in G<sub>1</sub>-phase. Our results demonstrate that the overexpression of LPP2 causes fibroblasts to be defective in arresting at the G<sub>1</sub>/S checkpoint following DNA damage induced by UV irradiation. Therefore, it is probable that LPP2 overexpressing cells accumulated DNA damage, but did not arrest in G<sub>1</sub>-phase. In response to UV, LPP2 overexpressing cells did increase the phosphorylation of p53 even though p53 phosphorylation was already 16-fold higher than in control cells. However, although the constitutive levels of p21<sup>Cip1</sup> and p27<sup>Kip1</sup> were high, their expression was not induced following p53 activation. Since the levels of p21<sup>Cip1</sup> and p27<sup>Kip1</sup> were already higher in the LPP2 overexpressing cells than the expression levels induced in control cells following UV irradiation, it may not have been possible or effective to induce their expression to a greater extent. Furthermore, based on the delay in G<sub>1</sub>-phase produced by more modest expression of p21<sup>Cip1</sup> in the control cells, the levels of p21<sup>Cip1</sup> and p27<sup>Kip1</sup> in LPP2 overexpressing cells should have been sufficient to produce arrest at the G<sub>1</sub>/S checkpoint. Therefore, in cells that overexpressed LPP2, the inhibition of cyclin-dependent kinase activities by the p53 pathway must have been overcome by the positive regulation of cyclin-dependent kinase activities that promoted S-phase entry. The cells that accumulated DNA damage but did not arrest in G<sub>1</sub>-phase did eventually arrest in G<sub>2</sub>-phase of the cell cycle, as described in Chapter 5.

## **CHAPTER 5**

### **PROLONGED LPP2 OVEREXPRESSION CAUSES DECREASED PROLIFERATION, THE ACCUMULATION OF FIBROBLASTS IN G<sub>2</sub>- PHASE, AND A SENESCENT PHENOTYPE**

*A version of this chapter has been published. Morris KE, Schang LM, Brindley  
DN. 2006. J Biol Chem. 281:9297-306.*

## 5.1. Introduction

Fibroblasts that overexpressed LPP2 entered S-phase prematurely as discussed in Chapter 4. These cells did not arrest at the G<sub>1</sub>/S checkpoint in response to DNA damage caused by UV radiation. Cells that do not arrest in G<sub>1</sub>-phase to repair randomly occurring DNA damage would likely accumulate DNA damage over time. Fibroblasts that overexpressed LPP2 had increased levels of activated p53 which indicates that they had accumulated DNA damage. Cells that overexpressed LPP2 had a functional G<sub>2</sub>/M checkpoint, and began to arrest at the G<sub>2</sub>/M checkpoint at high passage number. As this occurred, the proliferation of LPP2 overexpressing cells decreased significantly, and the cells showed hallmarks of senescence. Only cells that overexpressed active LPP2 and entered S-phase prematurely showed decreased proliferation rates and accumulation of fibroblasts in G<sub>2</sub>-phase at high passage. Cells overexpressing LPP1, LPP3, or catalytically inactive LPP2 [R214K] did not slow in proliferation, accumulate in G<sub>2</sub>-phase, or show hallmarks of senescence, even after 45 passages. This Chapter describes the characterization of LPP2 overexpressing cells at high passage.

To facilitate the interpretation of the following results, I will first discuss the fibroblast populations that were used in these studies and explain the terminology that will be used to describe the phenotypic characteristics of the cells in the following experiments. The passage number of a population of cells is an imprecise estimate of the average number of doublings of each cell in a population. The rate at which LPP2 overexpressing cells progressed toward a phenotype of slow growth and G<sub>2</sub>-phase arrest varied between cell populations.



This was expected, since the frequency of cell passing and the density at which cells were passed could not be entirely consistent between cell populations. Additionally, the initial density of cells immediately after retroviral transduction and puromycin selection was different in every cell population. Therefore, the number of doublings that occurred before passage 1, when selected cells first reached confluence, was different for every stably transduced cell population. For this reason, a given passage number in one cell population would represent a different number of cell doublings than the same passage number in another cell population. Additionally, LPP2 overexpressing fibroblasts were sensitive to freeze-thawing, and a much smaller percentage of LPP2 overexpressing cells survived routine freezing and thawing than cells that stably overexpressed the other LPPs or the empty vector. The cells that did survive thawing progressed toward the slow growth phenotype very rapidly, even if they were frozen at very low passage. Since the passage number of a population of cells did not correlate directly with the phenotype of the cells, I will not discuss specific passage numbers in this Chapter, but where necessary I will describe the cell populations that were used in particular experiments as higher or lower passage than others, based upon the approximate percentage of cells in the population that were in G<sub>2</sub>-phase. LPP2 overexpressing fibroblasts gradually accumulated more cells in G<sub>2</sub>-phase and progressively slowed in growth, and experiments were performed throughout this process. Therefore, most results are presented as representative results from populations having somewhere between 20% and 70% of cells in G<sub>2</sub>-phase. Some results are averages from cells at various different stages of arrest,

which accounts for the large standard errors in some of these experiments. It was impractical to work with cells only at one given stage of G<sub>2</sub>-phase arrest, since there would not have been enough cells available to perform experiments.

Eight different mixed populations of LPP2 or LPP2-GFP overexpressing cells were created. Three of these cell populations (two that overexpressed LPP2 and one that overexpressed LPP2-GFP) exhibited the phenotype described above. In the five other cases, LPP2 overexpressing cell populations that had entered S-phase prematurely for 5-20 passages did not arrest in G<sub>2</sub>-phase, but instead stopped entering S-phase prematurely and continued to grow normally in the presence of the continued overexpression of LPP2 activity. This presumably occurred because the cell population was gradually taken over by cells that had developed an unknown compensatory mutation. These cell populations were not used for subsequent studies, and will not be discussed in this Chapter. The results in this Chapter are primarily from two separately created populations of LPP2 overexpressing cells that each slowly accumulated cells in G<sub>2</sub>-phase and slowed in proliferation following at least 15 passages of premature S-phase entry. In these cells, the premature S-phase entry continued in the portion of the population that was not arrested in G<sub>2</sub>-phase until cycling became undetectable. The two cell populations were created approximately two years apart, and each were compared to vector controls and fibroblasts transduced with LPP2 [R214K] that were created in parallel. Both cell populations showed similar phenotypes of G<sub>2</sub>-phase arrest, slowed cell proliferation, and characteristics of senescence.

## 5.2. High passage LPP2 overexpressing cells slow in proliferation

5.2.1. *Fibroblasts overexpressing LPP2 have decreased proliferation at high passage* – Fibroblasts that overexpressed catalytically active LPP2 or LPP2-GFP that entered S-phase prematurely showed decreased proliferation at high passage (Fig. 5.1 A-B). Cells transduced with LPP2 [R214K] proliferated similarly to parental control cells at high passage (Fig. 5.1A). Additionally, cells that overexpressed LPP1 or LPP3 proliferated similarly to vector control cells at high passage (Fig. 5.1B).

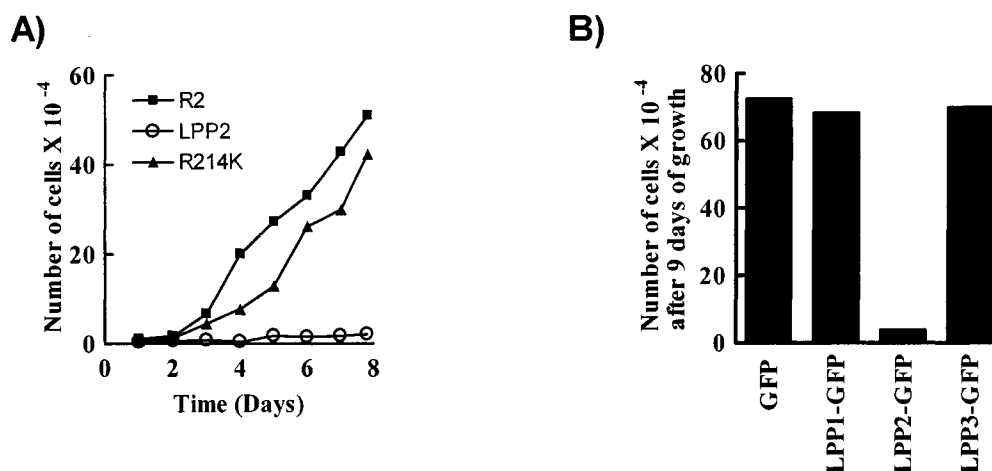


**Figure 5.1. Fibroblasts that overexpress LPP2 activity have decreased proliferation at high passage.** Panel A shows the proliferation of high passage rat2 fibroblasts or those stably transduced with LPP2 or LPP2[R214K]. Panel B shows the number of cells after 9 days of growth in high passage fibroblasts stably transduced with the GFP-tagged LPPs, or GFP alone. Results are from one representative of at least three independent experiments.

When the proliferation of the same cell populations at low and high passages were compared, only the overexpression of LPP2 caused the proliferation of cells to significantly decrease over time (Fig. 5.2A-D). This demonstrates that the decrease in proliferation at high passage is not an artifact of the stable transduction or a phenomenon that occurs in fibroblasts in general.

Populations of cells that were stably transduced with the empty vector or with LPP2 [R214K], LPP1, or LPP3 never showed decreased proliferation rates, even after 45 passages. The decreased proliferation occurred exclusively in cells that had entered S-phase prematurely as a consequence of LPP2 overexpression.

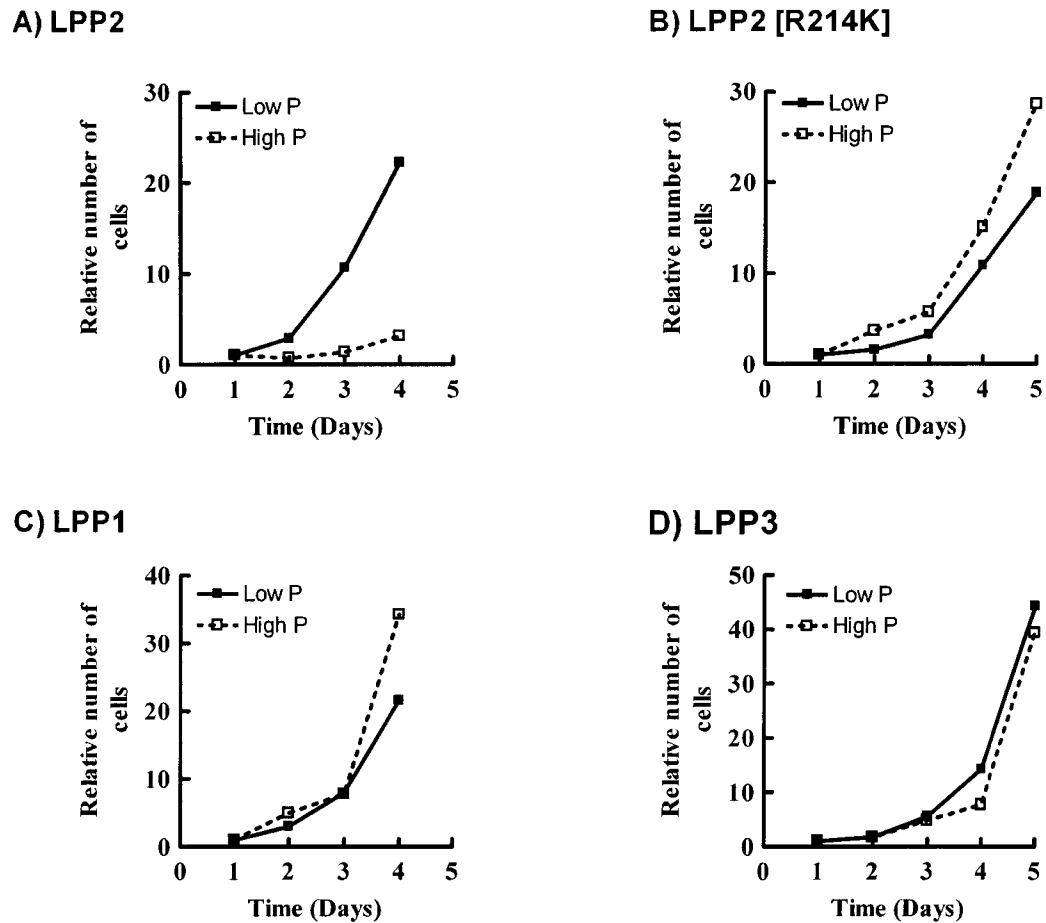


**Figure 5.2. The overexpression of LPP2 but not LPP2 [R214K], LPP1, or LPP3, causes proliferation to decline at high passage.** Panels A-D show the proliferation of cells stably transduced with LPP2, LPP2 [R214K], LPP1, or LPP3. Proliferation was measured in the same cells lines at low (P3 for Panels A-B and P14 for Panels C-D) and high (P23 for Panel A and P45 for Panels B-D) passage number. Results are from one experiment.

5.2.2. *The addition of LPA, S1P, or serum does not reverse the decreased proliferation of LPP2 overexpressing cells* – The decrease in proliferation of the LPP2 overexpressing cells could have been the result of a deficit of a bioactive lipid as a result of LPP2 activity. Media were supplemented with various concentrations of LPA or S1P, or with additional serum, and the proliferation of control and LPP2 overexpressing cells at high passage was measured. The addition of up to 5  $\mu\text{M}$  S1P, 10  $\mu\text{M}$  LPA, or up to 30% serum did not increase the proliferation of LPP2 overexpressing cells (Fig. 5.3A-C).

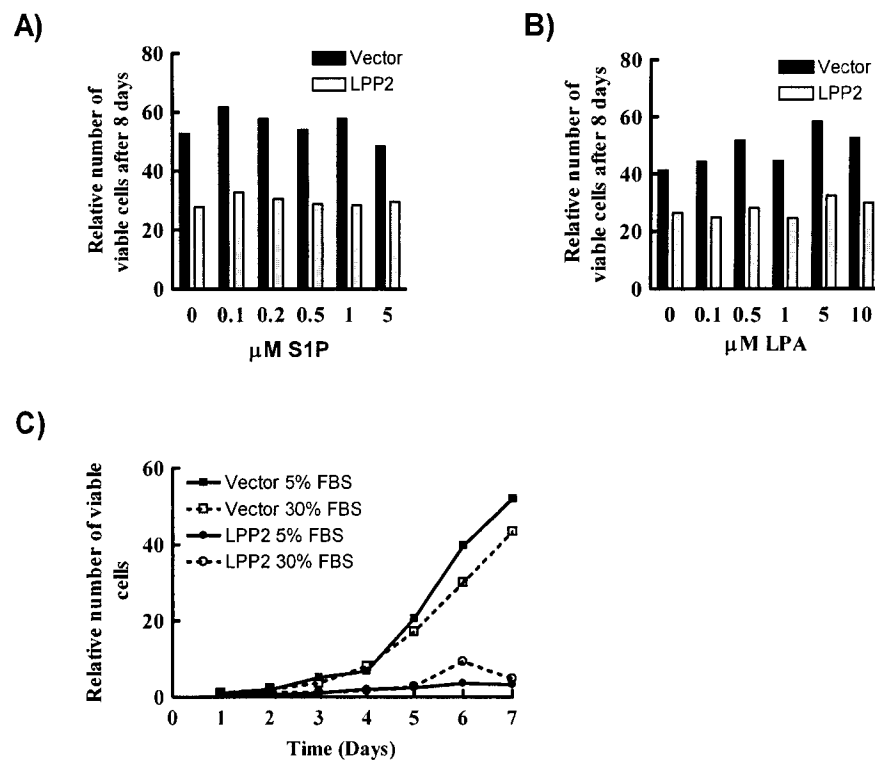


**Figure 5.3. The addition of LPA, S1P, or serum to the media does not reverse the decreased proliferation of high passage LPP2 overexpressing cells.** Panels A-B show the number of cells after 8 days of growth for fibroblasts stably transduced with the empty vector or LPP2 and treated with the indicated concentrations of S1P or LPA. Results are from one experiment. Panel C shows the proliferation of fibroblasts stably transduced with the empty vector or LPP2 and grown in media containing 5% or 30% FBS. Results are from one experiment.

*5.2.3. High passage LPP2 overexpressing cells do not exhibit increased apoptosis* – The decreased number of cells in LPP2 overexpressing populations could have been the result of increased apoptosis. The percentage of apoptotic cells in populations of fibroblasts stably transduced with the empty vector or LPP2 at high passage was evaluated by Hoescht staining. Cells transduced with the empty vector and treated with UV radiation to promote DNA damage had ~20% of cells showing an apoptotic phenotype of condensed DNA (Fig. 5.4). In untreated cells transduced with either the empty vector or LPP2 at high passage, there were less than 1% apoptotic cells in an average of 8 fields (Fig. 5.4). This indicated that the decrease in the number of cells in the LPP2 overexpressing populations was not due to increased apoptosis. Many of the fibroblasts that overexpressed LPP2 had significantly larger nuclei than were seen in the vector control cells of equivalent passage number (Fig. 5.4). This suggested that many of the LPP2 overexpressing cells had replicated their DNA but not divided.

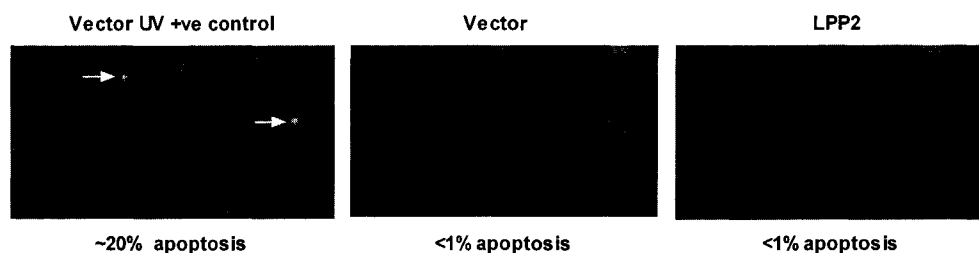


**Figure 5.4. High passage LPP2 overexpressing cells do not have increased apoptosis.** The Panels show fields from high passage cells stably transduced with empty vector or LPP2 that have been stained with Hoescht 33258 to visualize DNA. In the left panel, vector control cells were treated with 50 J/m<sup>2</sup> UV to promote apoptosis. Apoptotic nuclei are indicated by arrows. Results are from one representative of 8 fields that when averaged gave the percentages of apoptosis indicated. Results are from one of two independent experiments.

### **5.3. High passage LPP2 overexpressing cells accumulate in G<sub>2</sub>-phase following the activation of the G<sub>2</sub>/M checkpoint**

5.3.1. *High passage LPP2 transduced cells accumulate in G<sub>2</sub>-phase* – The DNA content of LPP2 overexpressing cells with decreased proliferation was evaluated by flow cytometry. In asynchronous parental rat2 fibroblasts, >80% of the cells were in G<sub>1</sub>-phase, approximately 6% of the cells were in each of S-phase and G<sub>2</sub>-phase, and less than 2% of the cells were apoptotic (Fig. 5.5A). In contrast, high passage cells that overexpressed LPP2 had approximately 30% of the cells in G<sub>1</sub>-phase, 10% of the cells in S-phase, 20% of the cells in G<sub>2</sub>-phase, and 5% of the cells in the apoptotic subdiploid population (Fig. 5.5A). The increase in apoptosis was minor, as expected from previous results, and the number of cells in G<sub>2</sub>-phase was significantly increased compared to control cells, in agreement with the large nuclei observed with Hoescht staining. Therefore, the decrease in proliferation of the LPP2 overexpressing cells could be attributed primarily to the arrest of cells in G<sub>2</sub>-phase of the cell cycle. Cells transduced with the empty vector, LPP2 [R214K], LPP1, or LPP3 all showed similar cell cycle distributions to parental control cells at high passage (Fig. 5.5A).

5.3.2. *LPP2 overexpressing cells with decreased proliferation have increased amounts of DNA and protein per cell* – High passage cells that overexpressed LPP2 and had ~20% of cells in G<sub>2</sub>-phase had approximately twice the amount of DNA per cell and approximately 2.5 times the amount of protein per cell compared to rat2 fibroblasts or vector control cells (Fig. 5.5B). Interestingly, since only 20% of the LPP2 overexpressing cells were in G<sub>2</sub>-phase,

we would expect only a 1.4-fold increase in the amount of DNA/ cell. The unexpectedly high increase in DNA/ cell meant that some cells in G<sub>1</sub>-phase, or G<sub>2</sub>-phase or both cell cycle phases had more than a normal complement of DNA.

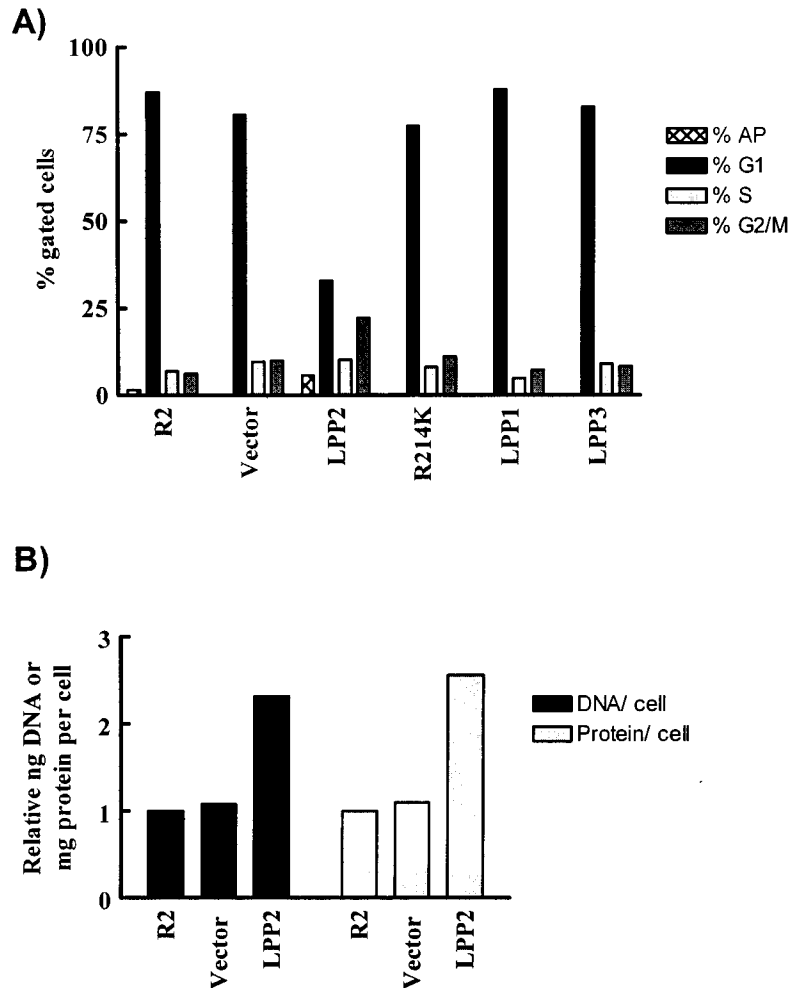


**Figure 5.5. Cells overexpressing LPP2 at high passage have an increased percentage of cells in G<sub>2</sub>-phase and increased amounts of DNA and protein per cell.** Panel A shows the cell cycle distribution after 10 days of growth of rat2 fibroblasts or those stably transduced with the empty vector, LPP2, LPP2[R214K], LPP1, or LPP3. Results are from one representative of two independent experiments. Panel B shows the amount of DNA (black bars) or protein (grey bars) per cell in rat2 fibroblasts or those stably transduced with the empty vector or LPP2. DNA and protein concentrations are expressed relative to the concentrations in rat2 cells which is given as 1. Results are from one representative of two independent experiments.

The arrested LPP2 overexpressing cells appeared more than twice as large as control cells under a microscope, in agreement with their higher amount of



protein per cell. The arrested LPP2 overexpressing cells also developed a morphology in which the cells were flattened and lost their reflectiveness under light. This type of morphology is a common feature of senescence. As populations increased in age, the LPP2 overexpressing cells slowed in proliferation progressively until proliferation was undetectable and more than 70% of cells were in G<sub>2</sub>-phase (not shown). When trypsinized, approximately 30% of the cells failed to reattach to plastic dishes. The remaining cells did attach and spread, but did not proliferate or undergo apoptosis. The fibroblasts remained permanently arrested and did not proliferate for several months, until eventually, cultures became contaminated and were disposed of.

*5.3.3. LPP2 overexpressing cells that are arrested in G<sub>2</sub>-phase have activated the G<sub>2</sub>/M checkpoint by maintaining high levels of phosphorylation of CDK1 on Tyr15* -Dephosphorylation of the inhibitory Tyr15 phosphorylation on CDK1 is required for cells to progress from G<sub>2</sub>-phase into mitosis. In cells where DNA damage is present, Tyr15 phosphorylation of CDK1 is maintained to prevent progression into mitosis. LPP2 transduced populations that had approximately 30% of cells in G<sub>2</sub>-phase and vector control cells of the same passage number were synchronized by serum deprivation and stimulated to cycle with the addition of FBS. In vector control cells, the levels of phosphorylated CDK1 (Tyr15) increased as the cell cycle progressed toward the G<sub>2</sub>/M transition, as expected (Fig. 5.6A). In arrested cells that overexpressed LPP2, the constitutive levels of inactive phosphorylated CDK1 were elevated and did not vary significantly over time (Fig. 5.6A). In asynchronous LPP2 overexpressing

cells with >50% of cells in G<sub>2</sub>-phase, the amount of phosphorylated CDK1 (Tyr15) was 14-fold higher than levels in asynchronous control cells (Fig. 5.6A). To ensure that the maintenance of CDK1 phosphorylation was not a direct function of the activity of LPP2, low passage vector control and LPP2 overexpressing cells were synchronized and the amount of phosphorylated CDK1 (Tyr15) was measured by Western blot. In very low passage LPP2 overexpressing cells that entered S-phase prematurely, the phosphorylation of CDK1 during cell cycle progression was not significantly different from that in vector control cells (Fig. 5.6B). The peak of CDK1 phosphorylation occurred approximately 2 h earlier in the LPP2 overexpressing cells due to the premature S-phase entry and consequently shorter cell cycle (Fig. 5.6B). These results demonstrate that the increase in CDK1 phosphorylation on Tyr 15 in high passage LPP2 overexpressing cells was not a direct effect of LPP2 activity, but a secondary effect of the repeated premature S-phase entry.

5.3.4. *LPP2 overexpressing cells that have arrested in G<sub>2</sub>-phase do not increase cyclin B expression in response to serum stimulation* – Cyclin B is a activating binding subunit of CDK1 that promotes progression from G<sub>2</sub>-phase into mitosis. The expression of cyclin B in high passage vector control and LPP2 overexpressing cells was evaluated by Western blotting. LPP2 overexpressing populations that had ~30% of cells in G<sub>2</sub>-phase had deregulated cyclin B expression compared to vector control cells of the same passage number (Fig. 5.6C). Cyclin B expression did not change over time after serum stimulation in the arrested cells, whereas it increased significantly as cells approached mitosis in

the control fibroblasts, as expected (Fig. 5.6C). Cyclin B levels were low in both asynchronous vector control cells that were predominantly in G<sub>1</sub>-phase, and in very high passage LPP2 cells with >50% of cells in G<sub>2</sub>-phase (Fig. 5.6C). The lack of increase in cyclin B expression in LPP2 overexpressing cell populations at high passage may have been the result of the fact that many of the cells in the population were not cycling and had undergone permanent arrest. Decreased cyclin B expression is common in cells that have undergone permanent cell cycle exit [178]. To ensure that cyclin B expression was not dysregulated directly by LPP2 activity, cyclin B expression in very low passage LPP2 overexpressing cells was measured during cell cycle progression. Cyclin B expression was not decreased or changed in timing in low passage LPP2 overexpressing cells compared to cells transduced with the empty vector (Fig. 5.6D).

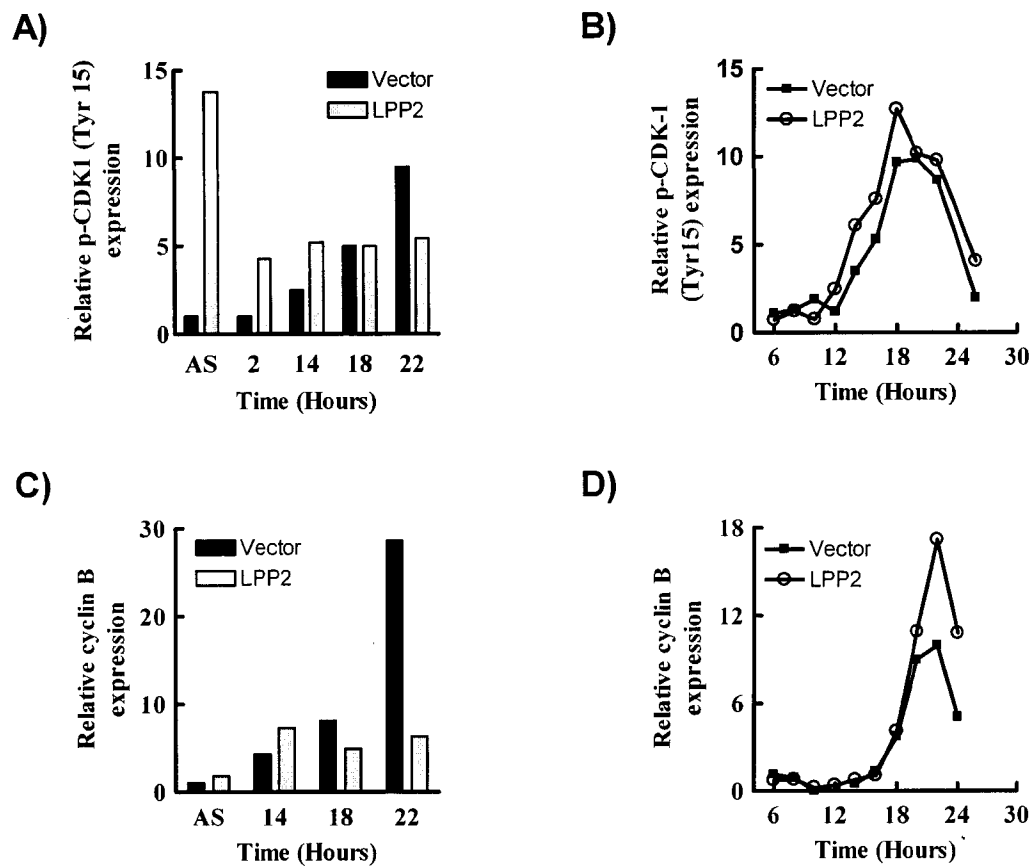


**Figure 5.6. The expression of phosphorylated CDK1 (Tyr15) and cyclin B are dysregulated in cells stably overexpressing LPP2 at high passage.** Panels A-D show the quantitation of Western blots for p-CDK1 (Tyr15) in Panels A-B or cyclin B in Panels C-D in asynchronous high passage cells (Panels A,C) or in low passage cells at various times after synchronization and the re-addition of FBS (Panels B,D). Cells were stably transduced with empty vector (black bar, ■) or LPP2 (grey bar, ○). Results are from one representative of at least two independent experiments.

#### 5.4. LPP2 overexpression is suppressed at high passage in cells arrested in G<sub>2</sub>-phase

##### 5.4.1. LPP2 mRNA expression is decreased in cells arrested in G<sub>2</sub>-phase –

Cells that overexpressed LPP2 activity, entered S-phase prematurely, and subsequently arrested in G<sub>2</sub>-phase, eliminated the overexpression of LPP2 mRNA at high passage (Fig. 5.7A). Fibroblasts that were stably transduced with LPP2

that had more than 30% of cells in G<sub>2</sub>-phase had not only eliminated the ~40-fold overexpression of LPP2 mRNA, but had decreased LPP2 mRNA expression to 33% of the endogenous expression in parental fibroblasts (Fig. 5.7A).

*5.4.2. LPP activity in lysates from cells arrested in G<sub>2</sub>-phase is reduced to control levels* – Lysates from cells transduced with LPP2 that had more than 30% of cells in G<sub>2</sub>-phase were assayed for LPP activity toward PA. High passage LPP2 transduced cells that had eliminated the overexpression and decreased the endogenous expression of LPP2 mRNA had similar total LPP activity in lysates to parental control cells (Fig. 5.7B).

*5.4.3. The concentrations of LPP1 mRNA and LPP3 mRNA in cells with suppressed LPP2 overexpression* – To determine whether the suppression of LPP2 expression affected the expression of the other LPP isoforms, the mRNA expression of LPP1 and LPP3 were measured in two independent high passage cell populations that had been transduced with LPP2. The concentration of LPP1 mRNA was not significantly changed in two populations of high passage cells that had suppressed LPP2 overexpression (Fig. 5.7C). However, the expression of LPP3 mRNA was significantly increased by 10-fold in one cell population and significantly decreased by 80% in the other cell population in which LPP2 overexpression was suppressed (Fig. 5.7C). This result was unexpected, since knock-down of endogenous LPP2 and overexpression of LPP2 did not change LPP3 mRNA expression. It is surprising that some G<sub>2</sub>-phase arrested cells had decreased LPP3 mRNA expression, and others increased LPP3 mRNA expression, yet both populations showed the same phenotypic characteristics of

cell cycle arrest and senescence and both populations had total LPP activities similar to those in control cells. The relationship between the changes in LPP3 mRNA expression and the suppression of LPP2 expression is unclear.

5.4.4. *The overexpression of LPP1, LPP3, and LPP2 [R214K] are not suppressed at high passage* – The suppression of LPP2 mRNA overexpression at high passage could have been a phenomenon related to the transduction system we used or the length of time in culture, or it could have been a general feature of LPP overexpression, rather than a result of the phenotype produced by LPP2. Therefore, we examined whether the expression of the other LPPs was suppressed at high passage using the same retroviral transduction techniques. Cells transduced with the empty vector, LPP1, LPP3, or LPP2 [R214K] were assayed for total LPP activity at high passage (passage 45). Lysates from high passage cells transduced with LPP1 and LPP3 still showed increased total LPP activity (Fig. 4.7D). Furthermore, lysates from high passage cells transduced with LPP2 [R214K] showed decreased LPP activity, as they did at low passage (Fig. 4.7D). These results indicate that the overexpression of the other LPPs was not suppressed at high passage, and that this phenomenon was specific to active LPP2, and therefore likely related to the cell cycle or senescent phenotype.

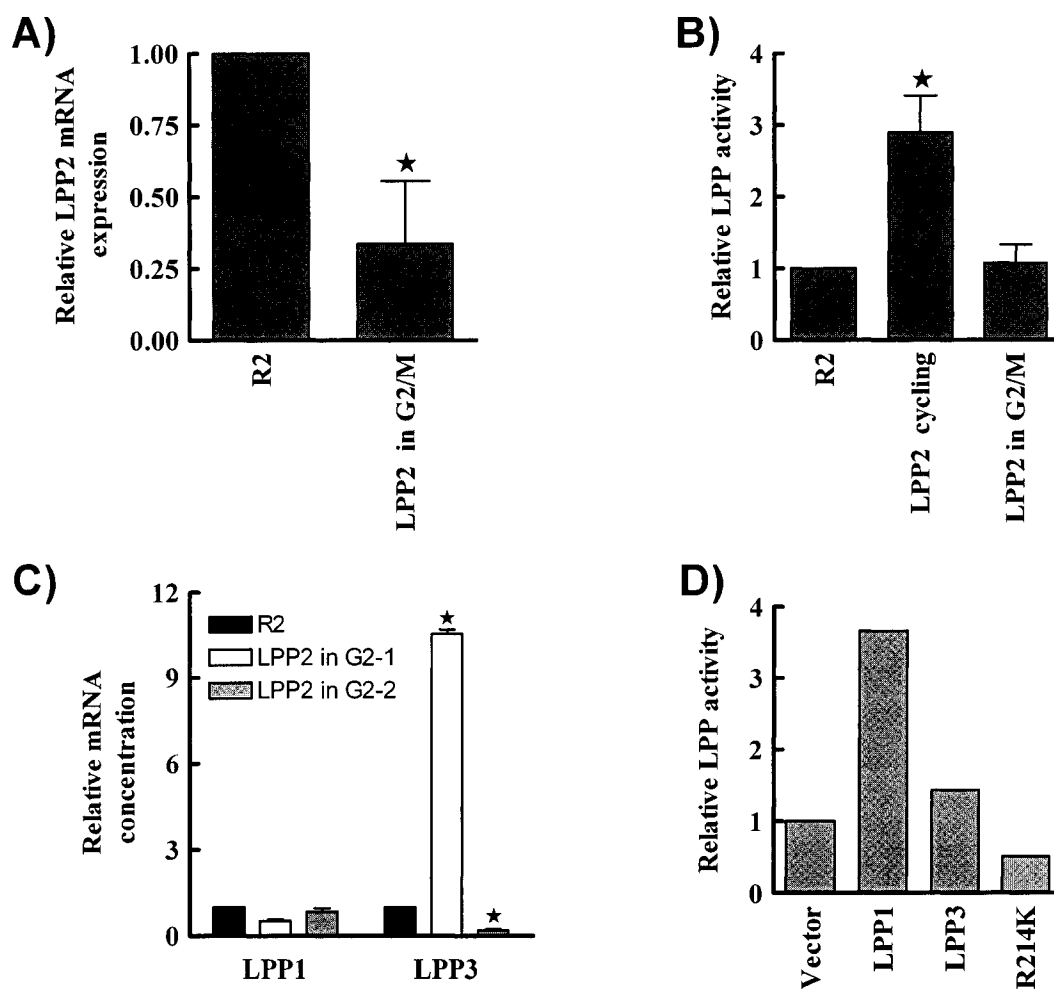


**Figure 5.7. The overexpression of LPP2 is suppressed at high passage.** Panel A shows LPP2 mRNA concentrations for parental fibroblasts or cells stably transduced with LPP2 at high passage that have >30% of cells in G<sub>2</sub>-phase. Panel B shows LPP activities of rat2 cells or those stably transduced with LPP2 at low passage (cycling) or high passage (G<sub>2</sub>/M). Results are expressed as fold change compared to rat2 fibroblasts which is given as 1. Panel C shows LPP1 or LPP3 mRNA concentrations, as indicated for parental fibroblasts or two different populations of cells stably transduced with LPP2 at high passage that have >30% of cells in G<sub>2</sub>-phase. Results from Panels A-C are means ± SD from at least 4 independent experiments. Statistically significant differences ( $p < 0.05$ ) from control are indicated by \*. Panel D shows LPP activities toward PA of lysates from fibroblasts stably transduced with the empty vector, LPP1, LPP3, or LPP2 [R214K] at passage 45. Results are expressed as fold change compared to vector control which is given as 1. Results are averages from one experiment. The results shown in Panel D are from an experiment performed by J. Dewald.

## **5.5. LPP2 transduced cells that are arrested in G<sub>2</sub>-phase show changes in protein expression and lipid concentrations that are characteristic of senescence**

*5.5.1. The expression of proteins involved in cell cycle progression and senescence are increased in cells arrested in G<sub>2</sub>-phase* – Lysates from cell populations that had overexpressed LPP2 and had >50% of cells in G<sub>2</sub>-phase were analyzed by Western blot and compared to lysates from parental rat2 fibroblasts and cells transduced with the empty vector at the same passage number. The arrested LPP2 transduced cells had increased the expression of cyclin D1 by 5-fold, cyclin D2 by 7-fold, cyclin D3 by 2-fold, and cyclin E by 4-fold (Fig. 5.8). These increases in cyclin expression are consistent with previous studies in which cyclin D and E levels were elevated in senescent cells [179, 180]. Since the expression of these proteins was normalized to cell number, it is also possible that some of the more modest increases in expression were due to the larger overall size of the arrested cells and their larger nuclei. The expression of Ser15-phosphorylated p53 was increased by 16-fold in arrested cells, and the expression of p21<sup>Cip1</sup> was increased 8-fold (Fig. 5.8). The expression of p27<sup>Kip1</sup> was also increased 6-fold, and the expression of p16<sup>INK4a</sup> was increased 7-fold (Fig. 5.8). The upregulation of active p53, p21<sup>Cip1</sup>, and p16<sup>INK4a</sup> are hallmarks of stress or oncogene-induced senescence [121, 137].



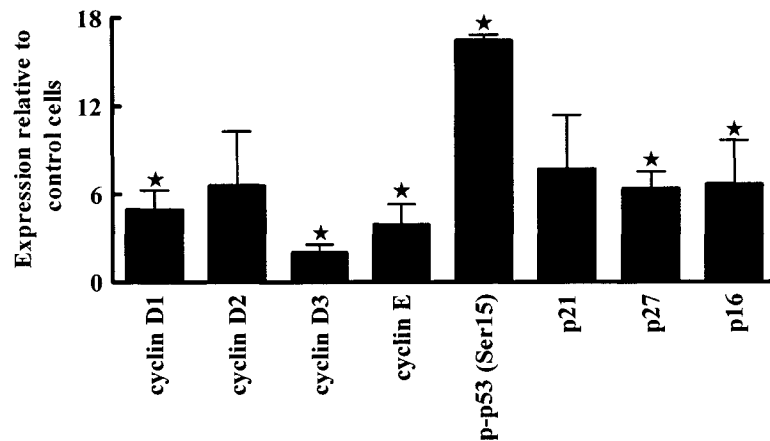


**Fig. 5.8. Cells stably transduced with LPP2 that are arrested in G<sub>2</sub>-phase show changes in the expression of proteins that are characteristic of senescence.** The panel shows quantitations of Western blots for cyclin D1, cyclin D2, cyclin D3, cyclin E, phospho-p53 (Ser15), p21<sup>Cip1</sup>, p27<sup>Kip1</sup>, and p16<sup>INK4a</sup> in cells transduced with LPP2 and grown asynchronously at high passage with >40% of cells in G<sub>2</sub>-phase. Expression is relative to the expression in the same number of cells transduced with empty vector and grown asynchronously at the same passage number. Results are means ± SD from at least three independent experiments. Statistically significant differences (p < 0.05) from vector control are indicated by \*.

#### 5.5.2. LPP2 transduced cells arrested in G<sub>2</sub>-phase have increased

*ceramide and decreased LPA levels*– Bulk lipid concentrations were compared in cell populations transduced with LPP2 at high passage that had >30% of cells in G<sub>2</sub>-phase and cells transduced with the empty vector at the same passage number. Cells that were arrested in G<sub>2</sub>-phase had increased ceramide concentrations by approximately 2-fold (Table 5.1). Different ceramide species were increased proportionally, and the predominant species, 16:0, comprised 50% of the total ceramide. It has been previously reported that ceramide levels increase in senescent cells, and that increased sphingomyelinase activity and high ceramide concentrations are instrumental in maintaining a senescent phenotype [140, 181]. Cells transduced with LPP2 and arrested in G<sub>2</sub>-phase also had decreased LPA concentrations by approximately 60% compared to parental control fibroblasts

(Table 5.1). The decrease in LPA was not a result of LPP2 activity, since the overexpression of LPP2 was suppressed in these cells. Additionally, the decrease in LPA occurred in the population of cells that had decreased LPP3 mRNA expression, so it could not be attributed to the increased expression of any of the LPP isoforms. Therefore, the reduction in the concentration of LPA in the G<sub>2</sub>-phase arrested cells was likely related to the senescent phenotype. The concentrations of sphingosine, sphingosine-1-phosphate, sphinganine, sphinganine-1-phosphate, and ceramide-1-phosphate were not significantly different in G<sub>2</sub>-phase arrested cells compared to control cells (Table 5.1).

**Table 5.1. Lipid composition of G<sub>2</sub> arrested cells**

Concentrations of bulk cellular sphingolipids were determined by mass spectrometry in parental fibroblasts (R2) and cells showing the G<sub>2</sub> arrest phenotype subsequent to LPP2 overexpression. Concentrations are expressed relative to total sphingomyelin. Samples were analyzed in triplicate and results are expressed as mean  $\pm$  SD for at least three independent determinations. LPA concentrations were determined in cells overexpressing the empty vector, low passage cells overexpressing LPP2, or cells formerly overexpressing LPP2 which were arrested in G<sub>2</sub>-phase. LPA concentration is normalized to total phospholipid, and expressed as the fold increase compared to the vector control which is given as 1. Results are means  $\pm$  SD for three independent experiments. Statistical significance ( $p < 0.05$ ) from rat2 fibroblasts or vector control is indicated by \*. Mass spectrometry was performed by E. Wang, S. Kelly, and Dr. A. Merrill Jr. at the Georgia Institute of Technology, Atlanta, GA.

	Relative concentration						Fold increase
	Ceramide	Ceramide phosphate	Sphingosine	Sphingosine phosphate	Sphinganine	Sphinganine Phosphate	Lysophosphatidic Acid
R2	3.81 $\pm$ 0.31	79.1 $\pm$ 5.47	0.333 $\pm$ 0.01	1.27 $\pm$ 0.201	0.553 $\pm$ 0.07	0.071 $\pm$ 0.021	1.00 $\pm$ 0.000
LPP2 (arrested in G <sub>2</sub> )	6.71 $\pm$ 0.47*	76.8 $\pm$ 2.19	0.429 $\pm$ 0.14	1.16 $\pm$ 0.273	0.676 $\pm$ 0.15	0.127 $\pm$ 0.031	0.368 $\pm$ 0.052*
Vector							1.00 $\pm$ 0.000
LPP2 (low passage)							1.07 $\pm$ 0.102

## 5.6. Discussion

Subsequent to repeated premature S-phase entry, cells that overexpressed active LPP2 began to accumulate in G<sub>2</sub>-phase of the cell cycle. Cells in G<sub>2</sub>-phase showed permanent cell cycle exit and irreversible proliferative arrest, characteristic of cellular senescence. It has been previously established that cells with unregulated and premature S-phase entry, which is often induced by the overexpression of G<sub>1</sub>-phase cyclins, exhibit genetic instability and increased dependence on checkpoint functions [81, 176, 177, 182]. Cells activate DNA damage response pathways after undergoing premature S-phase entry, likely as a result of the accumulation of random DNA damage that cannot be repaired due to the lack of arrest in G<sub>1</sub>-phase [81]. Cells undergoing repeated premature S-phase entry would be expected to activate the p53 DNA damage response pathway which would lead to the upregulation of p21<sup>Cip1</sup>. This could trigger cell cycle arrest at the G<sub>1</sub>/S checkpoint and/or at the G<sub>2</sub>/M checkpoint. Activation of the p53 DNA damage pathway can lead to apoptosis, temporary cell cycle and proliferative arrest (quiescence) while DNA damage is repaired, or permanent cell cycle and proliferative arrest (senescence). In Chapter 4 we provided evidence that cells that overexpress active LPP2 fail to arrest at the G<sub>1</sub>/S checkpoint in response to DNA damage caused by UV radiation. Although low passage LPP2 overexpressing cells did show increases in Ser15-phosphorylated p53 following UV irradiation, presumably as a result of the activation of ATR, cells continued to progress through G<sub>1</sub>-phase and into S-phase without arresting in response to the DNA damage.

DNA damage-induced G<sub>2</sub>/M arrest occurs by both p53-dependent and p53-independent mechanisms. After DNA damage, the kinases CHK1 and CHK2 are activated and phosphorylate the CDC25C phosphatase. The phosphorylated CDC25C is sequestered in the cytoplasm, and cannot enter the nucleus to dephosphorylate CDK1 and promote mitotic progression. Therefore, even in the absence of a functional p53 pathway and in the absence of G<sub>1</sub>/S checkpoint arrest, cells will arrest at the G<sub>2</sub>/M checkpoint due to the sustained inhibitory phosphorylation of CDK1 on Thr14 and Tyr15 (reviewed in [81]). The LPP2 overexpressing fibroblasts that repeatedly entered S-phase prematurely and failed to arrest at the G<sub>1</sub>/S checkpoint did arrest at the G<sub>2</sub>/M checkpoint. As expected, this arrest coincided with a sustained increased phosphorylation of CDK1 on Tyr 15. Studies on low passage LPP2 overexpressing cells demonstrated that the G<sub>2</sub>/M arrest did not occur because LPP2 activity directly dysregulated CDK1 phosphorylation or cyclin B expression. Therefore, the G<sub>2</sub>-phase arrest was most likely a consequence of G<sub>2</sub>/M checkpoint activation by the DNA damage pathway that was activated by repeated unchecked S-phase entry.

LPP2 overexpressing cells that arrested at the G<sub>2</sub>/M checkpoint did not undergo apoptosis to an increased extent compared to control cells. Instead, LPP2 overexpression led to the permanent and irreversible arrest of fibroblasts known as cellular senescence. Senescence typically refers to the arrest of cells in G<sub>1</sub>-phase, however other investigators have described the permanent arrest of cells in G<sub>2</sub>-phase [183]. Cells that overexpressed LPP2 exhibited the characteristic enlarged flat morphology of senescent cells in addition to showing permanent

proliferative arrest without apoptosis. In retrospect, it would have been informative to measure neutral  $\beta$ -galactosidase activity, a hallmark of senescence, in the G<sub>2</sub>-arrested cells. A limited number of experiments were performed to assay for hallmarks of senescence due to the small number of cells available for experimentation.

The LPP2 transduced cells that arrested in G<sub>2</sub>-phase had increased the levels of Ser15-phosphorylated p53, p21<sup>Cip1</sup>, and p16<sup>INK4a</sup>. This indicates that both pathways involved in the maintenance of a senescent phenotype were activated in the arrested cells. Interestingly, although p21<sup>Cip1</sup> did not appear to be upregulated in LPP2 overexpressing cells in response to UV, the p53 DNA damage pathway did induce p21<sup>Cip1</sup> expression subsequent to repeated premature S-phase entry. The upregulation of p16<sup>INK4a</sup> expression that is related to the activation of the Rb pathway is a hallmark of irreversible arrest and stress or oncogene-induced senescence in human fibroblasts. There is some discrepancy as to whether stress-induced senescence occurs differently in human and rodent cells. The oxidative stress induced in rodent cells by routine culture conditions causes an upregulation of p16<sup>INK4a</sup> without proliferative arrest, and unlike in human cells where Rb-induced senescence is irreversible, there is evidence to suggest that inactivating Rb can reverse senescence in mouse cells (reviewed in [132]). Whether or not there are differences in the induction of senescence in human and rodent cells, in our rat fibroblasts levels of p16<sup>INK4a</sup> were detectable but very low in vector control cells at very late passage, and were significantly upregulated in the LPP2 transduced cells arrested in G<sub>2</sub>-phase.

It has been well established that in cultured cells, some oncogenes can induce premature senescence after initially stimulating proliferation. Recently, several studies have demonstrated that cellular senescence is an important process involved in tumor suppression *in vivo*. These studies collectively demonstrate that benign but not malignant tumors contain cells with hallmarks of senescence, and that oncogene-induced cellular senescence is likely a potent anti-cancer response [129-131, 139, 184]. In one study, expression of an oncogenic mutant of BRAF, a downstream effector of Ras, initially accelerated cell cycle progression and stimulated the proliferation of melanocytes, but subsequently caused the induction of p16<sup>INK4a</sup> expression and a senescence-like growth arrest [131]. The phenotype produced in this *in vivo* study by oncogenic BRAF was very similar to the phenotype produced by LPP2 overexpression in our study. In both cases, initial stimulation of cell cycle progression was followed by eventual cell cycle exit and permanent proliferative arrest. Therefore, there is evidence that the type of phenotype observed in our study that resulted from LPP2 overexpression may represent a physiologically relevant process involved in the regulation of malignancy.

LPP2 transduced cells that arrested in G<sub>2</sub>-phase suppressed the overexpression of LPP2 and decreased the endogenous expression of LPP2 mRNA. In one cell population, the expression of LPP3 mRNA was increased, whereas in another cell population LPP3 mRNA expression was decreased. The significance of these observations is unknown. The population of cells that increased LPP3 mRNA overexpression by 10-fold did not show increased total

LPP activity, and showed the same senescent phenotype as the population that suppressed LPP3 expression, including similar expression of proteins involved in senescence, and similar changes in the concentrations of ceramide and LPA. Additionally, the changes in the expression of LPP3 did not allow the cells to overcome their proliferative arrest. It is not clear why the arrested cells suppressed the activity of LPP2. It is possible that the suppression of LPP2 activity may have been necessary in order for the cells to maintain their senescent phenotype or maintain the integrity of the G<sub>2</sub>/M checkpoint. It is also possible that cells that did not suppress the activity of LPP2 underwent apoptosis or were selected out of the population after a certain number of doublings. We have no evidence to support or reject any of these hypotheses, and understanding the significance of this observation will require further, more detailed study.

LPP2 transduced fibroblasts that were arrested in G<sub>2</sub>-phase had increased concentrations of ceramide. It has been previously shown that senescent human fibroblasts have elevated ceramide concentrations and that ceramide contributes to the senescent phenotype [140]. Although increased LPP activity could be expected to produce increased ceramide from ceramide-1-phosphate, the LPP2 transduced senescent cells had suppressed LPP2 overexpression, and increased ceramide levels were present in cell populations that had decreased LPP2 expression, decreased LPP3 expression, and unchanged LPP1 expression, compared to control cells. Additionally, the overexpression of LPP2 activity did not change bulk ceramide concentrations in low passage cells. Therefore, the increased ceramide is likely the result of increased neutral sphingomyelinase

activity as was previously reported in senescent fibroblasts [140]. LPP2 transduced senescent fibroblasts also had decreased LPA concentrations by approximately 60%. To our knowledge this is a novel finding which implicates intracellular LPA signaling in the development of cellular senescence. The LPA1 receptor can translocate to the nucleus and regulate transcription [22]. Additionally, LPA may be an agonist for the nuclear PPAR $\gamma$  receptor [24, 26] which decreases the expression of some of the proteins that were increased in our senescent cells such as cyclin D, cyclin E, p21<sup>Cip1</sup>, and p27<sup>Kip1</sup> [185]. Therefore, it is not surprising that decreased LPA might help to promote or maintain a senescent phenotype. Previous studies indicated that decreased sensitivity to LPA signaling by decreased LPA receptor expression or decreased downstream G $\alpha_i$  signaling may occur in some senescent cells [186, 187]. Therefore, it may be favorable for cells to decrease LPA production or secretion, or responsiveness to LPA to promote senescence. While decreased LPA could, in theory, result from increased LPP activity, the senescent LPP2 transduced fibroblasts that had low LPA concentrations had unchanged or decreased mRNA expression of all three LPP isoforms. Furthermore, overexpression of LPP2 activity in low passage cells did not decrease cellular LPA concentrations. Therefore, the decrease in LPA concentration is most likely related to the senescent phenotype.

In summary, the overexpression of active LPP2 leads to the eventual activation of the G<sub>2</sub>/M checkpoint and accumulation of cells in G<sub>2</sub>-phase after repeated premature S-phase entry. Cells that arrest in G<sub>2</sub>-phase exit the cell cycle



and show permanent proliferative arrest and characteristics of a senescent phenotype. LPP2 transduced cells that undergo cellular senescence have increased Ser15-phosphorylated p53, p21<sup>Cip1</sup>, and p16<sup>INK4a</sup> expression, increased ceramide, and decreased LPA concentrations. LPP2 transduced cells that undergo cellular senescence also eliminate the overexpression of LPP2 mRNA. Prolonged LPP2 overexpression produces a phenotype resembling typical oncogene-induced senescence that occurs in culture and *in vivo*. This constitutes an anti-malignancy program designed to halt the proliferation of cells with dysregulated cell cycle progression.

## **CHAPTER 6**

### **LPP2 REGULATES THE MIGRATION OF FIBROBLASTS TO LPA AND SECRETED MATRIX METALLOPROTEINASE ACTIVITIES**

## 6.1. Introduction

LPP1 overexpression inhibits fibroblast migration to LPA ([65], C. Pilquil, unpublished). It was determined in our laboratory that the conditioned media from fibroblasts that overexpressed LPP1 could inhibit the migration of parental fibroblasts (C. Pilquil, unpublished). Media from LPP1 overexpressing cells were analyzed, and we discovered that LPP1 overexpression changed the secreted activities of the gelatinases MMP2 and MMP9 (discussed later in this Chapter). As a follow-up to these observations, we investigated the effect of LPP2 overexpression and knock-down on fibroblast migration. We also investigated the effect of changing the expression of each of the LPPs on the secreted activities of MMP2 and MMP9. These studies are preliminary, but provide evidence that LPP2 can regulate fibroblast migration to LPA and MMP activities. The regulation of MMP activities and migration by LPP2 were evaluated using low passage cells that stably overexpressed LPP2 and entered S-phase prematurely. Since it has been reported that secreted MMP activities change in senescent cells, MMP activities were also analyzed in high passage LPP2 transduced senescent cells. The absolute values presented in this Chapter vary significantly between experiments when conditioned media were used. This is because in some cases media were concentrated up to 6-fold to optimize detection, whereas in other preliminary experiments media were not concentrated. Values can only be compared within experiments where media were treated equivalently.

## **6.2. Changes in LPP2 expression change the migration of fibroblasts to LPA**

*6.2.1. Fibroblasts that overexpress LPP2 migrate less to a variety of mitogens* – The migration of rat2 fibroblasts and those that stably overexpressed LPP2 or LPP2 [R214K] was measured in a Boyden chamber assay. Rat2 fibroblasts have a modest basal level of migration to starvation media (DMEM + 0.1% BSA). The optimal migration to LPA occurred at a concentration of 0.5  $\mu$ M LPA and the optimal migration to PDGF occurred at a concentration of 10 ng/ml PDGF. These agonists stimulated fibroblast migration by approximately 2-fold (Fig. 6.1A). The addition of 5% FBS stimulated a 5-fold increase in fibroblast migration, while 0.1  $\mu$ M S1P inhibited basal fibroblast migration by ~90% (Fig. 6.1A). Fibroblasts that stably overexpressed LPP2 migrated less than parental rat2 fibroblasts or cells that overexpressed inactive LPP2 [R214K] to untreated media, LPA, S1P, PDGF, and 5% serum (Fig. 6.1A). The decrease in migration of LPP2 overexpressing cells to all media suggests that LPP2 overexpression decreases the ability of fibroblasts to migrate. This does not necessarily imply that LPP2 overexpression attenuates the migratory response of cells to any specific agonist or signaling pathway.

*6.2.2. Knock-down of endogenous LPP2 decreases the migration of fibroblasts to LPA* - Cells that had LPP2 knocked down by approximately 40% showed a 25% decrease in migration toward LPA compared to parental control cells (Fig. 6.1B). The effect of the knock-down of endogenous LPP2 on the migration of fibroblasts to other agonists will be investigated in future experiments.

6.2.3. *Media from LPP2 overexpressing cells promotes the migration of parental fibroblasts to LPA* – Conditioned media (DMEM + 0.1% BSA) were collected from rat2 fibroblasts and those overexpressing the LPPs. Charcoal-stripped FBS and 0.5  $\mu$ M LPA were added to the media, and the media were used in the bottom chamber of transwells to stimulate migration. In two independent experiments, fibroblasts migrated approximately 1.5-fold more to media from LPP2 overexpressing cells than to media from parental control cells (Fig. 6.1C). In contrast, media from LPP1 overexpressing cells inhibited migration to LPA, and media from LPP3 overexpressing cells had no effect on migration to LPA (C. Pilquil, unpublished, and Fig. 6.1C). LPP2 could have conditioned media to promote migration by increasing the concentration or activity of factor that promotes migration, for example, MMP2 or LPA. Additionally, LPP2 could promote migration by decreasing the concentration of a factor that inhibits migration.

6.2.4. *Media from cells with LPP2 knocked down inhibits the migration of fibroblasts to LPA* – Conditioned media were collected from fibroblasts transfected with siRNAs for rat LPP2 or non-targeting control siRNAs. Media were concentrated 3-fold and charcoal-stripped FBS and 0.5  $\mu$ M LPA were added. Parental fibroblasts showed a ~50% decrease in migration to media from cells with LPP2 knocked down by ~50% (Fig. 6.1D). The effect of conditioned media from cells with LPP2 overexpressed or knocked down on fibroblast migration to other agonists or in the absence of agonist will be evaluated in future experiments.

### A) Migration of cells to various agonists (relative number of cells/field)

Stable cell line	Agonist added to DMEM + 0.1% BSA in bottom chamber				
	n.t.	0.5 $\mu$ M LPA	0.1 $\mu$ M S1P	10 ng/ml PDGF	5% FBS
Rat2	1.00	1.88	0.14	2.40	4.58
LPP2-GFP	0.63	0.77	0.08	1.30	2.75
LPP2[R214K]-GFP	0.71	1.92	0.10	2.62	4.67

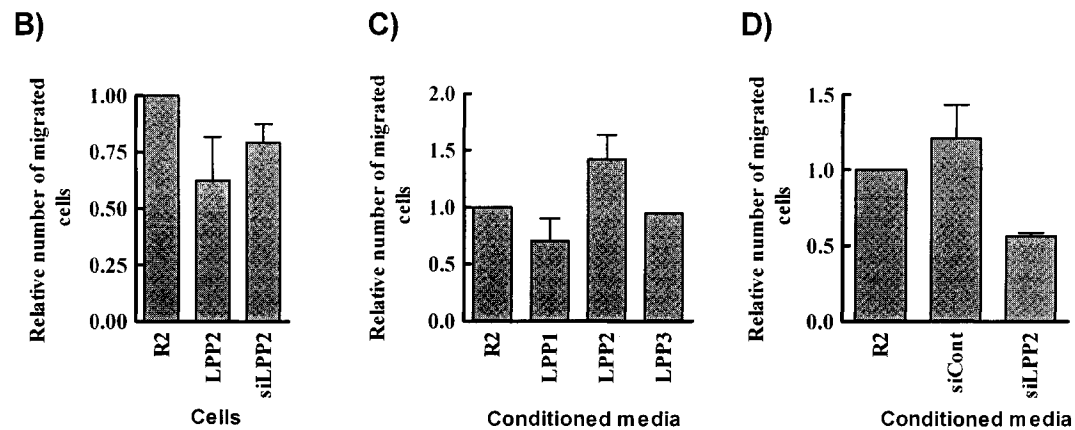


**Figure 6.1. Changes in expression of the LPPs affect the migration of fibroblasts.** Panels A-D show the average number of migrated cells per field after 6 h of migration. In panel A rat2 fibroblasts or those stably overexpressing LPP2-GFP or LPP2[R214K]-GFP migrated toward the indicated agonists. In panel B rat2 fibroblasts or those stably overexpressing LPP2 or transfected with siRNAs for rLPP2 migrated toward 0.5  $\mu$ M LPA. In panel C conditioned media (DMEM + 0.1% BSA) were collected from rat2 fibroblasts or those stably overexpressing LPP1, LPP2, or LPP3. Rat2 fibroblasts migrated toward this conditioned media supplemented with charcoal-stripped FBS and 0.5  $\mu$ M LPA. In panel D conditioned media were collected from rat2 fibroblasts or those transfected with non-targetting control siRNAs or siRNAs for rLPP2. Rat2 fibroblasts migrated toward this conditioned media supplemented with charcoal-stripped FBS and 0.5  $\mu$ M LPA. Results are expressed relative to the migration of rat2 cells in panels A-B or to the migration of cells to conditioned media from rat2 cells in Panels C-D which is given as 1. Typically, in a 6 h experiment, there are approximately 50 cells/field when rat2 cells migrate to 0.5  $\mu$ M LPA. Results are single experimental values or averages of values from at least two independent experiments where error bars are indicated. Some results shown in Panels A and C are from experiments performed by C. Gaetano and M. Sariahmetoglu, respectively.

## 6.3. LPP activities change the secreted activity and expression of MMP2

### 6.3.1. Secreted MMP2 activity is changed by the overexpression and

*knock-down of the LPPs* – The MMPs are secreted proteinases that can regulate the migration of many cells including fibroblasts. We wanted to evaluate whether

secreted MMP activities were changed in conditioned media from cells that had the LPPs overexpressed or knocked down. We measured the activities of the gelatinases MMP2 and MMP9 in conditioned media using gelatin zymography. Conditioned media from cells that stably overexpressed LPP2 had a 2-fold increase in 72 kDa pro-MMP2 activity compared to media from parental rat2 fibroblasts (Fig. 6.2A). In contrast, media from cells that overexpressed LPP1 and LPP3 had 80% and 70% decreases in pro-MMP2 activity, respectively (Fig. 6.2A). Media from cells that overexpressed LPP2 [R214K] had a 70% decrease in pro-MMP2 activity (Fig. 6.2A). This indicated that the inactive LPP2 [R214K] mutant may act as a dominant-negative in terms of regulating the secreted activity of MMP2. Media from fibroblasts transfected with siRNAs for non-targeting control or rLPP2 were collected and concentrated 3-fold. The knock-down of LPP2 by ~50% resulted in 15% and 60% decreases in 72 kDa pro-MMP2 and 62 kDa MMP2 activities, respectively (Fig. 6.2B). The decrease in pro-MMP2 activity produced by LPP2 knock-down was modest in comparison to the increase produced by LPP2 overexpression, but these results indicate that endogenous LPP2 may regulate MMP2 activity.

*6.3.2. MMP2 mRNA expression is changed by the overexpression and knock-down of the LPPs* – Changes in secreted MMP2 activity could be the result of changes in transcription or the protein concentration of MMP2, or changes in the secretion or activation of MMP2. We measured expression of MMP2 mRNA in cells that had the LPPs overexpressed or knocked down. Fibroblasts that stably overexpressed LPP2 had increased the expression of MMP2 mRNA by an

average of 14-fold compared to parental control cells (Fig. 6.2C). This increase in MMP2 mRNA was larger than the increase in secreted MMP2 activity produced by LPP2 overexpression, and likely accounted for most of the change in MMP2 activity. When the stable overexpression of LPP2 was knocked down with siRNAs for hLPP2, the MMP2 mRNA expression was knocked down to levels similar to the vector control (Fig. 6.2C). Therefore, even though the effect of overexpressing LPP2 was much greater than the effect of knocking down LPP2 on MMP2 activity, the increased MMP2 expression in the stably overexpressing cells was not due to an unrelated compensatory mutation in the cells, but was directly related to the overexpression of LPP2. Fibroblasts that were stably transduced with the inactive mutant LPP2 [R214K] had a 90% decrease in MMP2 mRNA expression (Fig. 6.2C). The decrease in MMP2 expression was similar the decrease in MMP2 activity produced by LPP2 [R214K]. Fibroblasts that stably overexpressed LPP1 and LPP3 each had decreased MMP2 mRNA levels by 90% (Fig. 6.2C). These decreases in MMP2 expression also paralleled the changes in MMP2 secreted activity produced by LPP1 and LPP3 overexpression but were of a greater magnitude. Therefore, the changes in the secreted activities of MMP2 produced by overexpression of the LPPs could be largely attributed to the regulation of MMP2 mRNA expression. Fibroblasts treated with siRNAs for rLPP2, but not non-targeting control siRNAs, had decreased the expression of MMP2 by 25% (Fig. 6.2D). This indicates that endogenous LPP2 regulates the transcription of MMP2. Again, the effect of knocking down endogenous LPP2



was much more subtle than the effect of overexpressing LPP2 in terms of MMP2 regulation.

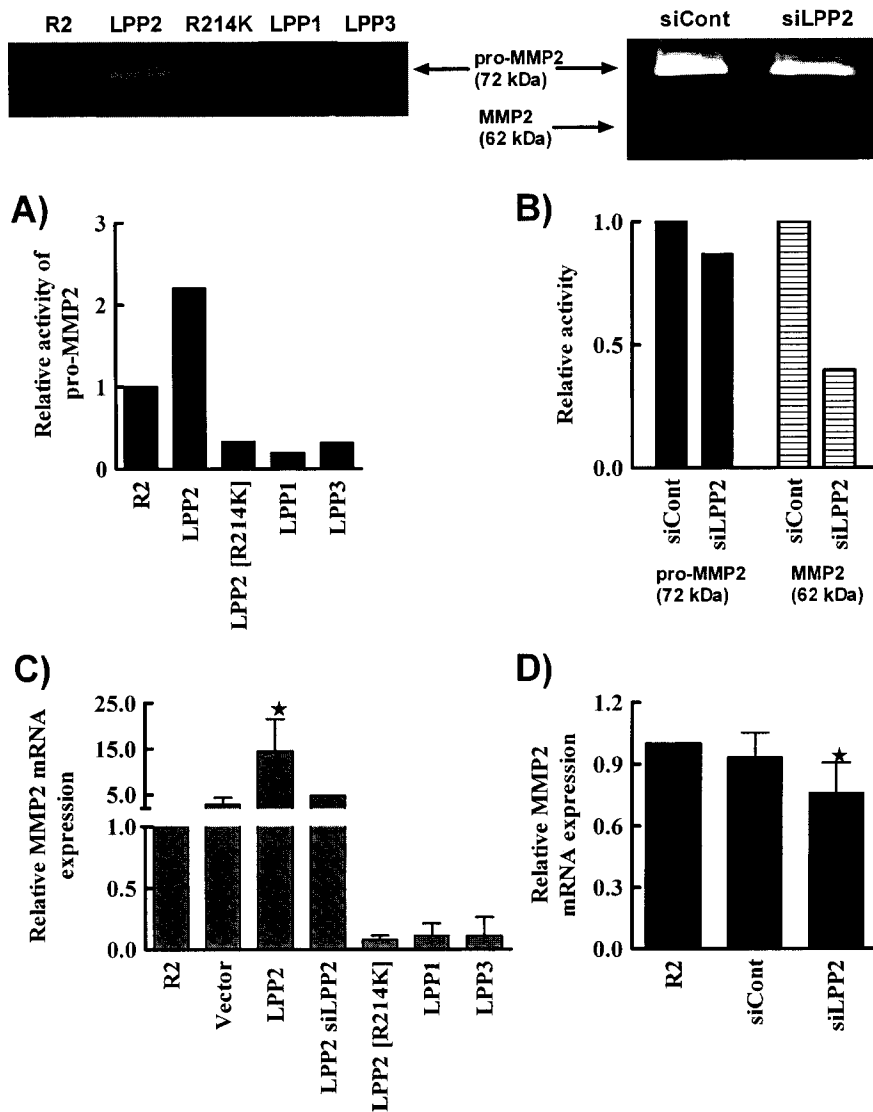


**Figure 6.2. Changes in LPP expression affect the activity and expression of MMP2.** Panels A-B show images and quantitation of the activity of the 72 kDa and 62 kDa bands on gelatin zymography. Conditioned media were collected from rat2 fibroblasts or those stably overexpressing LPP2, LPP2[R214K], LPP1, or LPP3, or those transfected with siRNAs for non-targeting control or rat LPP2. Results are from one representative of at least two experiments. Panel C shows the mRNA expression of MMP2 mRNA in lysates from rat2 fibroblasts or those stably transduced with empty vector, LPP2, LPP2[R214K], LPP1 or LPP3, or those stably overexpressing LPP2 and transfected with siRNAs for hLPP2. Panel D shows the mRNA expression of MMP2 mRNA in lysates from rat2 fibroblasts or those transfected with siRNAs for non-targeting control or rLPP2. mRNA concentrations are normalized to that of the housekeeping gene, cyclophilin A. Results are expressed as fold change compared to rat2 fibroblasts which is given as 1. Results are means  $\pm$  SD from at least 4 independent experiments. Statistically significant differences ( $p < 0.05$ ) from control are indicated by \*.

6.3.3. *The changes in MMP2 activity produced by the stable overexpression of LPP activities can be changed by transient adenoviral overexpression of different LPP activities* – Since LPP2 overexpression produced the opposite effect of LPP1 and LPP3 overexpression in terms of pro-MMP2 activity, we investigated whether transient adenoviral overexpression of one LPP isoform could change the MMP2 activity in cells stably overexpressing another LPP isoform. Cells that stably overexpressed LPP2 were infected with adenovirus containing the empty vector or LPP1. Infection with adenovirus for LPP1, but not empty vector, attenuated the increase in pro-MMP2 activity produced by LPP2 from 3-fold to 2-fold (Fig. 6.3A). Cells that stably overexpressed LPP3 were infected with adenovirus containing the empty vector or LPP2. Infection with adenovirus for LPP2, but not the empty vector, increased the pro-MMP2 activity in media from LPP3 cells from undetectable levels to 10% of control levels (Fig. 6.3A).

6.3.4. *LPA does not increase MMP2 expression in rat2 fibroblasts* - LPA stimulates secreted MMP2 activity in some cells [188, 189] and does not affect MMP2 activity in others [190, 191]. If LPA increased MMP2 in our fibroblasts, that could contribute to the induction of migration by LPA, and the LPPs might change this effect. We studied the effect of stimulating rat2 fibroblasts with 0.5  $\mu$ M, 2  $\mu$ M, and 10  $\mu$ M LPA on the mRNA expression of MMP2. LPA did not significantly change the mRNA expression of MMP2 (Fig. 6.2B). There may have been a small decrease in MMP2 expression following LPA treatment. Follow-up studies in the laboratory indicated that LPA did not change the secreted activity of

MMP2 (M. Sariahmetoglu, unpublished). Therefore, the LPPs likely did not change the expression or activity of MMP2 by changing LPA signaling.

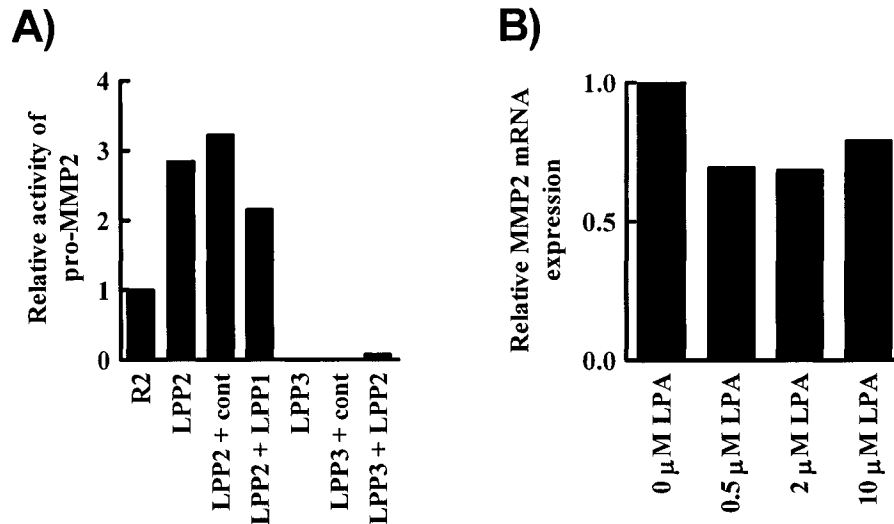


**Figure 6.3. Adenoviral overexpression of the LPPs alters MMP2 activity and LPA treatment does not change MMP2 expression in fibroblasts.** Panel A shows the quantitation of the activity of the 72 kDa band on gelatin zymography. Conditioned media were collected from rat2 fibroblasts or those stably overexpressing LPP2 or LPP3. Some LPP2 overexpressing cells were treated with adenovirus expressing empty vector (cont) or LPP1. Some LPP3 overexpressing cells were treated with adenovirus expressing empty vector (cont) or LPP2. Results are relative to the activity in rat2 media which is given as 1. Results are from one experiment. Panel B shows the mRNA expression of MMP2 in lysates from rat2 fibroblasts that have been treated with the indicated concentrations of LPA. mRNA concentrations are normalized to that of the housekeeping gene, cyclophilin A. Results are expressed as fold change compared to rat2 fibroblasts treated with no LPA which is given as 1. Results are from one representative of two independent experiments.

## 6.4. LPP activities change the secreted activity and expression of MMP9

6.4.1. *Secreted MMP9 activity is changed by the overexpression and knock-down of the LPPs* – Conditioned media from cells that had the LPPs overexpressed or knocked down were also assayed for 92 kDa MMP9 activity by gelatin zymography. Conditioned media from cells that stably overexpressed LPP2 had a 1.5-fold increase in MMP9 activity compared to parental rat2 fibroblasts (Fig. 6.4A). Media from cells that overexpressed LPP1 and LPP3 had

2.5-fold and 2-fold increases in MMP9 activity, respectively (Fig. 6.4A). Media from cells that were stably transduced with LPP2 [R214K] had decreased secreted MMP9 activity by 60% (Fig. 6.4A). Therefore, the inactive LPP2 [R214K] mutant may also have a dominant-negative effect in terms of regulating the secreted activity of MMP9. Media from fibroblasts treated with siRNAs for non-targeting control or rLPP2 were collected and concentrated 3-fold. The knock-down of LPP2 by ~50% resulted in decreased MMP9 activity by 15% (Fig. 6.4B). This decrease was again very modest, and may not have been significant, although it did suggest that knocking down endogenous LPP2 may produce the opposite effect on MMP9 activity from overexpressing LPP2.

*6.4.2. MMP9 mRNA expression is changed by the overexpression and knock-down of the LPPs* – The mRNA expression of MMP9 was measured in cells with changed expression of the LPPs to confirm that the LPPs regulate MMP9 and to determine whether, as in the case of MMP2, the regulation was predominantly at the level of mRNA expression. Fibroblasts that stably overexpressed LPP2 had increased mRNA expression of MMP9 by an average of 3-fold (Fig. 6.4C). Fibroblasts that stably overexpressed LPP1 and LPP3 had increased MMP9 mRNA levels by 55-fold and 20-fold, respectively (Fig. 6.4A). Therefore, the changes in secreted MMP9 activity produced by the overexpression of the three active LPPs could be attributed to changes in the mRNA expression of MMP9. Surprisingly, cells stably transduced with LPP2 [R214K] had a 4-fold increase in MMP9 mRNA expression (Fig. 6.4C). This indicated that although LPP2 [R214K] acted as a dominant-negative in terms of

regulating MMP9 secreted activity, the mutant acted as the wild-type enzyme in terms of regulating MMP9 transcription. This suggests that LPP2 may regulate MMP9 both by regulating its mRNA concentration, and by regulating the enzyme post-transcriptionally. Furthermore, it suggests that the catalytic activity of LPP2 is important for the post-transcriptional regulation, whereas regulation of mRNA expression may be a non-catalytic function of the enzyme. These results are preliminary, and should be investigated further. Fibroblasts treated with siRNAs for rLPP2, but not non-targeting control siRNAs, decreased MMP9 mRNA expression by 25% (Fig. 6.4D). This indicated that endogenous LPP2 can regulate MMP9 activity by regulating the mRNA expression of the protease.

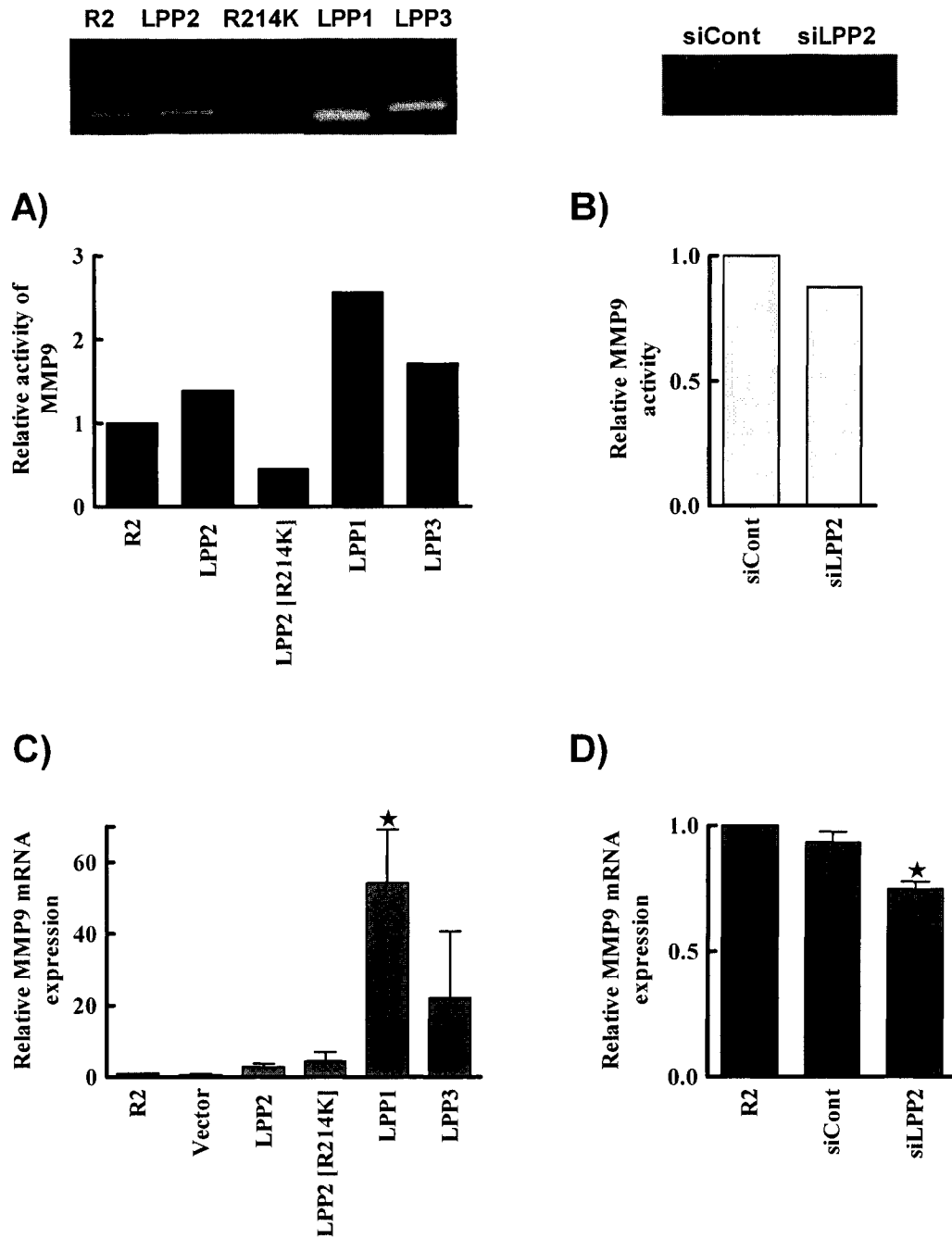


**Figure 6.4. Changes in LPP expression affect the activity and expression of MMP9.** Panels A-B show images and quantitation of the activity of the 92 kDa band on gelatin zymography. Conditioned media were collected from rat2 fibroblasts or those stably overexpressing LPP2, LPP2[R214K], LPP1, or LPP3, or those transfected with siRNAs for non-targeting control or rat LPP2. Results are from one representative of at least two experiments. Panels C-D show the mRNA expression of MMP9 in lysates collected from rat2 fibroblasts or those stably overexpressing LPP2, LPP2[R214K], LPP1, or LPP3, or those transfected with siRNAs for non-targeting control or rat LPP2. mRNA concentrations are normalized to that of the housekeeping gene, cyclophilin A. Results are expressed as fold change compared to rat2 fibroblasts which is given as 1. Results are means  $\pm$  SD from at least 4 independent experiments. Statistically significant differences ( $p < 0.05$ ) from control are indicated by \*.

## **6.5. The activity and expression of TIMP-2 are decreased in cells with LPP2 knocked down**

6.5.1. *Conditioned media from cells with LPP2 knocked down has decreased TIMP-2 activity* – Tissue inhibitor of metalloproteinase-2 (TIMP-2) inhibits activated MMP2 by direct binding, but also is required for the activation of MMP2 [149]. Therefore, the ratio of MMP2: TIMP-2 is important in determining the responses of cells. Preliminary work in the laboratory demonstrated that the overexpression of LPP1 changed the amount of secreted TIMP-2 in the media (C. Pilquil, unpublished). We wanted to investigate whether endogenous LPP2 regulated TIMP-2 activity or expression. TIMP-2 activity was measured as the decrease in recombinant MMP2 activity toward fluorescence-conjugated DQ™ gelatin in an *in vitro* fluorescence assay. The amount of recombinant MMP2 activity present in the assay overwhelmed any changes in MMP2 activity in the TIMP-2 containing conditioned media (M. Sariahmetoglu, unpublished). Conditioned media were collected from fibroblasts transfected with non-targeting control siRNAs or siRNAs for rLPP2. The ability of the media to inhibit MMP2 activity was measured, and the level of inhibition was presumed to represent the amount of TIMP-2 in the conditioned media. Media from cells with LPP2 knocked down had less ability to inhibit MMP2 activity (Fig. 6.5A). This indicated that the TIMP-2 activity in media from cells with LPP2 knocked down was decreased.

6.5.2. *Knock-down of LPP2 decreases TIMP-2 mRNA expression* – The mRNA expression of TIMP-2 was measured in cells transfected with non-

targeting control siRNAs or siRNAs for rLPP2. In one experiment, the knock-down of LPP2 by ~40% resulted in a 25% decrease in the expression of TIMP-2 mRNA (Fig. 6.5B).

### 6.5.3. Knock-down of LPP2 decreases the amount of secreted TIMP-2

*protein* – Cells were transfected with non-targeting siRNAs or siRNAs for rLPP2 and conditioned media were collected. Western blots were performed on the conditioned media. The knock-down of LPP2 by ~40% resulted in a decrease in the amount of TIMP-2 protein in the media (Fig. 6.5C). These results collectively indicate that endogenous LPP2 positively regulates TIMP-2. Since LPP2 also positively regulates the expression of MMP2, it may be that TIMP-2 levels are regulated in the same direction to promote continued activation of MMP2, since TIMP-2 is required to activate MMP2. These results should be followed up with future experiments.

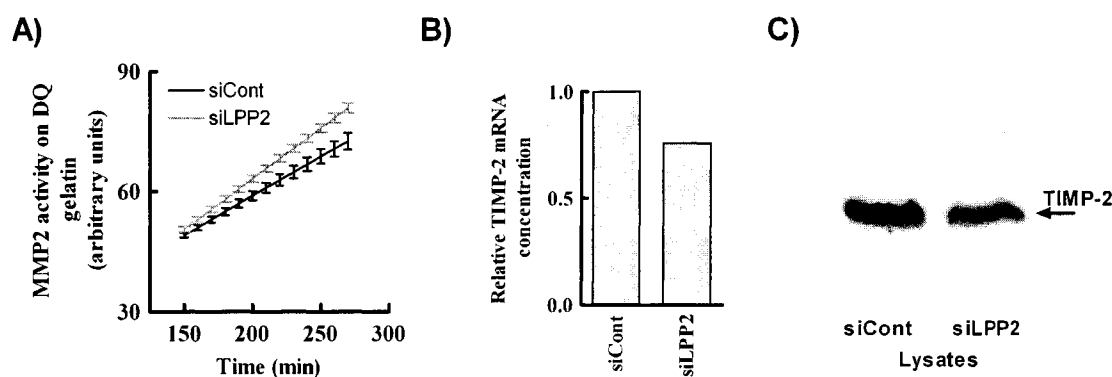


**Figure 6.5. Knock-down of LPP2 decreases the expression and activity of TIMP-2.** Panel A shows the activity of recombinant MMP2 toward DQ™ gelatin after the addition of conditioned media containing TIMP-2 from fibroblasts transfected with non-targetting control siRNAs or siRNAs for rLPP2. Panel B shows mRNA concentrations for untreated rat2 fibroblasts (R2) or cells treated with siRNAs for non-targetting control or rLPP2. mRNA concentrations are normalized to that of the housekeeping gene, cyclophilin A. Results are expressed as fold change compared to rat2 fibroblasts which is given as 1 and are from one experiment. Panel C shows a Western blot of the TIMP-2 protein in lysates from fibroblasts treated with siRNAs for non-targetting control or rLPP2. The image is a scan at 800 nm created on the Odyssey™ imager. The result is from one experiment.



## **6.6. The activities and expression of MMP2 and MMP9 are changed in high passage LPP2 transduced cells that are arrested in G<sub>2</sub>-phase**

*6.6.1. LPP2 transduced cells that are arrested in G<sub>2</sub>-phase have decreased MMP2 activity and expression* - It has been reported that senescent cells can increase the secretion of MMPs, and that this secretion may promote the migration of neighboring cells [192]. Therefore, we investigated the secreted activity and expression of MMP2 in cells that were arrested in G<sub>2</sub>-phase subsequent to the overexpression of LPP2. We analyzed the two arrested cell lines described in Chapter 5 (one with increased LPP3 expression and one with decreased LPP3 expression), and a third population of arrested cells in which the mRNA expression of the LPPs had not been evaluated. Conditioned media from two of the three cell populations arrested in G<sub>2</sub>-phase had decreased MMP2 activity by approximately 80% (Fig. 6.6A). The population with increased LPP3 mRNA expression showed a decrease in MMP2 activity, whereas the population with decreased LPP3 expression showed no change in MMP2 activity. The first population of arrested cells also had significantly decreased the mRNA expression of MMP2 by 90% (Fig. 6.6B). Since the cells that were arrested in G<sub>2</sub>-phase and did not have increased LPP3 expression did not show decreased MMP2 activity, it is possible that the decreases in MMP2 activity and expression in population 1 and 3 were artifacts of the increased LPP3 activity in the cells. It is clear that the senescent phenotype did not cause an increase in MMP2 expression or activity.

*6.6.2. LPP2 transduced cells that are arrested in G<sub>2</sub>-phase have increased MMP9 activity and expression* - Conditioned media from all three cell

populations that were arrested in G<sub>2</sub>-phase subsequent to the overexpression of LPP2 had increased secreted MMP9 activity by 1.5-fold to 5.5-fold (Fig. 6.6C). This suggests that increased MMP9 activity may have been a result of the senescent phenotype. The mRNA concentrations of MMP9 were increased by ~25-fold on average in the G<sub>2</sub>-arrested cells (Fig. 6.6D). This indicates the mRNA expression of MMP9 was increased in the senescent cells.

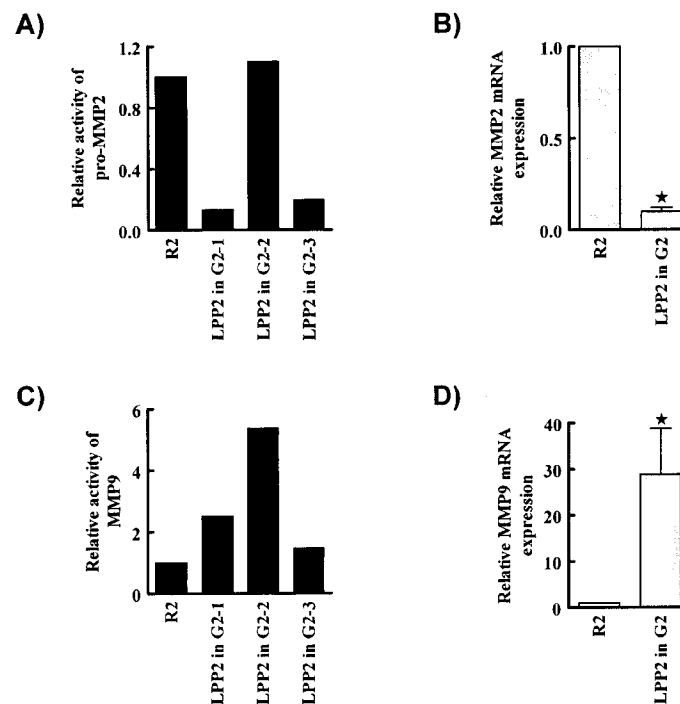


**Figure 6.6. The activity and expression of MMP2 and MMP9 are changed in cells arrested in G<sub>2</sub>-phase.** Panels A and C show the quantitation of the activities of the 72 kDa and 92 kDa bands, respectively, on gelatin zymography. Conditioned media were collected from rat2 fibroblasts or three populations of those stably transduced with LPP2 at high passage that were arrested in G<sub>2</sub>-phase. Results are from one experiment. Panels B and D show the mRNA expression of MMP2 and MMP9, respectively, in lysates collected from rat2 fibroblasts or those stably transduced with LPP2 that were arrested in G<sub>2</sub>-phase. mRNA concentrations are normalized to that of the housekeeping gene, cyclophilin A. Results are expressed as fold change compared to rat2 fibroblasts which is given as 1. Results are means  $\pm$  SD from at least 4 independent experiments. Statistically significant differences ( $p < 0.05$ ) from control are indicated by \*.

### **6.7. The premature S-phase entry of LPP2 overexpressing cells is not reversed with an MMP inhibitor**

LPP2 overexpression resulted in increased 72 kDa MMP2 activity in cells that entered S-phase prematurely. A general MMP inhibitor, Batimastat, was used at concentrations that reduced MMP2 activities to undetectable levels in zymography (M. Sariahmetoglu, unpublished) to evaluate the effect of MMP2 on cell cycle progression. We treated rat2 fibroblasts and those that overexpressed LPP2 with Batimastat during serum deprivation and after cells were stimulated to re-enter the cell cycle. Untreated and Batimastat-treated LPP2 overexpressing cells entered S-phase approximately 1.5 h before untreated or Batimastat-treated rat2 fibroblasts (Fig. 6.7). Therefore, the inhibition of MMP2 activity had no effect on the rate of cell cycle progression in parental control or LPP2 overexpressing fibroblasts. The premature S-phase entry caused by LPP2 overexpression was likely not a downstream effect of the increases in MMP2 activity produced by LPP2.

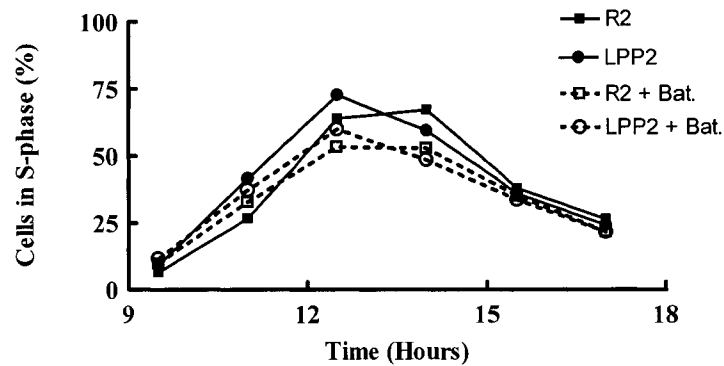


**Figure 6.7. The MMP inhibitor Batimastat does not change the effect of LPP2 overexpression on S-phase entry.** Rat2 fibroblasts or those that stably overexpressed LPP2 were synchronized by serum deprivation and stimulated to cycle by the re-addition of FBS in the presence or absence of MMP inhibitor Batimastat (Bat). The percentage of gated cells in S-phase at the indicated times after the re-addition of FBS is shown. Results are from one experiment.

## 6.8. Discussion

LPP1 activity can attenuate the migration of cells to LPA [63, 65]. Work in our laboratory confirmed that LPP1 attenuates the migration of rat2 fibroblasts to LPA, and suggested that conditioned media from LPP1 overexpressing cells could attenuate the migration of parental rat2 fibroblasts. Furthermore, media from LPP1 overexpressing cells had altered levels of MMP2 and MMP9 activities. We wanted to extend this work to investigate the effect of LPP2 and LPP3 overexpression on fibroblast migration and the regulation of MMP activities. We also used knock-down studies to investigate the role of endogenous LPP2 in the regulation of fibroblast migration and secreted MMP activities.

Conditioned media from cells that overexpressed LPP2 enhanced the migration of parental fibroblasts to LPA. This was an isoform-specific effect of LPP2, since media from LPP1 overexpressing cells decreased migration to LPA and media from LPP3 overexpressing cells did not change the migration of

fibroblasts to LPA. Conditioned media from cells with decreased levels of endogenous LPP2 attenuated the migration of parental fibroblasts to LPA. The ability of conditioned media from cells with LPP2 overexpressed or knocked down to change fibroblast migration to other agonists should be investigated in the future. Surprisingly, preliminary evidence from one experiment suggests that conditioned media from cells transduced with LPP2 [R214K] may also enhance migration to LPA. We reported in Chapter 3 that the overexpression of both wild-type and mutant LPP2 decreased the extracellular hydrolysis of LPA. If the effect of LPP2 overexpression on producing media that regulates LPA-induced migration is non-catalytic, then it may involve changes in the extracellular hydrolysis of LPA. The hydrolysis of extracellular LPA was increased significantly (2-fold) by LPP1 overexpression, decreased by wild-type or mutant LPP2 overexpression, and not significantly changed by LPP3 overexpression (Chapter 3, Fig 3.7). Similarly, migration of parental fibroblasts to LPA was decreased by media from LPP1 overexpression, increased by media from wild-type or mutant LPP2 overexpression, and not affected by media from LPP3 overexpression. Based on these results, it is possible that the ecto activity of the LPPs toward LPA is important for the regulation of LPA-induced migration. However, it is unlikely that the changes in LPA concentration in the conditioned media produced by the LPPs could account for this effect. Furthermore, other studies and our unpublished work have demonstrated LPP1 ecto activity is not responsible for regulating LPA-induced migration ([65], C. Pilquil, unpublished).

The use of a non-hydrolysable analog of LPA to stimulate migration would help to resolve this question.

Fibroblasts that had decreased endogenous LPP2 expression had decreased migration to LPA and produced media that decreased migration of parental fibroblasts to LPA. Their decreased migration to LPA could have been the result of the changes to the media that inhibited migration. In contrast, cells that overexpressed LPP2 produced media that stimulated the migration of parental fibroblasts, but LPP2 overexpressing cells migrated poorly to their own media. Fibroblasts that stably overexpressed LPP2 had decreased migration toward all agonists and in the absence of agonist. Therefore, LPP2 overexpression has two contrasting effects on the migration of fibroblasts. LPP2 overexpression reduces the ability of cells to migrate in general. LPP2 overexpression also causes increases or decreases in factors in the media that promotes the migration of wild-type cells.

Media from fibroblasts that overexpressed LPP2 had increased MMP2 and MMP9 activities that correlated with increases in MMP2 and MMP9 mRNA expression. Media from cells with endogenous LPP2 knocked down had small decreases in MMP2 and MMP9 activity that correlated with modest but significant decreases in MMP2 and MMP9 mRNA expression. The effects of LPP2 on the activity of the MMPs was dependent on its catalytic activity, since cells that were stably transduced with mutant LPP2 [R214K] had decreased activities of MMP2 and MMP9 in their media. This provides evidence of a possible dominant-negative type effect of LPP2 [R214K]. Although cells

transduced with LPP2 [R214K] had decreased MMP2 mRNA expression, surprisingly, their MMP9 mRNA expression was increased. This suggests that LPP2 may regulate both the expression and activity of MMP9 separately, and that the regulation of MMP9 expression may be a non-catalytic effect. These results should be investigated further.

There are a number of mechanisms whereby the LPPs could potentially regulate transcription. The ecto activity of the LPPs could regulate the amount of LPA or S1P that can signal through GPCRs. There are a number of signaling pathways that are activated by cell surface LPA and S1P receptors that can regulate transcription, and regulating extracellular LPA or S1P concentrations could alter these. For example, LPP1 overexpression partially attenuated LPA-induced NF- $\kappa$ B translocation to the nucleus in human bronchial epithelial cells [193]. Additionally, intracellular lipid hydrolysis by the LPPs could alter transcription. Intracellular LPA can activate nuclear LPA receptors that can regulate transcription. Intracellular DAG can activate PKCs which regulate transcription factors. Intracellular PA, C1P, and ceramide can all potentially regulate the localization and activity of kinases and phosphatases, which can lead to changes in the activity of transcription factors. Therefore, there are many ways that the LPPs could regulate the transcription of numerous genes, and it is not surprising that LPP activities would have a role in transcriptional regulation.

The LPPs regulated MMP activities in an isoform-specific manner. LPP2 increased both MMP2 and MMP9 activity, while LPP1 and LPP3 decreased MMP2 activity and increased MMP9 activity by far more than LPP2. The

mechanism whereby the LPPs differentially regulate the expression of MMP2 and MMP9 could be investigated in the future. Additionally, it should be determined if the changes in MMP activities produced by the LPPs are significant in regulating fibroblast migration. Recombinant MMP2 and TIMP-2 could be added to cells in conjunction with the overexpression or knock-down of each of the LPPs. Additionally, MMP2 and TIMP-2 could be knocked down with siRNA in conjunction with the overexpression or knock-down of each of the LPPs. Using these methods, we could evaluate whether changing the MMP2:TIMP ratio could reverse or exaggerate the effects of the LPPs on migration. This would help to establish whether the effects of the LPPs on migration are partially or wholly mediated by changes to MMP activities.

The preliminary evidence presented in this Chapter demonstrates that the LPPs have isoform-specific roles in the regulation fibroblast migration and secreted MMP activities. Endogenous LPP2 promoted the expression and activities of MMP2, MMP9, and TIMP-2. The regulation of MMP activities was not likely a factor in the regulation of cell cycle progression by LPP2, since MMP inhibitors did not effect the cell cycle in fibroblasts. The physiological relevance of the regulation of MMP and TIMP activities by LPP2 is still unclear. This Chapter provides insights into additional isoform-specific functions of LPP2 in fibroblasts that are worth investigating in the future.



## **CHAPTER 7**

### **GENERAL DISCUSSION AND FUTURE DIRECTIONS**

The LPPs regulate cell signaling and physiology by controlling the balance between the bioactive lipid phosphates LPA, S1P, PA, and C1P and their dephosphorylated products MAG, SPH, DAG, and Cer. *In vitro* studies and animal models have demonstrated that the LPPs have important and isoform-specific physiological roles. However, the role of LPP2 in cell signaling and physiology has been largely unexplored. This thesis demonstrates that LPP2 activity regulates cell cycle progression and proliferation in fibroblasts. The overexpression of catalytically active LPP2 in fibroblasts results in premature progression into S-phase after exit from quiescence. Knock-down of endogenous LPP2 results in delayed S-phase entry, demonstrating that the regulation of the timing of cell cycle progression is an endogenous function of LPP2 activity in fibroblasts. Cells that overexpress LPP2 eventually arrest in G<sub>2</sub>-phase of the cell cycle and display hallmarks of senescence. The induction of premature S-phase entry and eventual progression of cells toward a phenotype resembling oncogene-induced senescence were dependent on the increased catalytic activity of LPP2, since the expression of an inactive mutant did not reproduce these effects. The regulation of S-phase entry by LPP2 was dependent on the regulation of the timing of cyclin A expression, but could not be attributed to a change in the bulk cellular concentrations of LPA, S1P, PA, C1P, Cer, or DAG. In addition to regulating cell cycle progression, LPP2 expression regulated fibroblast migration and the secreted activity of matrix metalloproteinases. This thesis provides a detailed characterization of fibroblasts that stably overexpress LPP2 and mutant LPP2 [R214K], and describes phenotypes produced by the modification of LPP2

activity in fibroblasts. This thesis also provides the first evidence of an endogenous and isoform-specific role for LPP2 activity in regulating cell cycle progression.

We stably overexpressed and knocked down LPP2 in fibroblasts. Rat2 fibroblasts endogenously express all three LPP isoforms, and have high basal LPP activity. Our results demonstrate that most of the endogenous activity in rat2 cells can be attributed to LPP1, which is expressed to the highest extent. We achieved a 30 to 40-fold overexpression of LPP2 mRNA which resulted in a modest increase of approximately 2- to 3-fold in total cellular LPP activity. The level of protein overexpression could not be determined since LPP2 appeared on Western blots as high molecular mass aggregates and since the endogenous LPP2 protein was not detected by our antibodies. This level of overexpression did not result in changes to the bulk cellular concentrations of LPA, S1P, PA, C1P, Cer, or DAG, and did not change the PA: DAG ratio in cells. Additionally, the level of overexpression we achieved in fibroblasts did not attenuate p42/44 MAPK activation downstream of GPCRs. Other groups have reported that LPP2 overexpression changed the PA:DAG ratio and attenuated signaling by GPCRs in HEK293 cells [45, 46]. This discrepancy is likely explained by the fact that their overexpression produced a 20- to 300-fold increase in LPP activity, whereas our overexpression produced only a 2- to 3-fold increase in LPP activity. GFP-tagged wild-type and mutant LPP2 localized to the plasma membrane, endosomes, ER, and possibly other unidentified intracellular membranes in fibroblasts.

Interestingly, despite LPP2's plasma membrane localization, the overexpression of LPP2 did not increase the extracellular hydrolysis of LPA or S1P. Instead, overexpression of both wild-type and catalytically inactive mutant LPP2 decreased the hydrolysis of extracellular LPA and S1P. Therefore, LPP2 negatively regulates the hydrolysis of extracellular LPA and S1P in fibroblasts by a non-catalytic mechanism. Preliminary evidence suggests that a non-catalytic function of LPP2 overexpression may result in the secretion of factors into media or the depletion of factors from media that enhances the migration of fibroblasts to LPA. Therefore, it is worth investigating how LPP2 non-catalytically decreases extracellular phospholipid hydrolysis, and whether this has non-catalytic function of LPP2 expression has signaling consequences. It is possible that LPP2 decreased the extracellular hydrolysis of LPA and S1P by titrating out the more active LPP1 and LPP3 from the plasma membrane. This could be tested by biotinylating LPP1 and LPP3 or monitoring their localization by immunofluorescence microscopy and determining whether increasing amounts of LPP2 overexpression decreased their plasma membrane localization.

The mutant LPP2 [R214K] was expressed to a similar extent and showed the same subcellular localization as wild-type LPP2. The R214K mutation should eliminate the catalytic function of LPP2, since the equivalent mutation in LPP1 eliminated the activity of LPP1, and since the R214 residue is important for hydrogen bonding to the phosphate group of the substrate according to the proposed catalytic mechanism of the LPPs. Lysates from cells transduced with LPP2 [R214K] did not have increased total LPP activity and expression of LPP2

[R214K] did not produce the effects that wild-type LPP2 produced on cell cycle progression. Surprisingly, anti-GFP immunoprecipitates from cells transduced with LPP2 [R214K]-GFP had LPP activity toward PA. One explanation for this result is that the mutant LPP2 protein co-immunoprecipitated an active lipid phosphatase. The LPPs have been reported to homodimerize but not heterodimerize [56]. LPP2-GFP was unable to co-immunoprecipitate LPP1, the most abundant LPP activity in the fibroblasts, even when we optimized the possibility of detecting such an interaction. This agrees with the previous report that the LPPs do not heterodimerize. Therefore, it is more likely that LPP2 [R214K] co-immunoprecipitated endogenous active LPP2. Western blotting demonstrated that anti-GFP immunoprecipitates from cells transduced with LPP2 [R214K]-GFP exhibited high molecular mass bands that were immunoreactive for LPP2. This suggests that LPP2 exists in complexes of two or more proteins. Further studies with affinity tags are required to evaluate whether wild-type and mutant LPP2 can co-immunoprecipitate LPP2 or LPP3. Our studies suggest that LPP2 and LPP2 [R214K] may exist in active dimers or other undefined higher order complexes, and this possibility should be investigated further.

LPP2 has isoform-specific functions in fibroblasts. The overexpression of LPP2 produced unique and opposite effects compared to the overexpression of LPP1 or LPP3, and knock-down of LPP2 produced unique and opposite effects compared to the knock-down of LPP1 or LPP3. The timing of cell cycle progression was regulated by LPP2 activity, but not by LPP1 or LPP3. LPP2 overexpression decreased the extracellular hydrolysis of LPA and S1P, whereas

LPP1 and LPP3 overexpression increased the extracellular hydrolysis of LPA and S1P, respectively. Furthermore, the overexpression of LPP2 activity increased secreted MMP2 activity, while the overexpression of LPP1 or LPP3 decreased secreted MMP2 activity. Media from cells that overexpressed LPP2 increased fibroblast migration to LPA, whereas media from cells that overexpressed LPP1 decreased fibroblast migration to LPA. Therefore, it is evident from all our results that LPP2 has a very different function in fibroblasts from LPP1 and LPP3. LPP2 activity is not redundant with LPP1 or LPP3 activity, and in many cases produces opposite phenotypic effects from the other LPP isoforms. The fact that LPP2 has a very different function from LPP1 and LPP3 is expected, since animal models have demonstrated that knocking out LPP2 or LPP3 in mice produces extremely different results. Additionally, the tissue distribution of LPP2 is very different from the tissue distribution of LPP1 and LPP3, and the expression of LPP2 in tumor tissues is very different from the expression of LPP1 and LPP3 in tumor tissues. A summary of the opposite and unique effects of LPP2 activity compared with LPP1 or LPP3 activity is presented in Table 7.1. Importantly, the results presented in this thesis demonstrate that LPP2 has unique and significant functions in fibroblasts, despite its low level of endogenous expression in these cells compared to the other LPP isoforms. Therefore, in cells in which LPP2 is expressed at very low levels it still has important and isoform-specific endogenous functions in regulating cell signaling.

**Table 7.1. A comparison of the LPP isoforms**

The characteristics and functions of LPP1-3 are compared. Results pertaining to tissue distribution and tumor cell expression and knockout animals are cited in Chapter 1. *In vitro* substrate preferences are based on comparing the fold increases in hydrolysis of the indicated lipids in Triton X-100 micelles produced by the same levels of stable overexpression. Brackets indicate lipids whose hydrolysis was not significantly increased. For details, see Chapters 3-6.

Phenotype	LPP2	LPP1	LPP3
<b>Previous studies</b>			
Tissue Distribution	Restricted	Ubiquitous	Ubiquitous
Expression in breast, colon, and gastric tumors	Increased	Decreased	Decreased
Expression in ovarian tumors	No change	Decreased	No change
Expression in prostate and kidney tumors	Unchanged and decreased	Increased	Increased
Knockout mouse model	Viable, no obvious phenotype	Unknown	Embryonic lethal
<b>Results from this thesis in rat2 fibroblasts</b>			
<i>In vitro</i> substrate preference	S1P>PA>(LPA)	LPA≈PA>(S1P)	S1P>PA≈LPA
Ecto activity	Decreased LPA and S1P hydrolysis	Increased LPA hydrolysis	Increased S1P hydrolysis
Intracellular PA: DAG ratio	No change	Decreased PA:DAG	Unknown
LPA-induced p42/44 MAPK activation	No change	Attenuated activation	Unknown
Cell cycle regulation	Promoted premature entry into S-phase	No effect	No effect
Migration to LPA	Conditioned media increased	Conditioned media decreased	Conditioned media had no effect
MMP2 activity	Increased	Decreased	Decreased

Our results demonstrate that endogenous LPP2 activity regulates cell cycle progression in fibroblasts by regulating the timing of cyclin A expression and S-phase entry in cells re-entering the cell cycle following quiescence. Decreasing endogenous LPP2 expression by ~60% caused delayed S-phase entry in fibroblasts. LPP2 overexpression caused the premature entry of fibroblasts into S-phase and prevented fibroblasts from arresting at the G<sub>1</sub>/S checkpoint after the induction of DNA damage. Cells that overexpressed LPP2 eventually activated the G<sub>2</sub>/M checkpoint and permanently exited the cell cycle in G<sub>2</sub>-phase, showing characteristics of senescence. The regulation of the cell cycle was dependent on the catalytic activity of LPP2, but the mechanism whereby LPP2 activity increased the timing of cyclin A expression and promoted cell cycle progression could not be ascertained in these studies. The bulk concentrations of lipids that would be directly affected by LPP2 activity were not changed by LPP2 overexpression. Additionally, we did not observe changes in the phosphorylation state of several kinases in signaling pathways that might have promoted cell cycle progression. Determining the mechanism by which LPP2 activity increases cyclin A expression is a major future goal of this research.

Since LPP2 is an endogenous regulator of cell cycle progression in fibroblasts, we would expect that LPP2 activity would be regulated in relevant physiological situations to modulate the timing of S-phase progression. Very little is known about the regulation of LPP2. LPP2 could be regulated by post-translational modifications or translocation. These possibilities were not investigated in great detail in this study, but should be investigated further in the



future. Our results suggest that LPP2 is not regulated transcriptionally in fibroblasts during exit from quiescence or during cell cycle progression. LPP2 could be activated in situations such as wound healing, when fibroblasts that are normally quiescent need to proliferate rapidly. The mRNA expression of LPP2 was not changed by any individual wound healing regulating factor that we tested at the times we examined. This does not exclude the possibility that LPP2 expression is regulated by a mitogen or combination of mitogenic signals that we did not test. *In vivo* studies may be a more relevant way of evaluating whether LPP2 is transcriptionally regulated in situations where fibroblast cycling is changed. Interestingly, LPP2 is highly expressed in some tissues that undergo frequent proliferation, and LPP2 mRNA expression is increased in some human tumor tissues including breast, colon, and gastric where LPP1 and LPP3 are decreased. It would be interesting to determine if LPP2 can enhance cell cycle progression, proliferation, or migration in these tumor cells.

LPP2 knockout mice are viable and have no obvious phenotypic abnormalities [71]. Knockouts in mice of many genes that regulate the timing of S-phase progression including any one of the D-type or E-type cyclins and CDK2 result in viable animals that do not have major proliferative or developmental defects [79]. In some cases, cells from these animals exhibit subtle defects in cell cycle progression in culture [79]. It would be interesting to investigate whether fibroblasts or other cells from LPP2 knockout mice exhibit cell cycle defects when exposed to various stresses *in vitro*. For example, fibroblasts from LPP2 knockout mice may have a decreased ability to exit quiescence *in vitro*. LPP2

knockout mice may also respond differently in physiological situations that require the initiation of cycling in normally quiescent cells. For example, LPP2 knockout mice may have a decreased rate of wound healing. LPP2 knockout mice may also be less susceptible to tumor development in certain tissues. A re-examination of the knockout mice could be undertaken based on the information presented in this thesis about the functions of endogenous LPP2. Investigating the physiological relevance of the ability of LPP2 to regulate cell cycle progression is an essential area of future research.

The overexpression of many oncogenes including Ras, Myc, E2F, and BRAF induces cellular senescence [129, 131, 139, 194-197]. Oncogene-induced senescence is a mechanism that exists to prevent malignancy *in vivo* [184, 198, 199]. The overexpression of an oncogene initially stimulates cell cycle progression and increased proliferation, but the increased mitogenic signaling triggers a senescent response by activating the p14(ARF)/p53 and p16<sup>INK4a</sup>/Rb pathways. Oncogene-induced senescence can often be overcome by inactivating components of the p14(ARF)/p53 or p16<sup>INK4a</sup>/Rb pathways, or by disabling both pathways [198]. Similarly, *in vivo*, multiple oncogenic lesions are required to cause transformation [198]. The overexpression of LPP2 caused premature progression into S-phase of the cell cycle and prevented cells from arresting at the G<sub>1</sub>/S checkpoint. Subsequently, LPP2 overexpressing cells exited the cell cycle and showed characteristics of senescence including the activation of components of the p14(ARF)/p53 and p16<sup>INK4a</sup>/Rb pathways. LPP2 overexpression may have produced oncogene-induced senescence in fibroblasts, similar to the oncogene-

induced senescence produced by oncogenic BRAF that positively regulated the timing of cell cycle progression before promoting proliferative arrest [131]. If LPP2 overexpression produced oncogene-induced senescence, then the secondary loss of function of the p53 or Rb pathways might enable LPP2 overexpression to promote transformation. This is an interesting possibility that could be tested *in vitro*. The senescence responsive proteins p16<sup>INK4a</sup>, p53, Rb, or p14(ARF) could be inactivated individually or in combination in cells that overexpressed LPP2. The potential of these cells to promote colony formation or demonstrate other characteristics of transformed cells could then be assessed. This would be a very interesting area for future study.

The results presented in this thesis demonstrate that LPP2 regulates the timing of cell cycle progression, secreted matrix metalloproteinase activity, and migration toward LPA in fibroblasts, without altering the bulk cellular concentrations of its substrates or products. Our results suggest that LPP2 may exist in multimers, and may have non-catalytic functions that oppose the functions of LPP1 and LPP3. The relevance and details of these functions of LPP2 should be investigated further. Finally, this study demonstrates that an endogenous and isoform-specific function of LPP2 activity in fibroblasts is the regulation of the cell cycle. Decreasing LPP2 expression causes delayed progression into S-phase, while increasing LPP2 activity causes premature progression into S-phase. Sustained increased LPP2 activity results in cells exiting the cell cycle in G<sub>2</sub>-phase and displaying characteristics of senescence. The physiological implications of the regulation of cell cycle progression by LPP2 and the

mechanism by which LPP2 activity causes this regulation require further investigation. Although more work should be done to study the mechanism and implications of the role of LPP2 in cell cycle regulation, this study provides the first comprehensive description of an endogenous and isoform-specific function of LPP2 in fibroblasts. The information presented in this study about the specific role of LPP2 will be valuable in directing further studies into this intriguing enzyme.

## BIBLIOGRAPHY

1. Umezu-Goto, M., et al., *Lysophosphatidic acid production and action: validated targets in cancer?* J Cell Biochem, 2004. **92**(6): p. 1115-40.
2. Umezu-Goto, M., et al., *Autotaxin has lysophospholipase D activity leading to tumor cell growth and motility by lysophosphatidic acid production.* J Cell Biol, 2002. **158**(2): p. 227-33.
3. van Meeteren, L.A., et al., *Autotaxin, a secreted lysophospholipase D, is essential for blood vessel formation during development.* Mol Cell Biol, 2006. **26**(13): p. 5015-22.
4. Brindley, D.N., *Lipid phosphate phosphatases and related proteins: signaling functions in development, cell division, and cancer.* Journal of Cellular Biochemistry, 2004. **92**(5): p. 900-12.
5. Tokumura, A., *Metabolic pathways and physiological and pathological significances of lysolipid phosphate mediators.* J Cell Biochem, 2004. **92**(5): p. 869-81.
6. Mizugishi, K., et al., *Essential role for sphingosine kinases in neural and vascular development.* Mol Cell Biol, 2005. **25**(24): p. 11113-21.
7. Le Stunff, H., S. Milstien, and S. Spiegel, *Generation and metabolism of bioactive sphingosine-1-phosphate.* J Cell Biochem, 2004. **92**(5): p. 882-99.
8. Gardell, S.E., A.E. Dubin, and J. Chun, *Emerging medicinal roles for lysophospholipid signaling.* Trends Mol Med, 2006. **12**(2): p. 65-75.
9. Radeff-Huang, J., et al., *G protein mediated signaling pathways in lysophospholipid induced cell proliferation and survival.* J Cell Biochem, 2004. **92**(5): p. 949-66.
10. Sengupta, S., et al., *Biology of LPA in health and disease.* Semin Cell Dev Biol, 2004. **15**(5): p. 503-12.
11. Rosen, H. and E.J. Goetzl, *Sphingosine 1-phosphate and its receptors: an autocrine and paracrine network.* Nat Rev Immunol, 2005. **5**(7): p. 560-70.
12. Sanchez, T. and T. Hla, *Structural and functional characteristics of S1P receptors.* J Cell Biochem, 2004. **92**(5): p. 913-22.
13. Piiper, A. and S. Zeuzem, *Receptor tyrosine kinases are signaling intermediates of G protein-coupled receptors.* Curr Pharm Des, 2004. **10**(28): p. 3539-45.
14. Mills, G.B., et al., *Critical role of lysophospholipids in the pathophysiology, diagnosis, and management of ovarian cancer.* Cancer Treat Res, 2002. **107**: p. 259-83.
15. Mills, G.B. and W.H. Moolenaar, *The emerging role of lysophosphatidic acid in cancer.* Nat Rev Cancer, 2003. **3**(8): p. 582-91.
16. Chalfant, C.E. and S. Spiegel, *Sphingosine 1-phosphate and ceramide 1-phosphate: expanding roles in cell signaling.* J Cell Sci, 2005. **118**(Pt 20): p. 4605-12.

17. Spiegel, S. and S. Milstien, *Sphingosine-1-phosphate: an enigmatic signalling lipid*. Nat Rev Mol Cell Biol, 2003. **4**(5): p. 397-407.
18. English, D., et al., *Lipid mediators of angiogenesis and the signalling pathways they initiate*. Biochimica et Biophysica Acta, 2002. **1582**(1-3): p. 228-39.
19. Pyne, S. and N.J. Pyne, *Sphingosine 1-phosphate signalling in mammalian cells*. Biochemical Journal, 2000. **349**(Pt 2): p. 385-402.
20. Hsieh, H.L., et al., *Sphingosine-1-phosphate induces COX-2 expression via PI3K/Akt and p42/p44 MAPK pathways in rat vascular smooth muscle cells*. J Cell Physiol, 2006. **207**(3): p. 757-66.
21. Igarashi, N., et al., *Sphingosine kinase 2 is a nuclear protein and inhibits DNA synthesis*. J Biol Chem, 2003. **278**(47): p. 46832-9.
22. Gobeil, F., Jr., et al., *Modulation of pro-inflammatory gene expression by nuclear lysophosphatidic acid receptor type-1*. J Biol Chem, 2003. **278**(40): p. 38875-83.
23. Marrache, A.M., et al., *Intracellular signaling of lipid mediators via cognate nuclear G protein-coupled receptors*. Endothelium, 2005. **12**(1-2): p. 63-72.
24. McIntyre, T.M., et al., *Identification of an intracellular receptor for lysophosphatidic acid (LPA): LPA is a transcellular PPARgamma agonist*. Proc Natl Acad Sci U S A, 2003. **100**(1): p. 131-6.
25. Zhang, C., et al., *Lysophosphatidic acid induces neointima formation through PPARgamma activation*. J Exp Med, 2004. **199**(6): p. 763-74.
26. Simon, M.F., et al., *Lysophosphatidic acid inhibits adipocyte differentiation via lysophosphatidic acid 1 receptor-dependent down-regulation of peroxisome proliferator-activated receptor gamma2*. J Biol Chem, 2005. **280**(15): p. 14656-62.
27. Jenkins, G.M. and M.A. Frohman, *Phospholipase D: a lipid centric review*. Cell Mol Life Sci, 2005. **62**(19-20): p. 2305-16.
28. Jones, D., C. Morgan, and S. Cockcroft, *Phospholipase D and membrane traffic. Potential roles in regulated exocytosis, membrane delivery and vesicle budding*. Biochim Biophys Acta, 1999. **1439**(2): p. 229-44.
29. Pettus, B.J., et al., *Ceramide 1-phosphate is a direct activator of cytosolic phospholipase A2*. J Biol Chem, 2004. **279**(12): p. 11320-6.
30. Topham, M.K., *Signaling roles of diacylglycerol kinases*. J Cell Biochem, 2006. **97**(3): p. 474-84.
31. Ruvolo, P.P., *Intracellular signal transduction pathways activated by ceramide and its metabolites*. Pharmacol Res, 2003. **47**(5): p. 383-92.
32. Bollinger, C.R., V. Teichgraber, and E. Gulbins, *Ceramide-enriched membrane domains*. Biochim Biophys Acta, 2005. **1746**(3): p. 284-94.
33. Jamal, Z., et al., *Plasma membrane fractions from rat liver contain a phosphatidate phosphohydrolase distinct from that in the endoplasmic reticulum and cytosol*. J Biol Chem, 1991. **266**(5): p. 2988-96.
34. Brindley, D.N. and D.W. Waggoner, *Mammalian lipid phosphate phosphohydrolases*. Journal of Biological Chemistry, 1998. **273**(38): p. 24281-4.

35. Phan, J. and K. Reue, *Lipin, a lipodystrophy and obesity gene*. Cell Metab, 2005. **1**(1): p. 73-83.
36. Han, G.S., W.I. Wu, and G.M. Carman, *The Saccharomyces cerevisiae Lipin homolog is a Mg<sup>2+</sup>-dependent phosphatidate phosphatase enzyme*. J Biol Chem, 2006. **281**(14): p. 9210-8.
37. Sigal, Y.J., M.I. McDermott, and A.J. Morris, *Integral membrane lipid phosphatases/phosphotransferases: common structure and diverse functions*. Biochemical Journal, 2005. **387**(Pt 2): p. 281-93.
38. Stukey, J. and G.M. Carman, *Identification of a novel phosphatase sequence motif*. Protein Sci, 1997. **6**(2): p. 469-72.
39. Jasinska, R., et al., *Lipid phosphate phosphohydrolase-1 degrades exogenous glycerolipid and sphingolipid phosphate esters*. Biochemical Journal, 1999. **340**(Pt 3): p. 677-86.
40. Hemrika, W., et al., *From phosphatases to vanadium peroxidases: a similar architecture of the active site*. Proc Natl Acad Sci U S A, 1997. **94**(6): p. 2145-9.
41. Macedo-Ribeiro, S., et al., *X-ray crystal structures of active site mutants of the vanadium-containing chloroperoxidase from the fungus Curvularia inaequalis*. J Biol Inorg Chem, 1999. **4**(2): p. 209-19.
42. Renirie, R., et al., *Cofactor and substrate binding to vanadium chloroperoxidase determined by UV-VIS spectroscopy and evidence for high affinity for pervanadate*. Biochemistry, 2000. **39**(5): p. 1133-41.
43. Renirie, R., W. Hemrika, and R. Wever, *Peroxidase and phosphatase activity of active-site mutants of vanadium chloroperoxidase from the fungus Curvularia inaequalis. Implications for the catalytic mechanisms*. J Biol Chem, 2000. **275**(16): p. 11650-7.
44. Zhang, Q.X., et al., *Identification of structurally important domains of lipid phosphate phosphatase-1: implications for its sites of action*. Biochemical Journal, 2000. **345 Pt 2**: p. 181-4.
45. Alderton, F., et al., *G-protein-coupled receptor stimulation of the p42/p44 mitogen-activated protein kinase pathway is attenuated by lipid phosphate phosphatases 1, 1a, and 2 in human embryonic kidney 293 cells*. Journal of Biological Chemistry, 2001. **276**(16): p. 13452-60.
46. Long, J., et al., *Regulation of cell survival by lipid phosphate phosphatases involves the modulation of intracellular phosphatidic acid and sphingosine 1-phosphate pools*. Biochemical Journal, 2005. **391**(Pt 1): p. 25-32.
47. Jia, Y.J., et al., *Differential localization of lipid phosphate phosphatases 1 and 3 to cell surface subdomains in polarized MDCK cells*. FEBS Lett, 2003. **552**(2-3): p. 240-6.
48. Sciorra, V.A. and A.J. Morris, *Sequential actions of phospholipase D and phosphatidic acid phosphohydrolase 2b generate diglyceride in mammalian cells*. Mol Biol Cell, 1999. **10**(11): p. 3863-76.
49. Nanjundan, M. and F. Possmayer, *Pulmonary lipid phosphate phosphohydrolase in plasma membrane signalling platforms*. Biochemical Journal, 2001. **358**(Pt 3): p. 637-46.

50. Sun, W.S., et al., *Translocation of lysophosphatidic acid phosphatase in response to gonadotropin-releasing hormone to the plasma membrane in ovarian cancer cell*. Am J Obstet Gynecol, 2004. **191**(1): p. 143-9.
51. Tanyi, J.L., et al., *Role of decreased levels of lipid phosphate phosphatase-1 in accumulation of lysophosphatidic acid in ovarian cancer*. Clin Cancer Res, 2003. **9**(10 Pt 1): p. 3534-45.
52. Ulrix, W., et al., *Identification of the phosphatidic acid phosphatase type 2a isozyme as an androgen-regulated gene in the human prostatic adenocarcinoma cell line LNCaP*. J Biol Chem, 1998. **273**(8): p. 4660-5.
53. Kai, M., et al., *Cloning and characterization of two human isozymes of Mg<sup>2+</sup>-independent phosphatidic acid phosphatase*. J Biol Chem, 1997. **272**(39): p. 24572-8.
54. Barila, D., et al., *The Dri 42 gene, whose expression is up-regulated during epithelial differentiation, encodes a novel endoplasmic reticulum resident transmembrane protein*. J Biol Chem, 1996. **271**(47): p. 29928-36.
55. Wary, K.K. and J.O. Humtsoe, *Anti-lipid phosphate phosphohydrolase-3 (LPP3) antibody inhibits bFGF- and VEGF-induced capillary morphogenesis of endothelial cells*. Cell Commun Signal, 2005. **3**: p. 9.
56. Burnett, C., et al., *Lipid phosphate phosphatases dimerise, but this interaction is not required for in vivo activity*. BMC Biochemistry, 2004. **5**: p. 2.
57. Kanoh, H., et al., *Purification and properties of phosphatidic acid phosphatase from porcine thymus membranes*. J Biol Chem, 1992. **267**(35): p. 25309-14.
58. Waggoner, D.W., et al., *Purification and characterization of novel plasma membrane phosphatidate phosphohydrolase from rat liver*. Journal of Biological Chemistry, 1995. **270**(33): p. 19422-9.
59. Pyne, S., K.C. Kong, and P.I. Darroch, *Lysophosphatidic acid and sphingosine 1-phosphate biology: the role of lipid phosphate phosphatases*. Seminars in Cell & Developmental Biology, 2004. **15**(5): p. 491-501.
60. Roberts, R., V.A. Sciorra, and A.J. Morris, *Human type 2 phosphatidic acid phosphohydrolases. Substrate specificity of the type 2a, 2b, and 2c enzymes and cell surface activity of the 2a isoform*. J Biol Chem, 1998. **273**(34): p. 22059-67.
61. Smyth, S.S., et al., *Lipid phosphate phosphatases regulate lysophosphatidic acid production and signaling in platelets: studies using chemical inhibitors of lipid phosphate phosphatase activity*. J Biol Chem, 2003. **278**(44): p. 43214-23.
62. Roberts, R.Z. and A.J. Morris, *Role of phosphatidic acid phosphatase 2a in uptake of extracellular lipid phosphate mediators*. Biochim Biophys Acta, 2000. **1487**(1): p. 33-49.
63. Tanyi, J.L., et al., *The human lipid phosphate phosphatase-3 decreases the growth, survival, and tumorigenesis of ovarian cancer cells: validation of*



- the lysophosphatidic acid signaling cascade as a target for therapy in ovarian cancer.* *Cancer Res*, 2003. **63**(5): p. 1073-82.
64. Pagano, R.E. and K.J. Longmuir, *Phosphorylation, transbilayer movement, and facilitated intracellular transport of diacylglycerol are involved in the uptake of a fluorescent analog of phosphatidic acid by cultured fibroblasts.* *J Biol Chem*, 1985. **260**(3): p. 1909-16.
  65. Long, J.S., et al., *Lipid phosphate phosphatase-1 regulates lysophosphatidic acid- and platelet-derived-growth-factor-induced cell migration.* *Biochem J*, 2006. **394**(Pt 2): p. 495-500.
  66. Garcia-Murillas, I., et al., *lazar0 encodes a lipid phosphate phosphohydrolase that regulates phosphatidylinositol turnover during Drosophila phototransduction.* *Neuron*, 2006. **49**(4): p. 533-46.
  67. Escalante-Alcalde, D., et al., *The lipid phosphatase LPP3 regulates extra-embryonic vasculogenesis and axis patterning.* *Development*, 2003. **130**(19): p. 4623-37.
  68. Humtsoe, J.O., et al., *Regulation of cell-cell interactions by phosphatidic acid phosphatase 2b/VCIP.* *Embo J*, 2003. **22**(7): p. 1539-54.
  69. Humtsoe, J.O., et al., *Murine lipid phosphate phosphohydrolase-3 acts as a cell-associated integrin ligand.* *Biochem Biophys Res Commun*, 2005. **335**(3): p. 906-19.
  70. Yue, J., et al., *Mice with transgenic overexpression of lipid phosphate phosphatase-1 display multiple organotypic deficits without alteration in circulating lysophosphatidate level.* *Cell Signal*, 2004. **16**(3): p. 385-99.
  71. Zhang, N., J.P. Sundberg, and T. Gridley, *Mice mutant for Ppap2c, a homolog of the germ cell migration regulator wunen, are viable and fertile.* *Genesis*, 2000. **27**(4): p. 137-40.
  72. Sano, H., A.D. Renault, and R. Lehmann, *Control of lateral migration and germ cell elimination by the Drosophila melanogaster lipid phosphate phosphatases Wunen and Wunen 2.* *J Cell Biol*, 2005. **171**(4): p. 675-83.
  73. Burnett, C. and K. Howard, *Fly and mammalian lipid phosphate phosphatase isoforms differ in activity both in vitro and in vivo.* *EMBO Rep*, 2003. **4**(8): p. 793-9.
  74. Waggoner, D.W., et al., *Phosphatidate phosphohydrolase catalyzes the hydrolysis of ceramide 1-phosphate, lysophosphatidate, and sphingosine 1-phosphate.* *Journal of Biological Chemistry*, 1996. **271**(28): p. 16506-9.
  75. Hooks, S.B., et al., *Lysophosphatidic acid-induced mitogenesis is regulated by lipid phosphate phosphatases and is Edg-receptor independent.* *J Biol Chem*, 2001. **276**(7): p. 4611-21.
  76. Hooks, S.B., S.P. Ragan, and K.R. Lynch, *Identification of a novel human phosphatidic acid phosphatase type 2 isoform.* *FEBS Lett*, 1998. **427**(2): p. 188-92.
  77. Frederick, J.M., Zhang, K., Church-Kopish, J. and Baehr, W. in *ARVO 2002 Annual Meeting "Association of Research in Vision and Ophthalmology"*. 2002. Ft. Lauderdale, Florida.
  78. Noble, M.E., et al., *The cyclin box fold: protein recognition in cell-cycle and transcription control.* *Trends Biochem Sci*, 1997. **22**(12): p. 482-7.

79. Sherr, C.J. and J.M. Roberts, *Living with or without cyclins and cyclin-dependent kinases*. Genes Dev, 2004. **18**(22): p. 2699-711.
80. Fung, T.K. and R.Y. Poon, *A roller coaster ride with the mitotic cyclins*. Semin Cell Dev Biol, 2005. **16**(3): p. 335-42.
81. Samuel, T., H.O. Weber, and J.O. Funk, *Linking DNA damage to cell cycle checkpoints*. Cell Cycle, 2002. **1**(3): p. 162-8.
82. Malumbres, M. and M. Barbacid, *Mammalian cyclin-dependent kinases*. Trends Biochem Sci, 2005. **30**(11): p. 630-41.
83. Lolli, G. and L.N. Johnson, *CAK-Cyclin-dependent Activating Kinase: a key kinase in cell cycle control and a target for drugs?* Cell Cycle, 2005. **4**(4): p. 572-7.
84. Malumbres, M. and M. Barbacid, *To cycle or not to cycle: a critical decision in cancer*. Nat Rev Cancer, 2001. **1**(3): p. 222-31.
85. Sherr, C.J. and J.M. Roberts, *CDK inhibitors: positive and negative regulators of G1-phase progression*. Genes Dev, 1999. **13**(12): p. 1501-12.
86. Harbour, J.W. and D.C. Dean, *The Rb/E2F pathway: expanding roles and emerging paradigms*. Genes Dev, 2000. **14**(19): p. 2393-409.
87. Bandara, L.R., et al., *Functional synergy between DP-1 and E2F-1 in the cell cycle-regulating transcription factor DRTF1/E2F*. Embo J, 1993. **12**(11): p. 4317-24.
88. Wu, C.L., et al., *In vivo association of E2F and DP family proteins*. Mol Cell Biol, 1995. **15**(5): p. 2536-46.
89. Zhang, Y. and S.P. Chellappan, *Cloning and characterization of human DP2, a novel dimerization partner of E2F*. Oncogene, 1995. **10**(11): p. 2085-93.
90. DeGregori, J., *The genetics of the E2F family of transcription factors: shared functions and unique roles*. Biochim Biophys Acta, 2002. **1602**(2): p. 131-50.
91. Attwooll, C., E. Lazzerini Denchi, and K. Helin, *The E2F family: specific functions and overlapping interests*. Embo J, 2004. **23**(24): p. 4709-16.
92. Sherr, C.J. and J.M. Roberts, *Inhibitors of mammalian G1 cyclin-dependent kinases*. Genes Dev, 1995. **9**(10): p. 1149-63.
93. Welcker, M., et al., *Multisite phosphorylation by Cdk2 and GSK3 controls cyclin E degradation*. Mol Cell, 2003. **12**(2): p. 381-92.
94. Krude, T., et al., *Cyclin/Cdk-dependent initiation of DNA replication in a human cell-free system*. Cell, 1997. **88**(1): p. 109-19.
95. Hua, X.H. and J. Newport, *Identification of a preinitiation step in DNA replication that is independent of origin recognition complex and cdc6, but dependent on cdk2*. J Cell Biol, 1998. **140**(2): p. 271-81.
96. Coverley, D., H. Laman, and R.A. Laskey, *Distinct roles for cyclins E and A during DNA replication complex assembly and activation*. Nat Cell Biol, 2002. **4**(7): p. 523-8.
97. Resnitzky, D., L. Hengst, and S.I. Reed, *Cyclin A-associated kinase activity is rate limiting for entrance into S phase and is negatively*

- regulated in G1 by p27Kip1*. Molecular & Cellular Biology, 1995. **15**(8): p. 4347-52.
98. Mitra, J. and G.H. Enders, *Cyclin A/Cdk2 complexes regulate activation of Cdk1 and Cdc25 phosphatases in human cells*. Oncogene, 2004. **23**(19): p. 3361-7.
  99. Sicinski, P., et al., *Cyclin D1 provides a link between development and oncogenesis in the retina and breast*. Cell, 1995. **82**(4): p. 621-30.
  100. Sicinski, P., et al., *Cyclin D2 is an FSH-responsive gene involved in gonadal cell proliferation and oncogenesis*. Nature, 1996. **384**(6608): p. 470-4.
  101. Huard, J.M., et al., *Cerebellar histogenesis is disturbed in mice lacking cyclin D2*. Development, 1999. **126**(9): p. 1927-35.
  102. Lam, E.W., et al., *Cyclin D3 compensates for loss of cyclin D2 in mouse B-lymphocytes activated via the antigen receptor and CD40*. J Biol Chem, 2000. **275**(5): p. 3479-84.
  103. Geng, Y., et al., *Cyclin E ablation in the mouse*. Cell, 2003. **114**(4): p. 431-43.
  104. Sicinska, E., et al., *Requirement for cyclin D3 in lymphocyte development and T cell leukemias*. Cancer Cell, 2003. **4**(6): p. 451-61.
  105. Kozar, K., et al., *Mouse development and cell proliferation in the absence of D-cyclins*. Cell, 2004. **118**(4): p. 477-91.
  106. Malumbres, M., et al., *Mammalian cells cycle without the D-type cyclin-dependent kinases Cdk4 and Cdk6*. Cell, 2004. **118**(4): p. 493-504.
  107. Parisi, T., et al., *Cyclins E1 and E2 are required for endoreplication in placental trophoblast giant cells*. Embo J, 2003. **22**(18): p. 4794-803.
  108. Ortega, S., et al., *Cyclin-dependent kinase 2 is essential for meiosis but not for mitotic cell division in mice*. Nature Genetics, 2003. **35**(1): p. 25-31.
  109. Berthet, C., et al., *Cdk2 knockout mice are viable*. Curr Biol, 2003. **13**(20): p. 1775-85.
  110. Aleem, E., H. Kiyokawa, and P. Kaldis, *Cdc2-cyclin E complexes regulate the G1/S phase transition*. Nat Cell Biol, 2005. **7**(8): p. 831-6.
  111. Harris, S.L. and A.J. Levine, *The p53 pathway: positive and negative feedback loops*. Oncogene, 2005. **24**(17): p. 2899-908.
  112. Das, K.C. and R. Dashnamoorthy, *Hyperoxia activates the ATR-Chk1 pathway and phosphorylates p53 at multiple sites*. Am J Physiol Lung Cell Mol Physiol, 2004. **286**(1): p. L87-97.
  113. Delia, D., et al., *ATM protein and p53-serine 15 phosphorylation in ataxia-telangiectasia (AT) patients and at heterozygotes*. Br J Cancer, 2000. **82**(12): p. 1938-45.
  114. Niida, H. and M. Nakanishi, *DNA damage checkpoints in mammals*. Mutagenesis, 2006. **21**(1): p. 3-9.
  115. Maya, R., et al., *ATM-dependent phosphorylation of Mdm2 on serine 395: role in p53 activation by DNA damage*. Genes Dev, 2001. **15**(9): p. 1067-77.
  116. Hermeking, H., et al., *14-3-3 sigma is a p53-regulated inhibitor of G2/M progression*. Mol Cell, 1997. **1**(1): p. 3-11.

117. Peng, C.Y., et al., *Mitotic and G2 checkpoint control: regulation of 14-3-3 protein binding by phosphorylation of Cdc25C on serine-216*. *Science*, 1997. **277**(5331): p. 1501-5.
118. van Vugt, M.A., et al., *Inhibition of Polo-like kinase-1 by DNA damage occurs in an ATM- or ATR-dependent fashion*. *J Biol Chem*, 2001. **276**(45): p. 41656-60.
119. Hayflick, L.M.P.S., *The serial cultivation of human diploid cell strains*. *Experimental Cell Research*, 1961. **25**: p. 585-621.
120. Shay, J.W. and W.E. Wright, *The use of telomerized cells for tissue engineering*. *Nat Biotechnol*, 2000. **18**(1): p. 22-3.
121. Itahana, K., J. Campisi, and G.P. Dimri, *Mechanisms of cellular senescence in human and mouse cells*. *Biogerontology*, 2004. **5**(1): p. 1-10.
122. Krtolica, A. and J. Campisi, *Cancer and aging: a model for the cancer promoting effects of the aging stroma*. *International Journal of Biochemistry & Cell Biology*, 2002. **34**(11): p. 1401-14.
123. McClintock, B., *The stability of broken ends of chromosomes in Zea mays*. *Genetics*, 1941. **26**: p. 234-282.
124. de Lange, T., *Protection of mammalian telomeres*. *Oncogene*, 2002. **21**(4): p. 532-40.
125. Niida, H., et al., *Severe growth defect in mouse cells lacking the telomerase RNA component*. *Nature Genetics*, 1998. **19**(2): p. 203-6.
126. Chin, L., et al., *p53 deficiency rescues the adverse effects of telomere loss and cooperates with telomere dysfunction to accelerate carcinogenesis*. *Cell*, 1999. **97**(4): p. 527-38.
127. Sherr, C.J. and R.A. DePinho, *Cellular senescence: mitotic clock or culture shock?* *Cell*, 2000. **102**(4): p. 407-10.
128. Lowe, S.W. and C.J. Sherr, *Tumor suppression by Ink4a-Arf: progress and puzzles*. *Current Opinion in Genetics & Development*, 2003. **13**(1): p. 77-83.
129. Collado, M., et al., *Tumour biology: senescence in premalignant tumours*. *Nature*, 2005. **436**(7051): p. 642.
130. Chen, Z., et al., *Crucial role of p53-dependent cellular senescence in suppression of Pten-deficient tumorigenesis*. *Nature*, 2005. **436**(7051): p. 725-30.
131. Michaloglou, C., et al., *BRAFE600-associated senescence-like cell cycle arrest of human naevi. [see comment]*. *Nature*, 2005. **436**(7051): p. 720-4.
132. Campisi, J., *Senescent cells, tumor suppression, and organismal aging: good citizens, bad neighbors*. *Cell*, 2005. **120**(4): p. 513-22.
133. Parrinello, S., et al., *Stromal-epithelial interactions in aging and cancer: senescent fibroblasts alter epithelial cell differentiation*. *Journal of Cell Science*, 2005. **118**(Pt 3): p. 485-96.
134. Gire, V. and D. Wynford-Thomas, *Reinitiation of DNA synthesis and cell division in senescent human fibroblasts by microinjection of anti-p53 antibodies*. *Mol Cell Biol*, 1998. **18**(3): p. 1611-21.

135. Beausejour, C.M., et al., *Reversal of human cellular senescence: roles of the p53 and p16 pathways*. EMBO Journal, 2003. **22**(16): p. 4212-22.
136. Ohtani, N., et al., *The p16INK4a-RB pathway: molecular link between cellular senescence and tumor suppression*. J Med Invest, 2004. **51**(3-4): p. 146-53.
137. Narita, M. and S.W. Lowe, *Executing cell senescence*. Cell Cycle, 2004. **3**(3): p. 244-6.
138. Zhang, R., et al., *Formation of MacroH2A-containing senescence-associated heterochromatin foci and senescence driven by ASF1a and HIRA*. Dev Cell, 2005. **8**(1): p. 19-30.
139. Braig, M., et al., *Oncogene-induced senescence as an initial barrier in lymphoma development*. Nature, 2005. **436**(7051): p. 660-5.
140. Venable, M.E., et al., *Role of ceramide in cellular senescence*. Journal of Biological Chemistry, 1995. **270**(51): p. 30701-8.
141. Stamenkovic, I., *Extracellular matrix remodelling: the role of matrix metalloproteinases*. J Pathol, 2003. **200**(4): p. 448-64.
142. McCawley, L.J. and L.M. Matrisian, *Matrix metalloproteinases: they're not just for matrix anymore!* Curr Opin Cell Biol, 2001. **13**(5): p. 534-40.
143. Rundhaug, J.E., *Matrix metalloproteinases and angiogenesis*. J Cell Mol Med, 2005. **9**(2): p. 267-85.
144. Sottrup-Jensen, L. and H. Birkedal-Hansen, *Human fibroblast collagenase-alpha-macroglobulin interactions. Localization of cleavage sites in the bait regions of five mammalian alpha-macroglobulins*. J Biol Chem, 1989. **264**(1): p. 393-401.
145. Yang, Z., D.K. Strickland, and P. Bornstein, *Extracellular matrix metalloproteinase 2 levels are regulated by the low density lipoprotein-related scavenger receptor and thrombospondin 2*. J Biol Chem, 2001. **276**(11): p. 8403-8.
146. Santiskulvong, C. and E. Rozengurt, *Galardin (GM 6001), a broad-spectrum matrix metalloproteinase inhibitor, blocks bombesin- and LPA-induced EGF receptor transactivation and DNA synthesis in rat-1 cells*. Exp Cell Res, 2003. **290**(2): p. 437-46.
147. Mori, K., et al., *Lysophosphatidic Acid-Induced Effects in Human Colon Carcinoma DLD1 Cells Are Partially Dependent on Transactivation of Epidermal Growth Factor Receptor*. J Surg Res, 2006. **132**(1): p. 56-61.
148. Kue, P.F., et al., *Lysophosphatidic acid-regulated mitogenic ERK signaling in androgen-insensitive prostate cancer PC-3 cells*. Int J Cancer, 2002. **102**(6): p. 572-9.
149. Strongin, A.Y., et al., *Mechanism of cell surface activation of 72-kDa type IV collagenase. Isolation of the activated form of the membrane metalloprotease*. J Biol Chem, 1995. **270**(10): p. 5331-8.
150. Sato, H., et al., *A matrix metalloproteinase expressed on the surface of invasive tumour cells*. Nature, 1994. **370**(6484): p. 61-5.
151. Deryugina, E.I., et al., *MT1-MMP initiates activation of pro-MMP-2 and integrin alphavbeta3 promotes maturation of MMP-2 in breast carcinoma cells*. Exp Cell Res, 2001. **263**(2): p. 209-23.

152. Morgenstern, J.P. and H. Land, *A series of mammalian expression vectors and characterisation of their expression of a reporter gene in stably and transiently transfected cells*. Nucleic Acids Research, 1990. **18**(4): p. 1068.
153. Pear, W.S., et al., *Production of high-titer helper-free retroviruses by transient transfection*. Proceedings of the National Academy of Sciences of the United States of America, 1993. **90**(18): p. 8392-6.
154. Wigler, M., et al., *DNA-mediated transfer of the adenine phosphoribosyltransferase locus into mammalian cells*. Proceedings of the National Academy of Sciences of the United States of America, 1979. **76**(3): p. 1373-6.
155. Martin, A., et al., *Decreased activities of phosphatidate phosphohydrolase and phospholipase D in ras and tyrosine kinase (fps) transformed fibroblasts*. Journal of Biological Chemistry, 1993. **268**(32): p. 23924-32.
156. Labarca, C. and K. Paigen, *A simple, rapid, and sensitive DNA assay procedure*. Analytical Biochemistry, 1980. **102**(2): p. 344-52.
157. Sullards, M.C. and A.H. Merrill, Jr., *Analysis of sphingosine 1-phosphate, ceramides, and other bioactive sphingolipids by high-performance liquid chromatography-tandem mass spectrometry*. Science's Stake [Electronic Resource]: Signal Transduction Knowledge Environment, 2001. **2001**(67): p. PL1.
158. Song, M.S. and E.I. Posse de Chaves, *Inhibition of rat sympathetic neuron apoptosis by ceramide. Role of p75NTR in ceramide generation*. Neuropharmacology, 2003. **45**(8): p. 1130-50.
159. Pyne, S., K.C. Kong, and P.I. Darroch, *Lysophosphatidic acid and sphingosine 1-phosphate biology: the role of lipid phosphate phosphatases*. Semin Cell Dev Biol, 2004. **15**(5): p. 491-501.
160. Pines, J. and T. Hunter, *Human cyclin A is adenovirus E1A-associated protein p60 and behaves differently from cyclin B*. Nature, 1990. **346**(6286): p. 760-3.
161. Nevins, J.R., et al., *E2F transcription factor is a target for the RB protein and the cyclin A protein*. Cold Spring Harbor Symposia on Quantitative Biology, 1991. **56**: p. 157-62.
162. Girard, F., et al., *Cyclin A is required for the onset of DNA replication in mammalian fibroblasts*. Cell, 1991. **67**(6): p. 1169-79.
163. Wang, J., et al., *Modification of cyclin A expression by hepatitis B virus DNA integration in a hepatocellular carcinoma*. Oncogene, 1992. **7**(8): p. 1653-6.
164. Hinds, P.W., et al., *Regulation of retinoblastoma protein functions by ectopic expression of human cyclins*. Cell, 1992. **70**(6): p. 993-1006.
165. Cardoso, M.C., H. Leonhardt, and B. Nadal-Ginard, *Reversal of terminal differentiation and control of DNA replication: cyclin A and Cdk2 specifically localize at subnuclear sites of DNA replication*. Cell, 1993. **74**(6): p. 979-92.
166. Rosenberg, A.R., et al., *Overexpression of human cyclin A advances entry into S phase*. Oncogene, 1995. **10**(8): p. 1501-9.

167. Sunters, A., et al., *Accelerated cell cycle progression in osteoblasts overexpressing the c-fos proto-oncogene: induction of cyclin A and enhanced CDK2 activity*. Journal of Biological Chemistry, 2004. **279**(11): p. 9882-91.
168. Duncan, R.E., A. El-Sohemy, and M.C. Archer, *Mevalonate promotes the growth of tumors derived from human cancer cells in vivo and stimulates proliferation in vitro with enhanced cyclin-dependent kinase-2 activity*. Journal of Biological Chemistry, 2004. **279**(32): p. 33079-84.
169. Diehl, J.A., et al., *Glycogen synthase kinase-3beta regulates cyclin D1 proteolysis and subcellular localization*. Genes & Development, 1998. **12**(22): p. 3499-511.
170. Liang, J. and J.M. Slingerland, *Multiple roles of the PI3K/PKB (Akt) pathway in cell cycle progression*. Cell Cycle, 2003. **2**(4): p. 339-45.
171. Roovers, K., et al., *Nuclear translocation of LIM kinase mediates Rho-Rho kinase regulation of cyclin D1 expression*. Developmental Cell, 2003. **5**(2): p. 273-84.
172. Philips, A., et al., *Differential effect of Rac and Cdc42 on p38 kinase activity and cell cycle progression of nonadherent primary mouse fibroblasts*. Journal of Biological Chemistry, 2000. **275**(8): p. 5911-7.
173. Latonen, L. and M. Laiho, *Cellular UV damage responses--functions of tumor suppressor p53*. Biochimica et Biophysica Acta, 2005. **1755**(2): p. 71-89.
174. Coqueret, O., *New roles for p21 and p27 cell-cycle inhibitors: a function for each cell compartment?* Trends in Cell Biology, 2003. **13**(2): p. 65-70.
175. Yam, C.H., T.K. Fung, and R.Y. Poon, *Cyclin A in cell cycle control and cancer*. Cell Mol Life Sci, 2002. **59**(8): p. 1317-26.
176. Resnitzky, D., et al., *Acceleration of the G1/S phase transition by expression of cyclins D1 and E with an inducible system*. Molecular & Cellular Biology, 1994. **14**(3): p. 1669-79.
177. Ohtsubo, M., et al., *Human cyclin E, a nuclear protein essential for the G1-to-S phase transition*. Molecular & Cellular Biology, 1995. **15**(5): p. 2612-24.
178. Tsai, L.H., et al., *Activity and expression pattern of cyclin-dependent kinase 5 in the embryonic mouse nervous system*. Development, 1993. **119**(4): p. 1029-40.
179. Lucibello, F.C., et al., *Deregulation of cyclins D1 and E and suppression of cdk2 and cdk4 in senescent human fibroblasts*. Journal of Cell Science, 1993. **105**(Pt 1): p. 123-33.
180. Dulic, V., et al., *Altered regulation of G1 cyclins in senescent human diploid fibroblasts: accumulation of inactive cyclin E-Cdk2 and cyclin D1-Cdk2 complexes*. Proceedings of the National Academy of Sciences of the United States of America, 1993. **90**(23): p. 11034-8.
181. Marchesini, N., et al., *Role for mammalian neutral sphingomyelinase 2 in confluence-induced growth arrest of MCF7 cells*. Journal of Biological Chemistry, 2004. **279**(24): p. 25101-11.

182. Spruck, C.H., K.A. Won, and S.I. Reed, *Deregulated cyclin E induces chromosome instability*. Nature, 1999. **401**(6750): p. 297-300.
183. Baus, F., et al., *Permanent cell cycle exit in G2 phase after DNA damage in normal human fibroblasts*. Embo J, 2003. **22**(15): p. 3992-4002.
184. Campisi, J., *Suppressing cancer: the importance of being senescent*. Science, 2005. **309**(5736): p. 886-7.
185. Theocharis, S., et al., *Peroxisome proliferator-activated receptor-gamma ligands as cell-cycle modulators*. Cancer Treat Rev, 2004. **30**(6): p. 545-54.
186. Jang, I.S., et al., *Altered cAMP signaling induced by lysophosphatidic acid in senescent human diploid fibroblasts*. Biochem Biophys Res Commun, 2003. **302**(4): p. 778-84.
187. Jang, I.S., et al., *Lysophosphatidic acid-induced changes in cAMP profiles in young and senescent human fibroblasts as a clue to the ageing process*. Mech Ageing Dev, 2006. **127**(5): p. 481-9.
188. Fishman, D.A., et al., *Lysophosphatidic acid promotes matrix metalloproteinase (MMP) activation and MMP-dependent invasion in ovarian cancer cells*. Cancer Res, 2001. **61**(7): p. 3194-9.
189. Wu, W.T., et al., *Lysophospholipids enhance matrix metalloproteinase-2 expression in human endothelial cells*. Endocrinology, 2005. **146**(8): p. 3387-400.
190. Matsumoto, Y., et al., *Small GTP-binding protein, Rho, both increased and decreased cellular motility, activation of matrix metalloproteinase 2 and invasion of human osteosarcoma cells*. Jpn J Cancer Res, 2001. **92**(4): p. 429-38.
191. Shida, D., et al., *Lysophosphatidic acid (LPA) enhances the metastatic potential of human colon carcinoma DLD1 cells through LPA1*. Cancer Res, 2003. **63**(7): p. 1706-11.
192. Krtolica, A., et al., *Senescent fibroblasts promote epithelial cell growth and tumorigenesis: a link between cancer and aging*. Proceedings of the National Academy of Sciences of the United States of America, 2001. **98**(21): p. 12072-7.
193. Zhao, Y., et al., *Lipid phosphate phosphatase-1 regulates lysophosphatidic acid-induced calcium release, NF-kappaB activation and interleukin-8 secretion in human bronchial epithelial cells*. Biochem J, 2005. **385**(Pt 2): p. 493-502.
194. Ferbeyre, G., et al., *Oncogenic ras and p53 cooperate to induce cellular senescence*. Molecular & Cellular Biology, 2002. **22**(10): p. 3497-508.
195. Lazzerini Denchi, E., et al., *Deregulated E2F activity induces hyperplasia and senescence-like features in the mouse pituitary gland*. Mol Cell Biol, 2005. **25**(7): p. 2660-72.
196. Grandori, C., et al., *Werner syndrome protein limits MYC-induced cellular senescence*. Genes Dev, 2003. **17**(13): p. 1569-74.
197. Guney, I., S. Wu, and J.M. Sedivy, *Reduced c-Myc signaling triggers telomere-independent senescence by regulating Bmi-1 and p16(INK4a)*. Proc Natl Acad Sci U S A, 2006. **103**(10): p. 3645-50.



198. Lowe, S.W., E. Cepero, and G. Evan, *Intrinsic tumour suppression*. Nature, 2004. **432**(7015): p. 307-15.
199. Narita, M. and S.W. Lowe, *Senescence comes of age*. Nature Medicine, 2005. **11**(9): p. 920-2.